Natural oil nano-emulsion dispersions for the topical delivery of clofazimine, artemisone and decoquinate

C Burger

orcid.org/ 0000-0002-5188-4083

Thesis submitted for the degree *Doctor of Philosophy* in Pharmaceutics at the North-West University

Promoter:	Dr M Gerber
Co-promoter:	Prof J du Plessis
Co-promoter:	Prof ME Aucamp

Graduation May 2018

Student number: 21661308

Acknowledgements

2 Corinthians 12:9-10: “But he said to me: “My grace is sufficient for you, for my power is made perfect in weakness.” Therefore I will boast all the more gladly about my weaknesses, so that Christ’s power may rest on me. That is why, for Christ’s sake, I delight in weaknesses, in insults, in hardships, in persecutions, in difficulties. For when I am weak, then I am strong.”

First and foremost, I want to thank our **Heavenly Father**, for His abundant blessings, allowing me this opportunity to do my studies. Lord, without You, I would be lost.

To my two amazing parents, **Hennie and Martie Burger**, thank you for all your love and support, once again after three years of furthering my studies I would not be able to finish if it was not for you. Thank you for having the world`s patience with me even when I was frustrated relentlessly. Thank you for always believing in me, even when I stopped believing in myself. No words of appreciation will ever be enough. Love you forever and always.

To my brothers **Henro and Henning**, and sister-in law **Mariana**, thank you for always being there for me. You are a true example of what the word family means.

To **Stefan Erasmus**, not even a thank you is enough for what you have done for me. Thank you for staying up late with me, motivating me, comforting me, encouraging me and in general just being there. I am so grateful to have you in my life. I love you forever and a day.

To **Suzanne** and **Sumari**, there are no words to describe the thankfulness I have for you two. Thank you for picking up my late night phone calls, for calming me when I got stressed, for motivating and believing in me. Thank you for going out of your way to make sure that I am fine. You are the friends I would walk in storms for.

To my promoter, **Dr Minja Gerber**, what a privilege it has been to be one of your students again. I am truly blessed with you in my life. Thank you for all your expertise and showing me that struggles, no matter how big or small, can always be overcome if you have the right mind set. Thank you for being my mentor. Thank you for being the “People who make your problems their problems, just so you do not have to go through them alone“.

Prof Marique Aucamp, my co-promoter, thank you for your positive spirit and all your guidance during the course of the studies. Thank you for all the help and effort, it does not go unappreciated. It was a pleasure being one of your students.

Prof Wilna Liebenberg, thank you for all the help during the compatibility studies.

Prof Jan du Preez, thank you for your help with the HPLC.

Prof Jeanetta du Plessis, my co-promoter. Thank you for all the help.

Lizelle, thank you so much for helping me when I did not know which side to turn to. You are a blessing.

Marelize Pretorius. Thank you for helping help me with the data and statistical analysis of the diffusion studies.

Ms Hester de Beer. Thank you for all the help with the administrative work.

A very special thank you to **Gill Smithies,** with the proofreading and editing of my work. You are one of a kind!

The **National Research Foundation (NRF)**. Thank you for providing me with bursaries for three years of my study. "The financial assistance of the National Research Foundation (NRF) towards this research is hereby acknowledged. Opinions expressed and conclusions arrived at, are those of the author and are not necessarily to be attributed to the NRF."

Abstract

Tuberculosis (TB), which is caused by *Mycobacterium tuberculosis* (*Mtb*) (Godreuil *et al*., 2007:1), manifests as an extra-pulmonary disease in 3.7 to 8.4% of cases, whereas cutaneous tuberculosis (CTB), which is uncommon, compromises approximately 1.0 to 1.5% of all extra-pulmonary manifestations. The active pharmaceutical ingredients (APIs) chosen for this study were clofazimine (CLF), artemisone (ART) and decoquinate (DQ).

APIs should possess physicochemical characteristics by containing both hydrophilic properties (to permeate to other hydrophilic skin layers to reach the circulatory system) and lipophilic qualities (to permeate the stratum corneum) (Naik *et al*., 2000).

Penetration enhancers may be used to penetrate barrier properties of the skin to facilitate permeation. Literature suggests by using natural oils (fatty acids), the delivery of both hydrophilic and lipophilic APIs could be promoted (Williams & Barry, 2012:132) as they contain linoleic acid (C_{18} fatty acid) (Vermaak *et al.*, 2011:920-933).

The aim of this study was to investigate whether nano-emulsions containing natural oils would improve the topical delivery of CLF, DQ and ART, separately and in combination. The nano-emulsions were characterised by means of pH, viscosity, drug entrapment efficiency and zeta-potential. A novel high performance liquid chromatography (HPLC) method was developed and validated for the simultaneous analysis of CLF, ART and DQ throughout the study during experiments.

During membrane and skin diffusion studies, it was evident that no API was released from all eight nano-emulsions within the receptor fluid. The nano-emulsions containing a single API were found within the stratum corneum-epidermis (SCE) and showed similar results in the epidermis-dermis (ED), where only CLF and DQ were detected; no ART was observed within the ED. It is evident with the nano-emulsions containing the combination of APIs that CLF and ART was found within the SCE, but no DQ was found within the SCE. In the ED, it was evident that CLF and DQ were detected, but no ART was found, therefore nano-emulsions could deliver APIs topically without entering the blood stream.

In vitro cytotoxicity studies showed no cytotoxicity on immortalised human keratinocyte (HaCaT) cells, indicating the nano-emulsions were safe to use on human skin. From the *Mtb* cell line studies, all the formulations displayed %inhibition on the bacterial tuberculosis (52 – 63% inhibition).

During this study, a novel high performance liquid chromatography (HPLC) validation method was developed to determine the concentration of CLF, ART and DQ simultaneously. Subsequently, the validation method was published; in addition, a literature review on nano-emulsions was written and published. Novel contributions have been made to science where the compatibility of the combined use of CLF, ART and DQ were tested during microcalorimetry, differential scanning calorimetry (DSC) and hot stage microscopy (HSM) studies. Nano-emulsions containing natural oils were developed and tested for efficacy against TB strains. In the future, this knowledge can be applied for the possible treatment of CTB in conjunction with systemic treatment. Information gathered during this study serves as basic research, which forms the basis for further studies.

Keywords: Cutaneous tuberculosis; Topical delivery; Clofazimine; Artemisone; Decoquinate; Nano-emulsions; Natural oils.

References

Godreuil, S., Tazi, L. & Bañuls, A.-L. 2007. Pulmonary Tuberculosis and *Mycobacterium Tuberculosis:* Modern Molecular Epidemiology and Perspectives. (*In* Tibayrenc, M., *ed.* Encyclopedia of Infectious Diseases: Modern Methodologies. New Jersey: John Wiley & Sons, Inc doi: 10.1002/9780470114209.ch1.)

Naik, A., Kalia, Y.N. & Guy, R.H. 2000. Transdermal drug delivery: overcoming the skin's barrier function. *Pharmaceutical Science and Technology Today,* 3(9):318-326.

Vermaak, I., Kamatou, G.P.P., Komane-Mofokeng, B., Viljoen, A.M. & Beckett, K. 2011. African seed oils of commercial importance: cosmetic application. *South African Journal of Botany*, 77:920-933.

Williams, A.C. & Barry, B.W. 2012. Penetration enhancers. *Advanced Drug Delivery Reviews*, 64:128-137.

Table of Contents

Aknowledgements i

Abstract iii

References v

List of Figures xx

List of Tables xxv

Abbreviations xxx

Chapter 1: Introduction and problem statement

1. Introduction 1

References 6

Chapter 2: Traversing the skin barrier with nano-emulsions

Abstract 11

1. Introduction 11

2. Nano-emulsions vs. micro-emulsions 12

3. Formulation approaches 12

3.1. Low energy emulsification methods 12

3.1.1. Spontaneous emulsification 12

3.1.2. Phase Inversion Temperature 12

3.1.3. Phase Inversion Composition 13

3.2. High energy emulsification 13

3.2.1. Microfluidization method 13

3.2.2. High pressure homogenisation method 13

3.2.3. Ultrasonication method 13

4. Characterisation of nano-emulsions 14

5. Nano-emulsions as topical/transdermal vehicle 14

5.1. Nano-emulsions loaded with anti-inflammatory drugs 18

5.2. Nano-emulsions loaded with cardiovascular drugs 19

5.3. Nano-emulsions loaded with central nervous system drugs 20

5.4. Nano-emulsion loaded with anti-infective 20

5.5. Nano-emulsion loaded with hormones 21

5.6. Nano-emulsions loaded with anti-oxidants 21

5.7. Nano-emulsion loaded with sunscreen agents 22

Conclusion 22

Conflict of interest 22

Acknowledgements 22

Patient consent 22

References 22

Chapter 3: Development and validation of the simultaneous determination of artemisone, clofazimine and decoquinate with HPLC

Abstract 27

1. Introduction 27

2. Investigations, results and discussion 28

3. Experimental 29

Acknowledgements 30

Disclaimer 30

References 31

Chapter 4: Pre-formulation of natural oil nano-emulsions containing clofazimine, artemisone and decoquinate

Abstract 42

Introduction 44

Materials and methods 46

Materials 46

Solubility of compounds 46

Chromatographic conditions 47

Compatibility studies 47

Hot stage microscope (HSM) 47

Isothermal microcalorimetry 48

Preparation of nano-emulsions 48

Characterisation of nano-emulsion dispersions 48

pH 49

Viscosity 49

Droplet size 49

Zeta-potential 49

Drug entrapment efficacy 49

Results 50

Solubility determination/assay 50

Compatibility studies 50

Hot-stage microscopy 50

Isothermal microcalorimetry 51

Nano-emulsion formulation 52

Physicochemical Properties 52

pH 52

Viscosity 52

Droplet size 52

Zeta-potential 53

Discussion 53

Conclusion 54

Declaration of interest 55

References 56

Chapter 5: Formulation of natural oil nano-emulsions for the topical delivery of clofazimine, artemisone and decoquinate

Graphical abstract 71

Abstract 72

1. Introduction 73

2. Materials and methods 75

2.1 Materials 75

2.2 Methods 76

2.2.1 Nano-emulsion preparation 76

2.2.2 Preparation of PBS (pH 7.4) 76

2.2.3 HPLC analysis of clofazimine, artemisone and decoquinate 77

2.2.4 Standard preparation 77

2.2.5 Physicochemical properties 77

2.2.5.1 Aqueous solubility 77

2.2.5.2 Octanol-buffer distribution coefficient (log D) 78

2.3 Characterisation of the nano-emulsions 78

2.3.1 Droplet size, distribution and zeta-potential 78

2.3.2 pH 78

2.3.3 Viscosity of the nano-emulsions 79

2.3.4 Entrapment efficiency (EE) 79

2.4 Diffusion experiments 79

2.4.1 Membrane release studies 79

2.4.2 Skin preparation 80

2.4.3 Skin diffusion 80

2.4.4 Tape-stripping 81

2.5 Data and statistical analysis 81

2.6 *In vitro* cytotoxicity 81

2.6.1 Cell culture cultivation 81

2.6.2 Seeding of cells for toxicity assay 82

2.6.3 Determining cell death using LDH assay 82

2.7 *In vitro* cytotoxicity on *Mycobacterium* strains 82

2.7.1 Determination of the 90% minimum inhibitory concentration (MIC_{90}) 82

2.7.2 Intracellular efficacy of compounds against *Mycobacterium tuberculosis* H37Rv 83

3. Results and discussion 84

3.1 Formulation and semi-solid products 84

3.2 Physicochemical properties 84

3.2.1 Aqueous solubility 84

3.2.2 Log D 85

3.2.3 Characterisation of nano-emulsions 85

3.3 Membrane diffusion experiments 85

3.4 Diffusion experiment 85

3.4.1 Diffusion study 85

3.5 Tape-stripping 86

3.5.1 Stratum corneum-epidermis 86

3.5.2 Epidermis-dermis 87

3.6 Statistical analysis 88

3.6.1 Tape-stripping 88

3.7 *In vitro* cytotoxicity 89

3.8 *In vitro* cell culture studies on tuberculous cells 90

4. Conclusion 90

Acknowledgements 92

Declaration of interest 92

References 93

Tables 98

Figure legends 103

Figures 105

Chapter 6: Conclusion and future prospects

References 119

Appendix A: Validation of an HPLC analytical method for analysis of clofazimine, artemisone and decoquinate

A.1 Purpose of validation 121

A.2 Chromatographic conditions 121

A.3 Preparation of standard and samples 123

A.3.1 Standard preparation of clofazimine, artemisone and decoquinate 123

A.3.2 Preparation of samples for the analysis of nano-formulations 123

A.3.3 Placebo preparation 125

A.3.4 Sample preparation for diffusion studies 125

A.4 Validation parameters 126

A.4.1 Linearity 126

A.4.1.1 Detection limit (LOD) and quantitation limit (LOQ) 130

A.4.2 Accuracy 130

A.4.2.1 Accuracy analysis of clofazimine, artemisone and decoquinate 130

A.4.3 Precision 133

A.4.3.1 Intra-day precision (repeatability) 133

A.4.3.2 Inter-day precision (reproducibility) 135

A.4.4 Ruggedness 138

A.4.4.1 Sample stability 138

A.4.4.2 System repeatability (system suitability) 141

A.5 Conclusion 143

References 144

Appendix B: Pre-formulation, formulation and characterisation of nano-emulsions containing a natural oil and clofazimine, artemisone and decoquinate

B.1 Introduction 146

B.2 Materials 146

B.2.1 Ingredients used to formulate nano-emulsions 146

B.2.1.1 Natural oils 147

B.2.1.2 Clofazimine 147

B.2.1.3 Artemisone 147

B.2.1.4 Decoquinate 148

B.2.1.5 Emulsifiers 148

B.2.1.5.1 Emulsifiers classified by hydrophilic/lipophilic balance 148

B.2.1.5.2 Sorbitan monostearate 60 (Span® 60) 148

B.2.1.5.3 Polysorbate 80 (Tween® 80) 148

B.2.1.6 Water 149

B.3 Compatibility studies 149

B.3.1 Differential scanning calorimetry 149

B.3.2 Thermal activity monitor 150

B.3.3 Hot stage microscope (HSM) 155

B.4 Pre-formulation of nano-emulsions 158

B.4.1 Natural oil solubility of CLF, ART and DQ 158

B.4.2 Formulation of the nano-emulsion 158

B.5 Methods 160

B.5.1 General formulation method of the nano-emulsion 160

B.5.2 Formulation method of the eight pre-formulation natural oil nano-emulsions 160

B.6 Characterisation of pre-formulation nano-emulsions 160

B.6.1 pH 161

B.6.2 Viscosity 162

B.6.3 Droplet size 162

B.6.4 Zeta-potential 163

B.6.5 Drug entrapment efficacy 164

B.6.6 Morphology 165

B.7 Conclusion 167

References 168

Appendix C: Franz cell diffusion studies of natural oil nano-emulsions containing clofazimine, artemisone and decoquinate

C.1 Introduction 173

C.2 Methods 174

C.2.1 Preparation of nano-emulsions 174

C.2.2 Preparation of the receptor phase 174

C.2.3 HPLC analysis of clofazimine, artemisone and decoquinate 174

C.2.4 Standard sample preparation 175

C.2.5 Solubility and octanol-buffer distribution coefficient determination for clofazimine, artemisone and decoquinate 176

C.2.5.1 Solubility 176

C.2.5.2 Octanol-buffer distribution coefficient (log D) 176

C.2.6 Diffusion experiments 176

C.2.6.1 Membrane release studies 176

C.2.6.2 Skin preparation 178

C.2.6.3 *In vitro* skin permeation studies 178

C.2.6.4 Tape-stripping 179

C.2.7 Data analysis 179

C.2.8 Statistical analysis 179

C.3 Results and discussion 180

C.3.1 Formulation of natural oil nano-emulsions 180

C.3.2 Physicochemical properties 180

C.3.2.1 Solubility 180

C.3.2.2 Log D 181

C.3.3 Diffusion experiments 181

C.3.3.1 Membrane release studies 181

C.3.3.2 Transdermal studies 181

C.3.3.3 Tape-stripping results 182

C.3.3.3.1 Stratum corneum-epidermis concentration 187

C.3.3.3.2 Epidermis-dermis concentration 187

C.3.4 Statistical analysis 189

C.4 Conclusion 189

References 192

Appendix D**:** Cytotoxicity studies of natural oil nano-emulsions containing clofazimine, artemisone and decoquinate

D.1 Introduction 196

D.2 *In vitro* cell culture toxicity studies 197

D.2.1 Appropriate cell line selection 198

D.2.2 Cell line treatment 198

D.2.3 Experimental procedures 198

D.2.3.1 Materials 198

D.3 Cytotoxicity testing 199

D.3.1 LDH-assay 199

D.3.2 *In vitro* cell culture studies on tuberculous cells 200

D.3.2.1 Determination of the 90% minimum inhibitory concentration (MIC90) 200

D.3.2.2 Intracellular efficacy of compounds against *Mycobacterium tuberculosis* H37Rv 201

D.4 Results and discussion 201

D.4.1 LDH testing results on HaCaT cells 201

D.4.2 *In vitro* cell culture studies on tuberculous cells 203

D.5 Conclusion 205

References 207

Appendix E: Authors guide of 'Drug Development and Industrial Pharmacy'

Peer review 210

Preparing your paper 210

Structure 211

Word count 211

Style guidelines 211

Formatting and templates 211

References 212

Checklist: what to include 212

Using third-party material in your paper 213

Disclosure statement 214

Clinical Trials Registry 214

Complying with ethics of experimentation 214

Consent 214

Health and safety 215

Submitting your paper 215

Publication charges 215

Fast Track publication 215

Copyright options 215

Complying with funding agencies 215

Open access 216

Accepted Manuscripts Online (AMO) 217

My Authored Works 217

Article reprints 217

Sponsored supplements 217

Appendix F: International Journal of Pharmaceutics: Guide for Authors

F.1 Scope of the journal 219

F.2 Editorial Policy 219

F.3 Submission of Manuscripts 220

F.3.1 Europe, Africa, Near East 220

F.3.2 The Americas, Australia and New Zealand 221

F.3.3 Japan and far East 221

F.4 Manuscript Types 221

F.4.1 Full length manuscripts 221

F.4.1.1 Title 221

F.4.1.2 List of authors 221

F.4.1.3 Affiliation(s) Name(s) and address (es) of the establishment(s) where the work was done designated by superscript, lower-case letters where appropriate 221

F.4.1.4 Abstract 221

F.4.1.5 Keywords 221

F.4.1.6 Corresponding author 222

F.4.1.7 Text 222

F.4.1.8 Nomeclature 222

F.4.1.9 Figure legends, table legends, footnotes 222

F.4.1.10 References 222

F.4.2 Rapid communications 222

F.4.3 Notes 223

F.4.4 Reviews and mini reviews 223

F.5 References 223

F.5.1 Text citation 223

F.5.2 Reference list 223

F.5.3 Use of digital object identifier (DOI) 225

F.6 Articles in special issues 225

F.7 Figures and Tables 225

F.7.1 Figures 225

F.7.2 Tables 226

F.7.3 Dna and genbank accession numbers 226

F.8 Copyright guidelines for authors 226

F.9 Authors' rights 227

F.10 Proofs, Offprints and Page Charges 227

F.11 Language Services 227

F.12 Funding body agreements and policies 228

F.13 Author enquiries 228

List of Figures

Chapter 3: Development and validation of the simultaneous determination of artemisone, clofazimine and decoquinate with HPLC

Fig. 1: Molecular structures of A) clofazimine, B) artemisone and C) decoquinate 36

Fig. 2: Chromatographs of a standard solution containing clofazimine, artemisone and decoquinate, respectively. The top chromatogram signifying detection obtained at 284 nm and the bottom chromatogram showing detection at 210 nm 37

Fig. 3: Chromatographs obtained with a solution containing typical excipients used in formulation of solid oral dosage forms, observing clofazimine, artemisone and decoquinate, respectively. The top chromatogram signifying detection obtained at 284 nm and the bottom chromatogram showing detection at 210 nm 38

Fig. 4: Chromatographs of excipient solution for transdermal/topical delivery systems showing clofazimine, artemisone, and decoquinate, respectively. The top chromatogram signifying detection obtained at 284 nm and the bottom chromatogram showing detection at 210 nm 39

Chapter 4: Pre-formulation of natural oil nano-emulsions containing clofazimine, artemisone and decoquinate

Figure 1: Micrographs obtained from HSM observations with corresponding temperatures 67

Figure 2: a) Heat flow versus time graph obtained for a 1:1 combination of CLF and Tween® 80, b) heat flow versus time graph obtained for a 1:1 weight combination of CLF, Tween® 80 and safflower oil, c) heat flow versus time graph obtained for a 1:1 weight combination of CLF, Tween® 80 and olive oil, d) heat flow versus time graph obtained for a 1:1 weight combination of ART and Tween® 80, e) heat flow versus time graph obtained for a 1:1 weight combination of ART, Span® 60 and safflower oil and f) heat flow versus time graph obtained for a 1:1 weight combination of ART, Span® 60 and olive oil 68

Chapter 5: Formulation of natural oil nano-emulsions for the topical delivery of clofazimine, artemisone and decoquinate

Figure 1: Box-plot indicating the concentration (µg/ml) of **S1** (CLF), **S2** (ART) and **S3** (DQ) present in the SCE after tape-stripping. Concentration values are indicated by the lines and squares, respectively 104

Figure 2: Box-plot indicating the concentration (µg/ml) of **O1** (CLF), **O2** (ART) and **O3** (DQ) present in the SCE after tape-stripping. Concentration values are indicated by the lines and squares, respectively 105

Figure 3: Box-plot indicating the concentration (µg/ml) of CLF, ART and DQ present in **S4** in the SCE after tape-stripping. Concentration values are indicated by the lines and squares, respectively 106

Figure 4: Box-plot indicating the concentration (µg/ml) of CLF, ART and DQ present in **O4** in the SCE after tape-stripping. Concentration values are indicated by the lines and squares, respectively 107

Figure 5: Box-plot indicating the concentration (µg/ml) of **S1** (CLF) and **S3** (DQ) present in the ED after tape-stripping. Concentration values are indicated by the lines and squares, respectively 108

Figure 6: Box-plot indicating the concentration (µg/ml) of **O1** (CLF) and **O3** (DQ) present in the ED after tape-stripping. Concentration values are indicated by the lines and squares, respectively 109

Figure 7: Box-plot indicating the concentration (µg/ml) of CLF, ART and DQ present in **S4** in the ED after tape-stripping. Concentration values are indicated by the lines and squares, respectively 110

Figure 8: Box-plot indicating the concentration (µg/ml) of CLF, ART and DQ present in **O4** in the ED after tape-stripping. Concentration values are indicated by the lines and squares, respectively 111

Appendix A: Validation of an HPLC analytical method for analysis of clofazimine, artemisone and decoquinate

Figure A.1: Linear regression curve of CLF 127

Figure A.2: Linear regression curve of ART 128

Figure A.3: Linear regression curve of DQ 129

Appendix B: Pre-formulation, formulation and characterisation of nano-emulsions containing a natural oil and clofazimine, artemisone and decoquinate

Figure B.1: CLF, ART and DQ combination differential scanning calorimetry 150

Figure B.2: Heat flow *versus* time graph obtained for a 1:1 combination of CLF and Tween® 80 151

Figure B.3: Heat flow *versus* time graph obtained for a 1:1 weight combination of CLF, Tween® 80 and safflower oil 152

Figure B.4: Heat flow *versus* time graph obtained for a 1:1 weight combination of CLF, Tween® 80 and olive oil 152

Figure B.5: Heat flow *versus* time graph obtained for a 1:1 weight combination of ART and Tween® 80 152

Figure B.6: Heat flow *versus* time graph obtained for a 1:1 weight combination of ART, Tween® 80 and safflower oil 152

Figure B.7: Heat flow *versus* time graph obtained for a 1:1 weight combination of ART, Tween® 80 and olive oil 153

Figure B.8: Heat flow *versus* time graph obtained for a 1:1 weight combination of ART, Span® 60 and safflower oil 153

Figure B.9: Heat flow *versus* time graph obtained for a 1:1 weight combination of ART, Span® 60 and olive oil 154

Figure B.10: a) Light microscopy micrographs of the nano-emulsion containing safflower oil (**S1**, **S2**, **S3** and **S4**) 166

Figure B.11: a) Light microscopy micrographs of the nano-emulsion containing olive oil (**O1**, **O2**, **O3** and **O4**) 166

Appendix C: Franz cell diffusion studies of natural oil nano-emulsions containing clofazimine, artemisone and decoquinate

Figure C.1: Mixing of PBS: a) PBS mixing on magnetic stirrer, b) PBS being filtered, c) H_3PO_4 (used to lower pH), d) NaOH (used to increase pH) 177

Figure C.2: Nano-emulsions being formulated: a) water phase (Water and Tween® 80) being mixed on hot plate, b) APIs mixed separately in oil phase (safflower with Span® 60) 177

Figure C.3: Materials used during a diffusion study: a) Franz cells in Franz cell stand, b) Dow Corning® Vacuum grease and c) Grant water bath 177

Figure C.4: Materials used to dermatome skin: a) dermatome blade, b) power source, c) dermatome 178

Figure C.5: Box-plot indicating the concentration (µg/ml) of **S1** (CLF), **S2** (ART) and **S3** (DQ) present in the SCE after tape-stripping (n=7). Concentration values are indicated by the lines and squares, respectively. 183

Figure C.6: Box-plot indicating the concentration (µg/ml) **O1** (CLF), **O2** (ART) and **O3** (DQ) present in the SCE after tape-stripping (n=7). Concentration values are indicated by the lines and squares, respectively. 183

Figure C.7: Box-plot indicating the concentration (µg/ml) **S1** (CLF) and **S3** (DQ) present in the ED after tape-stripping (n=7). Concentration values are indicated by the lines and squares, respectively. 184

Figure C.8: Box-plot indicating the concentration (µg/ml) **O1** (CLF) and **O3** (DQ) present in the ED after tape-stripping (n=7). Concentration values are indicated by the lines and squares, respectively. 184

Figure C.9: Box-plot indicating the concentration (µg/ml) CLF, ART and DQ present in **S4** in the SCE after tape-stripping (n=7). Concentration values are indicated by the lines and squares, respectively. 185

Figure C.10: Box-plot indicating the concentration (µg/ml) CLF, ART and DQ present in **O4** in the SCE after tape-stripping (n=7). Concentration values are indicated by the lines and squares, respectively. 185

Figure C.11: Box-plot indicating the concentration (µg/ml) CLF, ART and DQ present in **S4** in the ED after tape-stripping (n=7). Concentration values are indicated by the lines and squares, respectively. 186

Figure C.12: Box-plot indicating the concentration (µg/ml) CLF, ART and DQ present in **O4** in the ED after tape-stripping (n=7). Concentration values are indicated by the lines and squares, respectively. 186

List of Tables

Chapter 2: Traversing the skin barrier with nano-emulsions

Table 1. Physicochemical characterisation of nano-emulsions 13

Table 2. NEs containing various APIs used in topical and transdermal delivery 14

Chapter 3: Development and validation of the simultaneous determination of artemisone, clofazimine and decoquinate with HPLC

Table 1: Solubility **(µg/ml)** (37 °C) determined for artemisone, clofazimine and decoquinate in nine different solvents 33

Table 2: Obtained validation parameters for the three compounds 34

Table 3: Precision data for artemisone, clofazimine and decoquinate 35

Chapter 4: Pre-formulation of natural oil nano-emulsions containing clofazimine, artemisone and decoquinate

Table 1: Formula used during the formulation of the nano-emulsions containing olive oil 62

Table 2: Formula used during the formulation of the nano-emulsions containing olive oil 63

Table 3: Solubility (µg/ml) of clofazimine, artemisone and decoquinate in selected solvents 64

Table 4: Interaction heat flow results of TAM 65

Table 5: Characterisation results of the nano-emulsions 66

Chapter 5: Formulation of natural oil nano-emulsions for the topical delivery of clofazimine, artemisone and decoquinate

Table 1: Formulas for the nano-emulsion containing olive oil 98

Table 2: Formulas for the nano-emulsion containing safflower oil 99

Table 3: Physicochemical properties of nano-emulsions 100

Table 4: LDH results for the nano-emulsions containing safflower oil and olive oil separately 101

Table 5: Percentage inhibition of the formulations against *M.tb* H37Rv relative to control culture 102

Appendix A: Validation of an HPLC analytical method for analysis of clofazimine, artemisone and decoquinate

Table A.1: Mobile phase gradient used during HPLC analysis 122

Table A.2: Formula of **S1** used during HPLC sample preparation 123

Table A.3: Formula of **S2** used during HPLC sample preparation 124

Table A.4: Formula of **S3** used during HPLC sample preparation 124

Table A.5: Formula of **S4** used during HPLC sample preparation 124

Table A.6: Formula of **O1** used during HPLC sample preparation 124

Table A.7: Formula of **O2** used during HPLC sample preparation 125

Table A.8: Formula of **O3** used during HPLC sample preparation 125

Table A.9: Formula of **O4** used during HPLC sample preparation 125

Table A.10: Linearity results of CLF 127

Table A.11: Linearity results of ART 128

Table A.12: Linearity results of DQ 129

Table A.13: Accuracy results of CLF 131

Table A.14: Statistical analysis results of CLF 131

Table A.15: Accuracy results of ART 131

Table A.16: Statistical analysis results of ART 132

Table A.17: Accuracy results of DQ 132

Table A.18: Statistical analysis results of DQ 132

Table A.19: Repeatability results of CLF 133

Table A.20: Repeatability results of ART 134

Table A.21: Repeatability results of DQ 134

Table A.22: Inter-day results of CLF 135

Table A.23: Inter-day results of ART 136

Table A.24: Inter-day results of DQ 136

Table A.25: Reproducibility results of CLF 137

Table A.26: Reproducibility results of ART 137

Table A.27: Reproducibility results of DQ 137

Table A.28: Results of sample stability of CLF 138

Table A.29: Results of sample stability of ART 139

Table A.30: Results of sample stability of DQ 140

Table A.31: Results of system repeatability of CLF 141

Table A.32: Results of system repeatability of ART 142

Table A.33: Results of system repeatability of DQ 142

Appendix B: Pre-formulation, formulation and characterisation of nano-emulsions containing a natural oil and clofazimine, artemisone and decoquinate

Table B.1: Ingredients used in the study 147

Table B.2: Experimental setup and conditions for DSC analysis 149

Table B.3: Interaction heat flow results of TAM 154

Table B.4: Results of hot stage microscopy for CLF 156

Table B.5: Results of hot stage microscopy for ART 156

Table B.6: Results of hot stage microscopy for DQ 157

Table B.7: Results of hot stage microscopy for the combination of **CLF**, **ART** and **DQ** 158

Table B.8: Pre-formulation nano-emulsion API concentrations 158

Table B.9: Pre-formulation nano-emulsion formulas 159

Table B.10: Results of pH of pre-formulated nano-emulsions 161

Table B.11: Results of viscosity of pre-formulated nano-emulsions 162

Table B.12: Results of droplet sizes of pre-formulated nano-emulsions 163

Table B.13: Results of zeta-potential of pre-formulated nano-emulsions 164

Table B.14: Results of EE% of pre-formulated nano-emulsions 165

Appendix D: Cytotoxicity studies of natural oil nano-emulsions containing clofazimine, artemisone and decoquinate

Table D.1: Materials used during the *in vitro* cytotoxicity study 199

Table D.2: LDH results from the nano-emulsions containing safflower oil 203

Table D.3: LDH results from the nano-emulsions containing olive oil 203

Table D.4: Volumes of nano-emulsions used in 5 ml culture (*M.tb* H37Rv) 204

Table D.5: Percentage inhibition of the nano-emulsions relative to control culture against *M.tb* H37Rv 204

Abbreviations

ACN	Analytical grade acetonitrile
ANOVA	Analysis of variance
API	Active pharmaceutical ingredient
ART	Artemisone
ATP	Adenosine triphosphate
attB	Phage attachment site
CFU	Colony-forming units
cGMP	Current Good Manufacturing Practice
CLF	Clofazimine
$CLFH_2$	Clofazimine reduced
CTB	Cutaneous tuberculosis
CYP	Cytochrome
CYP3A4	Cytochrome 3A4
DMEM	Dulbecco's modified eagle medium
DMSO	Dimethyl sulfoxide
DQ	Decoquinate
DSC	Differential scanning calorimetry
ED	Epidermis-dermis
EDTA	Trypsin-Versene®
EE%	Entrapment efficiency
FAD	Flavin adenine dinucleotide
$FADH_2$, reduced	Flavin adenine dinucleotide
FBS	Foetal bovine serum
Fe (II)	Iron
GAST/Fe	Glycerol-alanine-salts containing iron
GFP	Green fluorescent protein

HaCaT	Immortalised human keratinocyte cells
HEE	High-energy emulsification
He-Ne	Helium - neon
HPLC	High performance liquid chromatography
HSM	Hot stage microscopy
Hyg^{50}	Hygromycin B resistance gene
ICH	International Conference on Harmonisation
KH_2PO_4	Potassium dihydrogen orthophosphate
Kollidon® VA64	Vinylpyrrolidone-vinyl acetate copolymer
LDH	Lactate dehydrogenase
LEE	Low-energy emulsification method
LOD	Limit of detection
log P	Octanol-water partition coefficient
LOQ	Limit of quantitation
MDR-TB	Multidrug-resistant tuberculosis
MEM NEAA	L-glutamine and 1% MEM non-essential amino acids
MR	Mycothiol reductase
MRC	Medical Research Council
Mtb	*Mycobacterium tuberculosis*
MTT	3-(4, 5-dimethylthiazol-2-yl)-2, 5-diphenyltetrazolium bromide)
NAD^+	Oxidised nicotinamide adenine dinucleotide
NADH	Type-II nicotinamide adenine dinucleotide
NaOH	Sodium hydroxide
NDH-2	Oxidoreductase
NRF	National Research Foundation
O	Olive oil
OD_{600}	Optical density reading taken at 600 nm)
o/w	Oil-in-water

O_2	Oxygen
O1	Olive oil nano-emulsion containing clofazimine
O2	Olive oil nano-emulsion containing artemisone
O3	Olive oil nano-emulsion containing decoquinate
O4	Olive oil nano-emulsion containing clofazimine, artemisone and decoquinate
O5	Olive oil nano-emulsion placebo
PBS	Phosphate buffer solution
PdI	Polydispersed index
Pen/Strep	Penicillin/Streptomycin
PIC	Phase inversion composition
PIT	Phase inversion temperature
PVDF	Polyvinylidene fluoride
PVP 30	Polyvinylpyrrolidone
Q	Quinone
R_2	Correlation coefficient
ROS	Reactive oxygen species
ROS/RONS	ROS/reactive oxygen-nitrogen species
RSD	Relative standard deviation
S	Safflower oil
SCE	Stratum corneum-epidermis
SD	Standard deviation
Span® 60	Sorbitan monostearate
S1	Safflower oil nano-emulsion containing clofazimine
S2	Safflower oil nano-emulsion containing artemisone
S3	Safflower oil nano-emulsion containing decoquinate
S4	Safflower oil nano-emulsion containing clofazimine, artemisone and decoquinate
S5	Safflower oil nano-emulsion placebo

TAM	Thermal activity monitor
TB	Tuberculosis
THF	Tetrahydrofuran
Tween® 20	Polysorbate 20
Tween® 80	Polysorbate 80
Tris	Tris (hydroxymethyl) aminomethane
WHO	World Health Organizations
XDR-TB	Extensively drug-resistant TB

Chapter 1:

Introduction and problem statement

1. Introduction

Tuberculosis (TB) is a very deadly and contagious disease that is primarily caused by airborne *Mycobacterium tuberculosis,* but *Mycobacterium bovis* and *Mycobacterium africanum* (Cataldi & Romano, 2007:283-314; Ducati, 2006:697-714) can also cause it. TB primarily affects the lungs through the *M. tuberculosis and M. bovis* bacteria, but it can also manifest in other areas of the body, such as the skin, in which case it is referred to as cutaneous TB (CTB) (Ramarao *et al.,* 2012:378). TB only manifests in about 8.4 – 13.7% cases as an extra-pulmonary disease, of which CTB only consists of a small prevalence of 1 – 2% (Ilgazli *et al*., 2004:435; Wyrzykowska *et al*., 2012:293; Zouhair *et al*., 2007:209). Nevertheless, when the high incidence of TB in many developing countries is taken into account, these numbers can become significant (Bravo & Gotuzzo, 2007:173). Because CTB is usually unsightly, it significantly impacts the patient's social and emotional wellbeing. The biggest shortcoming is that no topical treatment has yet been developed for CTB, since no complete effectiveness has yet been achieved, despite current oral regimens showing good promise (Van Zyl *et al*., 2014:2). Although future topical therapy alone will not be used to substitute any systemic treatment; different active pharmaceutical ingredients (APIs), i.e. clofazimine (CLF), artemisone (ART) and decoquinate (DQ) will be investigated during this study, which formed part of the Medical Research Council (MRC) flagship program: MALTB:Redox, for the possible promotion of future topical CTB treatments.

The human skin consists of three main layers, i.e the epidermis, the dermis and the subcutaneous fatty layer (the hypodermis) (Potts *et al.,* 1992:14). Transdermal drug delivery comprises of permeation through the lipophilic stratum corneum, then through the hydrophilic epidermal and dermal layers, before reaching the capillaries of the human body (Perrie *et al*., 2012:392). APIs must therefore have both hydrophilic and lipophilic physicochemical qualities in order to permeate from the formulation into the skin, where they will accumulate. In order to permeate into and through the skin, an API should preferably possess the following physicochemical properties: a) log P (octanol-water partition coefficient) should be between 1

and 3 (Mbah *et al*., 2011:681), b) aqueous solubility should be above 1 mg/ml and c) the molecular weight should be below 500 Da (Naik *et al.,* 2000:319).

CLF is a poorly water soluble (10 mg/l) redox compound with a log D (octanol-buffer distribution coefficient) of 7.6 (US Pharmacopeia online, 2014), having anti-inflammatory (Cholo *et al.,* 2011:293) and dye properties (Anderson, 1983:139-144). CLF has a lipophilic character, which enables it to accumulate in the skin and among the nerves (Dutta, 1980:252-259; Imkamp, 1973:127-130; Imkamp, 1981:135-140). CLF shows *in vitro* activity against multidrug-resistant TB (MDR-TB), however the problem arises where it crystallises out of the macrophage. It can be used for treatment in TB patients who cannot tolerate the adverse effects of other drugs (Lu *et al*., 2011:5183). It acts as a substrate for the flavoenzyme *M. tuberculosis* Type-II nicotinamide adenine dinucleotide (NADH)-quinone (Q) oxidoreductase (NDH-2), which is a critical respiratory enzyme. It also oxidises hydroquinone form of flavin adenine dinucleotide ($FADH_2$, reduced) to flavin adenine dinucleotide (FAD) to generate reduced CLF ($CLFH_2$). $CLFH_2$ is then oxidised by oxygen (O_2) to produce CLF and reactive oxygen species (ROS). In each reaction cycle, CLF consumes $FADH_2$ and O_2, as well as produce ROS. It also enhances the NADH production (Haynes & Tang, 2012). The primary site of action of CLF is the outer skin membrane. When CLF is added to the organism's membrane in the presence of potassium cyanide (being a terminal cytochrome (CYP) respiratory chain inhibitor) and NADH (being an oxidisable co-factor); an oxidation and reduction action of CLF occurs, which produces super-oxides and hydrogen peroxide, better known as anti-microbial ROS. Bacterial death is therefore caused by ROS, as they interfere with adenosine triphosphate (ATP) production (Cholo *et al.,* 2011:293).

ART is a relatively new, semi-synthetic, 10-alkylaminoartemisinin that can be synthesised in a one-step process from dihydroartemisinin (Haynes *et al.*, 2004:1381-1385). ART with a log D of 2.49 (Dunay *et al*., 2009:4451) and aqueous solubility of 89 mg/l (Steyn *et al.,* 2011:261) shows no neurotoxicity, increased anti-plasmodial activity or metabolic stability (Von Keutz *et al.*, 2005:28). ART is active against all red blood cell stages of *Plasmodium falciparum* and demonstrates limited resistance. Three metabolites (M1, M2 and M3), obtained primarily from being metabolised by cytochrome 3A4 (CYP3A4) in the liver, possess intrinsic anti-malarial activity (Nagelschmitz *et al.,* 2008:3090) and due to their short half-lives, they should be used in combination with other APIs (Steyn *et al.,* 2011:260). Through cleavage of the peroxide bond by iron (Fe (II)), found in the heme proteins (Biamonte *et al.,* 2013:2831); toxic oxygen radicals are thought to be generated and as a result, this oxidant activity is important for ART to enhance activity against TB by accelerating the cycling of redox APIs (Haynes, 2013:7).

The third drug which will be added is DQ (quinolone) and has a different mechanism of action, which suppresses the selection for resistant pathogen strains and is this case amplifies the effect for the oxidative stress. DQ is however very lipophilic with a log D of 8.07 (Chembase, 2014) and should therefore be evaluated with lipophilic dosage preparations; since there is a problem with solubility in culture medium (dimethyl sulfoxide (DMSO)) (Haynes, 2015). DQ is an approved veterinary drug and has to date only been tested on animals and there is no available literature on aqueous solubility. The 4-hydroxy quinolone has demonstrated possible anti-TB activity, due to its high lipophilicity (Biamonte *et al.,* 2013:2838).

The rationale behind the combination of APIs is that the oxidant drug (ART) destroys reduced deazaflavin, which generates a pulse of ROS/RONS (reactive oxygen nitrogen species). It can also divert electron supply from the nicotinamide adenine dinucleotide phosphate (NADPH), which causes a cytotoxic effect. The redox drug (CLF), scavenges electron supply from NADPH and therefore enhances the oxidative stress, which is caused by the oxidant drug which also causes a cytotoxic effect. Therefore, the redox drug will amplify the oxidation drugs' mechanism (Haynes, 2013:7).

Taking the three aforementioned API`s into account it is indicated that ART is an ideal candidate for topical delivery, whilst CLF and DQ are expected to pose potential challenges towards achieving successful skin transport. To overcome the barrier properties of the skin, penetration enhancers may be used to facilitate drugs across the skin. Nano-emulsions, containing natural oils, were chosen as carriers for this study. The available literature suggests that the delivery of both lipophilic and hydrophilic compounds could be promoted by using fatty acids (Williams & Barry, 2012:132) such as olive- and safflower oil, as they contain linoleic acid (C_{18} fatty acid) (Vermaak *et al.*, 2011:920-933). Since linoleic acid is naturally found in human skin, they are expected to be less harmful, or irritating to the skin, than other available penetration enhancers (Dingler & Gohla, 2002:11-16).

Nano-emulsions have been chosen as the drug delivery system as it has been successfully implemented to improve the transport of hydrophobic compounds (Shakeel *et al*., 2012:953-973) and will therefore further enhance drug penetration (Chime *et al.,* 2014). Nano-emulsions have numerous advantages over other micro-counterparts, such as liposomes, micro-emulsions, niosomes and nano-particles, as they offer exceptional solubilisation ability to drugs. They have small droplet sizes with higher entrapment efficiencies and they offer ease of preparation, optical clarity and stability, which all contribute to them being attractive candidates for drug vectorisation (Chime *et al.,* 2014).

The research problem of this study is that 1) currently no topical preparation is available for CTB and 2) the APIs (CLF, ART and DQ) do not possess the ideal required physicochemical properties to penetrate the target site (epidermis-dermis (ED)).

The aim of this study is to investigate whether nano-emulsions containing natural oils would improve the topical delivery of CLF, DQ and ART, separately and in combination. Two natural oils will be examined, i.e. safflower- and olive oil and thus eight nano-emulsions will therefore be formulated, i.e. nano-emulsions containing safflower oil and CLF (**S1**), safflower oil and ART (**S2**), safflower oil and DQ (**S3**), olive oil and CLF (**O1**), olive oil and ART (**O2**) olive oil and DQ (**O3**), as well as the combinations of safflower oil with CLF, ART and DQ (**S4**) and olive oil with CLF, ART and DQ (**O4**). The compatibility of the three APIs will be tested with each other as well as with the different oils. The dermal toxicity will be investigated on the different constituents of the dispersions (i.e. APIs itself, natural oils and the nano-emulsions without API as well as the nano-emulsions combined with the API). The nano-emulsions containing any of the three different APIs separately or in single formulation (combination of all three APIs), will be chosen for *in vitro* cell culture studies against *M. tuberculosis* for further investigation regarding their potential use in the future treatment of CTB. *In vitro* studies of the nano-emulsions will be tested on inoculated, freeze-dried bacterial cells with and without APIs to ensure that cell death is not caused by the natural oils or the API itself.

Objectives of the study include the following:

- Develop and validate a high performance liquid chromatography (HPLC) analytical method to determine the concentration of CLF, DQ and ART, separately and in combination, in the test samples generated during this study.
- Determine the aqueous solubility, solubility in different solvents and log D values of CLF, DQ and ART.
- Testing drug with drug compatibilities by using the differential scanning calorimetry (DSC).
- Testing oil with drug compatibilities by using microcalorimetry.
- Formulate nano-emulsions containing CLF, DQ and ART, separately and in combination, by using safflower- and olive oil as the oil phase in the nano-emulsions.
- Determine *in vitro* efficacy on tuberculous bacterial cells of the entrapped APIs in the nano-emulsions containing safflower- and olive oil separately with any of the three different APIs, separately or in combination.

- Characterise (viscosity, zeta-potential, pH, droplet size, pH, morphology and drug entrapment efficiency) the nano-emulsions with and without the APIs.
- Conduct membrane release studies to establish whether the APIs are released from the different nano-emulsions.
- Determine the transdermal and topical delivery of the APIs from the nano-emulsions by performing diffusion studies followed by tape stripping, respectively.
- Conduct cell culture studies to determine the cytotoxic effects of the API(s), the oils, as well as the nano-emulsions on dermal fibroblast cells and on immortal human keratinocyte cell line (HaCaT) cells.

References

Anderson, R. 1983. The immunopharmacology of antileprosy agents. *Leprosy Review*, 54:139-44.

Biamonte, M.A., Wanner, J. & Le Roch, K.G. 2013. Recent advances in malaria drug discovery. *Bioorganic and Medicinal Chemistry Letters,* 23(10):2829-2843.

Bravo FG, & Gotuzzo E. 2007. Cutaneous tuberculosis. *Clinics in Dermatology*, 25(2):173-180.

Cataldi, A. & Romano, M.I. 2007. Tuberculosis caused by other members of the *M. tuberculosis* complex. (*In* Palomino, J.C., Lea˜o, S.C. & Ritacco, V., *eds*. Tuberculosis: from basic science to patient care. BourcillierKamps.com, p. 283-314.)

Chembase. 2014. http://en.chembase.cn/molecule-157442.html Date of access: 5 Aug 2015.

Chime, S.A., Kenechukwu, F.C. & Attama, A.A. 2014. Nanoemulsions — Advances in Formulation, Characterization and Applications in Drug Delivery, Application of Nanotechnology in Drug Delivery, http://www.intechopen.com/books/application-of-nanotechnology-in-drug-delivery/nanoemulsions-advances-in-formulation-characterization-and-applications-in-drug-delivery Date of access: 1 Mar 2015.

Cholo, M.C., Steel, H.C., Fourie, P.B., Germizhuizen, W.A. & Anderson, R. 2011. Clofazimine: current status and future prospects. *Journal of Antimicrobial Chemotherapy,* 67(2):290-298.

Dingler, A. & Gohla, S. 2002. Production of solid lipid nanoparticles (SLN): scaling up feasibilities. *Microencapsulation*, 19:11-16.

Ducati, R.G. 2006. The resumption of consumption: a review on tuberculosis. *The Memórias do Instituto Oswaldo Cruz,* 101:697-714.

Dunay, I.R., Chi Chan, W., Haynes, R.K. & Sibley, L.D. 2009. Artemisone and artemiside control acute and reactivated toxoplasmosis in a murine model. *Journal of Antimicrobial Agents and Chemotherapy,* 53(10):4450-4456.

Dutta, R.K. 1980. Clofazimine and dapsone: a combination therapy in erythema nodosum leprosum syndrome. *Leprosy India*, 52:252-259.

Haynes, R.K., Ho, W.Y., Chan, H.W. 2004. Highly antimalaria-active artemisinin derivatives: biological activity does not correlate with chemical reactivity. *Angewandte Chemie International Edition*, 43:1381-1385.

Haynes, R.K. & Tang, M.M.K.-T. Unpublished; M.M.K.-T. Tang, Ph.D. Thesis, The Hong Kong University of Science and Technology, 2012.

Haynes, R.K. 2013. MRC South African university flagship projects: project proposal: development to the clinical phase of oxidant and redox drug combinations for treatment of malaria: TB and related diseases. 21p.

Haynes, R.K., Wong, H., Guo, Z., Coghi, P. & Monti, D. 2014. Oxidant and Redox Drugs: Potential for Treatment of Malaria, TB and Other Diseases. Symposium on Chemico- and Biomedicinal Research, Rhodes University, Grahamstown, 27 Oct 2014.

Haynes, R.K. 2015. Development of Oxidant and Redox Drug Combinations for Treatment of Malaria, TB and Related Diseases. MRC/SAU Flagship project.

Ilgazli, A., Boyaci, H., Basyigit, I. & Yildiz, F. 2004. Extrapulmonary tuberculosis: clinical and epidemiologic spectrum of 636 cases. *Archives of Medical Research*, 35(5):435-441.

Imkamp, F.M. 1973. The treatment of corticosteroid-dependent lepromatous patients in persistent erythema nodosum leprosum with clofazimine. *Leprosy Review*, 44:127-130.

Imkamp, F.M. 1981. Clofazimine (lamprene or B663) in lepra reactions? *Leprosy Review,* 52:135-40.

Lu, Y., Zheng, M., Wang, B., Fu, L., Zhao, W., Li, P., Xu, J., Zhu, H., Jin, H., Yin, D., Huang, H., Upton, A.M. & Ma, Z. 2011. Clofazimine Analogs with Efficacy against Experimental Tuberculosis and Reduced Potential for Accumulation. *Antimicrobial Agents and Chemotherapy,* 55: 5183-5193.

Mbah, C.J., Uzor, P.F. & Omeje, E.O. 2011. Perspectives on Transdermal Drug Delivery. *Journal of Chemical and Pharmaceutical Research,* 3(3):680-700.

Naik, A., Kalia, Y.N. & Guy, R.H. 2000. Transdermal drug delivery: overcoming the skin's barrier function. *Pharmaceutical Science and Technology Today,* 3(9):318-326.

Nagelschmitz, J., Voith, B., Wensing, G., Roemer, A., Fugmann, B., Haynes, R.K., Kotecka, B.M., Rieckmann, K.H. & Edstein, M.D. 2008. First assessment in humans of the safety,

tolerability, pharmacokinetics, and *ex vivo* pharmacodynamic antimalarial activity of the new artemisinin derivative artemisone. *Antimicrobial Agents and Chemotherapy,* 52(9):3085-3091.

Perrie, Y., Badhan, R.J.K., Kirby, D.J., Lowry, D., Mohammed, A.R. & Ouyang, D. 2012. The impact of ageing on the barriers to drug delivery. *Journal of Controlled Release,* 161:392-393.

Potts, R.O., Bommannan, D.B. & Guy, R.H. 1992. Percutaneous absorption. (*In* Mukhtar, H., *ed*. Pharmacology of the skin. Florida: CRC Press. p. 22.)

Pharmacopeia online. 2014. http://www.usp.org/pdf/EN/referenceStandards/msds/1138904.pdf Date of access: 1 Mar 2015.

Ramarao, S., Greene, J.N., Casanas, B.C., Carrington, M.L., Rice, J. & Kass, J. 2012. Cutaneous Manifestations of Tuberculosis. *Infectious Diseases in Clinical Practice*, 20(6):376-383.

Shakeel, F., Shafiq, S., Haq, N., Alanzi, F.K. & Alsarra, I.A. 2012. Nanoemulsions as potential vehicles for transdermal and dermal delivery of hydrophobic compounds: an overview. *Expert Opinion on Drug Delivery*, 9(8):953-974.

Steyn, J.D., Wiesner, L., Du Plessis, L.H., Grobler, A.F., Smith, P.J., Chan, W.C., Haynes, R.K. & Kotze, A.F. 2011. Absorption of the novel artemisinin derivatives, artemisone and artemiside: potential application of Pheroid™ technology. *International Journal of Pharmaceutics,* 414(1-2):260-266.

Van Zyl, L., Du Plessis, J. & Viljoen, J. 2015. Cutaneous tuberculosis overview and current treatment regimens. *Tuberculosis,* 95:629-638.

Vermaak, I., Kamatou, G.P.P., Komane-Mofokeng, B., Viljoen, A.M. & Beckett, K. 2011. African seed oils of commercial importance: cosmetic applications. *South African Journal of Botany*, 77:920-933.

Von Keutz, E., Schmuck, G. & Haynes, R. 2005. Artemifone, a new antimalarial artemisinin derivative: lack of neurotoxicity. (*In* Abstracts of Medicine and Health in the Tropics Congress, Marseille, France, Abstract no. O-004, p. 28.)

Williams, A.C. & Barry, B.W. 2012. Penetration enhancers. *Advanced Drug Delivery Reviews*, 64:128-137.

Wyrzykowska, N., Wyrzykowski, M., Zaba, R. & Silny, W. 2012. Treatment of cutaneous infections caused by *Mycobacterium tuberculosis*. *Advances in Dermatology and Allergology*, 29(4):293-298.

Zouhair, K., Akhdari, N., Nejjam, F., Ouazzani, T. & Lakhdar, H. 2007. Cutaneous tuberculosis in Morocco. *International Journal of Infectious Diseases,* 11(3):209-212.

Chapter 2:

Article published in "Current Drug Delivery"

Chapter 2 is presented in the form of a review article and was published in the journal "Current Drug Delivery".

Send Orders for Reprints to reprints@benthamscience.ae

Current Drug Delivery, 2017, *14*, 458-472

REVIEW ARTICLE

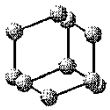

BENTHAM SCIENCE

Traversing the Skin Barrier with Nano-emulsions

Cornel Burger[1], Yasser Shahzad[2], Alicia Brümmer[1], Minja Gerber[1,*] and Jeanetta du Plessis[1]

[1]*Centre of Excellence for Pharmaceutical Sciences, North-West University, Private Bag X6001, Potchefstroom 2520, South Africa;* [2]*Faculty of Pharmacy, University of Central Punjab, Lahore 54000, Pakistan*

ARTICLE HISTORY

Received: April 23, 2016
Revised: July 27, 2016
Accepted: August 12, 2016

DOI:
10.2174/1567201813666160824125444

Abstract: ***Background***: In recent years, colloidal delivery systems based on nano-emulsion are gaining popularity; being used for encapsulation and delivery of many drugs. This review therefore aims at summarizing various methods of nano-emulsion formulation and their use as a topical and transdermal delivery vehicle for a number of active pharmaceutical ingredients from different pharmacological classes.

Methods: This article represents a systematic review of nano-emulsions for topical and transdermal drug delivery. A vast literature was searched and critically analysed.

Results: Nano-emulsions are thermokinetically stable dispersion systems, which have been used in topical and transdermal delivery of a number of pharmaceutically active compounds. Nano-emulsions have a narrow droplet size range with tuneable surface properties, which make them an ideal delivery vehicle. Nano-emulsions have a number of advantages over conventional emulsions, including easy preparation using various low and high energy methods, optical transparency, high solubilisation capacity, high stability to droplet aggregation and the ability to penetrate the skin; thus allowing the transdermal delivery of drugs.

Conclusion: This review indicated that nano-emulsions are promising vehicle for entrapping various drugs and are suitable for traversing the skin barrier for systemic effects.

Keywords: Emulsification, micro-emulsions, nano-emulsions, skin permeation, topical drug delivery, transdermal drug delivery.

1. INTRODUCTION

The skin has historically been used for the topical delivery of compounds since ancient Egyptian and Babylonian times [1]. However, the quest for understanding skin and its barrier properties was initiated in the 1800s. Many masters in this field have contributed tremendously in revealing the unseen and the unknown facts about the nature of the skin, and unfolded the concepts about the exact location of the skin barrier that is now established to limit the ingress of foreign entities and escape of water from the body. These investigations not only increased our fundamental understandings of the skin, but also the complexity of the skin's structure has become far more evident. It was the pioneering efforts of Blank, Scheuplein and co-workers that involved physical chemistry by applying Fick's laws of diffusion to explore the permeability of the skin [2-4], which later helped in the development of the first transdermal patch in 1978.

Whilst the skin has remained an area of great focus for years, and despite the ever increasing understanding of the skin's barrier properties, this area has yet to be explored to its full potential. The beauty of the skin is that it is impermeable for most compounds. The stratum corneum (SC), a unique biomembrane, which has been identified as the main hurdle in diffusion of compounds into and through the skin, is 15-20 μm thick and has excellent control over the absorption of chemicals [5, 6]. For a detailed morphology of the SC, readers are encouraged to read through recent publications authored by Iwai *et al.* [7] and Norlén [8].

When the traditional routes are not feasible because of the hepatic metabolism, patient inconvenience and pain associated with the injections; alternative routes are sought [9]. Skin has now been accepted as a potential alternative route for local and systemic delivery of some drugs. The development of transdermal drug delivery systems has enabled the sustained release of drugs with short biological half-lives; thus frequent dosing associated with the oral route can be avoided. Nevertheless, oral administration should be the delivery route of choice for the drugs with higher bioavailability and infrequent dosing that are well accepted by the patients. Success of dermal and transdermal delivery systems relies on the effective breaching of the SC, so that drugs can enter the skin or even pass through it for their systemic effects. Perhaps breaching this barrier has remained a major challenge for researchers over the years. There are certain physicochemical constraints associated with the drugs that can effectively pass through the skin barrier. For instance, transdermal candidates must have a molecular weight less than 500 Da, and the lipophilicity should be between one and three log values. Most importantly, candidates should be pharmacologically potent, requiring a low therapeutic dose (< 10 mg), and the therapeutic plasma concentration should be in the $ng.mL^{-1}$ range or less [6].

The efficiency of the SC can be effectively compromised by the use of physical and chemical methods of penetration

*Address correspondence to this author at the Centre of Excellence for Pharmaceutical Sciences, North-West University, Private Bag X6001, Potchefstroom 2520, South Africa; Tel: +2718 299 2328; Fax: +2787 231 5432; E-mail: Minja.Gerber@nwu.ac.za

Cornel Burger and Yasser Shahzad are Co-First Author.

1875-5704/17 $58.00+.00

© 2017 Bentham Science Publishers

enhancement [10]. Physical methods include the use of different sources of energy such as electrical, thermal, acoustic, or microneedles. On the other hand, chemical methods include the use of chemicals as permeation enhancers or as a delivery vehicle that can penetrate into the skin and consequently deliver the drug deeper in the skin layers. Recently, nanotechnology has proven to be effective in dermal and transdermal drug delivery. Specifically, nano-emulsions (NEs) have shown promise as a delivery vehicle for many hydrophilic and lipophilic drugs. NEs have shown endless opportunities as carrier systems with practical applications for pharmaceutical, cosmetic, chemical and food industry [11-14]. The success of NE as a carrier has led to the introduction of a number of drug-loaded NE based dosage forms in the pharmaceutical market. Most of the marketed products are recommended either for topical or oral administration. However, transdermal delivery of drugs using NE is limited because of the barrier properties of the skin. Recently, considerable efforts have been made in elucidating the transdermal fate of drugs when encapsulated in NEs. Therefore, this review article focuses on NEs for the delivery of drugs into and through the skin.

2. NANO-EMULSIONS VS MICRO-EMULSIONS

NEs, also known as colloidal dispersions, are fabricated by dispersing oil in an aqueous phase, stabilised by surfactants with or without the use of co-surfactants. NEs are thermokinetically stable dispersions, and the droplets are typically in the size range of up to 250 nm [15]. However, various literatures stated sizes that vary from 20 to 500 nm, typically in the range of 200-300 nm [16] and have been established on the basis of optical properties and on the intended use [17]. These oil droplets can exist as oil-in-water (o/w) or water-in-oil (w/o) form, where the main dispersion medium is water or oil, respectively. Bicontinuous is where water and oil are inter-dispersed within the nanosystem [18]. NEs have several advantages over other nano-counterparts, *i.e.* micro-emulsions, liposomes, niosomes, nanoparticles; for instance, NEs offer excellent solubilisation capacity for drugs, small droplet size with higher entrapment efficiency, ease of preparation, optical clarity and stability, thus making them attractive candidates for drug vectorisation [19]. Micro-emulsions are also nanosized colloidal dispersions similar to NEs, however, there have been misperceptions in the classification of colloidal dispersions and micro-emulsions that are often confused with NEs in the vast available scientific reports. The basic difference in both colloidal systems is that micro-emulsions are thermodynamically stable, whilst NEs are thermokinetically stable [15]. A NE is a thermodynamic unstable system that will breakdown over time at a rate that depends on the high energy barrier (Gibb's free energy) between NEs and the separated states [20]. There are also some methodological and structural dissimilarities. Micro-emulsions are formed spontaneously or with a minimum energy input upon addition of a higher percentage of surfactants to the oil and water phases. On the other hand, NEs usually require high energy input for emulsification with a lesser amount of surfactants [15].

3. FORMULATION APPROACHES

NEs can be formulated using a variety of approaches, commonly classified as low and high energy emulsification (HEE) methods. This section provides a brief description of methods that are routinely used to formulate NEs.

3.1. Low Energy Emulsification Methods

Low energy emulsification (LEE) methods make use of the internal chemical energy of the system, thus requiring simple stirring to produce NEs with a small droplet size [21]. LEE methods include spontaneous emulsification, phase inversion temperature (PIT) and phase inversion composition (PIC).

3.1.1. Spontaneous Emulsification

Spontaneous emulsification, also known as the self-emulsification, is the rapid diffusion of surfactant and/or solvent molecules from the dispersed phase to the continuous phase. This process operates without any change in the spontaneous curvature of the surfactant [17].

Generally, a dispersed phase is diluted with a continuous phase at a constant pressure without any phase transition. Afterwards diffusion occurs quickly, and the turbulence generated, it breaks down the larger droplets into nanosize, thus giving rise to NE [17]. NE formulation by self-emulsification was first reported by Taylor & Ottewill [22] using o/w micro-emulsion as a starting point and diluting it with alcohol until the micro-emulsion become thermodynamically unstable and transformed into a NE. Self-emulsification can be divided in two processes. The first process requires an o/w micro-emulsion as a start-up feed for emulsification. This process results in a NE with a small droplet size, independent on the dilution process and feed composition. In contrast, the second process requires a w/o micro-emulsion as a start-up feed and the process is dependent on both the micro-emulsion composition and the type of dilution.

Micro-emulsions with a low oil-to-surfactant ratio rapidly separate into two phases, which causes a turbid emulsion, independent of the dilution procedure adopted. Higher oil-to-surfactant ratio in w/o micro-emulsion would produce small sized droplets upon stepwise dilution, thus leading to an o/w NE when equilibrium ensues. This process can be seen as a two-step strategy for emulsification; the first step is adding water, which results in a change in the surfactant spontaneous curvature, whilst the second step involves the self-emulsification process without inducing any change in the surfactant spontaneous curvature [23].

Sole *et al.* [23] demonstrated that by selecting a suitable composition and dilution procedure, NE of similar droplet size can be obtained from both o/w and w/o micro-emulsions. This study refuted some of the previous claims that diluting a w/o micro-emulsion would produce NE with large droplet size [24].

3.1.2. Phase Inversion Temperature

Phase inversion methods make use of chemical energy released as a result of phase transitions; leading to changes in the surfactant spontaneous curvature during the emulsification process. Such phase transitions can be triggered either by changing the composition (PIC) or by changing the temperature (PIT) [17]. In order to obtain a NE with a low polydispersity index (PDI) and in nanosized range, a judicious choice of oil and surfactant is required.

Shinoda introduced the PIT method in 1968 [25], which explains that when temperature changes, there is a change in the surfactant's spontaneous curvature. The PIT procedure for NE formulation comprised of preparing the sample at a suitable hydrophilic-lipophilic balance (HLB) [26], since extremely low interfacial tension (10^{-2}-10^{-5} $mN.m^{-1}$) is required in order to achieve small droplet sized NE [27]. Thus, at a cross point of zero curvature and minimal interfacial tension, finely dispersed NEs are formed [28], which are very unstable since the droplets are extremely small at the HLB temperature. In order to obtain thermokinetically stable NE; the HLB temperature should be cooled or heated quickly (obtaining w/o or o/w emulsions, respectively), otherwise a polydispersed NE would form [29]. For heat labile drugs, the PIT method is not advisable.

3.1.3. Phase Inversion Composition

Instead, phase transitions are brought about by the PIC method, at a constant temperature during the emulsification process. The PIC method of obtaining NEs consists of stepwise addition of one component (water or oil) in a mixture of either oil-surfactant or water-surfactant, respectively [30]. However, the PIT method is considered more efficient than the PIC to obtain narrow size distributions and small droplets [31].

3.2. High Energy Emulsification

HEE methods operate by producing intensely disruptive forces to form NEs using mechanical devices, *i.e.* microfluidizers [32], high-pressure homogenisers and ultrasonicators [33]. The formation of nanosized droplets will depend on the type of mechanical device used and their processing attributes, such as the number of operating cycles, time, and temperature, along with formulation composition [34].

3.2.1. Microfluidization Method

Microfluidization technique involves the use of a microfluidizer device coupled with a high-pressure displacement pump (500-20000 psi). This device contains many microchannels which lets the materials pass through under extreme pressure on to an impingement area, thus resulting in conversion of larger droplets into nanosized scale. The aqueous and oil phases form a coarse emulsion with the in-line homogeniser. The coarse emulsion is then cycled again through the microfluidizer to form a fine NE. The desired particle size can be obtained by repeating the operating cycles, and is thereafter filtered under nitrogen to remove unwanted larger droplets [35].

3.2.2. High Pressure Homogenisation Method

High pressure homogenisation involves applying very high pressure to the aqueous and oil phases as well as to the surfactant with the help of a homogeniser. The process begins by micro-particles that enter the valve at low velocity. The positive-displacement pump generates the pressure and several forces such as hydraulic shear, intense turbulence and cavitation forces act simultaneously to yield NEs with extremely small droplet sizes [34, 36].

3.2.3. Ultrasonication Method

Ultrasonication method involves the use of ultrasonic energy, which produces cavitation forces on the coarse emulsion; thus resulting in disruption of the larger particles into nano-scaled droplets. This process uses two mechanisms; 1)

Table 1. Physicochemical characterisation of nano-emulsions.

Characteristics	Description	Influenced by
Particle size and PDI	Size and PDI of NEs are routinely characterised by photon correlation spectroscopy (PCS). Typically, PCS gives the hydrodynamic radius of the oil droplets based on the light scattering from droplets in random Brownian motion. PCS is a simple and a popular method for average droplet size analysis. NEs generally have a size range of 20-200 nm [60].	Either system composition or preparation conditions [55], surfactant type, surfactant-oil-water ratio, ionic strength, stirring speeds and temperature-time history [39].
Surface charge	NE surface charge is expressed in zeta-potential and the charge depends on surface active agents and the counter-ion concentration. Hence, the zeta-potential value should be more than 30 mV (positive or negative), which indicates a stable system [28]. Surface charge also dictates stability of a suspension through electrostatic interactions.	Adsorption of ionised emulsifiers, biopolymers or mineral ions on the droplet surface [39].
Stability	Stability is an important criterion that defines shelf-life of a formulation. NEs are metastable and have a clear/turbid appearance, [40] and a surface to mass ratio of 70-330 $m^2.g^{-1}$ [41].	Surfactant and oil type, surfactant-oil-water ratio, ionic strength, stirring speed and temperature-time history [39].
Morphology	Transmission electron microscopy (TEM) is a popular method for morphology assessment of the oil droplets in NEs. A typical NE is incapable of generating sufficient contrast, and thus, a negative staining method is typically used where the sample on the copper grid is further exposed to phosphotungstic acid or its salt or uranyl acetate [42]. TEM has also been used for accurate droplet size measurements.	Surfactant and oil type, surfactant-oil-water ratio, ionic strength, stirring speed.
Viscosity	Determines the flow behaviour of NEs low viscosity [61].	Requires lower surfactant concentration for formation [43].
Optical properties	Translucent or transparent systems which are kinetically stable [57].	Types of emulsions are fairly great due to their droplet sizes [57].
pH	Should be in the range of 3 to 8 [101].	Zeta-potential and ionisation changes with a change in pH [99].

interfacial waves that are produced by the use of an acoustic field, which then becomes unstable resulting in the eruption of the oil phase within the aqueous phase, therefore forming droplets and 2) low frequency ultrasound is applied which causes acoustic cavitation (forming and collapsing micro-bubbles by the pressure fluctuations of simple sound waves). When there is an implosion on a microscopic scale, extreme levels of highly localised turbulence are produced. These turbulent micro-implosions are very effective in breaking the primary droplets into sub-micron sized droplets [37].

Although HEE methods can produce NEs of desired attributes, they may not be suitable for heat sensitive drugs [38].

4. CHARACTERISATION OF NANO-EMULSIONS

Characterisation of NEs is very important in order to predict their performance in pre-clinical and clinical settings. Physicochemical properties such as stability, rheology, optical properties and release characteristics are mainly determined by the droplet characteristics (size distribution, interfacial properties, composition, entrapment efficiency and physical state) [39]. Various physicochemical characteristics have been discussed in detail in a previous publication [34], therefore, a summary has been presented in Table 1.

5. NANO-EMULSIONS AS TOPICAL/TRANSDERMAL VEHICLE

NEs in transdermal drug delivery offers steady-state controlled drug delivery over a certain period of time and also the advantage of self-administration, with a pleasant skin feel [40]. Drug diffusion therefore depends on the route of diffusion as well as physicochemical properties. Three routes are usually followed for drug penetration through the skin namely transcellular, intercellular and appendageal [44]. Nanosized oil droplets can pass through the pores without difficulty, due to the hydrophilic and hydrophobic properties of the NEs, which in turn can penetrate through both the hydrophobic SC as well as hydrophilic skin layers. Studies show that NE decreased the activation energy, indicating the disruption of the SC lipids, therefore showing that enhancement of skin permeation is possible [45]. Due to NEs small droplet size, they have a large surface area and have easy transport abilities [46]. NEs' small droplet sizes favour better targeting and drug absorption [47].

It was found that positively charged NEs penetrate better than negatively charged NEs; since positively charged NEs interact better with the negative charge present on the skin [48]. The PDI and droplet size of NEs decrease with an increase in surfactant concentration, which in turn lead to a decrease in interfacial tension with an increase in interfacial area [49]. Since NEs have the capability of solubilising a large proportion of hydrophobic drugs, they can enhance both, the permeation and the bioavailability [50].

Studies have confirmed that NE formulations show improved dermal and transdermal properties for both *in vitro* and *in vivo* studies (Table 2). Literature suggests that NEs can easily penetrate skin pores, thereby delivering the drugs deeper in the skin tissue, which results in the effective delivery of active pharmaceutical ingredients (APIs). Thus, NEs show enhanced transdermal penetration of APIs compared to gels and conventional emulsions [51-54]. Various drug classes along with the formulation composition and brief outcomes that have been used for topical and transdermal drug delivery by using NEs as a delivery vehicle are summarised in Table 2 [55-97].

Table 2. NEs containing various APIs used in topical and transdermal delivery.

Class of Drugs	API	Composition	Type of NE	Formulation Method	Droplet Size	Skin Model	Brief Outcome	Ref.
NSAIDs	Capsaicin	**Oil:** Oleoresin capsicum **Surfactants:** Tween®-80; Span®-80	o/w	High pressure homogenisation	20-65 nm	Strat-M synthetic membranes	Development of capsaicin-loaded NEs for anti-inflammatory and improved skin permeation effects	[55]
	Celecoxib	**Oil:** Sefsol®-218 and Triacetin (1:1) **Surfactant:** Cremophor®-EL **Co-surfactant:** Transcutol-P	o/w	Spontaneous emulsification	15-31 nm	Full thickness rat abdominal skin	Significant increase in permeation parameters compared with gel formulations	[56]
		Oil: Sefsol®-218 and Triacetin (1:1) **Surfactant:** Tween®-80 **Co-surfactant:** Transcutol-P	o/w	Spontaneous emulsification	34-86 nm	Full thickness rat abdominal skin	Significant enhancement of anti-inflammatory effects	[57]
	Etoricoxib	**Oil:** Triacetin **Surfactant:** Cremophor® RH 40 **Co-surfactant:** Transcutol® P	o/w	Spontaneous emulsification	50-90 nm	Porcine abdominal skin	Significant inhibition of inflammation using NE compared with conventional gel formulations	[58]
	Indomethacin	**Oil:** Lemon oil **Surfactant:** Tween®-20 **Co-surfactant:** Propylene glycol	o/w	Spontaneous emulsification	30-140 nm	Full thickness abdominal skin	Development of NEs for improved transdermal delivery of indomethacin	[59]

(Table 2) Contd...

Class of Drugs	API	Composition	Type of NE	Formulation Method	Droplet Size	Skin Model	Brief Outcome	Ref.
		Oil: Labrafil® M1944CS **Surfactant:** Tween®- 80 **Co-surfactant:** Transcutol® HP	o/w	Spontaneous emulsification	25-35 nm	Male Wistar rats	Significant inhibition of inflammation using NE compared with marketed gel formulations	[60]
		Oil: Labrafil M1944 CS **Surfactant:** Tween®-80 **Co-surfactant:** Transcutol®-HP	o/w	Spontaneous emulsification	25-73 nm	Rat abdominal skin	Development of indomethacin NE for transdermal drug delivery	[45]
	Piroxicam	**Oil:** Oleic acid **Surfactant:** Tween®-80 **Co-surfactant:** Ethanol	o/w	Spontaneous emulsification	120-150 nm	Full thickness Wistar rat abdominal skin	Development of NEs for transdermal delivery of piroxicam	[61]
		Oil: Palm oil esters **Surfactant:** Tween®-80 **Co-surfactant:** Span®-20	o/w	Continental method	140 nm	Full thickness rat skin	Advanced NE permeation characteristics for transdermal application of piroxicam	[62]
	Meloxicam	**Surfactant:** Cremophor® RH40 **Co-surfactants:** Capmul® MCM C8, Tween®-60, PEG-400	o/w	Spontaneous emulsification	11-26 nm	Rat abdominal skin	Significant solubility and improved skin permeation using NE	[63]
		Oil: Caprylic acid **Surfactant:** Tween®-80 **Co-surfactant:** Propylene glycol	o/w	Spontaneous emulsification	125 nm	Rat abdominal skin	Significant permeation of meloxicam from NE gel compared to drug solution	[64]
	Lornoxicam	**Oil:** Labrafac® **Surfactant:** Tween®-80 **Co-surfactant:** Pluronic® F68	o/w	Spontaneous emulsification	102-967 nm	Porcine abdominal skin	Development of lornoxicam NE for enhanced solubility and permeation	[65]
	Ketoprofen	**Oil:** Palm oil esters **Surfactant:** Tween®-80	o/w	Spontaneous emulsification	84-230 nm	Cellulose acetate membranes	Development of palm oil ester NEs for the topical delivery of ketoprofen	[46]
		Oil: Benzyl alcohol **Surfactant:** Solutol® HS 15 **Co-surfactant:** Ethanol	o/w	Spontaneous emulsification	20-226 nm	Mice skin	Significantly enhances permeation rate compared to control	[66]
	Aceclofenac	**Oil:** Labrafac® **Surfactant:** Tween®-80 **Co-surfactant:** Ethanol	o/w	Spontaneous emulsification	17-100 nm	Rat abdominal skin	Significant increase inhibition when compared to aceclofenac conventional gel	[67]
		Oil: Labrafil® and Triacetin **Surfactant:** Tween®-80 **Co-surfactant:** Transcutol® P	o/w	Spontaneous emulsification	35-70 nm	Rat abdominal skin	Development of NEs for the improved transdermal delivery of aceclofenac	[68]
	5,7-Dihydroxy-6-methyl-8-prenyl-flavanone; 5,7-Dihydroxy-6-methyl-8-prenyl-4_-Methoxy-flavanone; 5,7-Dihydroxy-6-prenylflavanone; 5-Hydroxy-7-methoxy-6-prenylflavanone	**Oil:** Labrafac® **Surfactant:** Labrasol® **Co-surfactant:** Plurol® Oleique **Hydrophilic phase:** Propylene glycol	w/o	Sonication in ultrasonic bath	48-68 nm	Franz cell diffusion using dermatomed abdominal skin	Significantly enhances anti-inflammatory activity	[69]
Cardio-vascular	Carvedilol	**Oil:** Oleic acid and isopropyl myristate **Surfactant:** Tween®-20 **Co-surfactant:** Carbitol	o/w	Spontaneous emulsification	78.1 nm	Rat skin	Significantly enhanced bioavailability of transdermally applied carvedilol NE.	[70]

(Table 2) Contd...

Class of Drugs	API	Composition	Type of NE	Formulation Method	Droplet Size	Skin Model	Brief Outcome	Ref.
		Oil: Miglyol® 812 **Surfactant:** Acconon®-CC6 **Co-surfactant:** CO-20 (PEG-20 castor oil)	o/w	Spontaneous emulsification	9-95 nm	Rat abdominal skin	Development of carvedilol NE for transdermal delivery.	[71]
	Metoprolol	**Oil:** Isopropyl myristate **Surfactant:** Lecithin **Co-surfactant:** Alcohol (butanol, isopropyl alcohol, n-propanol); water	w/o & o/w	Magnetic stirrer	17-300 nm	Full thickness abdominal skin of Wistar rats	Development of lecithin NE based organogels for permeation enhancement of metoprolol through rat skin	[72]
	Valsartan	**Oil:** Triacetin **Surfactant:** Cremophor® EL **Co-surfactant:** PEG-400; water	o/w	Spontaneous emulsification	4-60 nm	Full thickness rat abdominal skin	Development of NE as carrier for transdermal delivery of valsartan	[73]
	Ramipril	**Oil:** Sefsol®-218 **Surfactant:** Cremophor® EL **Co-surfactant:** Carbitol; water	o/w	Spontaneous emulsification	30-36 nm	N/A	Development of ramipril NE of transdermal delivery	[74]
	Nimodipine	**Oil:** Triacetin **Surfactant:** Tween®-80 **Co-surfactant:** PEG-400; water	o/w	Spontaneous emulsification	10-50 nm	N/A	Development of NEs for the transdermal drug delivery of nimodipine	[75]
	Amlodipine	**Oil:** Oleic acid **Surfactant:** Tween®-20 **Co-surfactant:** Transcutol® P	o/w	Spontaneous emulsification	59 nm	Rat skin	Significant enhances transdermal delivery of amlodipine	[76]
	Nicardipine hydrochloride	**Oil:** Isopropyl myristate **Surfactant:** Tween®-80 and Span®-80/20 **Co-surfactant:** Ethanol in water	w/o	Spontaneous emulsification	70-123 nm	Franz cell diffusion using rat skin	Development of NEs for the transdermal drug delivery of nicardipine hydrochloride	[77]
Central nervous system	Clozapine	**Oil:** Oleic acid **Surfactant:** Tween®-20 **Co-surfactant:** Transcutol® P; water	o/w	Spontaneous emulsification	50-100 nm	Full thickness albino rat abdominal skin	Significantly enhanced bioavailability of transdermally applied clozapine	[78]
	Huperzine A	**Oil:** Capmul® MCM **Surfactant:** Tween®-80 **Co-surfactant:** Transcutol® P; water	w/o	Spontaneous emulsification	148.3 nm	Wistar rat abdominal skin	NEs promote the transport of huperazine A	[79]
Anti-infectives	Dapsone	**Oil:** Isopropyl myristate; N-methyl pyrrolidone; isobutanol **Surfactants:** Tween®-80; Span®-20; water	o/w	Spontaneous emulsification	8-12 nm	Porcine ear skin	Significant skin permeation for the treatment of leprosy	[80]
	Metronidazole	**Oil:** Labrafil® M1944CS **Surfactant:** Cremophor® EL **Co-surfactant:** Tetraethylene glycol; water	w/o & o/w	Spontaneous emulsification	13-140 nm	Porcine abdominal skin	Development of NEs for improved skin targeting of metronidazole	[81]
	3,5-Dihydroxy-4-isopropylstilbene	**Oil:** Isopropyl myristate **Surfactant:** EL-40 **Co-surfactant:** Ethanol; water	o/w	Phase inversion composition method	60.88 nm	Full thickness mouse abdominal skin	Significantly enhanced transdermal release of 3,5-dihydroxy-4-isopropylstilbene	[82]
	Eucalyptus oil	**Oil:** Eucalyptus oil **Surfactant:** Tween®-80	o/w	Ultrasonication	3-50 nm	Male albino Wistar rats	Development of eucalyptus oil NE for topical wound healing	[83]

(Table 2) Contd...

Class of Drugs	API	Composition	Type of NE	Formulation Method	Droplet Size	Skin Model	Brief Outcome	Ref.
	Nystatin	**Oil:** Labrafac® Lipophile **Surfactant:** Labrasol® **Co-surfactant:** Plurol® Oleique	w/o	Sonication in ultrasonic bath	70-500 nm	Dermatomed human abdominal skin	Significant improvement of nystatin NE compared to other formulations	[84]
		Oil: Labrafil® M1944 **Surfactant:** Tween®-80 **Co-surfactant:** Ethanol	o/w	Spontaneous emulsification	176-309 nm	Semipermeable membrane	Development of nystatin NE based gel for topical delivery	[85]
	Amphotericin B	**Oil:** Sefsol®-218 **Surfactant:** Tween®-80 **Co-surfactants:** PEG-400; propylene glycol; water	o/w	Spontaneous emulsification	67-150 nm	Full thickness Albino rat abdominal skin	Significantly enhanced topical delivery of amphotericin B	[86]
	Acyclovir	**Oil:** Miglyol 812 **Surfactant:** Solutol® HS15 **Co-surfactants:** Span®-80, Ryoto sugar ester S-1670/S-270	w/o/w	Phase inversion temperature method	63-125 nm	Dermatomed pig abdominal skin	Development of optimal multiple w/o/w NE for dermal delivery of acyclovir	[87]
Hormones	Testosterone	**Biolipid B2:** Oleic acid; phospholipids; other nutrients	o/w	Homogenisation	93.3-179.6 nm	-	Development of testosterone NE for hormone replacement	[88]
	Progesterone, estriol, estradiol	**Biolipid B2:** Oleic acid; phospholipids; other nutrients	o/w	Homogenisation	150-450 nm	-	Development of hormone replacement therapy to alleviate climacteric symptoms in postmenopausal women	[89]
	Progesterone	**Oil :** PCL-liquid; Lipoid E-80, propylene glycol; tocopherol **Aqueous:** distilled water; potassium sorbate **Surfactants:** Sucrose ester; CD α, β and γ	o/w	High pressure homogenisation	140-320 nm	Dermatomed porcine abdominal skin	Significant increase in skin permeation rates of progesterone compared to the control	[90]
Antioxidants	Idebenone	**Oil:** Medium chain fatty acid triglycerides **Surfactants:** Soybean phosphatidylcholine; Tween®-80; water	o/w	High-shear homogenisation	51.3 nm	Full thickness guinea pig skin	Development of NEs to improve chemical stability of idebenone and enhance skin permeation compared to other formulations	[91]
	Alpha-lipoic acid	**Oil:** Miglyol®-812 **Surfactant:** Pluronic®- F68; water	o/w	Hot homogenisation	113 nm	Polyethersulfone ultrafiltration membrane	Development of alpha-lipoic acid NEs for transdermal drug delivery	[92]
	Lutein	**Oil:** Miglyol®-812 **Surfactant:** Plantacare® 810; water	o/w	High pressure homogenisation	150-350 nm	Pig ear skin	Development of NEs as carriers for dermal delivery of lutein	[93]
UVA/UV B filters	Various UVA and UVB sun filters	**Oil:** Miglyol®-812 **Surfactant:** Pluronic® F68; water	o/w	High pressure homogenisation	118-290 nm	Human skin	Development of NEs as carriers for UV-filters	[94]
	Parasol MCX & Parasol 1789	**Oil:** Parasol® MCX, Parasol® 1789, Finsolv TN; water **Surfactants:** Tween®-80; Span®-80	o/w	Spontaneous emulsification	270-500 nm	Porcine ear skin	Significant protection from photo-degradation, controlled release from nanocapsules and limited penetration through pig ear epidermis	[95]
	Octyl methoxycinnamate and titanium oxide	**Oil:** Avocado oil **Surfactants:** Ultrol® L70; Ultrol® CE200; water	o/w	Ultrasonication	400-500 nm	Cellulose membrane	Development of NEs containing OMC and TiO_2 as anti-solar nanocosmetics	[96]
	Genistein	**Oil:** Octyldodecanol; medium chain triglycerides **Surfactant:** Egg lecithin **Organic solvent:** Acetonitrile; methanol; ethanol; water	o/w	Spontaneous emulsification	220-280 nm	Pig ear skin	Development of topical NEs containing isoflavone genistein	[97]

5.1. Nano-emulsions Loaded with Anti-inflammatory Drugs

This section provides an overview of various analgesics that have been loaded by NEs for improved skin permeation and subsequent anti-inflammatory and analgesic effects.

Kim *et al.* [55] developed a capsaicin-loaded NE for anti-inflammatory application which improved skin permeation effects. The NE consisted of oleoresin capsicum, Tween®-80, Span®-80 (oil phase) and water (water phase), and the droplet size ranged from 20 to 62 nm. Franz cells were used for skin permeation studies using Strat-M® membrane as a human skin mimic. Penetration of capsaicin from the NE was also visualised using confocal laser scanning microscopy (CSLM). Results from the permeation and CSLM studies indicated that capsaicin-loaded NE could penetrate all the layers of the skin and therefore, showed potential for transdermal delivery.

Cyclooxigenase-2 (COX-2) selective inhibitor is a subclass of NSAIDs (non-steroidal anti-inflammatory drugs) that inhibits the COX-2 enzyme, which is believed to be responsible for inflammation and pain. Shakeel *et al.* [56] developed and evaluated an o/w NE loaded with a COX-2 inhibitor, namely celecoxib. The spontaneous emulsification method was employed to formulate the NE using an oil phase (Sefsol®-218 and Triacetin in a 1:1 ratio), stabilised by Cremophor®-EL and Transcutol®-P as surfactant and co-surfactant, respectively. Subsequently, the NE was characterised for viscosity, droplet size, refractive index and morphology, and the formulation was subjected to stability test. The NE was compared with NE based gel and a conventional celecoxib gel where a significant increase ($p<0.05$) in permeation and anti-inflammatory effects was observed with a decrease in the droplet size. Similar results were also reported by Baboota *et al.* [57]. They formulated a celecoxib loaded NE using spontaneous emulsification method and tested for its transdermal drug delivery. The NE that was optimised (based on lowest viscosity, droplet size, PDI and optimum surfactant and co-surfactant concentration), consisted of 2% (m/m) of celecoxib, 10% (m/m) of oil phase (Sefsol®-218 and Triacetin), 50% (m/m) of surfactant mixture (Tween®-80 and Transcutol®-P) and 40% (m/m) water. The optimised formulation showed the highest skin permeation and inhibition of anti-inflammatory effects ($p<0.005$) after 24 h compared to NE based gel and conventional celecoxib gel. The small droplet size present in the optimised formulation (34.6 ± 1.0 nm) was considered to be helpful in penetrating the skin layers. Hence, the optimised formulation showed to be promising as dermal and transdermal delivery vehicle.

Lala & Awari *et al.* [58] also developed a NE for the transdermal delivery of a COX-2 inhibitor, namely etoricoxib for the treatment of inflammation. An o/w NE was formulated consisting of 2% (w/w) of etoricoxib, 20% (w/w) of Triacetin, 38% (w/w) of a surfactant mixture (Cremophor®-RH 40: Transcutol®-P) and 42% (w/w) of water using the spontaneous emulsification method. The optimised NE was characterised by droplet size, viscosity, *etc.* The NE formulations were tested for their *in vitro* permeability using Franz cells. The optimised NE was compared with a conventional etoricoxib gel and an increased permeation was observed. The anti-inflammatory capability of the formulations was evaluated using an *in vivo* carrageenan-induced paw edema test. After 6 h the percentage inhibition was 92.3% for the NE, 84.61% for the NE gel and 69.23% for the conventional gel. They concluded that the NE can serve as a potential vehicle for topically applied anti-inflammatory drugs.

Indomethacin is another drug from the class of NSAIDs, which has been loaded into NEs for improved topical delivery to aid inflammatory conditions. NEs prepared from different oils revealed enhanced drug permeation across the tested skin and a significant anti-inflammatory response was achieved, thus endorsing suitability of the NE as a vehicle for topical delivery of indomethacin. Droplet size also played an important role with the smallest being the most efficient [45, 59, 98].

Several attempts have been made to incorporate the oxicam class drugs such as piroxicam, meloxicam and lornoxicam into NEs for better analgesic and anti-inflammatory effects. Dhawan *et al.* [61] developed and evaluated piroxicam loaded NE for topical delivery. They formulated a NE without the use of chemical enhancers which may cause skin irritation. The NE that was optimised consisted of 10% oleic acid as oil, 35% Tween®-80 and ethanol as surfactant mixture, 55% water, 0.5% drug and 0.5% (w/w) Carbopol® (NE converted into nano-emulgel). NE components were chosen on the basis of emulsification and solubility. The NE was subsequently characterised for various attributes such as viscosity, droplet size, conductivity and permeation across rat skin which was studied using Franz diffusion cells. The nano-emulgel showed enhanced ($p<0.05$) cumulative drug permeation across the skin with less lag time and also less drug was retained within the skin as compared with the market product, namely Feldene®. Droplet sizes of <200 nm within a low PDI indicates uniformity of droplet sizes. The o/w NE showed high conductivity and the viscosity was too low to be applied on the skin, therefore Carbopol® was incorporated to form the nano-emulgel. Results obtained from Dhawan *et al.* [61] showed that the nano-emulgel could be used as an alternative for piroxicam without using any penetration enhancers. Similar results were reported by Abdulkarim *et al.* [62], where a NE based nanocream containing piroxicam was studied for anti-inflammatory effects. In this study, palm oil esters (POE) were chosen as oil-phase and the NE was stabilised by a mixture of Tween®-80 and Span®-20. Steady-state flux was higher for the NE compared with the marketed product. The NE exhibited an increased anti-inflammatory and analgesic activity owing to the small droplet sizes which helped with deeper penetration of drug into the skin. The authors concluded that the NE containing POE was successful for topical and transdermal delivery of Piroxicam.

Khurana *et al.* [64] developed a NE based gel for the transdermal delivery of meloxicam for anti-inflammatory activity. The NE consisted of caprylic acid, Tween®-80, propylene glycol and water, and was formulated using the spontaneous emulsification method. The NE was characterised for pH, zeta-potential, droplet size, rheology and *in vitro* skin permeation studies were conducted. The NE showed increased skin permeation when compared with that of the

drug solution (control). The NE gel formulation permeated to the deeper layers of the skin as observed using CLSM. The meloxicam NE gel had the highest inflammation reduction after 24 h when compared with the control. Khurana *et al.* [64] proposed that the NE gel (containing caprylic acid as oil phase) held a promising prospective as vehicle for topical and transdermal drug delivery of meloxicam.

Dasgupta *et al.* [65] investigated lornoxicam loaded NE gels for topical delivery and anti-inflammatory effects. Spontaneous self-emulsification method was adopted to formulate the NE that consisted of Labrafac®, Tween®-80, Pluronic® F68 and water. The formulated NE had droplet sizes ranging from 102 to 200 nm. *In vitro* studies showed that the NE performed better than the conventional gel when enhancement ratio, steady-state flux and permeability coefficients were compared. The NE increased permeability through the skin. Results depicted that components of the NE also played an important role in control over particle size, zeta-potential and drug solubility. Dasgupta *et al.* [65] concluded that lornoxicam NE is a better alternative vehicle than the conventional gel.

Continuing with the NSAIDs, Sakeena *et al.* [46] focused on developing and evaluating ketoprofen loaded o/w NE for topical delivery using POE. Palm oil is considered as a good pharmaceutical vehicle; therefore, the spontaneous emulsification method was employed for the NE preparation. The NE droplet size was below 500 nm and it was predicted that the small droplet size will increase surface area for the release of the drug, as well as the transfer and absorption, which was confirmed using *in vitro* permeation studies. Therefore, the authors proposed that POE can be used as a pharmaceutical ingredient for topical delivery of ketoprofen. Similar results were reported by Kim *et al.* [66]; they investigated ketoprofen loaded NE which were formulated using a different set of excipients. The o/w NE consisted of benzyl alcohol, Solutol® HS 15 and ethanol in water. Benzyl alcohol, because of its permeation enhancing and good solubilisation effects, was used in the oil phase. The NE which incorporated 4% benzyl alcohol showed an increased permeation when compared with 1% and 2%, as well as with the 1% Solutol® HS 15. Kim *et al.* [66] proposed that these results with small droplet sizes and lower surfactant contents could enhance transdermal delivery and hold promise for topical delivery using NE systems for poorly water soluble drugs, such as ketoprofen.

Modi & Patel [67] investigated a NE based gel formulation for the dermal delivery of aceclofenac to reduce pain and inflammation. The NE consisted of 2% (w/w) of aceclofenac, 10% (w/w) of Labrafac®, 45% (w/w) surfactant mixture (Cremophor®-EL:ethanol), and 43% (w/w) of distilled water and was prepared by the spontaneous emulsification method. Skin permeation was determined by Franz diffusion cells. An optimised NE was compared with the NE based gel and a conventional gel for its skin permeation capability. After 24 h, there was a significant increase in the magnitude of inflammation inhibition from the NE when compared to the NE based gel and the conventional gel. They concluded that the NE can be a potential dermal delivery vehicle for aceclofenac. Shakeel *et al.* [68] also developed a NE containing gel for the transdermal delivery of aceclofenac for anti-inflammatory effects. An o/w NE was prepared using the spontaneous emulsification method. The optimised NE consisted of 2% (w/w) of aceclofenac, 10% (w/w) of Labrafil®, 5% (w/w) of Triacetin, 35.33% (w/w) of Tween®-80, 17.66% (w/w) of Transcutol®-PR, and 32% (w/w) of distilled water. Different thermodynamic stability tests were applied to the NE and this was characterised using TEM, then refractive index and droplet size was also determined. The NE was compared with the NE gel and a conventional gel, and an increase of permeability parameters was seen for the NE as compared with its counterparts. After 24 h the optimised NE showed a significant increase in anti-inflammatory effects ($p<0.05$). The selected optimised NE was chosen on the basis of lowest viscosity, smallest droplet size, minimum concentration of surfactant and co-surfactant. Shakeel and co-workers concluded that the NE could possibly be used for topical and transdermal drug delivery of aceclofenac [68].

Domínguez-Villegas *et al.* [69] isolated four flavanones (5,7-dihydroxy-6-methyl-8-prenylflavanone; 5,7-dihydroxy-6-methyl-8-prenyl-4-methoxy-flavanone; 5,7-dihydroxy-6-prenylflavanone and 5-hydroxy-7-methoxy-6-prenylflavanone) from the *Eysenhardtia platycarpa* leaves, which were used as anti-inflammatory agents in topical formulations. These NEs were composed of Labrafac®, Labrasol®, Plurol® Oleique and propylene glycol. These NE had droplet sizes less than 70 nm, compared with nanoparticles which had sizes that ranged from 156-202 nm. It was reported that NEs are able to lower the interface tension between the skin and the vehicle which can result in faster permeation [95]. These NEs showed high drug entrapment efficiency (78-90%). Franz type diffusion cells were used for the *in vitro* and *ex vivo* permeation studies where the NEs showed a steady-state release as well as a steady increase of flavanones in the skin penetration study. These NEs showed increased anti-inflammatory activity. Domínguez-Villegas *et al.* [69] results suggest that these NEs could be used for topical treatment of anti-inflammatory disorders.

5.2. Nano-emulsions Loaded with Cardiovascular Drugs

In the previous section we have discussed various studies where NEs have been used for the topical and transdermal delivery of various anti-inflammatory drugs. The scope of NEs is thus not limited to only dermal delivery, but also shown potential in delivering the drugs systemically. This section is therefore focused on discussing transdermal delivery of cardiovascular drugs.

Pratap *et al.* [70] developed and evaluated a NE gel for the transdermal delivery of carvedilol. This study was aimed at enhancing the bioavailability of the drug. The o/w NE consisted of oleic acid and isopropyl myristate as oil phase, Tween®-20, carbitol and water, and was prepared by the spontaneous emulsification method. Different parameters were evaluated, such as droplet size, stability test and thermodynamics. Compared with the control, the NE showed a significant difference in the steady state flux (Jss), enhancement ratio (Es) and the permeability coefficient (K_p) ($p<0.001$). The highest flux value (211.8 $\mu g.cm^{-2}.h^{-1}$) was obtained by the optimised formulation after 24 h, which also had the lowest viscosity of 29.12 cP. Based on these results,

Pratap *et al.* [70] suggested that the NE containing carvedilol could be used for transdermal delivery. Similar results were reported by Rizwan *et al.* [71]. They prepared carvedilol loaded NEs which were optimised to find a suitable formulation. The optimised NE composed of Miglyol-810 (12.5% (w/w)) as oil phase with Acconon CC6/PEG-20 (1:1) and castor oil (50% (w/w)) as surfactant/co-surfactant mix. The maximum achievable flux from the optimised formulation was 161.53 $mg.cm^{-2}.h^{-1}$ across the rat skin. Interestingly, the optimised NE had the smallest droplet size of 9.28 nm, which in turn may have resulted in the high transdermal flux of carvedilol across the skin. *In vitro* skin permeation studies showed that the flux obtained was high enough and might achieve therapeutic drug level required in humans for 24 h, although this speculation cannot be justified from this study, and thus warrants further studies.

Varshosaz *et al.* [72] developed and evaluated a lecithin based NE for the transdermal delivery of metoprolol. Metoprolol has low oral bioavailability due to the first-pass metabolism. NEs contained isopropyl myristate, lecithin, alcohol (n-butanol, isopropyl alcohol, *n*-propanol) and water. Three NEs each contained different surfactant/co-surfactant weight ratios, various amounts of drug and different types of alcohol were prepared. Droplet sizes ranged from 17-49 nm. To study the drug release parameters, NEs with smaller droplet sizes were chosen based on transparency. They found that the drug dissolution rate increased with increasing metoprolol content in the NE, and decreased when lecithin concentration was increased. A significant increase was seen in metoprolol release when the water content of the NE was increased. The drug flux was the highest when *n*-butanol was used. Metoprolol-loaded NE showed higher flux and permeability across rat skin regardless of type of NE, *i.e.* o/w or w/o.

Another interesting research was reported by Malgope *et al.* [73]. They developed and evaluated a NE for the transdermal delivery of valsartan. Various o/w test formulations were prepared and optimised for optimum constituents. The optimised NE contained Triacetin (13.6%), Cremophor®-EL (23.9%), PEG-400 (7.9%), and water (54.6%) as oil, surfactant, co-surfactant and aqueous phase, respectively. The optimised NE had a small droplet size of 4.49 nm, PDI of 0.651 and very low viscosity of 85.55 cP. The optimised NE showed steady state flux of 283.119 ± 4.164 $\mu g.cm^{-2}.h^{-1}$ through rat skin. There was a 7.2-fold enhanced permeation of valsartan when compared with conventional gel formulation. Malgope and co-workers results therefore show that NEs can be a potential alternative carrier for valsartan transdermal delivery [73].

Other studies also showed successful transdermal permeation of antihypertensive drugs such as ramipril [74], nimodipine [75], amlodipine [76] and nicardipine [77].

5.3. Nano-emulsions Loaded with Central Nervous System Drugs

Shafaat *et al.* [78] developed a NE based transdermal formulation for delivery of clozapine as anti-psychotic drug. An o/w NE was prepared by the spontaneous emulsification method and consisted of oleic acid, Tween®-20, Transcutol®-P and water. Components such as oleic acid, Tween®-20 and Transcutol®-P were chosen on the basis of solubility. Significant increase was observed in the permeation parameters. The optimised NE was chosen on the basis of smallest droplet size, lowest viscosity and higher bioavailability. They concluded that NE for transdermal drug delivery depends on the appropriate combination of the components and therefore can be used for transdermal drug delivery of hydrophobic compounds.

Patel *et al.* [79] developed and evaluated huperzine A loaded NE for the treatment of Alzheimer's disease. In this study, solid lipid nanoparticles (SLN), NE and nanostructured lipid carriers (NLCs) were formulated and compared. SLN and NLC were incorporated into gels for transdermal delivery. LEE method was employed for o/w NE formulation using Capmul® MCM oil which was stabilised by Tween®-80 and Transcutol®-P as surfactant and co-surfactant mixture, respectively. Patel *et al.* [79] proposed that NE can increase the skin penetration of both hydrophilic and lipophilic drugs. Compared with the other nano-counterparts, the NE showed the highest permeation of huperzine A and could be explained on the basis that penetration of huperzine A can occur directly from the nanosized droplets without fusing to the SC. This enhancement could be due to the nanosized droplets which are dispersed in the continuous phase and therefore, can move freely into the SC. Literature suggests that NE can reduce the interfacial tension between the skin and the vehicle which results in faster permeation. Therefore, it is suggested that nanovehicles with highly negative charges would result in poor permeation across the SC. Due to negative residues of proteins; the surface of the skin is negatively charged [99].

5.4. Nano-emulsion Loaded with Anti-infective

Borges *et al.* [80] developed dapsone containing NEs for topical administration for possible treatment of leprosy. The NE consisted of isopropyl myristate or N-methyl pyrrolidone as oil phase, stabilised by a mixture of Tween®-80 and Span®-20 as surfactant and co-surfactant, respectively. Use of *n*-methyl-pyrrolidone provided a highly stable NE and higher solubilisation of dapsone and increased the *in vitro* release rate when compared with a NE prepared using isopropyl myristate. However, the use of isopropyl myristate increased epidermal permeation, which followed Higuchi type release kinetics. Borges *et al.* [80] concluded that isopropyl myristate as oil phase increased the permeation of dapsone through the skin when compared to N-methyl pyrrolidone, and therefore can be used as a potential vehicle for dermal delivery of dapsone for the treatment of leprosy.

Yu *et al.* [81] developed a metronidazole loaded NE for localised targeting in the deep skin layers to elicit anti-rosacea effects. A series of NE consisted of Labrafil®, a mixture of Cremophor®-EL/tetraethylene glycol (2:1; w/w), as a surfactant and co-surfactant mixture, at different weight ratios. The optimised NE formulation was assessed for its *in vitro* skin permeation studies, which was followed by a comparison with metronidazole gel. Metronidazole loaded NE permeated into the deeper layers of the skin compared with the gel. The results led to the conclusion that the NE had good mobility into the deeper skin layers because of the low viscosity of the system. Thus, the NE formulation could be a

promising vehicle for hydrophilic drugs for transdermal delivery.

Some other studies have focused on loading 3,5-dihydroxy-4-isopropylstilbene [82] and eucalyptus oil [83] to assess their skin permeation and their anti-bacterial activity. The NE formulations dramatically improved the skin permeation and anti-bacterial activity, thus endorsing the suitability of NE as potential transdermal vehicle.

Another important study carried out by Fernández-Campos *et al.* [84], focused on developing and evaluating a nystatin loaded NE for treatment of cutaneous *Candida* infections. Upon formulation, spherical shaped droplets with a mean droplet size of 70-80 nm were obtained. *In vitro* and *ex vivo* tests were conducted using Franz type cells which showed that the drug was retained in skin layers and did not cross the skin to make its way to the systemic circulation. The retained amount in the skin was sufficient to elicit anti-fungal effects. The results from this study were compared with a commercial ointment, namely Mycostatin®, and the NE was found to be potentially superior. Similar results were obtained in another study conducted by Elosaily [85], where a nystatin loaded NE was found superior than the marketed cream product.

Hussain *et al.* [86] prepared amphotericin B loaded NE for topical drug delivery. The o/w NE containing Sefsol®-218, Tween®-80, PEG-400 and propylene glycol was prepared by the spontaneous emulsification method. Higher steady state fluxes were observed for NE, with an enhancement ratio of 1.9 to 3.0-fold higher than that of the commercial formulation. Hussain and co-workers suggested that NE loaded with amphotericin B could potentially be a better option for topical delivery [86].

Schwarz *et al.* [87] developed a NE based formulation for the transdermal delivery of acyclovir for antiviral activity. The w/o/w NE was prepared by the PIT method and consisted of Miglyol®-812, Solutol® HS 15, Span®-80, Ryoto sugar ester S-1670/S-270 and water with added sodium chloride (NaCl) for phase inversion. The NE had a mean droplet size of 63-125 nm with a PDI of 0.1 nm. During Franz cell studies, the NE showed increased permeation of acyclovir across the skin. This study concluded that w/o/w NE is a potential transdermal delivery vehicle for acyclovir.

5.5. Nano-emulsion Loaded with Hormones

Botelho *et al.* [88] assessed the efficacy of Biolipid B2® nanostructured hormone loaded transdermal delivery system for the delivery of testosterone. An open label randomised prospective study was designed and 14 Brazilian middle aged men with testosterone deficiency were enrolled to conduct the studies. The study included the short term effects on C-reactive protein (CRP) serum levels, thyroid stimulating hormone (TSH) and blood pressure. Each volunteer received 50 mg testosterone nanostructured formulation, which was applied daily on the forearm for 3 months. Serum concentration and clinical parameters were compared between baseline and 3 months thereafter. TSH, CRP and testosterone serum concentration significantly changed ($p<0.05$) after treatment. There was also a significant change in the weight, body mass index and waist circumference when treatment was finished. Botelho and co-workers [88] found that the testosterone NEs were effective and safe to use in re-establishing testosterone levels and which may serve as perspective for hormone replacement. In another study by Botelho *et al.* [89], a nanostructured transdermal hormone replacement therapy was developed to relieve menopausal symptoms. The formulation was a combination of progesterone (10%), estriol (0.1%) and estradiol (0.25%). Subjects received the formulation on a daily basis for 60 months. Baseline was compared for serum concentration, blood pressure, and follicle stimulating hormone with 60 months post-treatment. No adverse effects were seen after treatment. An increase of climacteric systems (92.5%) and a significant increase of serum concentrations were found ($p<0.05$). The serum follicle stimulating hormone also decreased from 82.04 to 57.12 IU/mL, and no change in blood pressure was observed with the absence of vaginal bleeding or endometrial thickness. Botelho *et al.* [89] concluded that this nanostructured formulation could alleviate menopausal symptoms.

Klang *et al.* [90] developed and evaluated progesterone loaded positively and negatively charged NEs without the use of skin-irritating surfactants. High pressure homogenisation was employed to produce NEs, which comprised of PCL-liquid, Lipoid E-80, propylene glycol, tocopherol, and potassium sorbate. Natural substances such as sucrose esters and different cyclodextrins (CDs; α, β and γ) were additionally used as stabilising agents. Both the negatively and positively charges NEs were able to enhance the skin permeation of progesterone. The skin permeation was greatly enhanced when sucrose ester S-970 was used as additional stabilising agent. Furthermore, the natural CDs (α, β and γ) proved to be of great interest as additional compounds. The CDs seemed to induce fundamental changes in formulation structure, thus leading to increased skin permeation rates of progesterone. Klang *et al.* [90] results demonstrated that without the use of conventional synthetic surfactants such as polysorbates, NE with long term stability can be obtained with superior skin permeation capabilities.

5.6. Nano-emulsions Loaded with Anti-oxidants

Li & Ge [91] developed a NLC to improve skin permeation and chemical stability of idebenone. NLCs were also compared with NE and oil solutions to determine permeation enhancing effects across guinea pig skins. The idebenone permeation in epidermis, dermis and acceptor medium from NLC was three-fold higher than that from the NE or oil solution, however, there was no significant difference observed between oil solution and NE. NLC also showed the highest stability (90.1%) compared to the NE (65.4%) and the oil solution (51.3%) stored at 40°C. Li & Ge [91] concluded that NLC showed: 1) better permeation within the skin layers and 2) higher stability when it is compared with the NE and oil solution of idebenone. Similarly, Ruktanonchai *et al.* [92] and Mitri *et al.* [93] demonstrated that nanoparticulate formulations such as SLNs and NLCs were better distributed within the skin layer without significant crossing the skin and their long-term stability make them potential carriers for topical delivery of alpha-lipoic acid and lutein, respectively. Other studies also highlighted that NEs have the capability of traversing the skin compared with other counterpart nanocar-

riers and therefore a judicious choice of delivery vehicle is necessary when a dermatological or cosmetic purpose is required [100, 101].

5.7. Nano-emulsion Loaded with Sunscreen Agents

Puglia *et al.* [94] developed and evaluated NE loaded with UV-filters for photoprotective properties. The NE and NLC were formulated for the topical application of a variety UVA/UVB sun filters such as ethylhexyl triazone (EHT) or diethylamino hydroxybenzoyl hexyl benzoate (DHHB). The *in vitro* transdermal permeation was evaluated using excised human skin. The skin permeation of the UV-filters was reduced when incorporated in NLC; therefore, it only remained on the skin surface. Nevertheless, EHT and DHHB retained their photostability when incorporated either in NE or NLC. Similarly, Hanno *et al.* [95] also highlighted that nanocapsules were able to retain the sunscreening agents such as Parsol® MCX and Parsol® 1789, because of the slow penetration into the skin as compared with the NE.

In Contrast, Silva *et al.* [96] prepared octyl methoxycinnamate and titanium dioxide containing NEs for sun protection. Ultrasound processed o/w NE were composed of avocado oil/non-ionic surfactant/water (5%, 12%, 83% (w/w), respectively). A long chained surfactant (ethylene oxide) was used to stabilise the small oil droplets in the NE. Titanium dioxide did not significantly affect the *in vitro* release profile, which showed the diffusion-dependent kinetics of the active ingredient in the formulation. They concluded that the NE containing octyl methoxycinnamate and titanium dioxide shows promising results for cosmetic purpose. In another study by Silva *et al.* [97], genistein (a photoprotective agent) loaded NE showed a slow permeation across pig ear skin, thus endorsing the suitability of NE as a vehicle for sun screening agents.

CONCLUSION

NEs are small, kinetically stabilised oil droplets dispersed in water, with each droplet being surrounded by a protective coating of an emulsifier. These nanosized oil droplets are potential carriers for the topical and transdermal delivery of various drugs. NE is a versatile carrier system, which is equipped with interesting features such as lower surfactant concentration with tuneable physical and biological properties, which can improve therapeutic strategies of drugs that face problems, including low bioavailability, poor aqueous solubility and product stability. When NEs are charged (usually positive), they could act as drug reservoirs where the high concentration of drugs in the NEs can result in a concentration gradient, and therefore, the small droplet sizes of these NEs can permeate into the SC.

This review has presented topical and transdermal delivery of various drug classes. Since NEs have the ability to disrupt the skin barrier; transdermal delivery is much feasible compared to topical delivery. Despite the fact that NEs have tendency to breach the skin barrier effectively, there is no current market share of NE based transdermal formulations. We have summarised many studies focused on transdermal delivery of a number of pharmaceutical compounds and future directions should be towards elucidating skin penetration of such compounds in more clinically relevant situations. Furthermore, involving human volunteers for the generation of true clinical data would be invaluable in interpreting the interaction of NE components with the human skin and subsequent translation into product formulation.

For cosmetic purposes, an active ingredient should only cross the SC and remain in the skin, therefore nanoparticles and NLCs are more suitable for topical delivery than NEs. Hence, NEs may not be the ideal candidates for cosmetic products, since they are more prone to deliver the active ingredient deeper into the skin and may even reach the systemic circulation. Nevertheless, further optimisation of NEs or with the incorporation of penetration retardants, may lead to the successful use of NEs in cosmetics.

CONFLICT OF INTEREST

The authors confirm that this article content has no conflict of interest.

ACKNOWLEDGEMENTS

The authors would like to express their sincere gratitude towards the National Research Foundation (NRF) of South Africa (CPRR13091742482 and IFRR81178) and the Centre of Excellence for Pharmaceutical Sciences (01544021G662825) (North-West University, Potchefstroom, South Africa) for the financial support. Any opinion, findings and conclusions, or recommendations expressed in this material are those of the authors, and therefore, the NRF does not accept any liability in regard thereto.

PATIENT CONSENT

Declared none.

REFERENCES

[1] Perumal, O.; Murthy, S.N.; Kalia, Y.N. Turning theory into practice: the development of modern transdermal drug delivery systems and future trends. *Skin Pharmacol. Physiol.*, **2013**, *26*, 331-342.
[2] Scheuplein, R.J. Mechanism of percutaneous adsorption. I. Routes of penetration and the influence of solubility. *J. Invest. Dermatol.*, **1965**, *45*, 334-346.
[3] Scheuplein, R.J. Mechanism of percutaneous absorption. *J. Invest. Dermatol.*, **1967**, *48*, 79-88.
[4] Scheuplein, R.J; Blank, I.H. Permeability of the skin. *Physiol. Rev.*, **1971**, *51*, 702-747.
[5] Hadgraft J. Skin, the final frontier. *Int. J. Pharm.*, **2001**, *224*, 1-18.
[6] Naik, A.; Kalia, Y.N.; Guy, R.H. Transdermal drug delivery: overcoming the skin's barrier function. *Pharm. Sci. Tech. Today*, **2000**, *3*, 318-326.
[7] Iwai, I.; Han, H; Hollander, L.D.; Svensson, S.; Öfverstedt, L.G.; Anwar, J.; Brewer, J.; Bloksgaard, M.; Laloeuf, A.; Nosek, D.; Masich, S.; Bagatolli, L.A.; Skoglund, U.; Norlén, L. The human akin barrier is organized as stacked bilayers of fully extended ceramides with cholesterol molecules associated with the ceramide sphingoid moiety. *J. Invest. Dermatol.*, **2012**, *132*, 2215-2225.
[8] Norlén, L. Current understanding of skin barrier morphology. *Skin Pharmacol. Physiol.*, **2013**, *26*, 213-216.
[9] Shahzad, Y.; Sohail, S.; Arshad, M.S.; Hussain, T.; Shah, S.N.H. Development of solid dispersions of artemisinin for transdermal delivery. *Int. J. Pharm.*, **2013**, *457*, 197-205.
[10] Alexander, A.; Dwivedi, S.; Ajazuddin; Giri, T.K.; Saraf, S.; Saraf, S.; Tripathi, D.K. Approaches for breaking the barriers of drug

permeation through transdermal drug delivery. *J. Control. Rel.*, **2012**, *164*(1), 26-40.
[11] Parikh, R.H.; Patel, R.J. Nanoemulsions for intranasal delivery of riluzole to improve brain bioavailability: formulation development and pharmacokinetic studies. *Curr. Drug Deliv.*, **2016**, *13*(7), 1130-1143.
[12] Tan, L.S.; Stanslas, J.; Basri, M.; Karjiban, R.; Kirby, B.P.; Sani, D.; Basri, B.H. Nanoemulsion-based parenteral drug delivery system of carbamazepine: Preparation, characterization, stability evaluation and blood-brain pharmacokinetics. *Curr. Drug Deliv.*, **2015**, *12*, 795-804.
[13] Liu, Z.; Zhang, Q.; Ding, L.; Li, C.; Yin, Z.; Yan, G.; Pi, J.; Li, J.; Li, N.; Qi, D. Preparation procedure and pharmacokinetic study of water-in-oil nanoemulsion of Panax notoginseng saponins for improving the oral bioavailability. *Curr. Drug Deliv.*, **2016**, *13*, 600-610.
[14] Sanz, R.; Calpena, C.A.; Mallandrich, M.; Clares, B. Enhancing topical analgesic administration: review and prospect for transdermal and transbuccal drug delivery systems. *Curr. Pharm. Des.*, **2015**, *21*, 2867-2882.
[15] Lopes, L.B. Overcoming the cutaneous barrier with microemulsions. *Pharmaceutics*, **2014**, *6*, 52-77.
[16] Guglielmini, G. Nanostructured novel carrier for topical application. *Clin. Dermatol.*, **2008**, *26*, 341-346.
[17] Solans, C.; Solé, I. Nano-emulsions: Formation by low-energy methods. *Curr. Opin. Colloid Interface Sci.*, **2012**, *17*, 246-254.
[18] Devarajan, V.; Ravichandran, V. Nanoemulsions: As modified drug delivery tool. *Int. J. Comprehen. Pharm.*, **2011**, *2*(4), 1.
[19] Chime, S.; Kenechukwu, F.; Attama, A. Nanoemulsions—advances in formulation, characterization and applications in drug delivery. Ali, D.S. Application of nanotechnology in drug delivery. Croatia: *In Tech.*, **2014**, ch. 3, 77-111.
[20] McClements, D.J. Nanoemulsions versus microemulsions: Terminology, differences, and similarities. *Soft Matter*, **2012**, *8*, 1719-1729.
[21] Solè, I.; Maestro, A.; González, C.; Solans, C.; Gutiérrez, J.M. Optimization of nano-emulsion preparation by low-energy methods in an ionic surfactant system. *Langmuir*, **2006**, *22*, 8326-8332.
[22] Taylor, P. Ottewill, R.H. The formation and ageing rates of oil-in-water miniemulsions. *Colloids Surf. A*, **1994**, *88*, 303-316.
[23] Solè, I.; Solans, C.; Maestro, A.; González, C.; Gutiérrez, J. Study of nano-emulsion formation by dilution of microemulsions. *J. Colloid Interface Sci.*, **2012**, *376*, 133-139.
[24] Pons, R.; Carrera, I.; Caelles, J.; Rouch, J.; Panizza, P. Formation and properties of miniemulsions formed by microemulsions dilution. *Adv. Colloid Interface Sci.*, **2003**, *106*, 129-146.
[25] Shinoda, K.; Saito, H. The effect of temperature on the phase equilibria and the types of dispersions of the ternary system composed of water, cyclohexane, and nonionic surfactant. *J. Colloid Interface Sci.*, **1968**, *26*, 70-74.
[26] Shinoda, K.; Kunieda, H. Phase properties of emulsions: PIT and HLB. In: *Encyclopedia of Emulsion Technology: Basic Theory*; Schuste, D., ed.; Marcel Dekker: New York, **1983**; *1*, pp. 337.
[27] Kunieda, H.; Friberg, S.E. Critical phenomena in a surfactant/water/oil system. basic study on the correlation between solubilization, microemulsion, and ultralow interfacial tensions. *Bull. Chem. Soc. Japan*, **1981**, *54*, 1010-1014.
[28] Mansoor, M.A.; Sandip, B.T. Nanoemulsion formulations for tumor-targeted delivery. In: *Nanotechnology for Cancer Therapy; ed.;* CRC Press, **2006**; pp. 723-739.
[29] Izquierdo, P.; Esquena, J.; Tadros, T.F.; Dederen, J.C.; Feng, J.; Garcia-Celma, M.J.; Azemar, N.; Solans, C. Phase behavior and nano-emulsion formation by the phase inversion temperature method. *Langmuir*, **2004**, *20*, 6594-6598.
[30] Sadurní, N.; Solans, C.; Azemar, N.; García-Celma, M.J. Studies on the formation of O/W nano-emulsions, by low-energy emulsification methods, suitable for pharmaceutical applications. *Eur. J. Pharm. Sci.*, **2005**, *26*, 438-445.
[31] Roger, K.; Cabane, B.; Olsson, U. Emulsification through surfactant hydration: the PIC process revisited. *Langmuir*, **2010**, *27*, 604-611.
[32] Bouchemal, K.; Briançon, S.; Couenne, F.; Fessi, H.; Tayakout, M. Stability studies on colloidal suspensions of polyurethane nanocapsules. *J. Nanosci. Nanotechnol.*, **2006**, *6*, 3187-3192.
[33] Tadros, T.; Izquierdo, P.; Esquena, J.; Solans, C. Formation and stability of nano-emulsions. *Adv. Colloid Interface Sci.*, **2004**, *108*, 303-318.
[34] Ganta, S.; Talekar, M.; Singh, A.; Coleman, T.P.; Amiji, M.M. Nanoemulsions in translational research-opportunities and challenges in targeted cancer therapy. *AAPS Pharm. Sci. Tech.*, **2014**, *15*, 694-708.
[35] Sharma, N.; Bansal, M.; Visht, S.; Sharma, P.; Kulkarni, G. Nanoemulsion: A new concept of delivery system. *Chron. Young Sci.*, **2010**, *1*, 2.
[36] Floury, J.; Desrumaux, A.; Axelos, M.A.; Legrand, J. Effect of high pressure homogenisation on methylcellulose as food emulsifier. *J. Food Eng.*, **2003**, *58*, 227-238.
[37] Kentish, S.; Wooster, T.; Ashokkumar, M.; Balachandran, S.; Mawson, R.; Simons, L. The use of ultrasonics for nanoemulsion preparation. *Innov. Food Sci. Emerg. Technol.*, **2008**, *9*, 170-175.
[38] Lovelyn, C.; Attama, A.A. Current state of nanoemulsions in drug delivery. *J. Biomater. Nanobiotechnol.*, **2011**, *2*, 626.
[39] McClements, D.J. Food emulsions: principles, practices, and techniques. CRC Press, **2015**.
[40] Mason, T.; Graves, S.; Wilking, J.; Lin, M. Extreme emulsification: formation and structure of nanoemulsions. *Condens. Matter Phys.*, **2006**, *9*, 193-199.
[41] Mason, T.G.; Wilking, J.; Meleson, K.; Chang, C.; Graves, S. Nanoemulsions: formation, structure, and physical properties. *J. Phys.: Condens. Matter*, **2006**, *18*, R635.
[42] Klang, V.; Matsko, N.B.; Valenta, C.; Hofer, F. Electron microscopy of nanoemulsions: An essential tool for characterisation and stability assessment. *Micron*, **2012**, *43*, 85-103.
[43] Fernandez, P.; André, V.; Rieger, J.; Kühnle, A. Nano-emulsion formation by emulsion phase inversion. *Colloids Surf. A*, **2004**, *251*, 53-58.
[44] Shahzad, Y.; Louw, R.; Gerber, M.; du Plessis, J. Breaching the skin barrier through temperature modulations. *J. Control. Release*, **2015**, *202*, 1-13.
[45] Shakeel, F.; Ramadan, W.; Ahmed, M.A. Investigation of true nanoemulsions for transdermal potential of indomethacin: characterization, rheological characteristics, and *ex vivo* skin permeation studies. *J. Drug Target.*, **2009**, *17*, 435-441.
[46] Sakeena, M.; Muthanna, F.; Ghassan, Z.; Kanakal, M.; Elrashid, S.; Munavvar, A.; Azmin, M. Formulation and *in vitro* evaluation of ketoprofen in palm oil esters nanoemulsion for topical delivery. *J. Oleo Sci.*, **2009**, *59*, 223-228.
[47] Desai, N. Challenges in development of nanoparticle-based therapeutics. *AAPS J.*, **2012**, *14*, 282-295.
[48] Azeem, A.; Talegaonkar, S.; Negi, L.M.; Ahmad, F.J.; Khar, R.K.; Iqbal, Z. Oil based nanocarrier system for transdermal delivery of ropinirole: a mechanistic, pharmacokinetic and biochemical investigation. *Int. J. Pharm.*, **2012**, *422*, 436-444.
[49] Friberg, S.; Larsson, K.; Sjoblom, J. Food emulsions. CRC Press, **2003**.
[50] Shakeel, F.; Baboota, S.; Ahuja, A.; Ali, J.; Shafiq, S. Celecoxib nanoemulsion: Skin permeation mechanism and bioavailability assessment. *J. Drug Target.*, **2008**, *16*, 733-740.
[51] Prakash, R.; Thiagarajan, P. Nanoemulsions for drug delivery through different routes. *Res. J. Biotechnol.*, **2011**, *2*, 1-13.
[52] Lu, W-C.; Chiang, B-H.; Huang, D-W.; Li, P-H. Skin permeation of d-limonene-based nanoemulsions as a transdermal carrier prepared by ultrasonic emulsification. *Ultrason. Sonochem.*, **2014**, *21*, 826-832.
[53] Sandig, A.G.; Campmany, A.C.C.; Campos, F.F.; Villena, M.J.M.; Naveros, B.C. Transdermal delivery of imipramine and doxepin from newly oil-in-water nanoemulsions for an analgesic and anti-allodynic activity: Development, characterization and *in vivo* evaluation. *Colloids Surf., B*, **2013**, *103*, 558-565.
[54] Gönüllü, Ü.; Üner, M.; Yener. G.; Karaman, E.F.; Aydoğmuş, Z. Formulation and characterization of solid lipid nanoparticles, nanostructured lipid carriers and nanoemulsion of lornoxicam for transdermal delivery. *Acta Pharm.*, **2015**, *65*(1), 1-13.
[55] Kim, J.H.; Ko, J.A.; Kim, J.T.; Cha, D.S.; Cho, J.H.; Park, H.J.; Shin, G.H. Preparation of a capsaicin-loaded nanoemulsion for improving skin penetration. *J. Agric. Food Chem.*, **2014**, *62*, 725-732.
[56] Shakeel, F.; Baboota, S.; Ahuja, A.; Ali, J.; Shafiq, S. Celecoxib nanoemulsion for transdermal drug delivery: Characterization and *in vitro* evaluation. *J. Disper. Sci. Technol.*, **2009**, *30*, 834-842.

[57] Baboota, S.; Shakeel, F.; Ahuja, A.; Ali, J.; Shafiq, S. Design, development and evaluation of novel nanoemulsion formulations for transdermal potential of celecoxib. *Acta Pharm.*, **2007**, *57*, 315-332.

[58] Lala, R.; Awari, N. Nanoemulsion-based gel formulations of COX-2 inhibitors for enhanced efficacy in inflammatory conditions. *Appl. Nanosci.*, **2014**, *4*, 143-151.

[59] Abdelaziz, A.E.; Elmowafy, M.; Salama, A.; Samy, A.; Kassem, A.; Raslan, M.A.; El-Eraky, W.I. Development and transdermal efficacy assessment of indomethacin nanoemulsion formulation. *Inter. J. Pharma. Sci.*, **2014**, *4*, 611-621.

[60] Shakeel, F.; Ramadan, W.; Gargum, H.M.; Singh, R. Preparation and *in vivo* evaluation of indomethacin loaded true nanoemulsions. *Scientia Pharm.*, **2010**, *78*, 47-56.

[61] Dhawan, B.; Aggarwal, G.; Harikumar, S. Enhanced transdermal permeability of piroxicam through novel nanoemulgel formulation. *Int. J. Pharm. Invest.*, **2014**, *4*, 65.

[62] Abdulkarim, M.F.; Abdullah, G.Z.; Chitneni, M.; Salman, I.M.; Ameer, O.Z.; Yam, M.F.; Mahdi, E.S.; Sattar, M.A.; Basri, M.; Noor, A.M. Topical piroxicam *in vitro* release and *in vivo* anti-inflammatory and analgesic effects from palm oil esters-based nanocream. *Int. J. Nanomed.*, **2010**, *5*, 915.

[63] Badran, M.M.; Taha, E.I.; Tayel, M.M.; Al-Suwayeh, SA. Ultrafine self nanoemulsifying drug delivery system for transdermal delivery of meloxicam: Dependency on the type of surfactants. *J. Mol. Liq.*, **2014**, *190*, 16-22.

[64] Khurana, S.; Jain, N.; Bedi, P. Nanoemulsion based gel for transdermal delivery of meloxicam: physico-chemical, mechanistic investigation. *Life Sci.*, **2013**, *92*, 383-392.

[65] Dasgupta, S.; Ghosh, K.S.; Ray, S.; Kaurav, S.; Mazumder, B. *In vitro & in vivo* studies on lornoxicam loaded nanoemulsion gels for topical application. *Curr. Drug Deliv.*, **2014**, *11*, 132-138.

[66] Kim, B.S.; Won, M.; Lee, K.M.; Kim, C.S. *In vitro* permeation studies of nanoemulsions containing ketoprofen as a model drug. *Drug Deliv.*, **2008**, *15*, 465-469.

[67] Modi, J.D.; Patel, J.K. Nanoemulsion-based gel formulation of aceclofenac for topical delivery. *Int. J. Pharm. Pharm. Sci. Res.*, **2011**, *1*, 6-12.

[68] Shakeel, F.; Baboota, S.; Ahuja, A.; Ali, J.; Aqil, M.; Shafiq, S. Nanoemulsions as vehicles for transdermal delivery of aceclofenac. *AAPS Pharm. Sci. Tech.*, **2007**, *8*, 191-199.

[69] Domínguez-Villegas, V.; Clares-Naveros, B.; García-López, M.L.; Calpena-Campmany, A.C.; Bustos-Zagal, P.; Garduño-Ramírez, M.L. Development and characterization of two nano-structured systems for topical application of flavanones isolated from Eysenhardtia platycarpa. *Colloids Surf. B*, **2014**, *116*, 183-192.

[70] Pratap, S.B.; Brajesh, K.; Jain, S.; Kausar, S. Development and characterization of a nanoemulsion gel formulation for transdermal delivery of carvedilol. *Int. J. Drug Dev. Res.*, **2012**, *4*, 151-161.

[71] Rizwan, M.; Aqil, M.; Azeem, A.; Talegaonkar, S.; Sultana, Y.; Ali, A. Enhanced transdermal delivery of carvedilol using nanoemulsion as a vehicle. *J. Exp. Nanosci.*, **2010**, *5*, 390-411.

[72] Varshosaz, J.; Andalib, S.; Tabbakhian, M.; Ebrahimzadeh, N. Development of lecithin nanoemulsion based organogels for permeation enhancement of metoprolol through rat skin. *J. Nanomater.*, **2013**, 6.

[73] Malgope, A.; Murthy, P.; Ramani, R.; Dey, S. Development of nanoemulsion as carrier for transdermal delivery of valsartan. *Int. J. Pharm. Chem. Sci.*, **2013**, *2*, 1655-1665.

[74] Shafiq-un-Nabi, S.; Shakeel, F.; Talegaonkar, S.; Ali, J.; Baboota, S.; Ahuja, A.; Khar, R.K.; Ali, M. Formulation development and optimization using nanoemulsion technique: a technical note. *AAPS Pharm. Sci. Tech.*, **2007**, *8*, E12-E17.

[75] Yadav, S.; Singh, D.; Poddar, S. Influence of components of nanoemulsion system for transdermal drug delivery of nimodipine. *Asian J. Pharm. Clin. Res.*, **2012**, *5*, 209-214.

[76] Kumar, D.; Aqil, M.; Rizwan, M.; Sultana, Y.; Ali, M. Investigation of a nanoemulsion as vehicle for transdermal delivery of amlodipine. *Die Pharmazie*, **2009**, *64*, 80-85.

[77] Wu, P.C.; Lin, Y-H.; Chang, J-S.; Huang, Y-B.; Tsai, Y-H. The effect of component of microemulsion for transdermal delivery of nicardipine hydrochloride. *Drug Dev. Ind. Pharm.*, **2010**, *36*, 1398-1403.

[78] Shafaat, K.; Kumar, B.; Das, S.k.; Rizwan, U-H.; Prajapati, S.K. Novel nanoemulsion as vehicles for transdermal delivery of clozapine: *In vitro* and *in vivo* studies. *Int. J. Pharm. Pharm. Sci.*, **2013**, 5.

[79] Patel, P.A.; Patil, S.C.; Kalaria, D.R.; Kalia, Y.N.; Patravale, V.B. Comparative *in vitro* and *in vivo* evaluation of lipid based nanocarriers of Huperzine A. *Int. J. Pharm.*, **2013**, *446*, 16-23.

[80] de Almeida, B.V.R.; Simon, A.; Sena, A.R.C.; Cabral, L.M.; de Sousa, V.P. Nanoemulsion containing dapsone for topical administration: a study of *in vitro* release and epidermal permeation. *Int. J. Nanomed.*, **2013**, *8*, 535-544.

[81] Yu, M.; Ma, H.; Lei, M.; Li, N.; Tan, F. *In vitro/in vivo* characterization of nanoemulsion formulation of metronidazole with improved skin targeting and anti-rosacea properties. *Eur. J. Pharm. Biopharm.*, **2014**, *88*, 92-103.

[82] Zhang, Y.; Gao, J.; Zheng, H.; Zhang, R.; Han, Y. The preparation of 3, 5-dihydroxy-4-isopropylstilbene nanoemulsion and *in vitro* release. *Int. J. Nanomed.*, **2011**, *6*, 649-657.

[83] Sugumar, S.; Ghosh, V.; Nirmala, M.J.; Mukherjee, A.; Chandrasekaran, N. Ultrasonic emulsification of eucalyptus oil nanoemulsion: Antibacterial activity against *Staphylococcus aureus* and wound healing activity in Wistar rats. *Ultrason. Sonochem.*, **2014**, *21*, 1044-1049.

[84] Fernández-Campos, F.; Clares, N.B.; López, S.O.; Alonso, M.C.; Calpena, C.A. Evaluation of novel nystatin nanoemulsion for skin candidosis infections. *Mycoses*, **2013**, *56*, 70-81.

[85] Elosaily, G.H. Formulation and *in-vitro* evaluation of nystatin nanoemulsion-based gel for topical delivery. *J. Am. Sci.*, **2012**, *8*(12), 541-548.

[86] Hussain, A.; Samad, A.; Nazish, I.; Ahmed, F.J. Nanocarrier-based topical drug delivery for an antifungal drug. *Drug Dev. Ind. Pharm.*, **2013**, *40*, 527-541.

[87] Schwarz, J.C.; Klang, V.; Karall, S.; Mahrhauser, D.; Resch, G.P.; Valenta, C. Optimisation of multiple W/O/W nanoemulsions for dermal delivery of aciclovir. *Int. J. Pharm.*, **2012**, *435*, 69-75.

[88] Botelho, M.A.; Queiroz, D.B.; Freitas, A.; Guerreiro, S.; Umbelino, S.; Barros, G.; Borges, B.; Ruela, R.; Almeida, J.G.; Quintans Jr, L. Effects of a new testosterone transdermal delivery system, Biolipid B2®-testosterone in healthy middle aged men: A confocal raman spectroscopy study. *J. Pharm. Sci. Innov.*, **2013**, *2*(2), 1.

[89] Botelho, M.A.; Queiroz, D.B.; Barros, G.; Guerreiro, S.; Fechine, P.; Umbelino, S.; Lyra, A.; Borges, B.; Freitas, A.; de Queiroz, D.C.; Ruela, R.; Almeida, J.G.; Quintans, L. Nanostructured transdermal hormone replacement therapy for relieving menopausal symptoms: a confocal Raman spectroscopy study. *Clinics*, **2014**, *69*, 75-82.

[90] Klang, V.; Matsko, N.; Zimmermann, A-M.; Vojnikovic, E.; Valenta, C. Enhancement of stability and skin permeation by sucrose stearate and cyclodextrins in progesterone nanoemulsions. *Int. J. Pharm.*, **2010**, *393*, 153-161.

[91] Li, B.; Ge, Z-Q. Nanostructured lipid carriers improve skin permeation and chemical stability of idebenone. *AAPS Pharm. Sci. Tech.*, **2012**, *13*, 276-283.

[92] Ruktanonchai, U.; Bejrapha, P.; Sakulkhu, U.; Opanasopit, P.; Bunyapraphatsara, N.; Junyaprasert, V.; Puttipipatkhachorn, S. Physicochemical characteristics, cytotoxicity, and antioxidant activity of three lipid nanoparticulate formulations of alpha-lipoic acid. *AAPS Pharm. Sci. Tech.*, **2009**, *10*, 227-234.

[93] Mitri, K.; Shegokar, R.; Gohla, S.; Anselmi, C.; Müller, R.H. Lipid nanocarriers for dermal delivery of lutein: preparation, characterization, stability and performance. *Int. J. Pharm.*, **2011**, *414*, 267-275.

[94] Puglia, C.; Damiani, E.; Offerta, A.; Rizza, L.; Tirendi, G.G.; Tarico, M.S.; Curreri, S.; Bonina, F.; Perrotta, R.E. Evaluation of nanostructured lipid carriers (NLC) and nanoemulsions as carriers for UV-filters: Characterization, *in vitro* penetration and photostability studies. *Eur. J. Pharm. Sci.*, **2014**, *51*, 211-217.

[95] Hanno, I.; Anselmi, C.; Bouchemal, K. Polyamide nanocapsules and nano-emulsions containing Parsol® MCX and Parsol® 1789: *in vitro* release, *ex vivo* skin penetration and photo-stability studies. *Pharm. Res.*, **2012**, *29*, 559-573.

[96] Silva, F.F.; Ricci-Júnior, E.; Mansur, C.R. Nanoemulsions containing octyl methoxycinnamate and solid particles of TiO_2: preparation, characterization and *in vitro* evaluation of the solar protection factor. *Drug Dev. Ind. Pharm.*, **2013**, *39*, 1378-1388.

[97] Silva, A.; Nunes, B.; De Oliveira, M.; Koester, L.S.; Mayorga, P.; Bassani, V.L.; Teixeira, H.F. Development of topical nanoemulsions containing the isoflavone genistein. *Pharmazie*, **2009**, *64*, 32-35.

[98] Shakeel, F.; Ramadan, W.; Gargum, H.M.; Singh, R. Preparation and *in vivo* evaluation of indomethacin loaded true nanoemulsions. *Scientia Pharm.*, **2010**, *78*, 47.

[99] Baspinar, Y.; Borchert, H-H. Penetration and release studies of positively and negatively charged nanoemulsions-Is there a benefit of the positive charge? *Inter. J. Pharm.*, **2012**, *430*, 247-252.

[100] Abla, M.; Banga, A. Formulation of tocopherol nanocarriers and *in vitro* delivery into human skin. *Inter. J. Cosmet. Sci.*, **2014**, *36*, 239-246.

[101] Clares, B.; Calpena, A.C.; Parra, A.; Abrego, G.; Alvarado, H.; Fangueiro, J.F.; Souto, E.B. Nanoemulsions (NEs), liposomes (LPs) and solid lipid nanoparticles (SLNs) for retinyl palmitate: Effect on skin permeation. *Int. J. Pharm.*, **2014**, *473*, 591-598.

Chapter 3:

Article for publication in “Die Pharmazie”

Chapter 3 is accessible in the form of a research article which was accepted in the journal entitled “Die Pharmazie” for publication.

Centre of Excellence for Pharmaceutical Sciences, North-West University, Private Bag X6001, Potchefstroom, 2520, South Africa

Development and validation of the simultaneous determination of artemisone, clofazimine and decoquinate with HPLC

Authors: Jan L. du Preez, Marique E. Aucamp, Cornel Burger, Minja Gerber*, Joe M. Viljoen, Lindi van Zyl and Jeanetta du Plessis.

* Corresponding author: Centre of Excellence for Pharmaceutical Sciences, North-West University, Private Bag X6001, Potchefstroom, 2520, South Africa. Tel.: +2718 299 2328; Fax: +2787 231 5432. E-mail address: Minja.Gerber@nwu.ac.za

Abstract

The aim of this study is to develop and validate a novel HPLC method for the simultaneous analysis of artemisone, clofazimine and decoquinate. Detection was obtained at two wavelengths; 284 nm (clofazimine) and 210 nm (artemisone and decoquinate). Gradient elution was used with mobile phase A (**A**) consisting of 0.005 M sodium octanesulphonic-acid (pH 3.5) and mobile phase B (**B**) of HPLC grade acetonitrile. The flow rate was set to 1.0 ml/min with (**A**) at 35% and (**B**) at 65% for 2 min, followed by a gradient shift of 10/90% ((**A**)/(**B**)) over a duration of 4 min. After 10 min, the initial gradient conditions were readjusted to 35/65% ((**A**)/(**B**)). Distinctive peaks were identified for clofazimine, artemisone and decoquinate, respectively. The proposed HPLC assay method was validated and found to be reliable, reproducible and accurate for simultaneous analysis of the three compounds.

1. Introduction

Tuberculosis (TB) poses a significant public health threat, with 20 - 40% of the world's population being affected. Less than 14% of TB cases are extra-pulmonary, of which only 1.0 - 1.5% manifests as cutaneous tuberculosis (CTB). CTB is quite an exceptional presentation of TB; resulting in it being undefined and often misdiagnosed [Bravo and Gotuzzo, 2007; Rullán et al. 2012; Carman and Patel, 2014; Galagan et al. 2014].

A fixed-dose combination of artemisone, clofazimine and decoquinate formulated in a topical dosage form was chosen as a possible therapy to effectively treat CTB. The combination of these three APIs (active pharmaceutical ingredients) was based on the combination strategy of oxidant and redox APIs for the treatment of malaria and TB. The combination of the three APIs formed part of an investigative study; since the effectivity of decoquinate against TB has not yet been established, but its lipophilicity renders it an attractive compound for assessment. Although clofazimine was considered ineffective against pulmonary TB, recent advances in technology have renewed the use thereof for TB treatment, and therefore it was included in this combination as an API with redox capabilities. Artemisone is effective against *Plasmodium falciparum* (malaria), but was included in this study as an oxidant API [Cholo et al. 2011; Steyn et al. 2011; Haynes, 2013].

Clofazimine ($C_{27}H_{22}Cl_2N_4$) (Fig. 1A) [modified from Cholo et al. 2011] has an aqueous solubility of 10 mg/L, a log P of 7.60, a pKa of 8.51, a melting point of 210 - 212°C and a molecular weight of 473.40 g/mol [Holdiness, 1989; Brittain and Florey, 1992; Cholo et al. 2011; Bolla and Nangia, 2012; Srikanth et al. 2014].

Artemisone ($C_{19}H_{31}NO_6S$) (Fig. 1B) [modified from Biamonte et al. 2013], in addition, has an aqueous solubility of 89 mg/L (pH 7.2, water), a log P of 2.49, a melting point of ≈199°C and a molecular weight of 401.52 g/mol [Nagelschmitz et al. 2008; Dunay et al. 2011; Steyn et al. 2011]. Very little information is available for decoquinate; since it has mainly been used as a veterinary API. Decoquinate ($C_{24}H_{36}NO_5$) (Fig. 1C) [modified from Biamonte et al. 2013] has a log P of 7.80, a pKa of 10.76, a melting point of ≈219°C and a molecular weight of 417.54 g/mol [Nam et al. 2011; Iglesias et al. 2014]. Currently, no HPLC method for the simultaneous determination of these three compounds is available in literature. Therefore, this method was developed and validated to determine the concentration assays of the three compounds simultaneously for different routes of administration such as solid oral dosage forms or transdermal formulations. This method was developed and validated based on the International Conference on Harmonisation (ICH) and current Good Manufacturing Practice (cGMP) guidelines and parameters [ICH, 2005; FDA, 2011].

2. Investigations, results and discussion

The proposed method was validated in terms of linearity, accuracy, precision, limit of detection (LOD), limit of quantitation (LOQ), system suitability and robustness. Thereafter the solubility of all three APIs was determined in different solvents (Table 1). The solubility of decoquinate, when compared to the other two APIs, was the lowest in all investigated solvents, consequently the solubility thereof was used as the deciding parameter during the method development steps. The solubility of decoquinate in tetrahydrofuran (THF) was the highest, however, since it is considered a toxic solvent; it will not be the solvent of choice during pre-formulation, dosage form development or API release testing from either solid or semi-solid formulations. Hence, ethanol was chosen as the main solvent.

The linearity was determined by constructing a regression plot of API concentration versus peak area response, allowing the calculation of a regression equation for each API. The resulting equations are listed in Table 2. The correlation coefficient (r^2) was also determined, where the strongest linear relationship is indicated by a correlation coefficient of 1 [Krause, 2003; UNODC, 2009]. The accuracy of the three compounds can be seen in Table 2. The mean recovery percentages were all between 98 - 102% (%RSD < 15%), thus complying with validation requirements for accuracy parameters.

Precision was conducted during a three-day period at three concentration levels (Table 2). All the parameters mentioned adhered to the specifications and thus the method was found to be accurate and precise. The stability of artemisone, clofazimine and decoquinate was evaluated, and no significant instability was observed for at least 24 h (Table 2). None of the API concentrations deviated with more than 15% and were consequently found to be stable for at least 24 h after preparation. System suitability was determined with the injection precision for retention times and peak areas as depicted in Table 2. System suitability was determined from six replicate injections. The obtained peaks were analysed in terms of peak area and retention times. All %RSD values were less than 2% (Table 2) and as a result the method was found to be suitable for the HPLC system.

The LOQ is the lowest concentration of API that can be quantitatively ascertained, above which analysis is possible with the specified degree of accuracy and precision. LOQ is used particularly for determining impurities and/or degradation products [ICH, 2005; VICH, 2015]. To ensure whether LOQ is accurate, the

API should be injected at the calculated LOQ concentration (n = 6) and the %RSD should be calculated for each concentration. %RSD variation should not exceed 20 [Krause, 2003; ICH, 2005; Westgard, 2008; Huber, 2010; VICH, 2015; González et al. 2014]. The LOD, on the other hand, can be determined according to several methods, though the method used in this study is based on the standard deviation of the regression line or the y-intercept and the slope of the calibration curve. The calculated LOD was 1.98 µg/ml for artemisone, 3.11 µg/ml for clofazimine and 2.29 µg/ml for decoquinate. Confirmation of the LOD required injecting the samples at the calculated concentration six times. The experimental LOD obtained was thus 4.42 µg/ml (%RSD 19.68), 0.042 µg/ml (%RSD 17.73) and 0.703 µg/ml (%RSD 17.79) for artemisone, clofazimine and decoquinate, respectively. LOQ was subsequently determined as 13.39 µg/ml for artemisone, 0.13 µg/ml for clofazimine and 2.13 µg/ml for decoquinate.

Since there is currently no dosage form containing this combination of compounds available on the market, it was decided to make two solutions containing possible excipients that is normally included in a solid oral dosage form and a transdermal/topical delivery system, in order in order to test the sensitivity and selectivity of the method. The solution for solid oral dosage form contained the three APIs, talc, microcrystalline cellulose, polyvinylpyrrolidone (PVP 30), lactose, magnesium stearate, vinylpyrrolidone-vinyl acetate copolymer (Kollidon® VA64) and Pluronic® F-127 dissolved in absolute ethanol in unspecified concentrations. The solution prepared for transdermal/topical delivery contained the three APIs, polysorbate 20 (Tween® 20), polysorbate 80 (Tween® 80), sorbitan monostearate (Span® 60), phosphatidylcholine, cholesterol, safflower oil and olive oil dissolved in absolute ethanol in unspecified concentrations. As observed from Fig. 2 - 4 the three compounds delivered peaks at the determined retention times with little to no interference from the different excipients, which can possibly be used during formulation of solid oral dosage forms and transdermal/topical delivery systems. In addition to the novelty for the simultaneous quantification of artemisone, clofazimine and decoquinate the method is reliable and sensitive which complies with the ICH guidelines for method validation. Validation parameters such as linearity, limit of detection and quantitation, accuracy, precision, sample stability and system suitability were established. The reproducible method was also used to determine sensitivity of the method when applying it to an excipient mixture for a possible solid oral dosage form and for a transdermal/topical delivery system. The method was found to be adequate in quantifying the three APIs with virtually no interference.

3. Experimental

An Agilent® 1100 Series HPLC which was used during this study consisted of an Agilent® 1100 pump, diode array detector, and an autosampler injector module, and ChemStation Rev. A.10.02 software was utilised for data acquisition and analysis (Agilent Technologies, Palo Alto, CA). A Restek Ultra C_{18} fully endcapped reversed phase column (250 x 4.6 mm, 5 µm) was used with 100 Å pores, a 20% carbon load (Restek corporation, Bellefonte, US), a pH range of 2.5 – 8.0 and a temperature limit of 80°C. Gradient elution was used with mobile phase A (**A**) consisting of 0.005 M sodium octanesulphonic-acid (pH 3.5) and mobile phase B (**B**) comprising of HPLC grade acetonitrile. The flow rate was set to 1.0 ml/min with (**A**) at 35% and (**B**) at 65% for 2 min, followed by a gradient shift of 10/90% ((**A**)/(**B**)) over a duration of 4 min. After 10 min the initial gradient conditions were readjusted to 35/65% ((**A**)/(**B**)). An injection volume of 20 µl was used and the UV detection was set at 210 and 284 nm. Retention times were approximately 6.3 min, 7.3

min and 9.8 min for clofazimine, artemisone and decoquinate, respectively and the run time was set to 15 min. Ethanol absolute (99.7%) was used as the solvent throughout the method validation.

Acknowledgements

This work was carried out with the financial support of the South African National Research Foundation (NRF) (Grants no. IFRR81178 and CPRR13091742482); the South African Medical Research Council (MRC) for the Flagship Project MALTB-Redox; and the Centre of Excellence for Pharmaceutical Sciences (Pharmacen) of the North-West University, Potchefstroom Campus, South Africa.

Disclaimer

Any opinions, findings and conclusions, or recommendations expressed in this material are those of the authors and therefore the NRF does not accept any liability in regard thereto.

References

Biamonte MA, Wanner J, Le Roch KG (2013) Recent advances in malaria drug discovery. Bioorg Med Chem Lett 23: 2829 - 2843.

Bolla G, Nangia A (2012) Clofazimine Mesylate: A high solubility stable salt. Cryst Growth Des 12: 6250 - 6259.

Bravo FG, Gotuzzo E (2007) Cutaneous tuberculosis. Clin Dermatol 25: 173 - 180.

Brittain HG, Florey K (1992) Profiles of drug substances, excipients and related methodology. In: Brittain H (ed.) 1st ed., London, 696p.

Carman AS, Patel AG (2014) Science with societal implications: detecting Mycobacterium tuberculosis in Africa. Clin Microbiol Newsl 36: 73 - 77.

FDA (2011) Current good manufacturing process Guidance for Industry. Process validation: General principles and practices .CGMP [online]. Available from: https://www.fda.gov/ohrms/dockets/98fr/fda-2008-d-0559-gdl.pdf [Accessed 20 July 2016].

Cholo MC, Steel HC, Fourie PB, Germishuizen WA, Anderson R (2011) Clofazimine: current status and future prospects. J Antimicrob Chemother 67: 290 - 298.

Dunay IR, Chi Chan W, Haynes RK, Sibley LD (2009) Artemisone and artemiside control acute and reactivated toxoplasmosis in a murine model. Int J Antimicrob Agents 53: 4450 - 4456.

Galagan JE (2014) Genomic insights into tuberculosis. Nat Rev Genet 15: 307e20.

González O, Blanco ME, Iriarte G, Bartolomé L, Maguregui MI, Alonso RM (2014) Bioanalytical chromatographic method validation according to current regulations, with special focus on the non-well defined parameters limit of quantification, robustness and matrix effect. J Chromatogr A 1353: 10 - 27.

Haynes, R.K. (2013) MRC South African University Flagship Projects: Project Proposal. Development to the clinical phase of oxidant and redox drug combinations for treatment of malaria. TB and related diseases [online]. Available from: http://www-chem.ust.hk/Seminars/2016/201610/Haynes%20Abstract%20Chem%20Dep%20HKUST%20041016.pdf [Accessed 20 April 2017]

Holdiness MR (1989) Clinical pharmacokinetics of clofazimine: a review. Clin Pharmacokinet 16: 74 - 85.

Huber l (2010) Validation of Analytical Methods. A Primer, Agilent Technologies, Germany, (Publ. No. 5990-5140EN).

ICH (2005) International conference on harmonisation of technical requirements for registration of pharmaceuticals for human use Validation of analytical procedures: Text and methodology Q2(R1). [online]. Available from: https://www.ich.org/fileadmin/Public_Web_Site/ICH_Products/Guidelines/Quality/Q2_R1/Step4/Q2_R1__Guideline.pdf [Accessed 20 April 2017].

Iglesias A, Nebot C, Vázquez BI, Miranda JM, Abuín CMF, Cepeda A (2014) Detection of veterinary drug residues in surface waters collected nearby farming areas in Galicia, North of Spain. Environ Sci Pollut Res 21: 2367 - 2377.

Krause SO (2003) Good analytical method validation practice: Deriving acceptance criteria for the AMV protocol – Part II. J Val Tech 9: 162 - 178.

Nagelschmitz J, Voith B, Wensing G, Roemer A, Fugmann B, Haynes RK, Kotecka BM, Rieckmann KH, Edstein MD (2008) First assessment in humans of the safety, tolerability, pharmacokinetics, and *ex vivo* pharmacodynamics antimalarial activity of the new artemisinin derivative artemisone. Antimicrob Agents Chemother 52: 3085 - 3091.

Nam T, McNamara CW, Bopp S, Dharia NV, Meister S, Bonamy GMC, Plouffe DM, Kato N, McCormack S, Bursulaya B, Ke H, Vaidya AB, Schultz PG, Winzeler EA (2011) A chemical genomic analysis of decoquinate, a *Plasmodium falciparum* cytochrome b inhibitor. ACS Chem Biol 6: 1214 - 1222.

Rullán J, Seijo-Montes RE, Vaillant A, Sánchez NP. Cutaneous manifestations of pulmonary disease. In: Sánchez NP (ed.) Atlas of dermatology in internal medicine. 14th ed., San Juan, Puerto Rico, p. 17 - 30.

Srikanth CH, Joshi P, Bikkasani AK, Porwal K, Gayen JR (2014) Bone distribution study of antileprotic drug clofazimine in rat bone marrow cells by a sensitive reverse phase liquid chromatography method. J Chromatogr B 960: 82 - 86.

Steyn JD, Wiesner L, Du Plessis LH, Grobler AF, Smith PJ, Chan WC, Haynes RK, Kotzé AF (2011) Absorption of the novel artemisinin derivatives artemisone and artemiside: potential application of Pheroid™ technology. Int J Pharm 414: 260 - 266.

VICH: International cooperation on harmonisation of technical requirements for registration of veterinary medicinal products (2015) Guidance for industry. Studies to evaluate the metabolism and residue kinetics of veterinary drugs in food-producing animals: Validation of analytical methods used in residue depletion studies (VICH GL49(R)). 23p.

Westgard JO (2008) Basic Method Validation: training in analytical quality management for healthcare laboratories. In: Westgard WI (ed.) 3rd ed. Madison QC, 320 pp.

Table 1: Solubility **(µg/ml)** (37°C) determined for artemisone, clofazimine and decoquinate in nine different solvents

	Artemisone	Clofazimine	Decoquinate
Water	100.50	0.05	0.00
PBS (pH 7.4)	86.01	0.00	1.21
Trisaminomethane (pH 7.4)	99.07	0.00	0.00
Ethanol	44 600.00	1 824.70	181.70
Methanol	46 541.60	827.74	163.13
Isopropanol	26 351.00	1 018.53	160.08
Acetone	105 923.00	2 181.64	18.95
Acetonitrile	201 960.00	1 207.80	12.98
THF	194 190.00	143 410.00	241.13

Table 2: Obtained validation parameters for the three compounds

Linearity			
	Artemisone (n = 9)	**Clofazimine (n = 7)**	**Decoquinate (n = 9)**
Concentration range (µg/ml)	5.00 - 400.10	0.93 - 55.86	1.50 - 120.10
Regression equation	y = 1.079x - 0.375	y = 72.623x + 42.390	y = 23.261x + 51.866
Correlation coefficient (r^2)	0.9999	0.9937	0.9989
Accuracy			
Mean recovery (%) (%RSD)	99.9 (± 1.4)	100.0 (± 0.3)	99.3 (± 7.5)
Stability			
Max sample deviation from hour zero (%) (%RSD)	2.5 (± 0.8)	0.2 (± 0.5)	5.0 (± 1.1)
System suitability			
Retention time (min) (%RSD)	7.3 (± 0.1)	6.3 (± 0.3)	9.9 (± 0.1)
Peak area (%RSD)	23.19 (± 0.16)	430.76 (± 0.90)	187.10 (± 1.71)

Table 3: Precision data for artemisone, clofazimine and decoquinate

		Artemisone	Clofazimine	Decoquinate
Concentration (µl/ml)		393.0	74.0	128.0
Repeatability (intra-day)	**%RSD**	1.03	0.21	4.55
	Mean recovery (%)	99.86	99.99	99.57
Intermediate precision (inter-day)	**%RSD (day 2)**	0.78	0.17	3.68
	Mean recovery percentage (day 2)	99.96	100.01	99.67
	%RSD (day 3)	1.20	0.14	4.33
	Mean recovery percentage (day 3)	99.89	99.99	99.63
	p-value of ANOVA (for the three days)	0.938	0.958	0.862

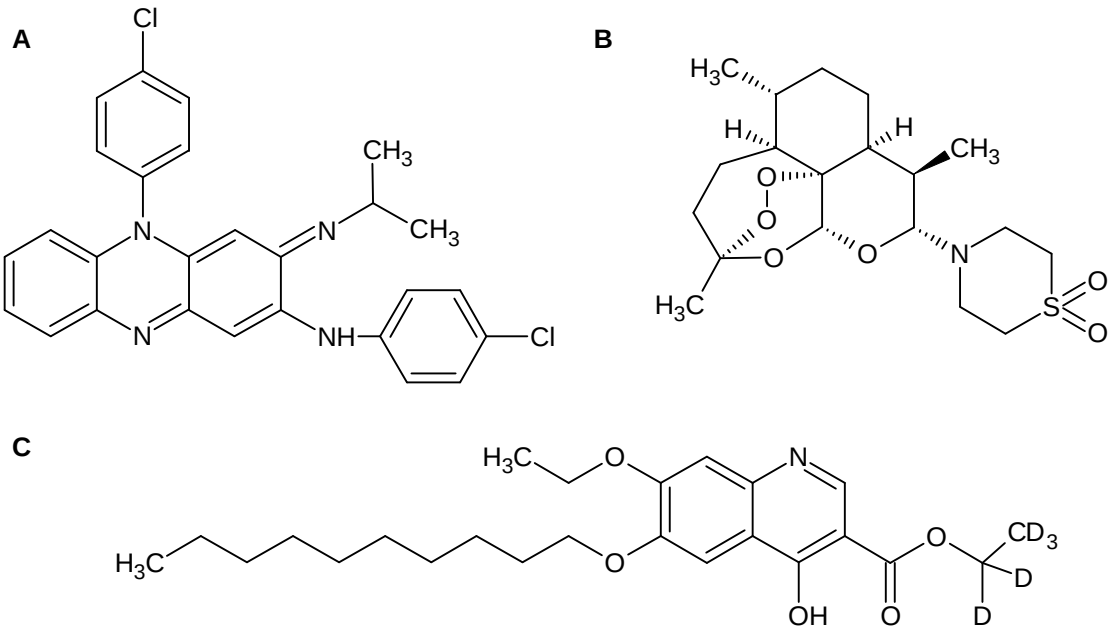

Fig. 1: Molecular structures of A) clofazimine, B) artemisone and C) decoquinate.

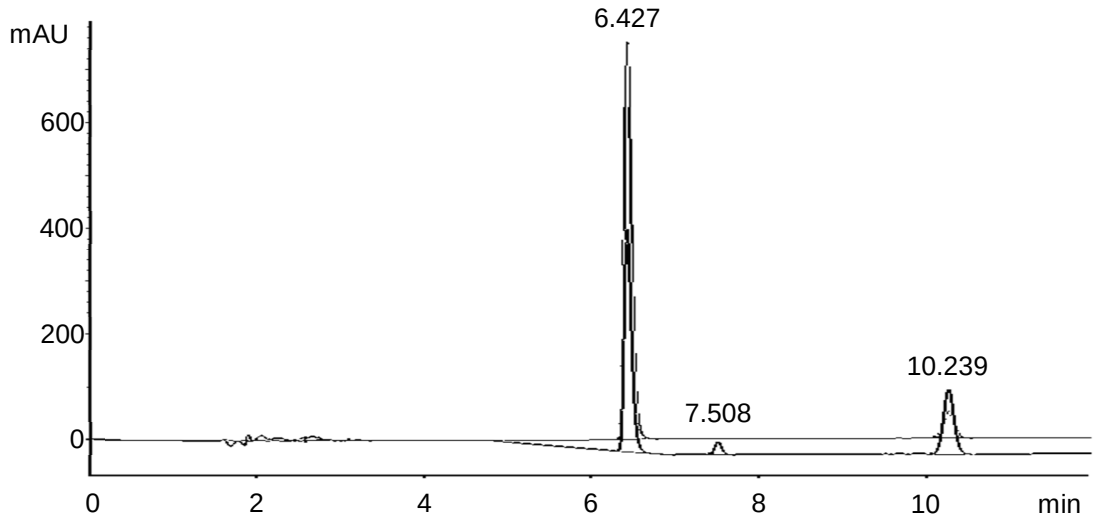

Fig. 2: Chromatographs of a standard solution containing clofazimine, artemisone and decoquinate, respectively. The top chromatogram signifying detection obtained at 284 nm and the bottom chromatogram showing detection at 210 nm.

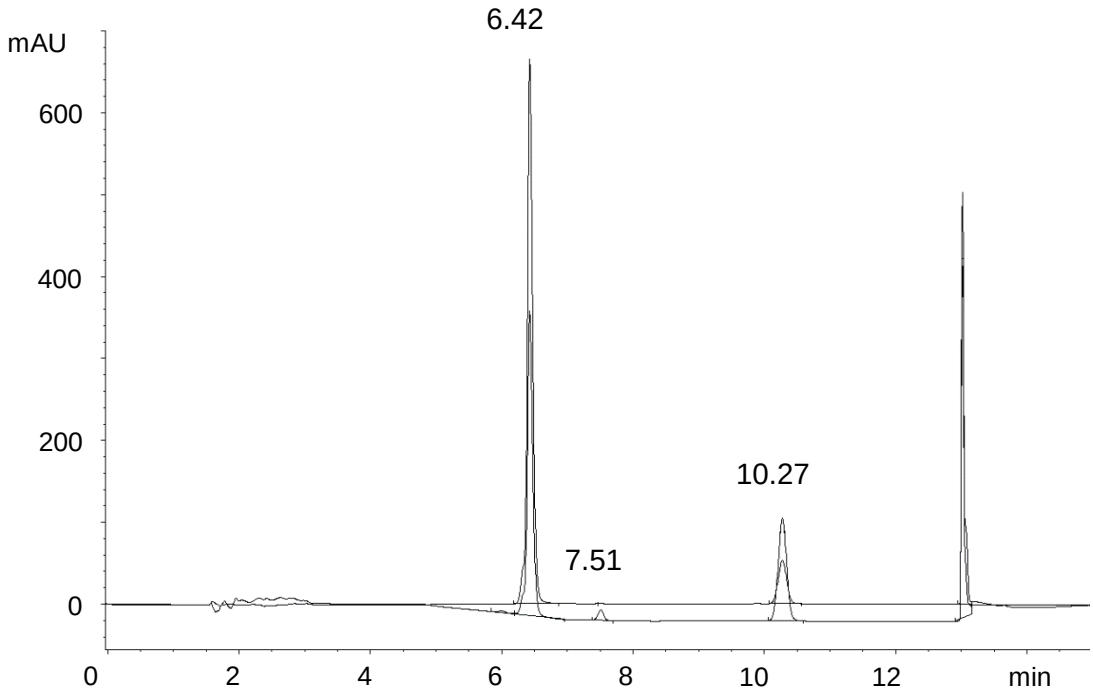

Fig. 3: Chromatographs obtained with a solution containing typical excipients used in formulation of solid oral dosage forms, observing clofazimine, artemisone and decoquinate, respectively. The top chromatogram signifying detection obtained at 284 nm and the bottom chromatogram showing detection at 210 nm.

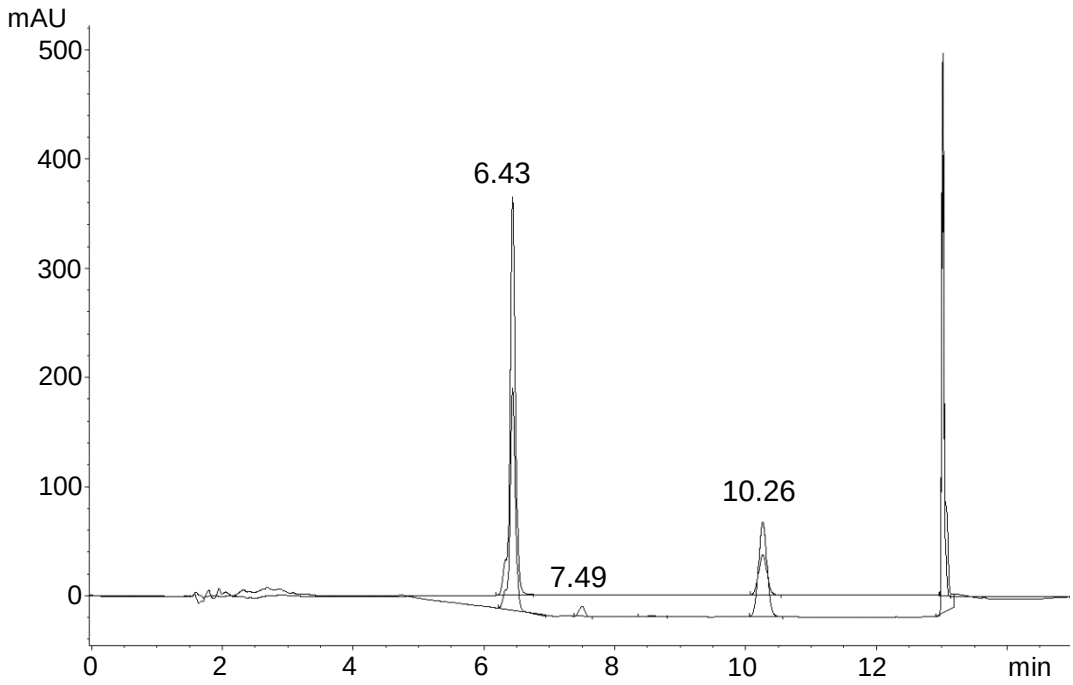

Fig. 4: Chromatographs of excipient solution for transdermal/topical delivery systems showing clofazimine, artemisone, and decoquinate, respectively. The top chromatogram signifying detection obtained at 284 nm and the bottom chromatogram showing detection at 210 nm.

Chapter 4:

Article for the publication in "Drug Development and Industrial Pharmacy"

Chapter 4 is accessible in the form of a research article, which will be submitted to the journal "Drug Development and Industrial Pharmacy" for publication. The authors guide for this journal can be seen in Appendix E; the article is written in Times New Roman font (12 point) with double line spacing and US English and formatted according to their specifications.

Pre-formulation of nano-emulsions containing clofazimine, artemisone and decoquinate together with natural oils for topical applications

Cornel Burger, Minja Gerber*, Jeanetta du Plessis and Marique Aucamp

Centre of Excellence for Pharmaceutical Sciences (Pharmacen™), North-West University, Private Bag X6001, Potchefstroom, 2520, South-Africa.

*Corresponding author: Tel: +2718 299 2328; Fax: +2787 231 5432. E-mail address: Minja.Gerber@nwu.ac.za (M. Gerber).

Currently a suitable formulation containing anti-tuberculosis drugs for the treatment of cutaneous tuberculosis does not exist. In this study clofazimine, artemisone and decoquinate were prepared separately and in combination with one another in nano-emulsions containing natural oils. This study shows that the three compounds can be combined successfully without drug-drug or drug-oil incompatibility.

Pre-formulation of nano-emulsions containing clofazimine, artemisone and decoquinate together with natural oils for topical applications

Objective: To assess the solubility, compatibility and characterization of clofazimine (CLF), artemisone (ART) and decoquinate (DQ) in nano-emulsions containing natural oils.

Significance: CLF, ART and DQ can now be combined in a formulation for the possible future treatment of cutaneous tuberculosis (CTB)

Methods: Solubility determination was done in triplicate in 9 different solvents at 32±1°C. Compatibility studies with all the possible active pharmaceutical ingredient (API)/excipient combinations were done by means of hot-stage microscopy (HSM) and isothermal microcalorimetry. Nano-emulsion characterization included the testing of pH, viscosity, morphology, zeta-potential, drug entrapment efficiency and droplet size.

Results: CLF, ART and DQ are poorly to completely insoluble in water (0.05 µg/ml, 100.5 µg/ml and 0.00 µg/ml, respectively) and the best solubility was seen in tetrahydrofuran (THF) (143.41 mg/ml, 194.19 mg/ml and 0.241 mg/ml, respectively). At a pH of 5, CLF, ART and DQ unionized species were calculated to be 99.69%, 0.098% and 99.98%, respectively. In terms of pre-formulation studies all APIs are compatible with either olive or safflower oil, separately or in combination. CLF and ART depicted some incompatibilities when combined with excipients such as Tween® 80 or Span® 60. DQ showed no incompatibilities with either oils or excipients. Zeta-potential ranged from -30 mV to -38 mV, which indicated that the nano-emulsions were stable. Viscosity was very low and droplet sizes ranged from 83-130 nm. Drug entrapment yielded very high percentages (>96%).

Conclusions: No incompatibility was seen during microcalorimetry or HSM studies indicating that the APIs can be combined and used in the tested formulations. Stable nano-emulsions containing natural oils can be formulated and incorporated with APIs such as CLF, ART and DQ for possible future topical delivery of CTB.

Keywords: pre-formulation, nano-emulsions, characterization, natural oil, clofazimine, artemisone, decoquinate, microcalorimetry, hot stage microscopy

Introduction

Tuberculosis (TB) is an contagious disease, primarily caused by airborne *Mycobacterium tuberculosis*[1,2], which results in a chronic bloody cough, amongst other serious symptoms. This highly contagious disease is life threatening and still leads to great global health problems. At least one out of three individuals is infected worldwide[3,4,] with at least two million deaths and nine million new cases reported each year[5]. However, although this is a disease with a high morbidity and mortality rate, most TB patients can be treated successfully through proper medicinal therapy[6]. TB primarily affects the lungs through *M. bovis* and the *M. tuberculosis* bacteria and can manifest in other body areas, such as the epidermis, referred to as cutaneous TB (CTB)[7]. TB manifests as an extra-pulmonary disease in about 8.4 to 13.7%, regardless of being such a prevalent infection. A small predominance of 1 to 2% of all cases involving extra-pulmonary TB consists of CTB[8-10], nevertheless, when the extraordinary incidence of TB is taken into consideration in many developing countries, these statistics can become noteworthy[11].

Challenges are faced in TB treatment, since regimens are very lengthy and become limited in effectiveness, which affects the patient's compliance to the treatment regimes. CTB is frequently unappealing and therefore has a significant impact on a patient's societal and emotive welfare. The main limitation is that no topical medical treatment has been developed for CTB yet, nonetheless current oral regimes show worthy potential[12]. No complete effectiveness has been achieved for CTB. Different active pharmaceutical ingredients (APIs), i.e. clofazimine (CLF), artemisone (ART) and decoquinate (DQ), were investigated during this study, for the possible promotion of future topical CTB treatments. Although future topical therapy will not substitute any systemic treatment, it is still necessary to investigate alternative compounds, which can be used as adjunct therapy to the normal TB treatment regimens. Difficulty arises to treat patients while the progression of infection and antibiotic resistance[4,13] develops leading to multidrug-resistant TB (MDR-TB) and extensively drug-resistant TB (XDR-TB)[14-16]. The amplified

occurrence of MDR-TB creates a critical necessity for alternative therapy regimens, as well as new effective anti-tuberculosis drugs[17].

CLF is a poorly water soluble redox API, which belongs to the riminophenazine class[19,21]. Marketed as an anti-mycobacterial drug for the treatment of leprosy[18], it also has proven anti-inflammatory[19] and dye properties[20]. Even though CLF crystallizes out of the macrophage, it still shows *in vitro* activity against *Mycobacterium tuberculosis* MDR-TB[21-23]. Currently, it is included in the World Health Organizations (WHO) recommended triple drug regime for the treatment of multi-bacillary leprosy[24].

ART is also known as a 10-alkylaminoartemisinin, which can be synthesized from dihydroartemisinin in a one-step process[25]. No metabolic stability, neurotoxicity or increased plasmodial activity is seen in ART[26]. Three metabolites (M1, M2 and M3) are primarily acquired from the metabolizing process by cytochrome 3A4 (CYP3A4) in the liver and possess inherent anti-malarial activity[27] and attributable to their diminutive half-lives, they should be combined with other compounds to increase their half-lives[28].

DQ is a 4-hydroxy quinolone approved veterinary drug[29]. The compounds mechanism of action is to disrupt mitochondrial cytochrome system electron transport and respiration in coccidia[30,31]. No anti-TB activity has been established for DQ yet, but it is incorporated as a third component due to its high lipophilicity. The rationale of the compounds being combined is that ART (oxidant drug) generates a pulse of reactive oxygen species/reactive oxygen-nitrogen species (ROS/RONS) by terminating reduced deazaflavin. It can also cause a cytotoxic effect by diverting electron supply from the nicotinamide adenine dinucleotide phosphate-oxidase (NADPH) in mycothiol reductase (MR). CLF (redox drug) enhances the oxidative stress by scavenging electron supply from NADPH caused by the oxidant drug also producing a cytotoxic effect. Consequently, CLF will intensify the ART's drug mechanism[32.] In this combination, the function of DQ will complement the mechanisms of the aforementioned compounds, where it will disrupt the electron transport[33,34].

Materials and methods

Materials

CLF and ART were kindly donated from Cipla (India), whilst DQ was obtained from the Hohance (Shanghai, China). Safflower and olive oil were purchased from CJP Chemicals (Johannesburg, South Africa). Analytical grade acetonitrile (ACN), Span® 60 and Tween® 80 were obtained from Merck (Johannesburg, South Africa). Absolute ethanol (99.7%) was obtained from Associated Chemical Enterprises (Johannesburg, South Africa). Potassium dihydrogen phosphate, sodium hydroxide, acetone, methanol, isopropanol, tetrahydrofuran and Tris (hydroxymethyl) aminomethane, sodium octanesulfonic-acid, and ammonia were all of analytical grade and purchased from Merck (Johannesburg, South Africa). The water used in this study was purified by a Milli-Q® water purification system from Millipore (Milford, USA).

Solubility of compounds

Equilibrium solubility concentrations of CLF, ART and DQ were determined in nine different solvents. Solubility studies were done to determine which solvent would be exceptionally suitable to dissolve all three APIs simultaneously, since CLF's and DQ's solubility is particularly poor in most aqueous diluents[35,36]. The solvents used for the solubility study were absolute ethanol (99.7%), ACN, acetone, methanol, phosphate buffer solution (pH7.4), propan-2-ol (isopropanol), Tris buffer solution (pH 7.5), tetrahydrofuran (THF) and water. The solubility concentrations of all three drugs were determined in the manner described below.

An excess amount of drug was placed in a test tube with 5 ml of the solvent; thereafter the tube was placed in a water bath continuously mixing at 32°C ± 1°C (temperature of skin surface) for 24 hrs. Throughout the study, the tubes were checked regularly to ensure that an excess amount of drug was still present within the sample. After 24 hrs, the solution was filtered through a 0.45 µm membrane filter. Ethanol was used to dilute the solution if needed to prevent precipitation. Subsequently, the samples were transferred to HPLC vials to be analysed by means of HPLC analysis. For each drug and solvent combination, the experiment was performed in triplicate.

Chromatographic conditions

An Agilent® 1100 Series HPLC was used, which consisted of an Agilent® 1100 pump, diode array detector, autosampler injection mechanism and ChemStation Rev. A.10.02 software for data acquisition and analysis (Agilent Technologies, USA). A Restek Ultra C_{18} fully end-capped reversed phase column (250 x 4.6 mm, 5 µm) was used as stationary phase (Restek Corporation, USA). The HPLC analyses were done by applying a gradient method. Mobile phase A consisted of 0.005 M sodium 1-octanesulfonate solution, 2% v/v 2 M ammonia solution with the pH adjusted to 3.5 with 2 M phosphoric acid and HPLC grade ACN (mobile phase B). The flow rate for both mobile phases was set at 1 ml/min at 35% for A and 65% for B for 2 min. After 4 min the gradient shifted to 10/90% (A:B). Initial conditions were regained to 35/65% after 10 min. The UV detection was set at 210 nm and 284 nm and 20 µl was used as the injection volume. The run time was set at 15 min and retention times were approximately 6.3 min, 7.3 min and 9.8 min for CLF, ART and DQ, respectively. For sample preparation, all three APIs were dissolved in ethanol (99.7%). The prepared samples were subsequently filtered through a 0.45 µm polyvinylidene fluoride (PVDF) filter[37].

Compatibility studies

Compatibility between APIs and excipients are of utmost importance, since the stability and therefore subsequent bioavailability of the dosage forms can be affected. These studies determined potential physical, as well as chemical interactions between a compound and the excipient[38].

Hot stage microscope (HSM)

A Nikon Eclipse E4000 microscope, fitted with a Nikon DS-Fi1 camera (Nikon, Japan) and a Linkam THMS600 heating stage, equipped with a T95 LinkPad temperature controller (Surrey, England), was used for HSM experiments. A small amount of sample was placed on the center of a glass microscope slide. The sample was heated at a rate of 10°C/min and photomicrographs were taken during the heating process.

Isothermal microcalorimetry

Compatibility testing was done by means of a 2277 thermal activity monitor (TAMIII) (TA Instruments, USA), equipped with an oil bath, with a stability of ±100 µK over 24 hrs. For compatibility studies, the heat flow was measured for the individual constituents, as well as the combinations. Approximately 50 mg of each sample to be analyzed was weighed into a glass ampoule and subsequently sealed. The compatibility testing was performed at 32°C

Preparation of nano-emulsions

Nano-emulsions were prepared in the ratios provided in Table 1 and 2. Prior to formulation, all the ingredients were accurately weighed. The nano-emulsions were prepared by mixing Tween® 80 and water (water phase) in a beaker. In another beaker, Span® 60 and olive or safflower oil (oil phase) were mixed. Both mixtures were mixed using a magnetic stirrer hotplate (60°C). After the temperature of 60°C was reached and each phase was stable after 15 min of mixing, the oil phase was added very slowly to the water phase, while continuing to mix at a constant stirring speed and maintaining the temperature at 60°C. Subsequently, it was placed in a beaker with ice and sonicated for 10 min at a power of 40 Watt[39]. Subsequently the following emulsions were made, i.e. safflower and CLF (S1), safflower and ART (S2), safflower and DQ (S3), safflower combined with CLF, ART and DQ (S4), olive and CLF (O1), olive and ART (O2), olive and DQ (O3) and olive combined with CLF, ART and DQ (O4).

[Table 1 near here]

[Table 2 near here]

Characterization of nano-emulsion dispersions

The physical characterization of the nano-emulsion dispersions were performed according to the following parameters: pH, viscosity, droplet size, zeta-potential and drug entrapment efficiency.

pH

The pH of the formulations was determined by means of the Mettler Toledo SevenMulti pH meter (InLab® 410 NTC electrode 9823) (Greifensee, Switzerland). Accuracy of the pH meter was verified by calibration each time prior to use.

Viscosity

The viscosity was determined using a Brookfield® Viscometer (Stoughton, USA). A water bath was connected to the viscosity meter and by means of a Brookfield® temperature controller, the temperature was maintained at 25.0±0.5°C. The consistency of the formulations was very thin and therefore a CS-14 spindle was used to ensure appropriate torque. The Helipath stand (D20733) rose and lowered the spindle at a rate of 7/8 inch/min. During this time, the T-bar spindle rotated at 100 rpm in the formulation. Viscosity readings were taken every 10 sec over a period of 5 min. Subsequently, the mean viscosity value for each formulation was calculated.

Droplet size

A Zetasizer Nano ZS (Malvern® Instruments LTD, Worcestershire, UK) was used to determine the droplet size of the formulations at ambient temperature. Triplicate samples were prepared and analyzed.

Zeta-potential

The zeta-potential for each formulation was determined at ambient temperature by means of the Zetasizer Nano ZS (Malvern® Instruments LTD, Worcestershire, UK). Samples were prepared and analyzed in triplicate.

Drug entrapment efficacy

The entrapment efficiency (EE%) was used to determine the difference between the total amount of the drug and the free drug in a sample. The eight nano-emulsion samples were centrifuged at 25 000 rpm for 90 min at room temperature (23.0°C ±0.5°C), using an Optima™ L-100 XP ultracentrifuge (Beckman Coulter, California, USA). The free drug (supernatant fluid) was separated from the nano-emulsion dispersions containing the entrapped drug (sediment material),

thereafter free and trapped drug were determined by means of HPLC analyses. Consequently, by using the following equation, drug entrapment was determined[40].

$$\text{Drug entrapment (\%)} = \{(\text{drug}_{\text{total}} - \text{drug}_{\text{supernatant}}) \div \text{drug}_{\text{total}}\} \times 100 \quad (1)$$

Results

Solubility determination/assay

The determined solubility concentrations of CLF, ART and DQ in nine different solvents were presented in Table 2. CLF, ART and DQ were very poor to insoluble in water. ART contained the highest solubility in ACN (201.6 mg/ml), CLF and DQ in THF (143.4 mg/ml and 0.241 mg/ml).

[Table 3 near here]

Compatibility studies

It is considered common practice to perform differential scanning calorimetry (DSC) analysis during compatibility studies, however when the API or excipients that need to be analyzed are in liquid form, it poses problematic to rely on DSC analyses. The only combinations that may be tested effectively during this study, by means of DSC analysis, are the combination of the ART, CLF and DQ. If the melting points of the three compounds are however taken into consideration, it is clear that DSC analyses will not provide useful information pertaining to possible interactions because ART starts to melt at 137°C. This subsequently could result in the solubilization of CLF and DQ in the molten ART, thereby showing no melting endotherms of the CLF and DQ; this will mistakenly be identified as an incompatibility. It was therefore decided that a more-visual method, such as hot stage microscopy in combination with isothermal microcalorimetry, would provide the best data for the identification of possible incompatibilities.

Hot-stage microscopy

[Figure 1 near here]

The HSM micrographs with corresponding melting points are depicted in Figure 1. When all three APIs were combined, it was observed that ART first starts to melt, whereas CLF and DQ start to dissolve in the liquefied ART, thereby resulting in a molten solubilized mass. No crystallization, unexplainable thermal event or phase transitions were identified during the HSM observation of the three APIs or the combination thereof.

Isothermal microcalorimetry

The microcalorimetry results are represented in Table 4. Figures 2 depicts the incompatibilities (heat flow *versus* time data) which were found during the microcalorimetry study. All samples were tested in a combination ratio of 1:1 (w/w), at a temperature of 32°C. Table 4 represents the interaction heat flow between the combinations, and whether there was any incompatibility identified. Should any interaction or incompatibility arise, there would be clear and pronounced deviations visible from the slopes of the individual curves and the measured heat flow would differ substantially from the calculated heat flow error. As can be seen in Fig. 2, when surface-active agents, such as Span® 60 or Tween® 80 are added, the compatibility of some combinations are significantly affected.

Individual combinations of CLF, ART and DQ were tested in combination with each other, as well as in combination with either olive or safflower oil and no conflicts were noticed for any API with oil combination. The aforementioned indicates that the APIs can be combined with the two natural oils separately and in combination with no incompatibility. The same trend was seen with ART, as well as with DQ, in combination with either olive or safflower oil. The same results were found where all three APIs were combined in either safflower oil or olive oil. When the APIs were separately combined with Span® 60, no incompatibility occurred. When CLF was combined with Span® 60 in combination with either olive or safflower oil no incompatibility was observed. Incompatibility was however observed when CLF was combined with Tween® 80 (Fig. 2a), as well as in combination with either safflower (Fig. 2b) or olive oil (Fig. 2c). ART depicted more incompatibility when combined separately with Tween® 80 (Fig. 2d). The same results were seen

when ART combined with Span® 60 with either safflower (Fig. 2e) or olive oil (Fig. 2f). DQ showed no incompatibility when combined separately with Tween® 80 or Span® 60, or the combination of the surfactants with the different oils. Consequently, it can be assumed that all three APIs, either in single, combination or multiple combinations are compatible.

[Figure 2 near here]

[Table 4 near here]

Nano-emulsion formulation

All nano-emulsions had a homogenous texture, with no phase separation, creaming or aggregation.

Physicochemical Properties

Table 5 depicts the results obtained from the physicochemical properties of the nano-emulsions.

[Table 5 near here]

pH

At a pH of 5, CLF, ART and DQ were dissociated at 99.69%, 0.098% and 99.98%, respectively. ART would indicate some difficulty to permeate through the skin, but CLF and DQ indicated they would permeate adequately[41].

Viscosity

The viscosity readings of all the formulations were very low (2.56-2.73 cP) and this could be attributed to the high water content (95%), as well as the low amount of Tween 80 and oil used in the formulations[42].

Droplet size

The measured droplet sizes ranged from 83 to 130 nm for the formulations; this falls within the acceptable range for emulsions (10 nm to 10 μm). For topical delivery, accumulation of the compound within the skin is preferred. Studies report that when the size of the droplet changes, there is a change in total area of the dispersed phase[43] and the droplet size decreases when the

entrapment efficiency increases[44]. Due to the hydrophilic and hydrophobic nature of the nano-emulsions when droplets sizes are nano-ranged, it can permeate the skin without much effort and in turn can permeate the hydrophilic and hydrophobic strata of the skin[45]. Easy transport abilities is another characteristic of small droplet sizes, since they penetrate a great surface area[46] and support better drug targeting and absorption[47]. Permeation, which may aid in increased bioavailability, is enhanced by nano-emulsions, since they have the capacity to solubilize large parts of hydrophilic drugs[48].

Zeta-potential

When zeta-potential values range from below -30 mV to above 30 mV, the suspension is stable[49]. Results differ from -30 mV to -38 mV, which is in the acceptable range above 30 mV or below -30 mV, indicating the nano-emulsion formulations were stable.

Drug entrapment efficiency

Table 5 illustrates all the formulations had a high drug entrapment efficiency of >91%, indicating the APIs were dispersed through the nano-emulsions.

Discussion

TB related alternative drug therapy has gained significant interest over the past few years due to multidrug resistant and extreme drug resistant infections caused by lengthy treatment and poor patient compliance[4,13]. To date, CLF, ART and DQ have never been characterized in nano-emulsions. Furthermore, there is no literature available on compatibility studies of CLF, ART and DQ, which may hold great clinical significance for the possible future treatment of CTB. In this study, we have characterized the solubility profile of CLF, ART and DQ and found CLF and DQ are the most soluble in THF and ART in ACN. These results are consistent with prior finding of poor solubility in water[50, 51] of CLF and DQ. Results obtained can be prescribed to the high lipophilicity of these two APIs[50,52]. Data obtained from the compatibility studies shows that all three APIs can be incorporated in natural oils, separately and in combination, with no interaction or incompatibility observed; data obtained from the HSM confirmed these results. Therefore, it

can be inferred that all three APIs, either in single, combination or in multiple combinations containing all three APIs, are compatible with each other as well as the natural oils. The incompatibilities can possibly be explained by the use of excipients, such as Tween® 80 and Span® 60, which have chemical and physical interactions and can affect the stability, the bioavailability and the chemical nature of the API and consequently, involuntary increased effects of drug degradation[53,54]. It is acknowledged that the chemical compatibility of a binary API mixture might vary from a multicomponent sample formulation indicating incompatibility and therefore in future, an alternative is to test sample formulations[55].

High entrapment efficiency was observed in all eight nano-emulsions. Droplet sizes were all in range, the nano-emulsions were also stable as can be seen by the zeta-potential values, but they all had very low viscosity possibly due to the low concentration of Tween® 80 and oil used. The study shows that CLF, ART and DQ can effectively be incorporated in nano-emulsions containing natural oils and further investigation is needed into *in vivo* studies with these nano-emulsions to confirm whether they can be used as a possible treatment for CTB.

Conclusion

In this study, we investigated the solubility of CLF, ART and DQ in nine different solvents, performed compatibility studies by means of HSM and microcalorimetry and tested the nano-emulsion's physicochemical properties, including the pH, zeta-potential, viscosity, droplet size and drug entrapment efficiency. CLF and DQ had the highest solubility in THF, whilst ART had the highest solubility in ACN. No incompatibilities were observed between the individual APIs during HSM studies, or when they were tested separately or in combination with the natural oils, but there were some during microcalorimetric analyses, when the APIs were combined with surface-active agents, such as Span® 60 and Tween® 80. Nano-emulsions were stable and had acceptable droplet sizes. Viscosity was very low due to the small amount of oil and Tween® 80 used. Drug entrapment was very high ranging from 91 to 99%. The pre-formulation studies

delivered an additional understanding about the physical and chemical properties of CLF, ART and DQ separately and in combination.

Declaration of interest

The authors wish to offer sincere thanks to the South African Medical Research Council (Flagship programme MALTB-Redox) and the Centre of Excellence for Pharmaceutical Sciences, Faculty of Health Sciences, North West University, South Africa, for their financial contribution to this project.

References

1. Cataldi A, Romano, MI. Tuberculosis caused by other members of the *M. tuberculosis* complex. 2007. (*In* Palomino, J.C., Lea˜o, S.C. & Ritacco, V., *eds*. Tuberculosis: from basic science to patient care. BourcillierKamps.com, p. 283-314.)
2. Ducati RG. The resumption of consumption: a review on tuberculosis. *The Memórias do Instituto Oswaldo Cruz.* 2006, 101:697-714.
3. Davies J, Davies, D. 2010. Origins and Evolution of Antibiotic Resistance. Microbiol. Mol Biol Rev. 2010, 74:417.
4. Manning T, Plummer S, Baker T, et al. Development of a three component complex to increase isoniazid efficacy against isoniazid resistant and non-resistant *Mycobacterium tuberculosis*. Bioorganic Med Chem Lett. 2012, 25:4621-4627.
5. WHO. Global tuberculosis control 2009: epidemiology, strategy, financing http://www.who.int/entity/tb/publications/global_report/2009/pdf/full_report.pdf (accessed on 29 May 2016).
6. American Thoracic Society, Centers for Disease Control and Prevention, Infectious Diseases Society of America. Treatment of tuberculosis.Am J Respir Crit Care Med. 2003; 167: 603–662.
7. Ramarao S. Greene, JN. Casanas, BC, et al. Cutaneous Manifestations of Tuberculosis. Infect Dis Clin Pract. 2012, 20(6):376-383.
8. Ilgazli A, Boyaci H, Basyigit I, et al. Extrapulmonary tuberculosis: clinical and epidemiologic spectrum of 636 cases. Arch Med Res. 2004, 35(5):435-441.
9. Wyrzykowska N, Wyrzykowski M, Zaba R, et al. Treatment of cutaneous infections caused by *Mycobacterium tuberculosis*. Adv Dermatol Allergol. 2012, 29(4):293-298.
10. Zouhair K, Akhdari N, Nejjam F, et al. Cutaneous tuberculosis in Morocco. Int J Infect Dis. 2007, 11(3):209-212.
11. Bravo FG, Gotuzzo E. Cutaneous tuberculosis. Clin Dermatol. 2007, 25(2): 173-180.

12. Van Zyl L, du Plessis J, Viljoen J. Cutaneous tuberculosis overview and current treatment regimens. Tuberculosis. 2015, 95:629-638.
13. Ena J, Valls V. Short-course therapy with rifampin plus isoniazid, compared with standard therapy with isoniazid, for latent tuberculosis infection: a meta-analysis. Clin Infect Dis. 2005, 40:670.
14. Iseman MD. Treatment of multidrug-resistant tuberculosis. N Engl J Med. 1993; 329: 784–791.
15. Nachega JB, Chaisson RE. Tuberculosis drug resistance. A global threat. Clin Infect Dis. 2003; 36 (suppl 1): 24–30.
16. Centers for Disease Control and Prevention. Revised definition of extensively drug-resistant tuberculosis. MMWR. 2006; 55: 1176.
17. Xu HB, Jiang RH, Xiao HP. Clofazimine in the treatment of multidrug-resistant tuberculosis. Clin Microbiol Infect. 2012; 18:1104-1110.
18. Sansarricq H. (ed). 2004. Multidrug therapy against leprosy: development and implementation over the past 25 years. http://www.who.int/lep/resources/MDT_Full.pdf Date of access: 1 March 2015
19. Cholo MC. Steel HC. Fourie PB. et al. Clofazimine: current status and future prospects. J Antimicrob Chemother, 2011, 67(2):290-298.
20. Anderson R. The immunopharmacology of antileprosy agents. Leprosy review. 1983, 54:139-144.
21. Barry VC, Belton JG, Conalty ML. et al. A new series of phenazines (rimino-compounds) with high antituberculosis activity. Nature. 1957, 179:1013-1015.
22. Reddy VM, O`Sullivan JF, Gangadharam PR. Antimycobacterial activities of riminophenazines. J Antimicrob Chemother. 1999, 43:615-623.

23. Van Rensburg CEJ,·Jooné GK, Sirgel FA, et al. *In vitro* investigation of the antimicrobial activities of novel tetramethylpiperidine-substitued phenazines against *Mycobacterium* tuberculosis. Chemother. 2000, 46:43-48.

24. WHO. WHO Model List of Essential Medicines, 17th Edition (Updated: March 2011). http://www.who.int/medicines/publications/essentialmedicines/en/ (12 April 2016, date last accessed).

25. Haynes RK, Ho WY, Chan HW. Highly antimalaria-active artemisinin derivatives: biological activity does not correlate with chemical reactivity. Angew Chem. 2004, 43:1381-1385.

26. Von Keutz E, Schmuck G, Haynes R. Artemisone, a new anti-malarial artemisinin derivative: lack of neurotoxicity. Abstracts of the Medicine and Health in the Tropics Congress, Marseille, France, Abstract no. O-004, 2005, p. 28.

27. Nagelschmitz J, Voith B, Wensing G, et al. First assessment in humans of the safety, tolerability, pharmacokinetics, and *ex vivo* pharmacodynamic antimalarial activity of the new artemisinin derivative artemisone. Antimicrob Agents Chemother. 2008, 52(9):3085-3091.

28. Steyn JD, Wiesner L, Du Plessis LH, et al. Absorption of the novel artemisinin derivatives, artemisone and artemiside: potential application of Pheroid™ technology. Int J Pharm. 2011, 414(1-2):260-266.

29. Biamonte MA, Wanner J, Le Roch KG. Recent advances in malaria drug discovery. Bioorganic Med Chem Lett. 2013, 23(10):2829-2843.

30. Fry M, Williams RB. Effects of decoquinate and clopidol on electron transport in mitochondria of *Eimeria tenella (*Apicomplexa: coccidia*)* Biochem Pharmacol. 1984, 33:229-240.

31. Mikota SK, Plumb DC. 2014. http://www.elephantcare.org/Drugs/decoquin.htm Date of access: 12 June 2016.

32. Haynes RK. MRC South African university flagship projects: project proposal: development to the clinical phase of oxidant and redox drug combinations for treatment of malaria: TB and related diseases. 2013, 21p.
33. Williams RB. The mode of action of anticoccidial quinolones (6-decyloxy-4-hydroxyquinoline-3-carboxylates) in chickens. Int. J. Parasitol, 1997, 27(1):101-111.
34. Pogany SA, Tanol M, Baltezor MJ. University Of Kansas, 2013.*Decoquinate prodrugs*. U.S. Patent Application 13/495,772.
35. O'driscoll CM, Griffin BT. Biopharmaceutical challenges associated with drugs with low aqueous solubility—the potential impact of lipid-based formulations. Adv Drug Deliv Rev. 2008, 60(6):617-624.
36. Du Preez J, Aucamp M,. Burger C, et al. Development and validation of the simultaneous determination of artemisone, clofazimine and decoquinate with HPLC. Pharmazie, 73:139-142.
37. Corvi MP, Cirri M, Mura P. Differential scanning calorimetry as a screening technique in compatibility studies of DHEA extended release formulations. J Pharm Biomed Anal. 2006, 42: 3-10.
38. Borhade V, Pathak S, Sharma S, et al. Clotrimazole nanoemulsion for malaria chemotherapy. Part 2: Stability nassesment, *in vivo* pharamcodynamic evaluations and toxicological studies. Int J Pharm. 2012, 431:149-160.
39. Xuan T, Zhang JA, Ahmad I. HPLC method for determination of SN-38 content and SN-38 entrapment efficiency in a novel liposome-based formulation, LE-SN38. J Pharm Biomed Anal. 2006, 41:582–588.
40. Admescope. 2012. pKa-Dissociation constant, pH partition. http://www.admescope.com/learnadme/physicochemical-properties/pka-dissociation-constant-ph-partition.html. Date of access: 13 April 2016.

41. Djordjevic L, Primorac M, Stupar M, et al. Characterization of capryocaproyl macrogolycerides based microemulsion drug delivery vehicles for an amphilic drug. Int J Pharm. 2004, 271: 11-19.

42. Wiechers JW, Kelly CL, Blease TG, et al. Formulating for efficacy. Int J Cosmet Sci. 2008, 26:173-175,177.

43. Chime SA, Kenechukwu FC, Attama AA. Nanoemulsions — Advances in Formulation, Characterization and Applications in Drug Delivery, Application of Nanotechnology in Drug Delivery, PhD. Ali Demir Sezer (Ed.), InTech. 2014.

44. Shakeel F, Ramadan W, Ahmed MA. Investigation of true nanoemulsions for transdermal potential of indomethacin: characterization, rheological characteristics, and ex vivo skin permeation studies. J Drug Target. 2009; 17:435-441.

45. Sakeena M, Muthanna F, Ghassan Z, et al. Formulation and in vitro evaluation of ketoprofen in palm oil esters nanoemulsion for topical delivery. J Oleo Sci. 2009; 59:223-228.

46. Desai N. Challenges in development of nanoparticle-based therapeutics. AAPS Pharm. 2012; 14:282-295.

47. Shakeel F, Baboota S, Ahuja A, et al. Celecoxib nanoemulsion: Skin permeation mechanism and bioavailability assessment. J Drug Target. 2008; 16:733-740.

48. Djordjevic L, Primorac M, Stupar M, et al. Characterization of capryocaproyl macrogolycerides based microemulsion drug delivery vehicles for an amphilic drug. Int J Pharm. 2004, 271:11-19.

49. Pharmacopeia online. 2014. http://www.usp.org/pdf/EN/referenceStandards/msds/1138904.pdf Date of access: 1 March 2015.

50. European Food Safety Authority (EFSA). Opinion of the Scientific Panel on additives and products or substances used in animal feed (FEEDAP) on a request from the Commission

on the coccidiostat DECCOX in accordance with article 9G of Council Directive 70/524/EEC. p.6 http://onlinelibrary.wiley.com/doi/10.2903/j.efsa.2004.17 Date of access: 13 Apr 2016.

51. Chembase. 2014. http://en.chembase.cn/molecule-157442.html Date of access: 5 Augustus 2015.
52. Clas SD; Dalton CR; Hancock BC. Differential scanning calorimetry: applications in drug development. Pharm Sci Technol Today. 1999, 2:311-320.
53. Bharate SS, Bharate SB, Bajaj AN. Interactions and incompatibilities of pharmaceutical excipients with active pharmaceutical ingredients: a comprehensive review. :J Excipients Food Chem. 2010, 1(3):1-26.
54. Thomas VH, Naath M. Design and utilization of the drug–excipient chemical compatibility automated system. Int J Pharm. 2008, 35:150–157.

Tables

Table 1: Formula used during the formulation of the nano-emulsions containing olive oil

Nano-emulsion	Water phase	Weight (w/v)	Oil phase	Weight (w/v)
O1	Water Tween® 80	40.0 ml 3.6 ml	Olive oil Span® 60 Clofazimine	10% (4.6 ml) 1000.0 mg 61.5 mg
O2	Water Tween® 80	40.0 ml 3.6 ml	Olive oil Span® 60 Artemisone	10% (4.6 ml) 1000.0 mg 179.8 mg
O3	Water Tween® 80	40.0 ml 3.6 ml	Olive oil Span® 60 Decoquinate	10% (4.6 ml) 1000.0 mg 1.9 mg
O4	Water Tween® 80	40.0 ml 3.6 ml	Olive oil Span® 60 Clofazimine Artemisone Decoquinate	10% (4.6 ml) 1000.0 mg 70.8 mg 379.2 mg 8.1 mg

Table 2: Formula used during the formulation of the nano-emulsions containing olive oil

Nano-emulsion	Water phase	Weight (w/v)	Oil phase	Weight (w/v)
S1	Water Tween® 80	40.0 ml 3.6 ml	Safflower oil Span® 60 Clofazimine	10% (4.6 ml) 1000.0 mg 72.1 mg
S2	Water Tween® 80	40.0 ml 3.6 ml	Safflower oil Span® 60 Artemisone	10% (4.6 ml) 1000.0 mg 199.3 mg
S3	Water Tween® 80	40.0 ml 3.6 ml	Safflower oil Span® 60 Decoquinate	10% (4.6 ml) 1000.0 mg 3.4 mg
S4	Water Tween® 80	40.0 ml 3.6 ml	Safflower oil Span® 60 Clofazimine Artemisone Decoquinate	10% (4.6 ml) 1000.0 mg 136 mg 210.4 mg 8.4 mg

Table 3: Solubility (µg/ml) of clofazimine, artemisone and decoquinate in selected solvents

	Clofazimine	Artemisone	Decoquinate
Acetone	2.18 ± 0.02	105.92 ± 6.52	0.02 ± 0.00
Acetonitrile	1.21 ± 0.06	201.96 ± 2.97	0.01 ± 0.00
Ethanol	1.83 ± 0.02	44.60 ± 1.51	0.18 ± 0.00
Isopropanol	1.02 ± 0.04	26.35 ± 0.75	0.16 ± 0.02
Methanol	0.83 ± 0.01	46.54 ± 0.33	0.16 ± 0.00
THF	143.41 ± 0.06	194.19 ± 0.05	0.24 ± 0.03
Tris	0.00 ± 0.00	0.1 ± 0.00	0.00 ± 0.00
PBS	0.00 ± 0.00	0.09 ± 0.00	0.00 ± 0.01
Water	0.00 ± 0.000	0.10 ± 0.00	0.00 ± 0.00

Table 4: Interaction heat flow results of TAM

Formulation	Interactive heat flow (μW/g)	Incompatibility identified
CLF and olive oil	2.330 ± 2.806	None
CLF and safflower oil	2.159 ± 2.592	None
CLF and Tween® 80	65.86 ± 0.00	Possible incompatibility
CLF, Tween® 80 and safflower oil	-27.71 ± 36.35	Possible incompatibility
CLF, Tween® 80 and olive oil	3580 ± 0.00	Possible incompatibility
CLF and Span® 60	6.82 ± 7.46.	None
CLF, Span® 60 and safflower oil	-19.14 ± 25.41	None
CLF, Span® 60 and olive oil	-22.42 ± 29.83	None
ART and olive oil	16.79 ± 16.82	None
ART and safflower oil	20.89 ± 20.91	None
ART and Tween® 80	93.43 ± 0.00	Possible incompatibility
ART, Tween® 80 and safflower oil	69.82 ± 70.61	None
ART, Tween® 80 and olive oil	93.26 ± 95.16	None
ART and Span® 60	-6.43 ± 6.68	None
ART, Span® 60 and safflower oil	48.47 ± 53.42	Possible incompatibility
ART, Span® 60 and olive oil	77.32 ± 85.45	Possible incompatibility
DQ and olive oil	4.25 ± 4.39	None
DQ and safflower oil	4.515 ± 4. 67	None

DQ and Tween® 80	2.63 ± 8.37	None
DQ, Tween® 80 and safflower oil	17.84 ± 20.11	None
DQ, Tween® 80 and olive oil	8.50 ± 12.23	None
DQ and Span® 60	13.35 ± 15.39	None
DQ, Span® 60 and safflower oil	0.713 ± 1.150	None
DQ, Span® 60 and olive oil	-7.64 ± 9.11	None
Olive oil combination of CLF, ART and DQ	16.54 ± 16.59	None
Safflower oil combination of CLF, ART and DQ	13.04 ± 13.12	None

Table 5: Characterisation results of the nano-emulsions

Formulations	pH	Viscosity(cP)	Droplet size (nm)	Zeta-potential (mV)	Drug entrapment efficiency (%)
O1	5.01 ± 0.10	2.59 ± 0.50	101.36 ± 2.05	-33.3 ± 1.10	94.12 ± 1.20
S1	5.10 ± 0.05	2.91 ± 0.08	126.47 ± 1.75	-30.00 ± 0.10	91.35 ± 1.38
O2	5.15 ± 0.07	2.60 ± 0.08	101.47 ± 1.56	-36.60 ± 0.12	96.30 ± 1.01
S2	5.08 ± 0.02	2.62 ± 0.05	104.63 ± 1.42	-37.90 ± 0.05	98.95 ± 2.05
O3	5.30 ± 0.08	2.72 ± 0.08	91.39 ± 1.30	-35.40 ± 0.80	93.01 ± 1.45
S3	5.24 ± 0.04	2.73 ± 0.03	83.61 ± 1.72	-34.40 ± 1.33	91.90 ± 0.99
O4	5.19 ± 0.08	2.63 ± 0.07	83.05 ± 0.90	-32.00 ± 1.28	94.12 ± 2.40 96.30 ± 1.34 93.01 ± 1.57
S4	5.26 ± 0.07	2.56 ± 0.08	88.14 ± 1.52	-30.1 ± 0.05	94.42 ± 1.20 98.5 ± 1.75 98.02 ± 1.35

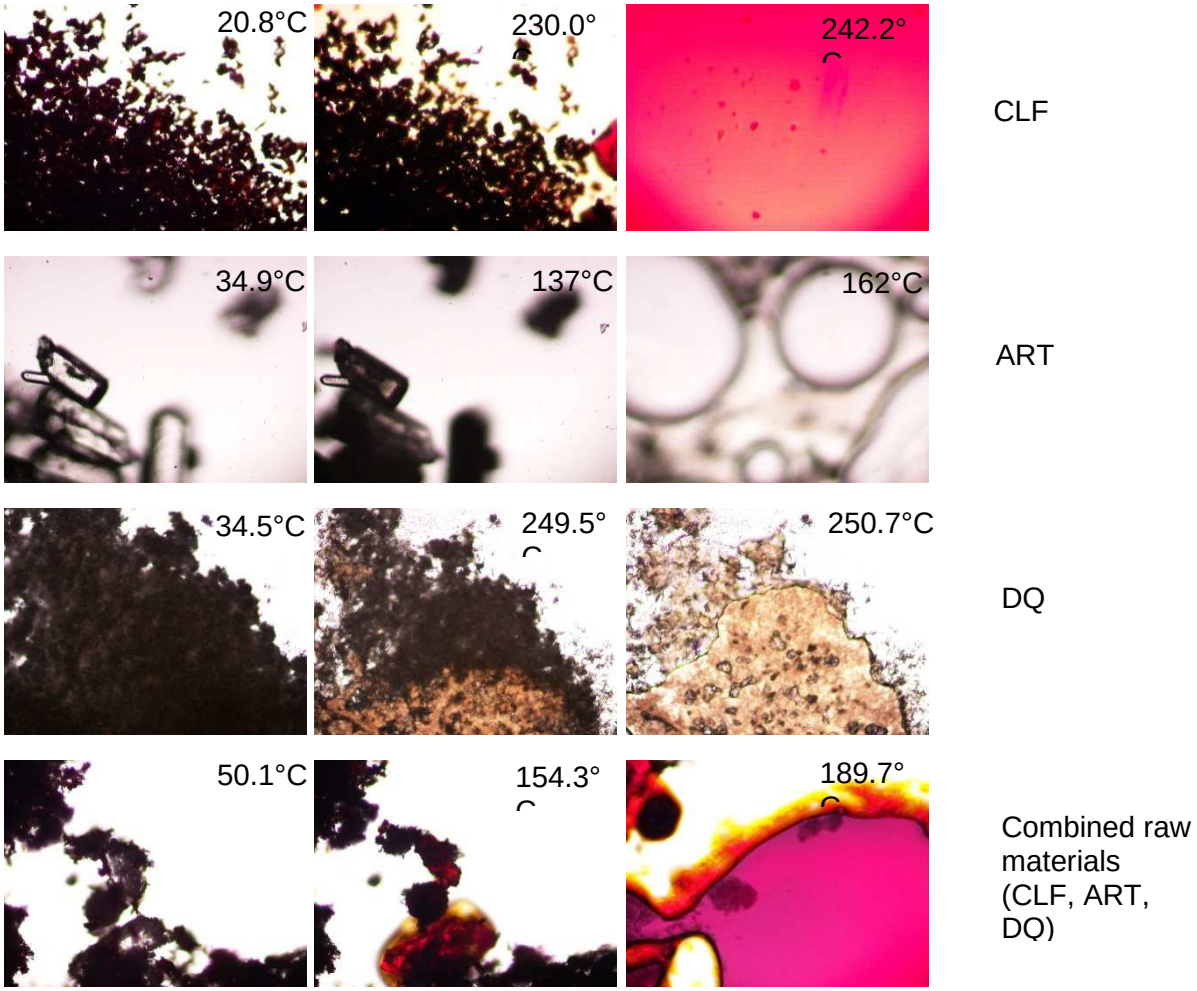

Figure 1: Micrographs obtained from HSM observations with corresponding temperatures

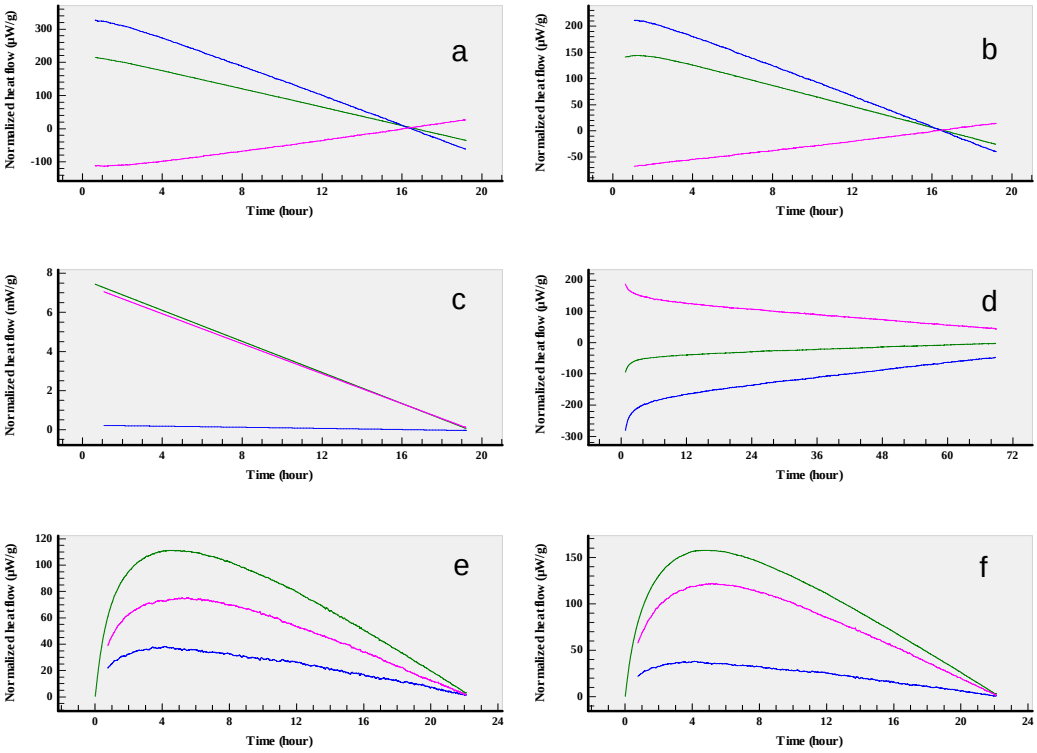

Figure 2: a) Heat flow *versus* time graph obtained for a 1:1 combination of CLF and Tween® 80, b) heat flow *versus* time graph obtained for a 1:1 weight combination of CLF, Tween® 80 and safflower oil, c) heat flow *versus* time graph obtained for a 1:1 weight combination of CLF, Tween® 80 and olive oil, d) heat flow *versus* time graph obtained for a 1:1 weight combination of ART and Tween® 80, e) heat flow *versus* time graph obtained for a 1:1 weight combination of ART, Span® 60 and safflower oil and f) heat flow *versus* time graph obtained for a 1:1 weight combination of ART, Span® 60 and olive oil.

Chapter 5:

Article for the publication in "The International Journal of Pharmaceutics"

Chapter 5 is written in article format for the purpose of publication in the International Journal of Pharmaceutics and the authors guide is stipulated in Appendix F. For ease of reading the paragraphs of this chapter have been justified.

Formulation of natural oil nano-emulsions for the topical delivery of clofazimine, artemisone and decoquinate

Cornel Burger[a], Marique Aucamp[a], Jan du Preez[a], Richard Haynes[a], Ronnett Seldon[b], Joanna Evans[b], Digby Warner[b], Liezl Gibhard[c], Minja Gerber[a]* and Jeanetta du Plessis[a]

a) Centre of Excellence for Pharmaceutical Sciences, North-West University, Private Bag X6001, Potchefstroom 2520, South Africa

b) MRC/NHLS/UCT Molecular Mycobacteriology Research Unit, Department of Pathology and Institute of Infectious Disease and Molecular Medicine, Faculty of Health Sciences, University of Cape Town, South Africa.

c) Division of Clinical Pharmacology, Department of Medicine, Groote Schuur Hospital, Old Main Building K45, University of Cape Town, Observatory, 7925

* Corresponding author. Tel.: +2718 299 2328; Fax: +2787 231 5432. E-mail address: Minja.Gerber@nwu.ac.za (M Gerber).

Graphical abstract

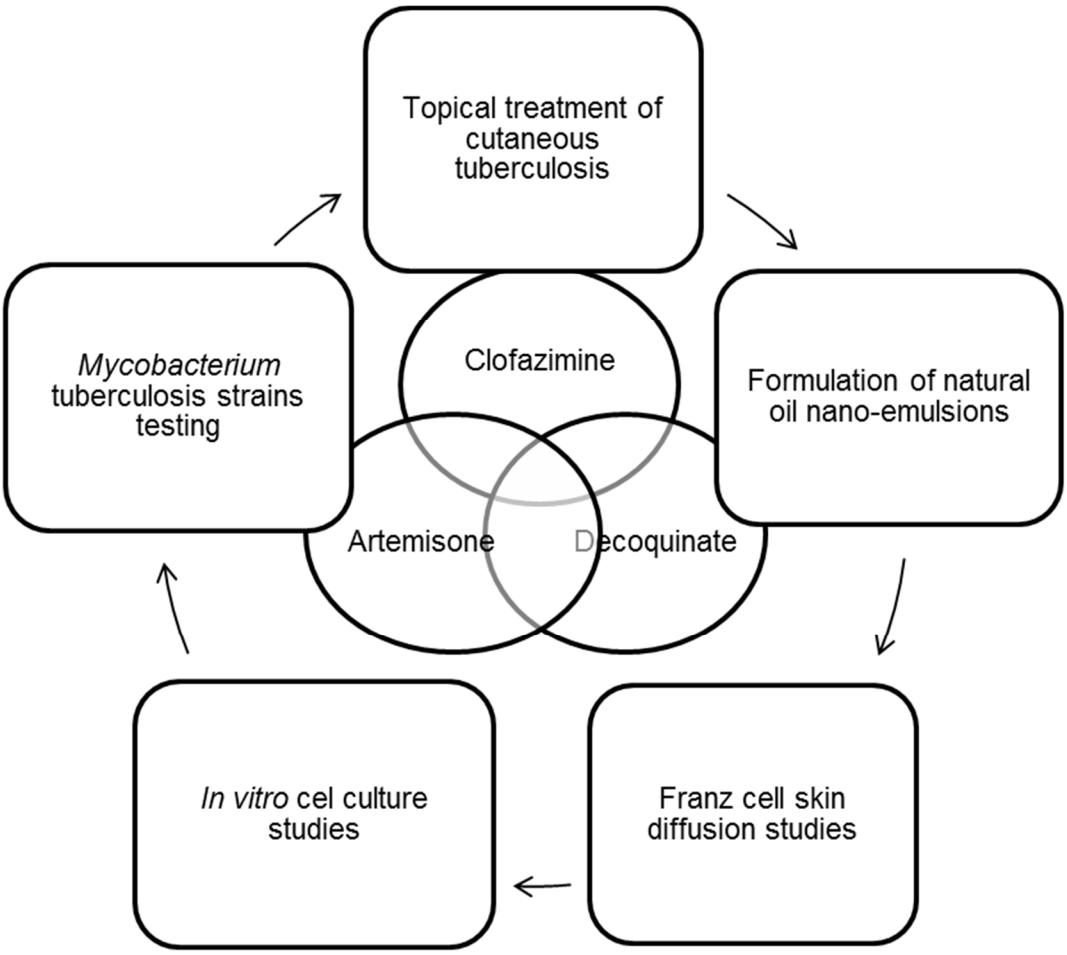

Abstract

Cutaneous tuberculosis which only makes up a minor percentage (1-2%) of tuberculosis patients, is still of utmost importance, since TB causes death of nearly 2 million patients each year of which 2 billion patients are infected worldwide. The aim of this study was to formulate novel nano-emulsions for the topical delivery of clofazimine (CLF), artemisone (ART) and decoquinate (DQ). Membrane release studies were performed, which were followed by skin diffusion studies and tape-stripping studies to determine the release of the active pharmaceutical ingredient (API) from the nano-emulsions. By using Franz cells, the skin diffusion studies were employed. By using the lactate dehydrogenase (LDH) assay, *in vitro* toxicity studies were done on immortalised human keratinocytes (HaCaT) cell line to determine the possible cell death caused by the APIs itself and the carrier system incorporated with the different APIs. No concentration of APIs was found in the receptor phase during the membrane release and skin studies. During tape-stripping studies, it was evident that the APIs accumulated within the stratum corneum-epidermis and the epidermis-dermis. During the *in vitro* studies, it was evident that all nano-emulsions were non-cytotoxic ($p<0.05$). *In vitro* studies on *Mycobacterium* strains performed exceptionally well where all nano-emulsions depicted %inhibition.

Keywords: Cutaneous tuberculosis, clofazimine, artemisone, decoquinate, nano-emulsions, natural-oils

1 Introduction

Tuberculosis (TB) is one of the most prevalent and lethal infectious diseases in the world (Hurtley & Ash, 2010), causing approximately 1.7 million deaths worldwide in 2016, and nearly one-quater of the world's populace are currently infected with the bacterium (WHO*.,* 2018).

Cutaneous tuberculosis (CTB) involves only a minor percentage (1-2%) in all cases of TB. Nonetheless, considering the increase in incidence of TB in numerous evolving countries, these statistics become substantial (Bravo & Gotuzzo, 2007). There is a need for novel drugs and other therapeutic methods, since current anti-tuberculosis therapeutics are not adequately effective against multidrug-resistant tuberculosis (MDR-TB). Consequently, to improve therapeutic options, it has been proposed that second-line treatment, i.e. clofazimine (CLF), can be repurposed for the treatment of MDR-TB (Dey *et al*., 2013). The leading difficulty of most second-line drugs is the insufficient effectiveness, as well as undesirable toxicity profiles (Dooley *et al*., 2013).

CLF can be classified as a riminophenazine antibiotic with a hydrophobic character (WHO, 2011), which possesses immune-pharmacological, pro-oxidative and anti-inflammatory properties (Reddy *et al*., 1999). CLF exhibits a half-life of 65 to 70 days. This compound has gained some interest over years as an anti-mycobacterial drug, which has shown increased success in clinical studies for diseases caused by *Mycobacterium leprae*, *Mycobacterium avium complex* and *Mycobacterium kansasii* (Cholo *et al*., 2012; Telles *et al*., 2005). Current *in vitro* and *in vivo* regimes indicate good effectiveness and low toxicity against MDR-TB mycobacterial strains (Dey *et al*., 2013; Jagannath *et al*., 1995).

Artemisone (ART), a semi-synthetic second generation derivate of artemisinin, does not show any neurotoxicity in both *in vitro* and *in vivo* assays (Guiguemde *et al*., 2014; Ramharter *et al*., 2006). Physicochemical property values of ART, such as an octanol-buffer distribution coefficient (log D) and aqueous solubility, limits transdermal drug delivery (Haynes *et al*., 2006).

Decoquinate (DQ), which belongs to the quinolone class (Wiiliams, 2006), is implemented as an anti-coccidial drug and currently used for avian coccidiosis prevention; it also has an effect on secondary early schizonts (Wiiliams, 1997). DQ possibly complements ART and CLF, as its

mechanism affects the disruption of electron transport in the coccidian system within the mitochondrial cytochrome leading to the suppression of resistance (Mikota & Plumb, 2014).

One of the most important functions of the skin is to form an active barrier between indigenous and exogenous substances. The stratum corneum, which is known as the upper layer of the skin, is mostly lipophilic and consists of macrophages, acids, lipids, hydrolytic enzymes and anti-microbial peptides (Proksch *et al*., 2008). Difficulty arises when active pharmaceutical ingredients (APIs) have low penetration abilities to overcome the intrinsic barrier of the human skin, which leads to restricted drug uptake and low permeation rates (Lam & Gambardi, 2014). Permeation of the skin is possible if the API possesses ideal physicochemical properties. APIs should possess both lipophilic qualities (to permeate the stratum corneum) and hydrophilic properties (to permeate to the other hydrophilic layers of the skin to reach the blood stream) (Colombo *et al*., 2013; Naik *et al*., 2000). According to Naik *et al*. (2000), other properties, such as log D ($1 < \log D < 3$), molecular weight (< 500 g/mol) and aqueous solubility (> 1 mg/ml), are needed for successful skin permeation. By looking at the log D of CLF (7.66) (Pharmacopeia, 2014), ART (2.49) (Dunay *et al*., 2009) and DQ (7.80) (Chembase, 2014), only ART shows a favourable log D to permeate the skin. Observing the aqueous solubility of CLF (10 mg/l) (Pharmacopeia, 2014), ART (89 mg/l) (Dunay *et al*., 2009; Steyn *et al*., 2011) and DQ (no data), none of the APIs show favourable aqueous solubility to permeate the skin. As a possible way to improve the permeation of these compounds, natural oils will be used, i.e. safflower and olive oil.

Natural oils, are purported to promote the delivery of both lipophilic and hydrophilic APIs (Williams & Barry, 2012), since natural oils and human skin (stratum corneum) both contain linoleic acid (C_{18} fatty acid) (Dingler & Gohla, 2002), which can disturb intercellular lipid packaging and in turn, increase penetration (Williams & Barry, 2012). Recently nano-emulsions have established to be effective in transdermal and topical delivery, which have shown great potential as a delivery system for a variety of lipophilic and hydrophilic drugs (Lui *et al*., 2016; Parikh & Patel, 2016; Sanz *et al*., 2015; Tan *et al*., 2015). Advantages of nano-emulsions include excellent solubilisation capacity for a variety of drugs, higher entrapment with small droplet size, effortlessness

preparation, visual stability and clarity, which makes nano-emulsions attractive applicants as drug delivery systems (Chime *et al*., 2014).

The aim of the study was to formulate eight different nano-emulsions, containing either olive oil or safflower oil, with CLF, ART and DQ as the APIs separately and in combination in order to investigate the topical drug delivery since the epidermis-dermis is the target site for CTB. The nano-emulsion containing safflower oil consisted of CLF (**S1**), ART (**S2**) and DQ (**S3**), the combination of all three APIs (**S4**) and without APIs (placebo: **S5**), while the nano-emulsions containing olive oil comprised CLF (**O1**), ART (**O2**) and DQ (**O3**), the combination of all three APIs (**O4**) and without APIs (placebo: **O5**). Tape-stripping studies offer insight into whether nano-emulsions containing natural oils could be used as penetration enhancers for the topical delivery of the selected APIs.

2 Materials and methods

2.1 Materials

CLF and ART were generously donated by Sangrose Laboratories Pvt Ltd (India) for the flagship programme. DQ was acquired from Hohance (Shanghai, China). Natural oils (safflower-and olive oil) were obtained from CJP Chemicals (Johannesburg, South Africa). Absolute ethanol (99.7%) was obtained from Associated Chemical Enterprises (South Africa). Span® 60 and Tween® 80, as well as sodium hydroxide (NaOH) and orthophosphate, used for the preparation of phosphate buffered solution (PBS), were supplied by Merck Laboratory Supplies (Midrand, South Africa). Deionised high-pressure liquid chromatography (HPLC) grade water (Millipore, Milford, USA) was used throughout this study. The immortalised human keratinocytes (HaCaT) cell line, which was used during the cell culture cytotoxicity studies, was received as a gift from the University of the Witwatersrand (WITS). Growth media was obtained from HyClone™ (GE Healthcare Life Sciences, South Logan, Utah), which included preparations such as Non-Essential Amino Acids, Dulbecco's modified eagle medium (DMEM), L-glutamine, phosphate buffered saline (1x) and foetal bovine serum. Other consumables used during the cytotoxicity studies, such as Trypan Blue Solution, were obtained from Sigma-Aldrich® (St. Louis, Missouri), Penicillin/Streptomycin

(Pen/Strep) and Trypsin-Versene® (EDTA) from Lonza™ (Basel, Switzerland) and the CytoTox 96® Non-Radioactive Cytotoxicity Assay Kit from Promega™ (Madison, Wisconsin).

2.2 Methods

2.2.1 Nano-emulsion preparation

Table 1: Formulas for the nano-emulsion containing olive oil

Table 2: Formulas for the nano-emulsion containing safflower oil

Tables 1 and 2 provide the quantities used for the formulation of the nano-emulsions. All the ingredients were accurately weighed prior to formulation. The nano-emulsions were prepared by mixing Span® 60 and the natural oil (olive or safflower oil) (oil phase) in one beaker and Tween® 80 and water (water phase) in another beaker; using a magnetic stirrer hotplate, both mixtures were mixed (60°C) separately. Each phase was stable after 15 min of mixing and reached a temperature of 60°C. Thereafter the oil phase was added very slowly to the water phase, while continuously mixing at a constant stirring speed. The temperature was maintained at 60°C. Subsequently the nano-emulsions were placed in a beaker with ice and sonicated for 10 min at a power of 40 Watt (Borhade *et al.,* 2012).

2.2.2 Preparation of PBS (pH 7.4)

During the skin diffusion studies, PBS (pH 7.4) was used as the receptor phase. PBS (pH 7.4) was prepared by dissolving 3.025 g of NaOH in 800 ml of Milli-Q® water and 13.65 g of potassium dihydrogen orthophosphate (KH_2PO_4) in 500 ml of Milli-Q® water, according to the British Pharmacopoeia (BP) standards (BP, 2013a; BP, 2013b), separately in volumetric flasks each containing a magnetic stirrer. Both solutions were placed on a magnetic stirrer and mixed continuously to ensure complete dissolution. Subsequently the NaOH solution was slowly added to the KH_2PO_4 solution and stirred continuously with a magnetic stirrer. Milli-Q® water (700 ml) was added to make up to the volume of 2000 ml. If needed, the solution's pH was set and adjusted to a pH of 7.4 using either NaOH or orthophosphoric acid. The solution was filtered and degassed.

2.2.3 HPLC analysis of clofazimine, artemisone and decoquinate

A novel HPLC method had been developed and validated for the simultaneous analysis of CLF, ART and DQ. The HPLC (Agilent 1200 Series) was equipped with an Agilent 1200 pump, a diode array detector, an auto sampler injection mechanism and ChemStation Rev. A.10.01 software for data analysis (Agilent Technologies, Palo, Alto, CA). The UV-detector was set at a two different wavelengths of 210 nm for ART and DQ and 284 nm for CLF to be detected. Two mobile phases were used in this study; mobile phase A consisted of 0.005 M sodium octanesulfonic acid (pH 3.5) and mobile phase B of HPLC grade acetonitrile using gradient elution. The injection volume was set at 2 µl and the flow rate at 1.0 ml/min with mobile phase A at 35% and mobile phase B at 65% for 2 min. This was followed by a gradient which was 10% (mobile phase A)/90% (mobile phase B) over a period of 4 min. The initial gradient conditions were regained after 10 min to 35% (mobile phase A)/65% (mobile phase B). The runtime was set at 15 min and individual peaks were identified for CLF, ART and DQ at 6.3 min, 7.3 min and 9.8 min, respectively. Analytical tests were achieved in a laboratory with a measured setting of 25°C. Limit of detection (LOD) values of CLF, ART and DQ were determined to be 0.04 µg/ml, 4.42 µg/ml and 0.70 µg/ml, respectively. Limit of quantification (LOQ) was 0.05 µg/ml, 5.50 µg/ml and 4.00 µg/ml for CLF, ART and DQ, respectively (Du Preez *et al*., 2017).

2.2.4 Standard preparation

The standard preparation of CLF, ART and DQ was prepared by accurately weighing 7 mg of CLF, 40 mg of ART and 12 mg of DQ and thereafter transferring it to a 100 ml volumetric flask. The APIs were dissolved in 100 ml of absolute ethanol (99.7%) (Standard 1). Standard 1 (5 ml) was taken and diluted to 50 ml with absolute ethanol (99.7%) (Standard 2), thereafter the two standard solutions were filtered into HPLC vials using 0.45 µm polyvinylidene fluoride (PVDF) filters.

2.2.5 Physicochemical properties

2.2.5.1 Aqueous solubility

Aqueous solubility was determined by pre-heating the water bath to 32°C (temperature on top of the skin during a diffusion study). Water was inserted in the separate test tubes with magnetic stirrers and an excess of CLF, ART and DQ was added to these and regularly checked to ensure

the solution was saturated throughout. After 24 h, the solutions were removed then filtered using a 0.45 µm membrane filter; thereafter the solutions were centrifuged for 10 min at 5000 rpm and ethanol was added to prevent precipitation. Samples were transferred from each test tube to HPLC vials to be analysed by means of HPLC. This experiment was repeated in triplicate.

2.2.5.2 Octanol-buffer distribution coefficient (log D)

The log D was determined by pre-weighing a certain mass of API which was added to 20 ml pre-saturated *n*-octanol in a test tube; 3 ml of each solution was then transferred into a test tube followed by an equal volume of the extracted PBS (pH 7.4) phase and left to equilibrate overnight. From each separate test tube, 1 ml of the PBS-phase and the *n*-octanol-phase was extracted and placed into different test tubes and thereafter diluted in 10 ml of ethanol. From each different test tube, 1 ml of diluted PBS (pH 7.4) solution and *n*-octanol solution was transferred into vials. The concentration of the API was determined in each separate phase by means of HPLC.

2.3 Characterisation of the nano-emulsions

The eight formulations were characterised by measuring the following: viscosity, pH, entrapment efficiency, zeta-potential and droplet size.

2.3.1 Droplet size, distribution and zeta-potential

The droplet size and distribution, together with the zeta-potential of the individual formulations, were determined by means of the Zetasizer Nano ZS (Malvern® Instruments LTD, Worcestershire, UK). The eight dispersions were tested at ambient temperature and samples were prepared in triplicate and analysed.

2.3.2 pH

The pH of the eight different nano-emulsions was determined by means of a Mettler Toledo SevenMulti pH meter (InLab® 410 NTC electrode 9823) (Greifensee, Switzerland). The pH of each individual formulation was measured in triplicate at the same conditions (32°C) and accuracy was verified by calibrating the pH meter each time prior to use.

2.3.3 Viscosity of the nano-emulsions

The viscosity of the eight nano-emulsions was determined by using of a Brookfield® Viscometer (model DV II, Stoughton, Massachusetts, USA). A rotating spindle determining resistance was

immersed in the formulation medium whilst spinning at a specific rate (measured in rpm). The individual formulations were placed in a water bath, which was connected to the viscosity meter by means of a Brookfield® temperature controller to maintain the temperature at 25°C ±0.5°C. Each formulation was removed and positioned in the apparatus while the spindle (Stoughton, MA) was placed in the formulation. A CS-14 spindle was used to ensure appropriate torque since the consistency of the formulations was very thin. At a rate of 7/8 inch/min, the Helipath stand (D20733) rose and lowered the spindle. Over a period of 5 min, viscosity readings were taken every 10 sec; after 30 readings were obtained, the mean viscosity value for each formulation was calculated.

2.3.4 Entrapment efficiency (EE)

The EE% was determined by transferring 10 ml of prepared nano-emulsion dispersions into Eppendorf® tubes, thereafter the samples were centrifuged at 3000 g for 30 min at room temperature using an Optima L-100 XP ultracentrifuge (Beckman Coulter, South Africa. The resultant supernatant was extracted and diluted with 5 ml of ethanol absolute (99.7%). The diluted supernatant (1 ml) was extracted and transferred to vials to be determined by means of HPLC.

2.4 Diffusion experiments

2.4.1 Membrane release studies

To evaluate the different APIs release from the nano-emulsions, membrane release studies were conducted for the **S1**-**S5** and **O1**-**O5** nano-emulsions. The Franz cells consisted of a donor phase and a receptor phase, with a magnetic stirring rod placed into the latter (±2 ml). To ensure no leaking took place, vacuum grease was placed on both the donor and the receptor phase. Synthetic PVDF membrane filters (FP Vericel, 0.45 µm, 25 mm, Pall®) were placed on the lower half of the Franz cells (receptor phase), thereafter the phases were placed together and secured with a horseshoe clamp. During the experiment, nine Franz cells were used; two cells were used as the placebo (control) and the other seven consisted of the prepared nano-emulsions. The receptor phase was filled with PBS (pH 7.4), which mimics the temperature of the blood flow (37°C), and the donor compartment consisted of the prepared nano-emulsions at a temperature mimicking that of the skin (32°C). To prevent any loss of the constituents, the donor compartment

was covered with Parafilm®. The Franz cells were placed in a water bath, which was maintained at a temperature of 32°C, so diffusion could take place. Every hour for 6 h, the receptor compartment was extracted with a syringe and refilled with PBS (pH 7.4) at 37°C. The samples were analysed by means of HPLC to determine the concentration of the API that permeated through the membrane within the receiver fluid (PBS) and the release rate could be determined for all the formulations.

2.4.2 Skin preparation

Full-thickness Caucasian abdominal skin (ethical approval reference number: NWU-00114-11-A5) was collected from plastic surgeons following abdominoplastic surgery. Upon receipt, the skin was kept in a refrigerator at -20°C for a period of no more than 24 h to ensure the skin could be easily separated from the fatty layer. The skin was dermatomed using a dermatome™ (Zimmer TDS, United Kingdom) with a thickness of 400 µm, then cut into circles (±15 mm in diameter) and placed on Whatman® filter paper to dry. Aluminium foil was used to wrap to skin, which was then kept at -20°C in the freezer. The frozen skin samples were thawed and visually examined for defects before diffusion studies commenced, and thereafter mounted on the diffusion apparatus.

2.4.3 Skin diffusion

Refer to Section 2.4.1. Instead of a membrane filter, dermatome skin was used. The skin was placed on the receptor compartment (stratum corneum facing upwards) and covered with the donor compartment. PBS (pH 7.4) was used to fill the receptor compartment. After a period of 12 h, the entire receptor compartment was withdrawn. The API that permeated into the receiver fluid (PBS) through the skin was determined by analysing samples by means of HPLC (Baert *et al.,* 2011).

2.4.4 Tape-stripping

Tape-stripping studies were conducted once skin diffusion studies were completed, to determine to which extent CLF, ART and DQ permeated into the different layers of the skin. The process is described as follows: all nine Franz cells were dismantled after skin diffusion studies and skin samples pinned onto a solid surface, which was covered with Parafilm® to ensure no leakage of the formulation onto the surface. Residual formulation on the skin was carefully dabbed dry with paper towel (Walters & Brain, 2008). 3M Scotch® Crazy™ tape was cut into the same size as the diffusion area. The first tape strip of fifteen, which was used per skin sample, was disposed of due to potential contamination with formulation remaining on the skin samples. The remainder of the skin sample strips were used to remove the stratum corneum-epidermis (SCE; upper layer of the skin containing API) until the skin glistened, after which the tape strips were transferred to separate polytops filled with 5 ml of absolute ethanol (99.7%). The remaining skin samples (epidermis-dermis (ED)) were cut into smaller pieces and placed in separate polytops, which also contained 5 ml of ethanol absolute. These polytops were left overnight, in a fridge at (±4°C), for the API to dissolve in the extraction fluid (Pellet *et al*., 1997). The solutions were filtered afterwards and analysed by means of HPLC.

2.5 Data and statistical analysis

A two-way analysis of variance (ANOVA) test was performed on the tape-stripping data to determine the statistical difference between the APIs (CLF, ART and DQ), the skin layers (SCE and ED) and the natural oils (olive oil (O) and safflower oil (S)). An acceptable significance level for the ANOVA is illustrated by a p-value smaller than 0.05 ($p<0.05$).

2.6 *In vitro* cytotoxicity

2.6.1 Cell culture cultivation

The cytotoxicity of the nano-emulsions was determined using an epidermal (mammalian) cell line (HaCaT). The HaCaT cell line was cultivated with a growth medium of DMEM in a humidified incubator at 37°C and 5% CO2 in a 75 cm^2 flask, where the cells were enriched with 10% foetal bovine serum, 1% Pen/Strep, 4 mM L-glutamine and 1% Non-Essential Amino Acids

supplements. The cells were fed everyday with fresh growth media then split after a confluence of 80% was reached (Abcam, 2017).

2.6.2 Seeding of cells for toxicity assay

To determine and visualise the cell viability, a haemocytometer was used. The Trypan Blue dye 0.4% (w/v) exclusion approach was used to stain identical cell suspensions of 10 µl each. The cells were stained for 3 min each then transferred to an etched counting chamber (9 mm^2) to be evaluated. The process of dye takes place as dead (non-viable) cells take up the dye; living (viable) cells do not take up any dye.

2.6.3 Determining cell death using LDH assay

To determine the cell death by means of lactate dehydrogenase (LDH) assay, a CytoTox 96® Non-Radioactive Cytotoxicity Assay Detection Kit was used. The measurement of cell death was implemented with the following: 1) a positive control with 100% LDH release (full cell damage), 2) a negative control, which is a medium containing no API or nano-emulsion dispersion and 3) samples of **S1**, **S2**, **S3**, **S4**, **S5**, **O1**, **O2**, **O3**, **O4** and **O5** (Ahn *et al*., 2012). During the process, the CytoTox 96® Non-Radioactive Cytotoxicity Assay Detection Kit's directions were followed to determine the LDH-release for the cells. The growth medium and cells were placed in the 96-well assay plate and made up to volume (100 µl) with the prepared samples at the predetermined concentrations.

2.7 *In vitro* cytotoxicity on *Mycobacterium* strains

The nano-emulsions used for the evaluation of *in vitro* cytotoxicity on *Mycobacterium* strains were sent to University of Cape Town (UCT), South Africa.

2.7.1 Determination of the 90% minimum inhibitory concentration (MIC_{90})

The broth microdilution method (Collins & Franzblau, 1997) was used to assess the MIC_{90} (minimum concentration of API). The eight nano-emulsions, together with their placebos, were tested in one 96-well microtiter plate. A culture of mutant *Mycobacterium tuberculosis* (M.tb H37RvMA::*gfp*) strain expressing recombinant green fluorescent protein (GFP) off a plasmid integrated at the phage attachment site (*attB)* locus was grown to OD_{600} (optical density reading taken at 600 nm) between 0.6 and 0.7. This culture was diluted (1:100) in glycerol-alanine-salts

containing iron and Tween® 80 (GAST/Fe) medium. In row 1, 640 µm of the 10 nano-emulsions that were tested was added in duplicate, and a total volume of 50 µl of GAST/Fe medium was added to rows 2 to 12 of the plate. In addition to the test nano-emulsions in row 1, other wells contained GAST/Fe medium, 5% dimethyl sulfoxide (DMSO), kanamycin and rifampicin as a control. Two-fold serial dilution was followed by transferring 50 µl of the nano-emulsion solution from each preceding row to the following row ensuring that all the wells contain 50 µl (not for control wells), thereafter plates were incubated at 37°C (humid conditions) for 14 days. MIC_{90} values were scored using quantitative fluorescence at 7-days and 14-days post inoculation by means of a FLOUstar® Optima microplate reader (BMG Labtech). Consequently, digital images were captured and stored. According to Van der Ven *et al.* (2015), during the growth in different carbon sources, the efficacy of the APIs is determined.

2.7.2 Intracellular efficacy of compounds against *Mycobacterium tuberculosis* H37Rv

The J774 macrophage cell line grown in DMEM was plated on a 96-well plate (100 µl/well) and incubated overnight at 37°C in a CO_2 incubator. The plate was transferred to Biosafety Level 3 for infection with the H37RvMA::*gfp* (OD_{600} 0.4-0.6) and this culture was grown in 7H9/OADC and DMEM, ensuring 10^5 cells per ml. J447 cells were washed with PBS-Tween^{80}. Following the aforementioned, the cells were infected with the H37RvMA::*gfp* (100 µl) in DMEM, then H37RvMA::*gfp* in 7H9/OADC was added in appropriate wells and incubated for 4 to 6 h. Ten-fold serial dilutions of plated cells were plated on the agar plates, which contained 7H10/OADC supplemented with hygromycin B resistance gene (Hyg^{50}) and incubated at 37°C. Following successful bacterial-uptake by macrophages, the medium was replenished with compound containing medium. By means of the FLOUstar® Optima microplate reader (BMG Labtech), the GFP signal was read and images of representative wells were captured using the fluorescent cell imager (ZOE Fluorescence Imager, BioRad). The medium was replenished every second day and the GFP was read daily. After GFP captured fluorescence image analysis, the cells were lysed for enumeration of viable colony-forming units (CFU) and compared with the GFP readouts on day 6. To determine whether the combination of the APIs in the nano-emulsions would have

a synergistic effect on their efficacy or whether the combination will cause cell death, a combination of the APIs were done.

3 Results and discussion

3.1 Formulation and semi-solid products

All eight nano-emulsions were very watery. The CLF formulations had a distinct brown colour and the ART and DQ were a white colour; no phase separation or sedimentation was present. Tables 1 and 2 summarise the ingredients used during formulation.

3.2 Physicochemical properties

3.2.1 Aqueous solubility

The aqueous solubility for CLF, ART and DQ were determined as 0.00 mg/ml, 0.10 mg/ml and 0.00 mg/ml, respectively, at a temperature of 32°C. These results indicate that CLF and DQ are practically insoluble in water and ART is slightly soluble in an aqueous medium. Naik *et al*. (2000) reported that for an API to be soluble in an aqueous medium, a solubility of more than 1 mg/ml was required to permeate ideally through the skin.

3.2.2 Log D

The log D values of CLF (7.60), ART (2.49) and DQ (7.80) indicated that both CLF and DQ do not show favourable properties to diffuse through the skin, whereas ART does (Naik *et al.,* 2000).

3.2.3 Characterisation of nano-emulsions

Table 3: Physicochemical properties of nano-emulsions

No TEM images could be taken since the oil in the nano-emulsions could damage the equipment. Table 3 summarises the different characterisation values (pH, viscosity, droplet size, zeta-potential and %drug entrapment). The pH of all eight formulations was in the ideal range (pH 5-9) for topical drug delivery (Naik *et al*., 2000), as the values were in a narrow range between 5.14 and 5.70. All the formulations had a zeta-potential ranging from -32.9 to -26.1 mV, indicating no phase separation would take place and were stable regarding the accepted range of zeta-potential, which should be more positive than +25 mV and more negative than -25 mV (Mothilal *et al*, 2014). The viscosity of nano-emulsions was very low (2.56-2.73 cP)

and could possibly be attributed to the fact that 80% of the formulation consisted of water, with no thickener used. The EE% of all eight nano-emulsions depicted results between 91.35 and 98.95 %.

3.3 Membrane diffusion experiments

The results from the membrane release studies show conclusive evidence that no API successfully permeated through the membrane into the receptor fluid. No data was obtained with all three actives, separately or in combination.

3.4 Diffusion experiment

3.4.1 Diffusion study

During skin diffusion studies, the exact method was followed in membrane diffusion studies except a skin sample was used instead of a synthetic membrane. Skin diffusion studies took place by extracting the receptor phase every 2 h for 12 h. No concentration of the APIs were obtained within the receptor fluid during this method and therefore it was decided to prolong the extraction time to only one single withdrawal after 12 h; after this withdrawal, the samples were analysed by means of HPLC. It was evident that no APIs permeated into the receiver fluid during the diffusion study.

3.5 Tape-stripping

3.5.1 Stratum corneum-epidermis

The tape-stripping results for the SCE are depicted in Figures 1 to 4. On comparing the median concentrations, the nano-emulsions containing safflower oil with a single API (**S1**, **S2** and **S3)**, it was evident **S2** depicted the highest median concentration, followed by **S3** and lastly, **S1**. When comparing the median concentrations, the nano-emulsions containing olive oil with a single API (**O1**, **O2** and **O3**), it was observed that **O2** depicted the highest median concentration, followed by **O1** and lastly, **O3**; the median concentration of both **O1** and **O3** did not differ much. With the nano-emulsion containing safflower oil with the combination of APIs (**S4**) it was observed that ART had the highest median concentration when compared to CLF and DQ, followed by CLF. With the nano-emulsion containing olive oil with the combination of APIs (**O4)**, it was evident that

ART depicted the highest median concentration followed by CLF. It can also be observed that neither **S4** nor **O4** delivered DQ within the SCE.

Figure 1: Concentration (µg/ml) of **S1** (CLF), **S2** (ART) and **S3** (DQ) present in the SCE after tape-stripping. Concentration values are indicated by the lines and squares, respectively.

Figure 2: Concentration (µg/ml) of **O1** (CLF), **O2** (ART) and **O3** (DQ) present in the SCE after tape-stripping. Concentration values are indicated by the lines and squares, respectively.

Figure 3: Concentration (µg/ml) of CLF, ART and DQ present in **S4** in the SCE after tape-stripping. Concentration values are indicated by the lines and squares, respectively.

Figure 4: Concentration (µg/ml) of CLF, ART and DQ present in **O4** in the SCE after tape-stripping. Concentration values are indicated by the lines and squares, respectively.

Figures 1 to 4, illustrated all the nano-emulsions containing a single API (**S1**, **S2**, **S3**, **O1**, **O2** and **O3**) accumulated within the SCE. It was also observed that the nano-emulsions containing safflower oil with a single API (**S1**, **S2** and **S3**) showed increased permeation when compared to the nano-emulsions containing olive oil with a single API (**O1**, **O2** and **O3**), excluding CLF (**O1** was higher than **S1**). It was apparent that when the nano-emulsions containing a single API were compared (**S1**, **S2**, **S3**, **O1**, **O2** and **O3**) regarding the API, ART permeated the SCE more than CLF and DQ. On comparing the nano-emulsions containing the combination of APIs (**S4** and **O4)**, it was noticed that ART permeated the SCE more than CLF and DQ, and that DQ did not accumulate in the SCE for both **S4** and **O4**. It cannot be said with certainty which oil improved the delivery more since the following was apparent: **O4** delivered CLF more than **S4** and **S4** delivered ART more than **O4**. The aforementioned was also true when the nano-emulsions containing a single API (**S1**, **S2**, **S3**, **O1**, **O2** and **O3**) were compared, although the safflower oil also increased the delivery of DQ more than the olive oil.

3.5.2 Epidermis-dermis

When the median concentrations were compared with the nano-emulsions containing safflower oil with a single API (**S1**, **S2** and **S3**), **S3** yielded the highest median concentration, followed by **S1**. When individual olive nano-emulsions (**O1**, **O2** and **O3)** were compared, **O3** depicted the highest median concentration, followed by **O1**. It was also evident that neither **S2** nor **O2** delivered ART in the ED. When examining **S4** and **O4**, it was apparent that DQ had the highest median concentration, followed by CLF. It was also seen that neither **S4** nor **O4** delivered ART into the ED.

Figure 5: Concentration (µg/ml) of **S1** (CLF) and **S3** (DQ) present in the ED after tape-stripping. Concentration values are indicated by the lines and squares, respectively.

Figure 6: Concentration (µg/ml) of **O1** (CLF) and **O3** (DQ) present in the ED after tape-stripping. Concentration values are indicated by the lines and squares, respectively.

Figure 7: Concentration (µg/ml) of CLF, ART and DQ present in **S4** in the ED after tape-stripping. Concentration values are indicated by the lines and squares, respectively.

Figure 8: Concentration (µg/ml) of CLF, ART and DQ present in **O4** in the ED after tape-stripping. Concentration values are indicated by the lines and squares, respectively.

Figures 5 to 8 illustrated that the nano-emulsions containing a single API (**S1**, **S3**, **O1**, and **O3**) accumulated in the ED (excluding **S2** and **O2**). It was evident with the nano-emulsions containing a single API (**S1**, **S3**, **O1**, and **O3**) that it was not possible to determine which natural oil improved permeation; since **O1** improved the permeation of the CLF more than **S1**, whilst **S3** improved the permeation of the DQ more than **O3**.

When the nano-emulsions containing a single API (**S1**, **S2**, **S3**, **O1**, **O2** and **O3**) were compared in terms of the API, it was observed that DQ had the highest concentration of API within the ED

compared to CLF and ART. In the case of DQ, it could possibly be due to other penetration routes being followed other than that of direct skin permeation, i.e. the annexial route (Williams, 2003). The annexial route (also known as the sebaceous glands) is situated within hair follicles and is known to secrete sebum (cholesterol, waxes, triglycerides, fatty acids and cellular debris) and subsequently lipophilic drugs can tend to cross this route, due to their lipophilic nature (Montage, 1965; Williams, 2003).

It was apparent when **S4** and **O4** were compared that a similar trend was followed, as with the nano-emulsions containing a single API (**S1**, **S2**, **S3**, **O1**, **O2** and **O3**), where DQ permeated the ED more than CLF (ART did not accumulate in the ED for any of the nano-emulsions). It was also observed that **S4** enhanced the permeation of the APIs more than the **O4** for both DQ and CLF. In general, it was apparent that the nano-emulsions containing safflower oil (**S3** and **S4**) permeated better than those containing olive oil (**O3** and **O4**); a possible explanation might be the amount of linoleic acid which is present in safflower (75.0%) and olive oil (1.5%). Since the first layer of the skin, the stratum corneum, also consists of linoleic acid, the increased amount of linoleic acid found in the safflower oil in comparison to the olive oil, might have cause an increased delivery of the APIs into the stratum corneum from the nano-emulsions containing safflower oil (Applewhite, 1966; Olive oil Source, 2017; Vermaak *et al.*, 2011). Consequently, more API can permeate through the stratum corneum (SCE) and in turn, the API is available to diffuse from the SCE to the ED (Cross & Roberts, 1993).

3.6 Statistical analysis

3.6.1 Tape-stripping

As mentioned before, no data was obtained during the membrane or diffusion studies, but only with the tape-stripping studies. Results found during tape-stripping studies from the two-way ANOVA between the APIs (CLF, ART and DQ), the skin layers (SCE and ED) and the natural oils (O and S) depicted statistical significance ($p<0.05$). The one-way ANOVA between the oils (O and S) showed no statistical significance ($p = 0.0531$).

3.7 *In vitro* cytotoxicity

To determine the cell cytotoxicity of the APIs within the formulations, the LDH assay was employed. CLF, ART and DQ, which was encapsulated separately and in combination in the nano-emulsions containing natural oil, were compared to a placebo. A non-cytotoxic reference was used as a control sample, and cell cytotoxicity was evaluated using the following ranges: 1) below 40% - non-cytotoxic, 2) between 60% and 40% - weak cytotoxicity, 3) between 80% and 60% - moderate cytotoxicity and 4) between 100% and 80% - strong cytotoxicity (Lopez-Garcia *et al*., 2014). The formulations were also analysed statistically by comparing the formulations with the control sample. By examining the p-value results of all the nano-emulsions, it was evident there was a statistical significance for all formulations ($p<0.05$). The control has a cytotoxic effect of 0% (no effect on cells), whereas lysis has a cytotoxic effect of 100% (complete cell death/cytotoxicity).

Table 4: LDH results for the nano-emulsions containing safflower oil and olive oil separately

Table 4 summarises the results of the cytotoxicity profiles of all eight nano-emulsions (**S1**-**S4** and **O1**-**O4**), together with their placebos (**S5** and **O5**). All eight nano-emulsions, including the placebos, depicted results of either non-cytotoxic (<40%) or weak cytotoxicity (<40-60%) on the HaCaT cells.

3.8 *In vitro* cell culture studies on tuberculous cells

Table 5: Percentage inhibition of the formulations against *M.tb* H37Rv relative to control culture

Table 5 depicts the %inhibition results of each nano-emulsion (**S1**-**S5** and **O1**-**O5**) used on *M.tb* H37Rv, respectively. The *in vitro* cell culture studies were executed to indicate the extent to which the nano-emulsions would inhibit the *M.tb* strains. It was evident, looking at Table 5, that the nano-emulsions showed exceptional results with regard to %inhibition. Isoniazid (INH) was used as the positive control within this study, since it is known to cause cell death to *Mycobacterium* strains. The eight nano-emulsions (**S1**-**S4** and **O1**-**O4**) showed exceptionally high %inhibition, ranging from values 52 to 63% inhibition, when compared to the positive control. When the

%inhibition results of the nano-emulsions containing safflower oil were compared with the nano-emulsions containing olive oil, it was evident the former had higher %inhibition values than the latter. The primary focus of this part of the study was to determine if the nano-emulsions containing the combination of APIs (**S4** and **O4**) would give better %inhibition results against *M.tb* H37Rv than those containing a single API (**S1**, **S2**, **S3**, **O1**, **O2** and **O3**). It was evident that the **S4** (60%) yielded a higher %inhibition than **O4** (53%). Due to natural oils used with the nano-emulsions, the placebos (**S5** and **O5**) depicted some degree of %inhibition. Consequently, the nano-emulsions containing APIs could possibly be used in the future for the topical treatment of CTB.

4 Conclusion

Eight nano-emulsions containing natural oil were formulated - six nano-emulsions containing a single API (**S1**-**S3** and **O1**-**O3**) and two containing the combination of APIs (**S4** and **O4**). When the membrane release studies were observed, it was evident that no API concentration (CLF, ART and DQ) was found within the receptor fluid. Similar results were observed with diffusion studies, as no API permeated through the skin within the receptor fluid. Tape-stripping studies revealed that when APIs were incorporated separately within nano-emulsions (**S1**-**S3** and **O1**-**O3**) it was possible to deliver CLF, ART and DQ in the SCE. It was also apparent, when APIs are incorporated separately within nano-emulsions (**S1**-**S3** and **O1**-**O3**), that ART cannot be delivered into the ED, whilst CLF and DQ can. It was observed that ART, a polar compound, had a higher affinity for both the safflower and olive oil during the pre-formulation studies, when compared to CLF and DQ (Haynes *et al*., 2006). During tape-stripping studies, it was seen that the ART concentration was higher in the SCE compared to CLF and DQ. The phenomenon of ART could possibly be ascribed to the high affinity ART had for the oil. The lipophilic oil also has a high affinity with the lipophilic stratum corneum, which in turn may have led to the higher entrapment of ART within the SCE. Subsequently, although ART has a polar nature, its affinity for the oil phase (both safflower and olive oil) was significantly higher than the affinity for the hydrophilic ED and therefore it can possibly be concluded that ART remained within the lipophilic SCE rather than permeating to the hydrophilic ED. On investigating the nano-emulsions

containing the combination of APIs (**S4** and **O**4), it was observed that DQ was only noticeable in the ED and not in the SCE. This could possibly be ascribed to the "saturation effect" which took place in the stratum corneum, as described by Teichmann *et al.* (2005) who concluded that even with prolonged application, the stratum corneum can be saturated and subsequently no concentration increase will be observed. Subsequently, before DQ could reach the stratum corneum, saturation may have occurred with ART and CLF within the SCE, therefore, another route of penetration could have been followed by DQ, such as the annexial route by permeating directly to the dermis (Teichmann *et al*., 2005). When compared to CLF and DQ, ART has more ideal physicochemical properties and could therefore imply that ART permeated the SCE first, followed by CLF; it may be possible that CLF and ART followed the intracellular route to permeate within the SCE, while no DQ was found within the SCE (N`Da, 2010). As the concentration gradient still plays a significant role, it might be possible that the CLF (which was entrapped within the SCE) diffused to the ED and consequently the nano-emulsion (which was still applied on top of the skin) provides the underlying skin layers with CLF and therefore CLF was seen in both the SCE and the ED. When the nano-emulsions containing the combination of APIs (**S4** and **O4**) are investigated, it is observed that DQ cannot be delivered in the SCE and ART cannot be delivered in the ED, therefore it is not possible to deliver all three APIs in either the SCE or the ED. When comparing the natural oils formulated in the nano-emulsions, it is evident that nano-emulsions containing safflower oil increased the permeation of the APIs more than the nano-emulsions containing olive oil.

During the LDH-assay, no cytotoxicity was observed from all eight nano-emulsions, which indicated that all the dispersions were safe for human usage. Decreased cytotoxicity might possibly be explained by the way the nano-emulsions encapsulate the APIs. The nano-emulsions possibly provide a barrier between the APIs and the interaction with the normal healthy cells, since there is no direct skin contact. A study by De Godoi *et al*. (2017) depicted similar results, where cytotoxicity decreased when using nano-emulsions as the API formed a barrier because it was encapsulated within an oil droplet. When viewing the cytotoxicity from the *Mycobacterium* cell lines, it was evident that all eight nano-emulsions depicted very good results regarding

%inhibition. Values ranged from 52 to 63% inhibition for the nano-emulsions, which contained APIs (**S1**-**S4** and **O1**-**O4**), and both placebos (**S5** and **O5**) depicted a small %inhibition also, 14% and 22%, respectively. On comparing the %inhibition results of the nano-emulsions containing safflower oil to those containing olive oil, it was clear the nano-emulsions containing safflower oil depicted higher %inhibition values than those containing olive oil. The results obtained from the placebo nano-emulsions could possibly be ascribed to the use of natural oils within the nano-emulsions. When the nano-emulsions containing APIs (**S1**-**S4** and **O1**-**O4**) were compared to the placebo nano-emulsions (**S5** and **O5**), the placebos depicted remarkable results in terms of %inhibition, consequently, it can be concluded that the natural oils within the nano-emulsions do have an impact on the %inhibition. The nano-emulsions containing safflower oil increased the delivery of the APIs more than those containing olive oil. Enhanced permeation from the nano-emulsions containing safflower oil could possibly be due to the increased amount of linoleic acid (75.0%), which is found in safflower oil (Applewhite, 1966), compared to olive oil (1.5%)(Olive oil Source, 2017), since the skin (stratum corneum) also consists of linoleic acid (Vermaak *et al.*, 2011).

Acknowledgements

The authors would like to express their appreciation towards the South African Medical Research Council (Flagship programme MALTB Redox), the Centre of Excellence for Pharmaceutical Sciences, Faculty of Health Sciences, North-West University, South Africa and the National Research Foundation of South Africa for their financial contribution to this project [grant number CPRR13091742482]. A special thank you to Marelize Pretorius, from Statistical Consultation Services for the statistical analysis of the data and Ms. A. Brümmer for the cytotoxicity studies at the North-West University, Potchefstroom Campus, South Africa.

Declaration of interest

Any opinions, findings, conclusions or recommendations expressed in this material are those of the authors and therefore the NRF does not accept any liability with regard thereto.

References

Abcam., 2017. http://www.abcam.com/ps/pdf/protocols/cell_culture.pdf Date of access: 14 Nov 2017.

Ahn, B., Kim, J., Kong, C., Seo, Y.,. Kim, S., 2012. Protective effect of (2'S)-columbianetin from corydalis heterocarpa on UVB-induced keratinocyte damage. J Photochem Photobiol B, 109, 20-27.

Baert, B., Vansteelandt, S., De Spiegeleer, B., 2011. Ion mobility spectrometry as a high-throughput technique for *in vitro* transdermal Franz diffusion cell experiments of ibuprofen. J Pharm Biomed Anal, 55, 472,473.

Borhade, V., Pathak, S., Sharma, S., Patravale, V., 2012. Clotrimazole nanoemulsion for malaria chemotherapy. Part 2: Stability nassesment, *in vivo* pharamcodynamic evaluations and toxicological studies. Int J Pharm, 431, 149-160.

Bravo, F.G., Gotuzzo E., 2007. Cutaneous tuberculosis. Clin Dermatol, 25, 2, 173.

British Pharmacopoeia. 2013a. Online version. http://www.pharmacopoeia.co.uk.nwulib.nwu.ac.za/bp2013/ixbin/bp.cgi?a=query&title=%22Phosphate%20Buffer%20Solution%20pH%207.4%22&tab=a-z%20index&l=P&xh=1 Date of access: 23 Aug 2017.

British Pharmacopoeia., 2013b. Online version. http://www.pharmacopoeia.co.uk.nwulib.nwu.ac.za/bp2013/ixbin/bp.cgi?a=query&title=%22Phosphate%20Buffer%20Solution%20pH%206.5%2c%200.1%3Csmallcaps%3Em%3C%2fsmallcaps%3E%22&tab=az%20index&l=P&xh=1 Date of access: 23 Aug 2017.

Chembase., 2014. http://en.chembase.cn/molecule-157442.html Date of access: 5 Aug 2015.

Chime, S., Kenechukwu, F., Attama, A., 2014. Nanoemulsions - Advances in Formulation, Characterization and Applications in Drug Delivery. Ali DS. Application of nanotechnology in drug delivery. In Tech, 2014, 77-111.

Cholo, M., Steel, H., Fourie, P., Germishuizen, W.A. Anderson, R., 2012. Clofazimine: current status and future prospects. J. Antimicrob. Chemother, 67, 290-298.

Collins, L., Franzblau, S.G., 1997. Microplate alamar blue assay versus BACTEC 460 systemfor high-throughput screening of compounds against *Mycobacterium tuberculosis* and *Mycobacterium avium*. J Antimicrob Chemother, 41, 1004-1009.

Colombo, P., Cagnani, S., Buttini, F., Santi, P., 2013. Biological *in vitro* models for absorption by non-oral routes. Reference Module in Chemistry, Molecular Sciences and Chemical Engineering, p. 1-19.

Dey, T., Helen, G., Shubber, C., Cooke, G., Ford, N., 2013. Outcomes of clofazimine for the treatment of drug-resistant tuberculosis: a systematic review and meta-analysis. J Antimicrob Chemother, 68, 2, 284-293.

Dingler, A., Gohla, S., 2002. Production of solid lipid nanoparticles (SLN): scaling up feasibilities. Microencapsulation, 19, 11-16.

Dooley, K.E., Obuku, E.A., Durakovic, N., Belitsky, V., Mitnick, C., Nuermberger, V., 2013. World Health Organization group 5 drugs for the treatment of drug-resistant tuberculosis: unclear efficacy or untapped potential? J Infect Dis*,* 207, 1352-1358.

Dunay, I.R., Chi Chan, W., Haynes, R.K., Sibley, L.D., 2009. Artemisone and artemiside control acute and reactivated toxoplasmosis in a murine model. Antimicrob Agents Chemother*,* 53, 10, 4450-4456.

Du Preez, J., Aucamp, M., Burger, C., Gerber, M., Viljoen, J.M., Van Zyl, L. Du Plessis, J., 2017. Development and validation of the simultaneous determination of artemisone, clofazimine and decoquinate with HPLC. Die Pharmazie, 73, 139-142.

Guiguemde, W.A., Hunt, N.H., Guo, J., Marciano, A., Haynes, R.K., Clark, J., Guy, R.K., Golenser, J., 2014. Treatment of Murine Cerebral Malaria by Artemisone in Combination with Conventional Antimalarial Drugs: Antiplasmodial Effects and Immune Responses. Antimicrob Agents Chemother, 58, 8, 4745-4754.

Hurtley, S., Ash, C., 2010. Tuberculosis & malaria. Landscapes of infection. Introduction. Science, 328, 841.

Jagannath, C., Reddy, M., Kailasam, S., O`Sullivan, J.F., Gangadharam, P.R., 1995. Chemotherapeutic activity of clofazimine and its analogues against *Mycobacterium tuberculosis*. *In vitro*, intracellular, and *in vivo* studies. Am J Respir Crit Care Med, 151, 1083-1086.

Telles, M., Chimara, E., Ferrazoli, L., Riley, L.W., 2005. *Mycobacterium kansasii*: antibiotic susceptibility and PCR-restriction analysis of clinical isolates. J Med Microbiol, 54, 975-979.

Haynes, R.K., Fugmann, B., Stetter, J., Rieckmann, K., Heilmann, H.D., Chan, H.W., Cheung, M.K., Lam, W.L., Wong, H.N., Croft, S.L., Vivas, L., Rattray, L., Stewart, L., Peters, W., Robinson, B.L., Edstein, M.D., Kotecka, B., Kyle, D.E., Beckermann, B., Gerisch, M., Radtke, M., Schmuck, G., Steinke, W., Wollborn, U., Schmeer, K., Romer, A., 2006. Artemisone – a highly active antimalarial drug of the artemisinin class. Angewandte Chemie, 45, 2082-2088.

Lam, P.L., Gambari, R., 2014. Advanced progress of microencapsulation technologies: *In vivo* and *in vitro* models for studying oral and transdermal drug deliveries. J Control Release, 178, 25-45.

Liu, Z., Zhang, Q., Ding, L., Li, C., Yin, Z., Yan, G., Pi, J., Li, J., Li, N., Qi, D., 2016. Preparation procedure and pharmacokinetic study of water-in-oil nano-emulsion of Panax notoginseng saponins for improving the oral bioavailability. Curr Drug Deliv, 13, 600-610.

Lopez-Garcia, J., Lehocky, M., Humpolicek, P., Saha, P., 2014. HaCaT keratinocytes response on antimicrobial atelocollagen substrates: extent of cytotoxicity, cell viability and proliferation. J Funct Biomater, 5, 43-57.

Mikota, S.K., Plumb, D.C., 2014. http://www.elephantcare.org/Drugs/decoquin.htm Date of access: 1 Mar 2015.

Mothilal, M., Chiatanya Krishna, M., Surya Teja, S.P., Manimaran, V., Damodharan, N., 2014. Formulation and evaluation of naproxen-eudragit® RS 100 nanosuspension using 32 factorial design. Int J Biol Pharm Allied Sci, 6, 7, 449-455.

Nagelschmitz, J., Voith, B., Wensing, G., Roemer, A., Fugmann, B., Haynes, R.K., Kotecka, B.M., Rieckmann, K.H., Edstein, M.D., 2008. First Assessment in Humans of the Safety, Tolerability, Pharmacokinetics, and *Ex Vivo* Pharmacodynamic Antimalarial Activity of the New Artemisinin Derivative Artemisone. Antimicrob Agents Chemother, 52, 9, 3085-3091.

N`Da, D., 2010. Prodrug strategies for enhancing percutaneous absorption of drugs. *Molecules*, 19, 20780-20807.

Naik, A., Kalia, Y.N., Guy, R.H., 2000. Transdermal drug delivery: overcoming the skin's barrier function. Pharm Sci Technol Today, 3, 9, 318-326.

Parikh, R.H., Patel, R.J., 2016. Nano-emulsions for Intranasal Delivery of Riluzole to Improve Brain Bioavailability: Formulation Development and Pharmacokinetic Studies, 13, 7, 1130-1143.

Pellet, M.S., Roberts, M., Hadgraft, J., 1997. Supersaturated solutions evaluated with an *in vitro* stratum corneum tape stripping technique. Int J Pharm, 151, 1, 94.

Pharmacopeia online., 2014. http://www.uspbpep.com/usp29/v29240/usp29nf245O_m22310.html Date of access: 1 Mar 2015.

Proksch, E., Brandner, J.M., Jensen, J., 2008. The skin: an indispensable barrier. ExpDermatol 17, 1063-1072.

Ramharter, M., Burkhardt, D., Nemeth, J., Adegnika, A.A., Kremsner, P.G., 2006. Short report: in vitro activity of artemisone compared with artesunate against Plasmodium falciparum. Am J Trop Med Hyg, 75, 4, 637-639, 694.

Sanz, R., Calpena, C.A., Mallandrich, M., Clares, B., 2015. Enhancing topical analgesic administration: review and prospect for transdermal and transbuccal drug delivery systems. Curr Pharm Des, 21, 2867-2882.

Reddy, V., O'Sullivan, J., Gangadharam, P., 1999. Antimycobacterial activities of riminophenazines. J Antimicrob Chemother, 43, 615-23.

Steyn, J.D., Wiesner, L., Du Plessis, L.H., Grobler, A.F., Smith, P.J., Chan, W.C., Haynes, R.K., Kotze, A.F., 2011. Absorption of the novel artemisinin derivatives, artemisone and artemiside: potential application of Pheroid™ technology. Int J Pharm, 414, 1-2, 260-266.

Tan, L.S., Stanslas, J., Basri, M., Karjiban, R., Kirby, B.P., Sani, D., Basri, B.H., 2015. Nano-emulsion-based Parenteral Drug Delivery System of Carbamazepine: Preparation, Characterization, Stability Evaluation and Blood-Brain Pharmacokinetics. Curr Drug Deliv, 12, 795-804.

Van der Ven, B.C., Fahey, R.J., Lee, W., Liu, Y., Abramovitch, R.B., Memmott, C., Crowe, A.M., Eltis, L.D., Perola, E., Deininger, D.D., Wang, T., Locher, C.P., Russell, D.G., 2015. Novel inhibitors of cholesterol degradation in *Mycobacterium tuberculosis* reveal how the bacterium's metabolism is constrained by the intracellular environment. PLoS Pathogens, 11, 1-20.

Walters, K.A., Brain, K.R., 2008. Methods for studying percutaneous absorption, in:Wiechers, J.W. (Ed), Science and applications of skin delivery systems. Carol Stream, IL:Allured Publishing Corporation. p. 29-48.

WHO. 2011/2012 Tuberculosis Global Facts. 2011. www.who.int/tb/publications/2011/factsheet_tb_2011.pdf Dtae of access: 29 Aug 2017.

WHO. 2018 Tuberculosis Global Facts. 2018. www.who.int/tb/publications/2011/factsheet_tb_2011.pdf Date of access: 6 Mar 2018.

Williams, R.B., 1997. The mode of action of anticoccidial quinolones (6-decyloxy-4-hydroxyquinolone-3-carboxylates) in chickens. Int J Parasitol, 27, 101-111.

Wiliams, R.B., 2006. Tracing the emergence of drug-resistance in coccidian (Eimeria spp.) of commercial broiler flocks medicated with decoquinate for the first time in the United Kingdom. Vet Parasitol, 135,1-14.

Williams, A.C., Barry, B.W., 2012. Penetration enhancers. Adv Drug Deliv Rev, 64, 128-137.

Tables

Table 1: Formulas for the nano-emulsion containing olive oil

Formula	Water phase	Weight (v/v)	Oil phase	Weight (w/v)
O1	Water	40 ml	Olive oil	10% (4.6 ml)
	Tween® 80	3.6 ml	Span® 60	1 g
			CLF	500 mg
O2	Water	40 ml	Olive oil	10% (4.6 ml)
	Tween® 80	3.6 ml	Span® 60	1 g
			ART	500 mg
O3	Water	40 ml	Olive oil	10% (4.6 ml)
	Tween® 80	3.6 ml	Span® 60	1 g
			DQ	500 mg
O4	Water	40 ml	Olive oil	5% (4.6 ml)
	Tween® 80	3.6 ml	Span® 60	1 g
			CLF	500 mg
			ART	500 mg
			DQ	500 mg
O5	Water	40 ml	Olive oil	5% (4.6 ml)
	Tween® 80	3.6 ml	Span® 60	1 g

Table 2: Formulas for the nano-emulsion containing safflower oil

Formula	Water phase	Weight (v/v)	Oil phase	Weight (w/v)
S1	Water	40 ml	Safflower oil	5% (4.6 ml)
	Tween® 80	3.6 ml	Span® 60	1 g
			CLF	500 mg
S2	Water	40 ml	Safflower oil	5% (4.6 ml)
	Tween® 80	3.6 ml	Span® 60	1 g
			ART	500 mg
S3	Water	40 ml	Safflower oil	5% (4.6 ml)
	Tween® 80	3.6 ml	Span® 60	1 g
			DQ	500 mg
S4	Water	40 ml	Safflower oil	5% (4.6 ml)
	Tween® 80	3.6 ml	Span® 60	1 g
			CLF	500 mg
			ART	500 mg
			DQ	500 mg
S5	Water	40 ml	Safflower oil	5% (4.6 ml)
	Tween® 80	3.6 ml	Span® 60	1 g

Table 3: Physicochemical properties of nano-emulsions

Formulation	pH	Viscosity (cP)	Droplet size (nm)	Zeta-potential (mV)	Drug entrapment efficiency (%)
O1	5.01 ± 0.10	2.59 ± 0.50	101.36 ± 2.05	-33.3 ± 1.10	94.12 ± 1.20
S1	5.10 ± 0.05	2.91 ± 0.08	126.47 ± 1.75	-30.00 ± 0.10	91.35 ± 1.38
O2	5.15 ± 0.07	2.60 ± 0.08	101.47 ± 1.56	-36.60 ± 0.12	96.30 ± 1.01
S2	5.08 ± 0.02	2.62 ± 0.05	104.63 ± 1.42	-37.90 ± 0.05	98.95 ± 2. 05
O3	5.30 ± 0.08	2.72 ± 0.08	91.39 ± 1.30	-35.40 ± 0.80	93.01 ± 1.45
S3	5.24 ± 0.04	2.73 ± 0.03	83.61 ± 1.72	-34.40 ± 1.33	91.90 ± 0.99
O4: CLFART DQ	5.19 ± 0.08	2.63 ± 0.07	83.05 ± 0.90	-32.00 ± 1.28	94.12 ± 2.40 96.30 ± 1.34 93.01 ± 1.57
S4: CLFART DQ	5.26 ± 0.07	2.56 ± 0.08	88.14 ± 1.52	-30.1 ± 0.05	94.42 ± 1.20 98.5 ± 1.75 98.02 ± 1.35

Table 4: LDH results for the nano-emulsions containing safflower oil and olive oil separately

Formulation	%Cytotoxicity	p-Value
Control	0	0.000
Lysis	100	-
S1	11.857	0.010
S2	20.165	0.000
S3	11.699	0.016
S4	53.076	0.000
S5	20.047	0.000
O1	34.072	0.000
O2	28.309	0.000
O3	15.378	0.001
O4	38.58	0.000
O5	15.834	0.004

Table 5: Percentage inhibition of the formulations against *M.tb* H37Rv relative to control culture

Formulation	CFU/ml	STDEV	%Inhibition (relative to control)
S1	6.67E+07	1.6	60
S2	6.17E+07	1.5	63
S3	8.00E+07	2.9	52
S4	6.67E+07	1.6	60
O1	7.17E+07	1.9	57
O2	7.50E+07	3.7	55
O3	7.67E+07	1.6	54
O4	7.83E+07	0.8	53
S5	1.43E+08	1.6	14
O5	1.30E+08	1.4	22
INH (isoniazid)(1 µg/ml)	3.17E+07	1.7	81
CLF	9.33E+07	2.0	44
ART	1.17E+08	3.4	30
DQ	1.18E+08	2.5	29
Control	1.67E+08	2.4	-

Figure legends

Figure 1: Box-plot indicating the concentration (µg/ml) of **S1** (CLF), **S2** (ART) and **S3** (DQ) present in the SCE after tape-stripping. Concentration values are indicated by the lines and squares, respectively.

Figure 2: Box-plot indicating the concentration (µg/ml) of **O1** (CLF), **O2** (ART) and **O3** (DQ) present in the SCE after tape-stripping. Concentration values are indicated by the lines and squares, respectively.

Figure 3: Box-plot indicating the concentration (µg/ml) of CLF, ART and DQ present in **S4** in the SCE after tape-stripping. Concentration values are indicated by the lines and squares, respectively.

Figure 4: Box-plot indicating the concentration (µg/ml) of CLF, ART and DQ present in **O4** in the SCE after tape-stripping. Concentration values are indicated by the lines and squares, respectively.

Figure 5: Box-plot indicating the concentration (µg/ml) of **S1** (CLF) and **S3** (DQ) present in the ED after tape-stripping. Concentration values are indicated by the lines and squares, respectively.

Figure 6: Box-plot indicating the concentration (µg/ml) of **O1** (CLF) and **O3** (DQ) present in the ED after tape-stripping. Concentration values are indicated by the lines and squares, respectively.

Figure 7: Box-plot indicating the concentration (µg/ml) of CLF, ART and DQ present in **S4** in the ED after tape-stripping. Concentration values are indicated by the lines and squares, respectively.

Figure 8: Box-plot indicating the concentration (µg/ml) of CLF, ART and DQ present in **O4** in the ED after tape-stripping. Concentration values are indicated by the lines and squares, respectively.

Figures

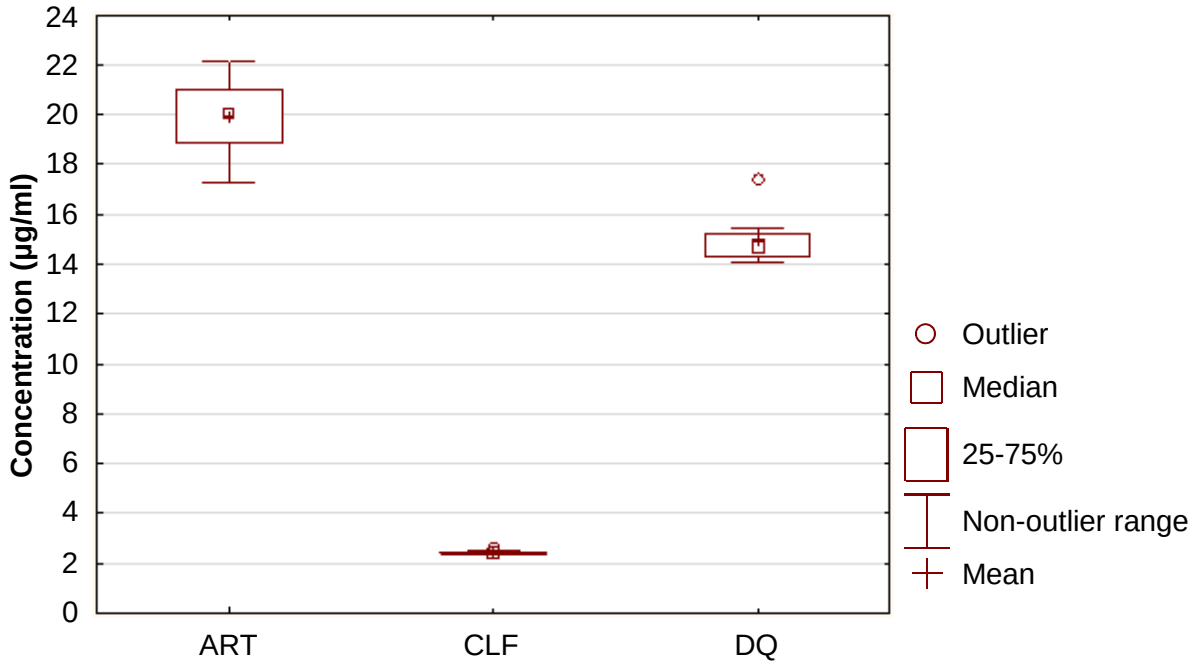

Figure 1: Box-plot indicating the concentration (µg/ml) of **S1** (CLF), **S2** (ART) and **S3** (DQ) present in the SCE after tape-stripping. Concentration values are indicated by the lines and squares, respectively.

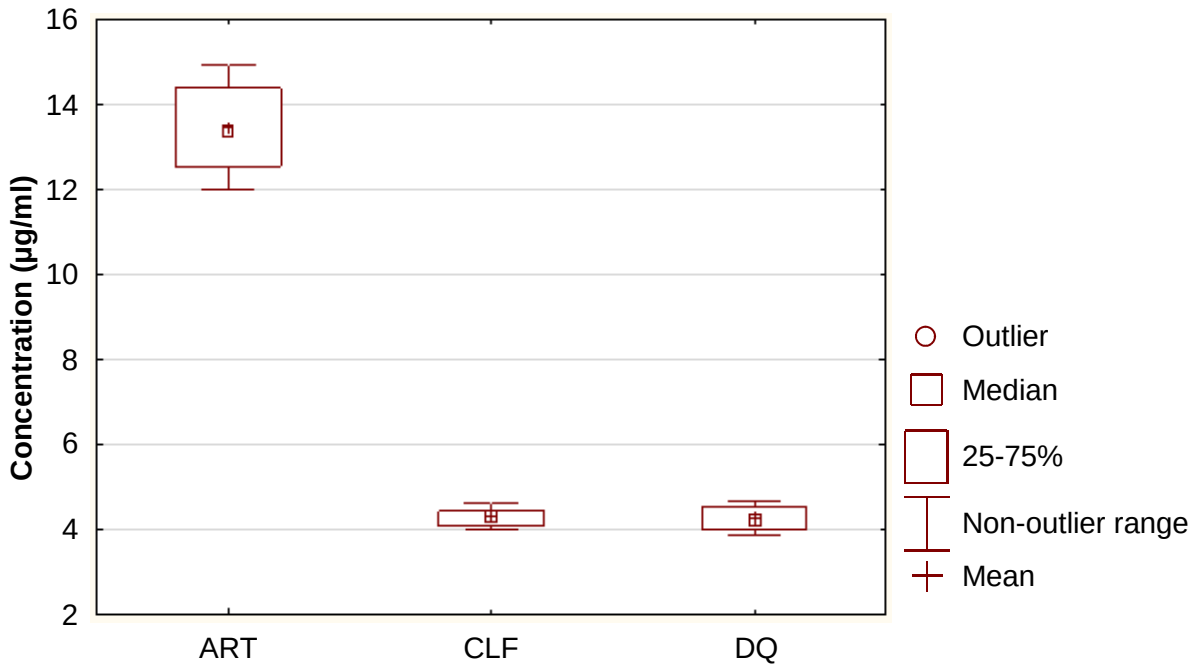

Figure 2: Box-plot indicating the concentration (µg/ml) of **O1** (CLF), **O2** (ART) and **O3** (DQ) present in the SCE after tape-stripping. Concentration values are indicated by the lines and squares, respectively.

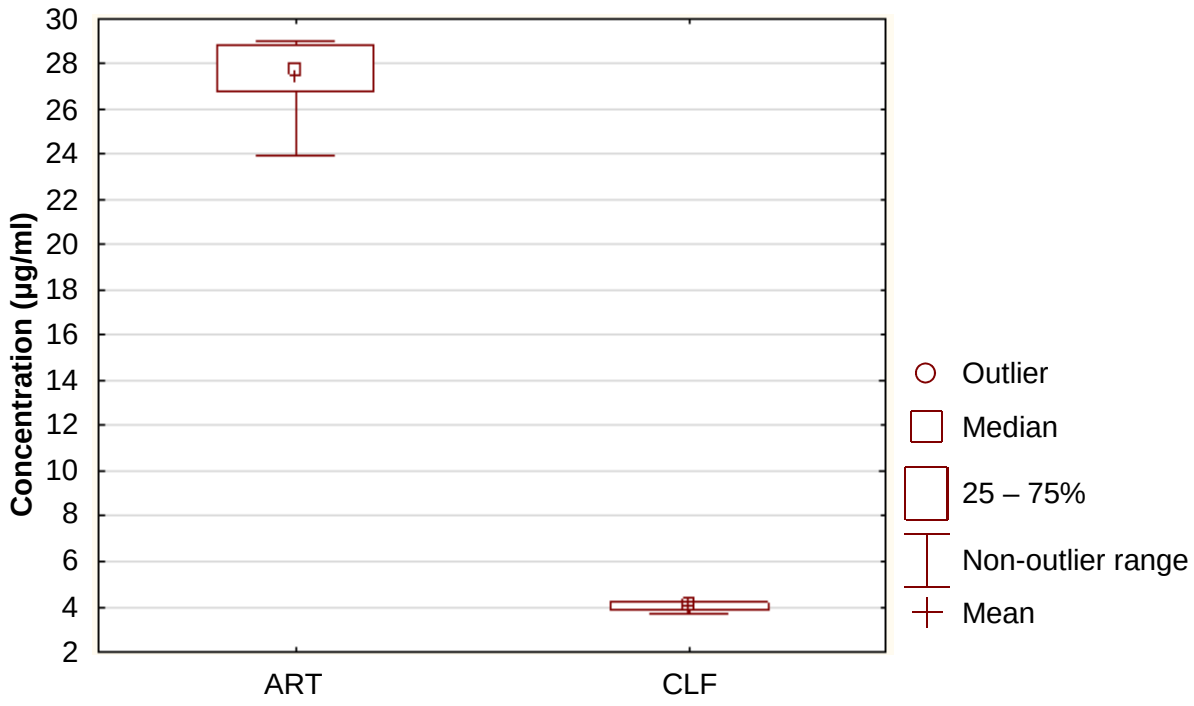

Figure 3: Box-plot indicating the concentration (µg/ml) of CLF, ART and DQ present in **S4** in the SCE after tape-stripping. Concentration values are indicated by the lines and squares, respectively.

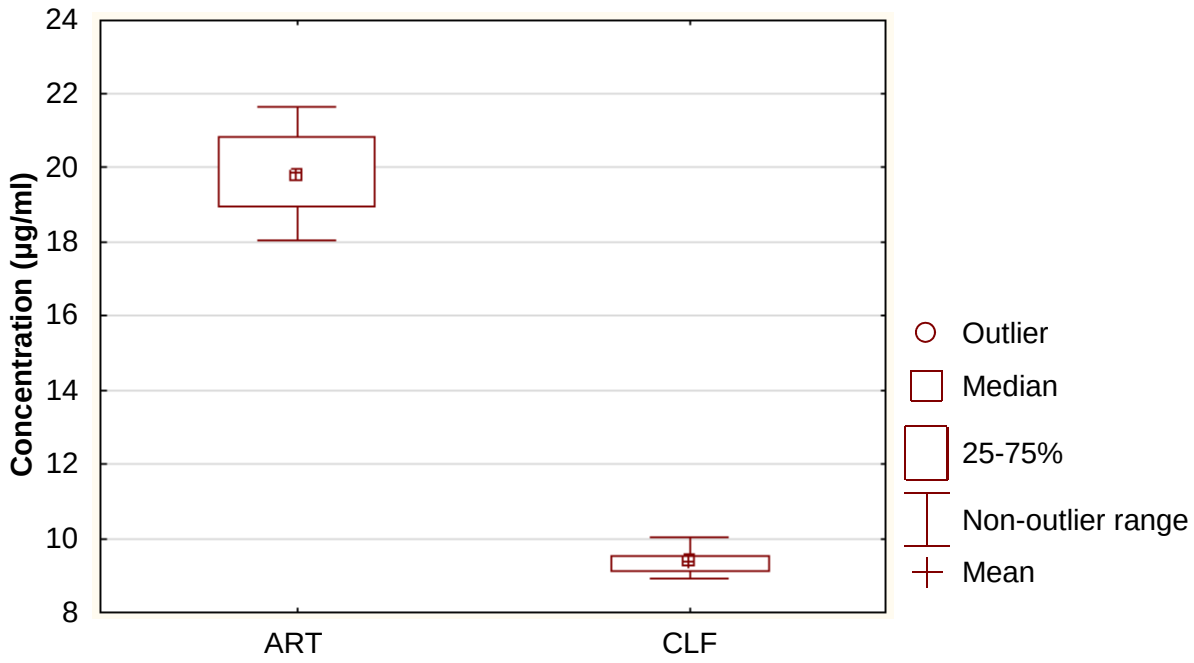

Figure 4: Box-plot indicating the concentration (µg/ml) of CLF, ART and DQ present in **O4** in the SCE after tape-stripping. Concentration values are indicated by the lines and squares, respectively.

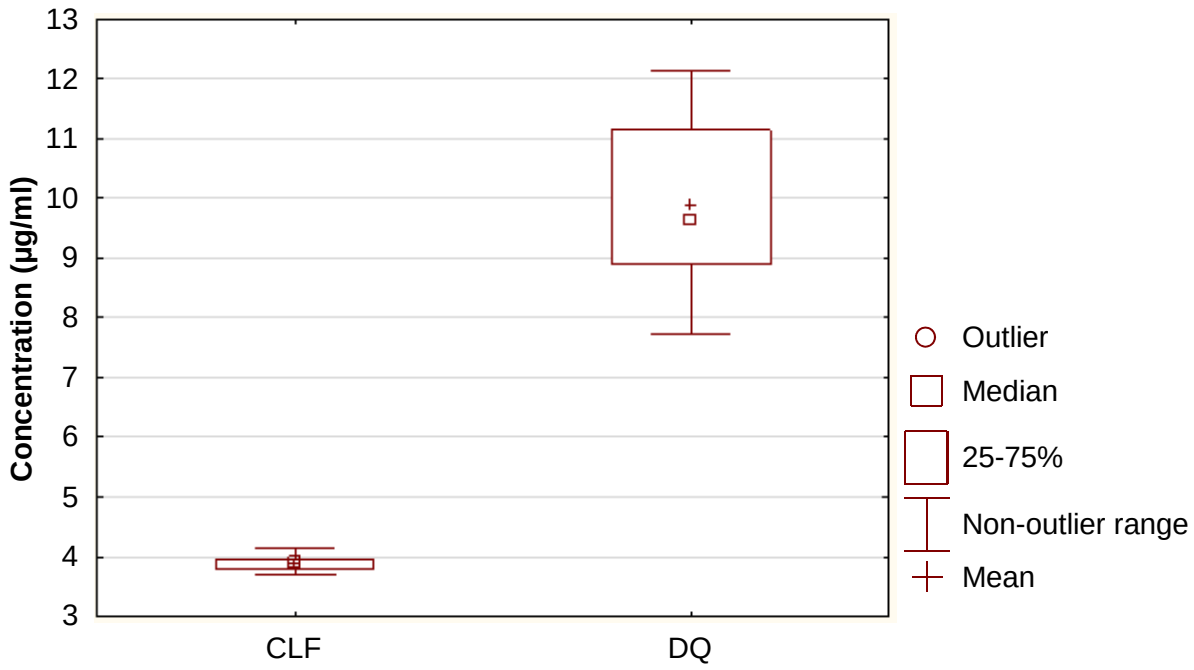

Figure 5: Box-plot indicating the concentration (µg/ml) of **S1** (CLF) and **S3** (DQ) present in the ED after tape-stripping. Concentration values are indicated by the lines and squares, respectively.

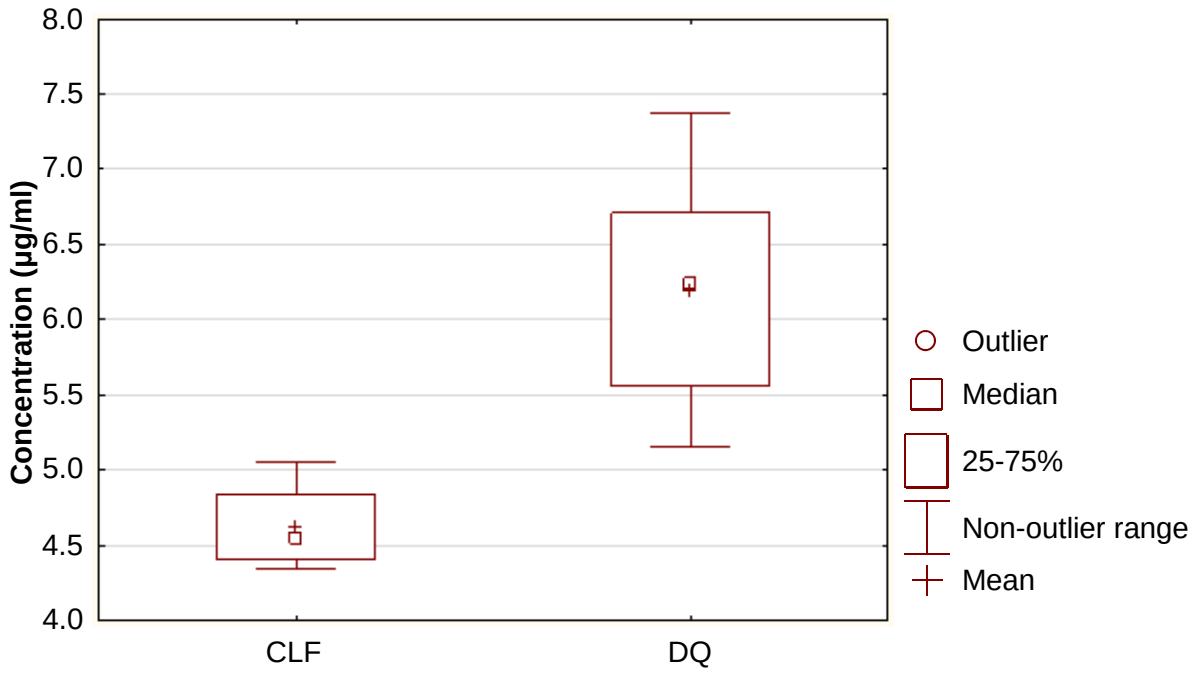

Figure 6: Box-plot indicating the concentration (µg/ml) of **O1** (CLF) and **O3** (DQ) present in the ED after tape-stripping. Concentration values are indicated by the lines and squares, respectively.

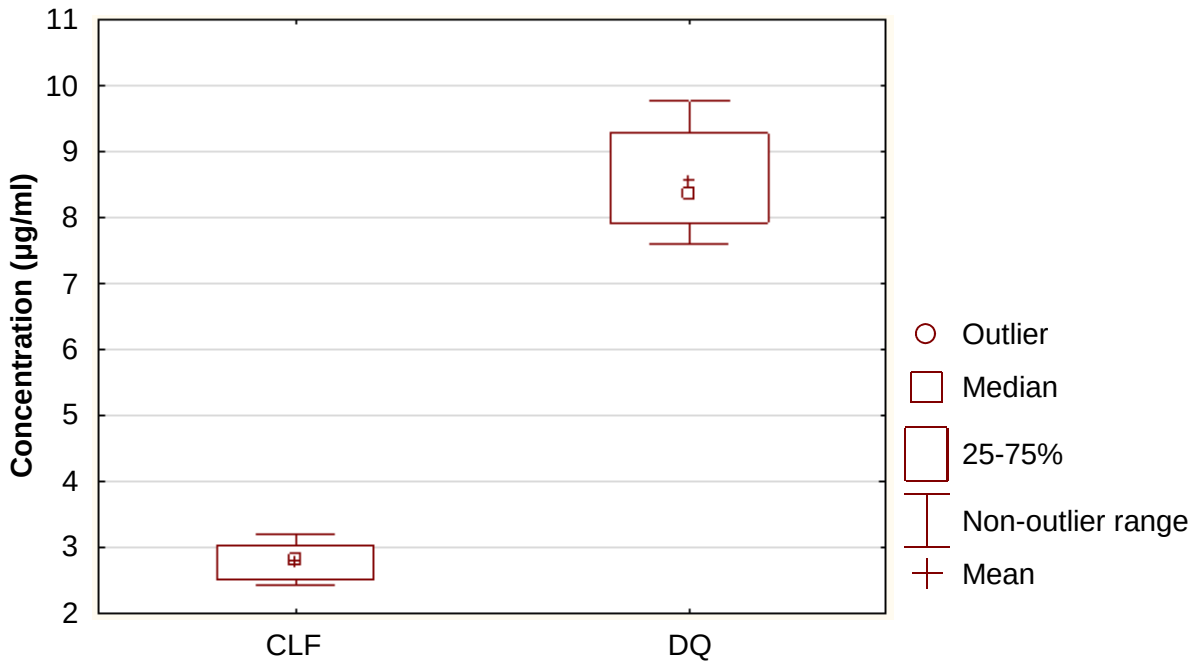

Figure 7: Box-plot indicating the concentration (µg/ml) of CLF, ART and DQ present in **S4** in the ED after tape-stripping. Concentration values are indicated by the lines and squares, respectively.

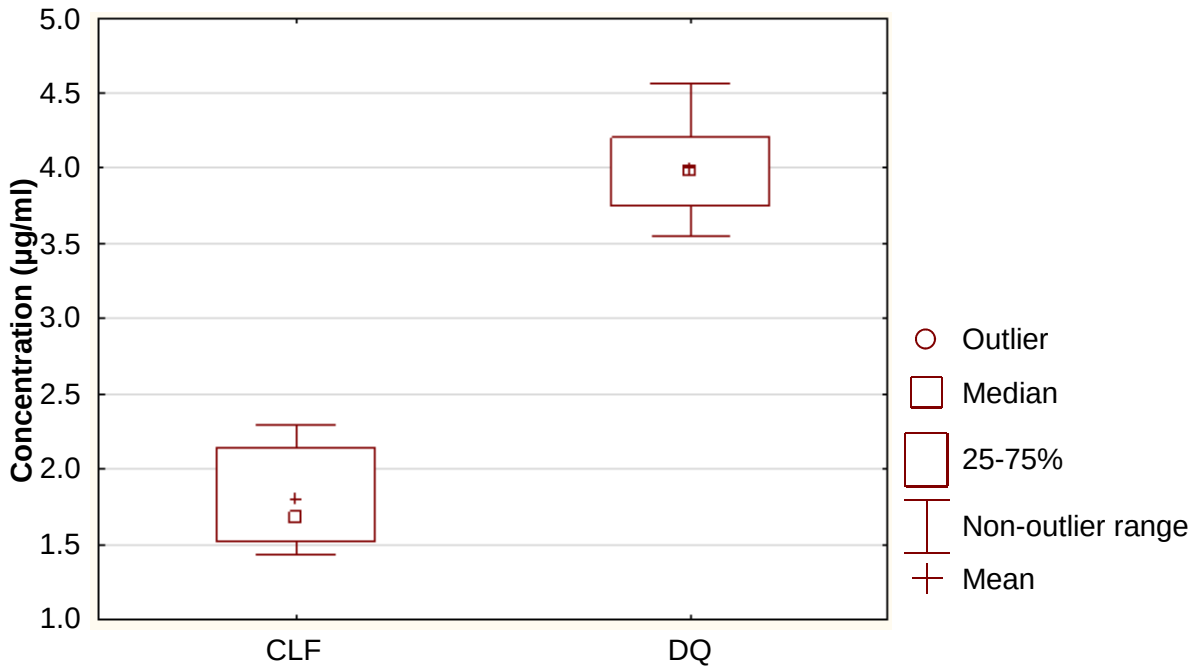

Figure 8: Box-plot indicating the concentration (µg/ml) of CLF, ART and DQ present in **O4** in the ED after tape-stripping. Concentration values are indicated by the lines and squares, respectively.

Chapter 6:

Conclusion and future prospects

The skin is comprised of three main layers (epidermis, dermis and hypodermis) and its responsibility is to act as the primary barrier of the body (El Maghraby *et al.,* 2008:203). This is due to the lipophilic nature of the stratum corneum, which is the upper most layer of the skin and consequently, the rate limiting step for topical and transdermal delivery (Potts *et al*., 1992:16).

TB is primarily caused by the bacterium *M. tuberculosis*. General manifestations are either pulmonary or extra-pulmonary presentations. Extra-pulmonary TB represents nearly 10% of all TB cases, of which CTB comprises only a trivial percentage of these cases (Almaguer-Chávez *et al.,* 2009:562; Kumar *et al.,* 2001:28). Lesions derived from CTB can either be acquired exogenously or endogenously, caused by *M. bovis*, *M. tuberculosis* and the Bacille Calmette Guerin (BCG) vaccine, which is an attenuated strain of *M. bovis* (Barbagallo *et al*., 2002:320; Dostrovsky & Saghar, 1963:188; Izumi & Matsunaga, 1982:171). True CTB skin lesions are only one of the extra-pulmonary presentations and show a variety of structural appearances, which are characterised by variable necrosis, variable vasculitis and granulomatous inflammation (Penneys *et al*., 1993:1596). Different lesions of CTB include lupus vulgaris, scrofuloderma, tuberculous chancre, TB verrucosa cutis, orificial TB, miliary TB and metastatic TB abscess (Barbagallo *et al*., 2002:320). Currently, no topical treatment against CTB exists and as a result of increasing drug resistance against TB, other alternative medications are required and therefore other routes of delivery should be investigated (Van Zyl *et al*., 2015:630). An important note is that topical therapy will not substitute systemic treatment, but rather be used in conjunction to shorten the treatment period of CTB. Consequently, proposing CLF is to repurpose the treatment of TB to increase therapeutic options (Dey *et al*., 2013:284).

CLF is a redox compound, belonging to the riminophenazine class, which was found to have good activity against *M. avium,* both *in vitro* and *in vivo,* and is consequently marketed as anti-mycobacterial drug that treats leprosy (Kailasam *et al*., 1994:273; Lindholm-Levy & Heifets, 1988:179; Mehta *et al*., 1993:2584; Sansarricq, 2005:5). CLF is lipophilic of nature and accumulates within the skin (Dutta, 1980:252-259; Imkamp, 1973:127-130; Imkamp, 1981:135-140), where the primary onset of action is the outer skin, but drug use is potentially restricted because of poor solubility and aesthetic side effects, such as skin discoloration (Kailasam *et al*., 1994:273; Lindholm-Levy & Heifets, 1988:179; Mehta *et al*., 1993:2584).

ART is a moderately new, semi-synthetic drug, derived from artemisinin, which can be synthesised in a one-step process from dihydroartemisinin (Haynes *et al.*, 2004:1381-1385). The Flagship programme proposed to use CLF and ART in combination, since ART can enhance activity against TB, by accelerating the cycling of redox APIs. The mechanism is oxidant activity by which toxic oxygen radicals are thought to be generated through the cleavage of the peroxide bond by iron (Fe (II)) (Biamonte *et al.,* 2013:2831).

DQ (4-hydroxy quinolone) is proposed by the Flagship programme to be combined with CLF and ART even though to date it has only been tested on animals. Due to high lipophilicity (Biamonte *et al.,* 2013:2838), the drug has demonstrated possible anti-TB activity. The compound can possibly complement CLF and ART, since the API's mechanism has an impact on the electron transport disruption within the mitochondrial cytochrome system of the coccidian (Mikota & Plumb, 2014). DQ (which has a different mode of action) in turn can possibly cause suppression of resistance and therefore make the combination of the three APIs more effective against the potential treatment of CTB.

Although the combination of these drugs shows possible effective anti-TB properties, the physicochemical properties present challenges during the topical drug delivery to the target skin site, the epidermis-dermis (ED) (Venus *et al.,* 2011:472).

Nano-emulsions have recently been successfully implemented to improve the transport of hydrophobic compounds and are seen as thermodynamically stable dispersions of oil and water (to form oil in water (o/w), or water in oil (w/o) emulsions), in combination with a surfactant and co-surfactant (Shakeel *et al*., 2012:953-973). Therefore, in this study, nano-emulsions were chosen as the drug carrier system as they offer exceptional solubilisation ability to drugs. They have small droplet sizes with higher entrapment efficiencies and offer ease of preparation, optical clarity and stability, all of which contributes to them being attractive candidates for drug vectorisation (Chime *et al.,* 2014).

The aim of this study was to investigate whether nano-emulsions containing natural oils would improve the topical delivery of CLF, DQ and ART, separately and in combination. Two natural oils were examined, safflower and olive oil, and eight nano-emulsions were therefore formulated, **S1**, **S2**, **S3**, **S4**, **O1**, **O2**, **O3** and **O4**. The compatibility of the three APIs was tested with each other as well as with the different oils. The dermal toxicity was investigated with the different constituents of the dispersions (i.e. APIs itself, the nano-emulsions without API and also combined with the API) on HaCaT cells. The nano-emulsions containing any of the three different APIs separately or in combination (**S1**, **S2**, **S3**, **S4**, **O1**, **O2**, **O3** and **O4**), were chosen for *in vitro* cell culture studies against *M. tuberculosis* for further investigation regarding their potential use in the future treatment of CTB. *In vitro* studies of the nano-emulsions were tested on inoculated, freeze-

dried bacterial cells, with and without APIs, to ensure that cell death was not caused by the natural oils or the API itself.

Objectives of the study included:

- Develop and validate an HPLC analytical method to determine the concentration of CLF, DQ and ART, separately and in combination, in the test samples generated during this study.
- Determine the aqueous solubility, solubility in different solvents and log D values of CLF, DQ and ART.
- Testing oil with drug compatibilities using microcalorimetry.
- Formulate nano-emulsions containing CLF, DQ and ART, separately and in combination, using safflower and olive oil as the oil phase in the nano-emulsions.
- Characterise (viscosity, droplet size, pH, zeta-potential, morphology and drug entrapment efficiency) the nano-emulsions with and without the APIs.
- Conduct membrane release studies to establish whether the APIs were released from the different nano-emulsions.
- Determine the transdermal and topical delivery of the APIs from the nano-emulsions by performing diffusion studies followed by tape-stripping, respectively.
- Conduct cell culture studies to determine the cytotoxic effects of the API(s), the oils, as well as the nano-emulsions on dermal fibroblast cells and HaCaT cells.
- Determine *in vitro* efficacy on tuberculous bacterial cells of the entrapped APIs in the nano-emulsions containing safflower and olive oil separately with any of the three different APIs, separately or in combination.

A novel HPLC method was developed and validated for the simultaneous analysis of CLF, ART and DQ to determine the different concentrations of the APIs. During validation the method was found to be accurate, precise and repeatable for the quantification of CLF, ART and DQ. The LOD was calculated to be 3.11 µg/ml for CLF, 1.98 µg/ml for ART and 2.29 µg/ml for DQ, whereas the LOQ was determined to be 0.13 µg/ml for CLF, 13.39 µg/ml for ART and 2.13 µg/ml for DQ.

To successfully permeate the skin, an API needs an aqueous solubility of more than 1 mg/ml (Naik *et al*., 2000:319), whilst the log D required should be between 1 and 3 therefore enabling the API to dissolve in both water and oil (Roberts & Walters, 1998:38). CLF, ART and DQ depicted an aqueous solubility of 0.000 mg/ml, 0.100 mg/ml and 0.000 mg/ml, respectively, at a temperature of 32°C. The log D of CLF, ART and DQ were extracted from literature as results differed too significantly. Hence, the log D of CLF, ART and DQ were found to be 7.6, 7.8 and 2.49, respectively. Taking both of the aforementioned physicochemical properties into account,

no favourable aqueous solubility was seen, but regarding the log D value, only ART yielded a favourable value for skin permeation.

Microcalorimetry was conducted to test compound compatibility and it was evident that the surfactants (Tween® 80 and Span® 60) showed some possible incompatibilities with CLF and ART, i.e.:

- CLF and Tween® 80;
- CLF, Tween® 80 and olive oil;
- CLF, Tween® 80 and safflower oil;
- ART and Tween® 80;
- ART, Tween® 80 and olive oil;
- ART, Tween® 80 and safflower oil;
- ART, Span® 60 and safflower oil;
- ART, Span® 60 and olive oil.

This could possibly be explained by using excipients such as Tween® 80 and Span® 60, which have both chemical and physical interactions and may influence the chemical nature of the compounds, as well as escalate the effects of drug degradation (Bharate *et al.*, 2010:1; Chas *et al*., 1999:312). Other alternatives are available for future use, such as testing sample nano-emulsions as the chemical compatibility of a two-component mixture can differ from a multicomponent mixture that indicates incompatibility (Bharate *et al.,* 2010: 312; Thomas & Naath, 2008).

During this study, eight o/w nano-emulsions containing 1% API and natural oil (**S1**, **S2**, **S3**, **S4**, **O1**, **O2**, **O3** and **O4**) were formulated, and were represented by a smooth and homogenous mixture. Pre-formulation studies were conducted upon formulating the eight natural oil nano-emulsions. Naik *et al.* (2000:319) stated that the suitable limits for a formulation on the skin should be between pH 5 and 9. All eight nano-emulsions had pH values between 5.1 and 5.77, which indicated the nano-emulsions all had acceptable pH. Viscosity of the nano-emulsions was very low (2.59 – 2.91 cP), which could be because 80% of the nano-emulsion contained water. Zeta-potential was depicted to be highly negative at - 30 mV to - 38 mV, indicating a stable dispersion for all eight nano-emulsions; all eight also depicted small droplet sizes, which ranged between 83 and 130 nm. This was within the size range for nano-emulsions (10 nm to 10 µm) (Wiechers, 2008:173).

During the membrane release studies, no API was found within the receptor phase. Skin diffusion studies presented the same after 2 h withdrawals. Consequently, the withdrawal period was

altered to only one extraction after 12 h. No data was obtained within the receptor phase after 12 h extractions, hence no transdermal penetration occurred.

After the skin diffusions studies, tape-stripping studies were conducted. From the individual nano-emulsions containing safflower oil (**S1**, **S2** and **S3**), it was evident that **S2** (19.922 ± 1.576 µg/ml) depicted the highest concentration in the stratum corneum-epidermis (SCE), whereas **S3** (9.905 ± 1.486 µg/ml) depicted the highest concentration in the epidermis-dermis (ED). By looking at the individual nano-emulsions containing olive oil (**O1**, **O2** and **O3**), it was evident that **O2** (13.433 ± 1.099 µg/ml) depicted the highest concentration in the SCE, whereas **O3** (6.195 ± 0.781 µg/ml) depicted the highest concentration in the ED. By comparing the combination nano-emulsions (**S4** and **O4**) in the SCE, it was evident that no trace of DQ was found. CLF within the **O4** (9.383 ± 0.362 µg/ml) depicted higher results than **S4** (4.035 ± 0.205 µg/ml), whereas ART within **S4** (27.455 ± 1.695 µg/ml) depicted higher results than that of **O4** (19.864 ± 1.241 µg/ml). By comparing **S4** and **O4** within the ED, it is evident that ART was not present. **S4** depicted higher concentrations with regards to CLF (2.793 ± 0.286 µg/ml) and DQ (8.556 ± 0.808 µg/ml), than CLF (1.801 ± 0.351 µg/ml) and DQ (3.998 ± 0.348 µg/ml) in **O4**. It was evident from the nano-emulsions that CLF and DQ from the individual nano-emulsions (**S1**, **S3**, **O1** and **O3)** reached both the SCE and ED, whereas ART only reached the SCE (**S2** and **O2**). It was evident from the combination nano-emulsions (**S4** and **O4**) that DQ reached only the ED, ART reached only the SCE and CLF reached both.

The eight nano-emulsions, together with their placebos, were used in the cytotoxic studies to investigate cell toxicity. A LDH-assay was conducted on HaCaT cell cultures, whereas all nano-emulsions (**S1** – **S5** and **O1** – **O5**) were determined to be non-cytotoxic with regard to only minimal cell death occurrence during treatment. All nano-emulsions depicted either as non-cytotoxic or weak cytotoxic, consequently, it can be seen that natural oil nano-emulsions are safe and non-cytotoxic.

After the cytotoxicity testing on HaCaT cells, *in vitro* efficacy on tuberculous bacterial cells was conducted on *Mycobacterium tuberculosis* (*M.tb*) strains. All the formulations illustrated very positive results with regard to %inhibition (**S1** – **S4** and **O1** – **O4**), which ranged from 52 to 63% inhibition. The results indicated that nano-emulsions containing safflower oil had increased %inhibition values compared to those containing olive oil. From the results obtained, it is apparent that both placebos (**S5** and **O5**) also depicted %inhibition. This could possibly be explained by the use of natural oils incorporated in the nano-emulsions and therefore could perhaps be used as a basic nano-emulsion formula to incorporate the APIs (ART, CLF and DQ separately or in combination) for the future topical treatment of CTB.

This study contributed to science in the following way:

- A literature review on nano-emulsions was written and published.
- A novel validated HPLC method to identify and quantify CLF, ART and DQ, simultaneously.
- No incompatibilities were detected when CLF, ART and DQ were combined with the natural oils, which in turn were incorporated within the nano-emulsions during HSM and microcalorimetry studies.
- It was also clear that the nano-emulsions could deliver APIs topically without entering the systemic circulation.
- From the dermal toxicity studies, it was evident the nano-emulsions displayed weak cytotoxicity and could be applied to the human skin without harm.
- By looking at the *in vitro* efficacy on tuberculous bacterial cells, it was evident that the eight formulated nano-emulsions did inhibit the growth of *Mycobacterium tuberculosis* cells and could therefore possibly be used in the future for the topical treatment of CTB, together with current systemic treatment regimens, since oral therapies for the treatment of CTB have shown no, to limited success.

Future prospects for this study include:

- Investigation of stability studies over extended periods to ensure that no flocculation, creaming, cracking (separation of dispersed phase as a layer), miscellaneous instability or phase inversion takes place.
- Alternative artemisinin derivatives, such as artemether, which has a higher lipophilic profile and demonstrates higher oil solubility, in combination with CLF and DQ may be used as APIs for the possible treatment of CTB topically.
- Other natural oils with a higher concentration of linoleic acid may be investigated as penetration enhancers.
- Investigation combining nano-emulsions in semi-solids, such as creams or emulgels, to determine if it would result in ideal topical delivery of CLF, ART and DQ.

References

Barbagallo, J., Tager, P., Ingleton, R., Hirsch, R.J. & Weinberg, J.M. 2002. Cutaneous Tuberculosis. *American Journal of Clinical Dermatology,* 3:319-329.

Bharate, S.S., Bharate, S.B., Bajaj, A.N. 2010. Interactions and incompatibilities of pharmaceutical excipients with active pharmaceutical ingredients: a comprehensive review. *Journal of Excipients and Food Chemicals,* 1(3):1-26.

Chong, L.Y. & Lo, K.K. 1995. Cutaneous tuberculosis in Hong Kong: a 10-year retrospective study. *International Journal of Dermatology,* 34:26-29.

Clas, S.D., Dalton, C.R. & Hancock, B.C. 1999. Differential scanning calorimetry: applications in drug development. *Pharmaceutical Science and Technology Today,* 2:311-320.

Dey, T., Helen, G., Shubber, C., Cooke, G. & Ford, N. 2013. Outcomes of clofazimine for the treatment of drug-resistant tuberculosis: a systematic review and meta-analysis. *Journal of Antimicrobial Chemotherapy,* 68(2):284-293.

Dostrovsky A. & Sagher F. 1963. Dermatological complication of BCG vaccination. *The British Journal of Dermatoly,* 75:180-190.

El Maghraby, G.M., Barry, B.W. & Williams, A.C. 2008. Liposomes and skin: from drug delivery to model membranes. *European Journal of Pharmaceutical Sciences,* 34:203-222.

Izumi, A.K. & Matsunaga, J. 1982. BCG vaccine-induced lupus vulgaris. *Archives of Dermatology,* 118:171-172.

Kailasam, S., Wise, D.L. & Gangadharam, P.R. 1994. Bioavailability and chemotherapeutic activity of clofazimine against *Mycobacterium avium* complex infections in beige mice following a single implant of a biodegradable polymer. *Journal of Antimicrobial Chemotherapy,* 3:273-279.

Kumar B., Rai R., Kaur I., Sahoo, B., Muralidhar, S. & Radotra, B.D. 2001. Childhood cutaneous tuberculosis: a study over 25 years from northern India. *International Journal of Dermatology,* 40:26-32.

Lindholm-Levy, P.J. & Heifets, L.B. 1988. Clofazimine and other rimino-compounds: minimal inhibitory and minimal bactericidal concentrations at different pHs for *Mycobacterium avium* complex. *Tubercle and Lung Disease,* 69:179-86.

Mehta, R.T., Keyhani, A., McQueen, T., Rosenbaum, B., Rolston, K. & Tarrand, J.J. 1993. *In vitro* activities of free and liposomal drugs against *Mycobacterium avium - M. intracellulare* complex and *M. tuberculosis*. *Antimicrobial Agents and Chemotherapy,* 37:2584-2587.

Naik, A., Kalia, Y.N. & Guy, R.H. 2000. Transdermal drug delivery: Overcoming the skin's barrier function. *Pharmaceutical Science and Technology Today,* 3:318-325.

Penneys, N.S., Leonardi, C.L., Cook, S., Blauvelt, A., Rosenberg, S., Eells, L.D., Konwiser, M. & Aaronson, C.M. 1993. Identification of *Mycobacterium tuberculosis* DNA in Five Different Types of Cutaneous Lesions by the Polymerase Chain Reaction. *Archives of Dermatology,* 129(12):1594-1598.

Potts, R.O., Bommannan, D.B. & Guy, R.H. 1992. Percutaneous absorption. (*In* Mukhtar, H., *ed.* Pharmacology of the skin. Boca Raton, Fla.: CRC Press. p. 13-28.)

Roberts, M.S. & Walters, K.A. 1998. The relationship between structure and barrier function of skin. (*In* Roberts, M.S. & Walters, K.A., *eds.* Dermal absorption and toxicity assessment. New York: Marcel Dekker. p. 1-42.)

Thomas, V.H. & Naath, M. 2008. Design and utilization of the drug-excipient chemical compatibility automated system. *International Journal of Pharmaceutics,* 35:150-157.

Appendix A:

Validation of an HPLC analytical method for analysis of clofazimine, artemisone and decoquinate

A.1 Purpose of validation

The purpose of method validation is to ensure the method of analysis is reliable, suitable and sensitive for the determination of the concentration of the APIs in different formulations (in this case nano-emulsions) (ICH, 1995:8; ICH 1996:8; ICH, 2014:7). In validation, data should be validated according to specific guidelines to establish the limits of a parameter, although these guidelines are only recommendations (cGMP, 2011; Singh, 2013). Before any validation process commences, the scope and the relevance of the analytical method should be defined and although there are various types of validation, only relevant methods will be discussed in this appendix (Singh, 2013). HPLC analyses were used to detect and analyse clofazimine, artemisone and decoquinate encapsulated in nano-emulsions used for topical delivery.

A.2 Chromatographic conditions

The analytical HPLC method for the analysis of clofazimine, artemisone and decoquinate, separately and in combination, was developed with the assistance of Prof Jan du Preez at the North-West University (NWU), Potchefstroom, and the experiments were carried out in a controlled laboratory environment in the Analytical Technology Laboratory (ATL), at a room temperature of 25 °C ± 2 °C.

Certain factors of the chromatographic conditions had been taken into account when this method of analysis was developed and these were:

Analytical instrument: The analysis of clofazimine, artemisone and decoquinate were performed using an Agilent® 1100 Series HPLC system in a temperature controlled environment (25 °C ± 2 °C). The instrument consisted of an Agilent® 1100 pump, diode array detector, autosampler injection mechanism and ChemStation Rev. A.10.02 software for data acquisition and analysis (Agilent Technologies, Palo Alto, CA).

Column: Restek Ultra C_{18} column, 250 x 4.6 mm, 5 µm, 100 Å pores, 20% carbon load, endcapped reversed phase column (Restek corporation, Bellefonte, USA), pH 2.5 – 8.0, temperature limit: 80 °C, USP phase code L1.

Mobile phase: The mobile phase consisted of two phases. Mobile phase A consisted of 0.005 M octanesulphonic-acid sodium salt in HPLC-grade water with added 2 ml of a 2 M ammonia solution adjusted to a pH of 3.5 with 2 M phosphoric acid. Mobile phase B contained chromatography grade acetonitrile.

Gradient: The mobile phase gradient given in Table A.1 was used to obtain elution of artemisone, clofazimine and decoquinate

Table A.1: Mobile phase gradient used during HPLC analysis

Time (min)	%A	%B
0.0	35	65
2.0	35	65
4.0	10	90
10.0	10	90
10.1	35	65
15.0	35	65

Flow rate: A mobile phase flow rate of 1.0 ml/min was maintained throughout all validation analyses.

Injection volume: 20 µl

Detection: UV at 210 nm and 284 nm

Retention time: Clofazimine: Approximately 6.3 min.

Artemisone: Approximately 7.3 min.

Decoquinate: Approximately 9.8 min.

Run time: 15.0 min

Solvent: Ethanol absolute (99.7%)

A.3 Preparation of standard and samples

A.3.1 Standard preparation of clofazimine, artemisone and decoquinate

The standard preparation of clofazimine, artemisone and decoquinate was as follows:

1. Approximately 7 mg of clofazimine, 40 mg of artemisone and 12 mg of decoquinate were accurately weighed and transferred to a 100 ml volumetric flask.
2. The clofazimine, artemisone and decoquinate were dissolved in 100 ml of absolute ethanol (99.7%) (Standard 1).
3. From this solution, 5 ml was diluted to 50 ml with absolute ethanol (99.7%) (Standard 2).
4. Subsequently the two standard solutions were filtered into HPLC vials using 0.45 µm polyvinylidene fluoride (PVDF) filters.

A.3.2 Preparation of samples for the analysis of nano-formulations

The following ingredients and quantities were weighed as shown in Table A.2. **A** and **B** were heated separately at 60 °C in beakers, whilst stirring continuously with magnetic stirrers. Once all the ingredients in beaker **B** were dissolved, the magnetic stirrer was removed from the oil phase. The oil phase was drawn up by a syringe and added drop-wise into the water phase. The formulation was placed under the ultrasonic probe for 3 to 6 min and thereafter in the ultrasonic bath for 15 to 20 min. After the nano-emulsion was prepared, 1 ml was transferred to a 100 ml volumetric flask and diluted with absolute ethanol (99.7%) for HPLC analysis. Natural oils used in this study presented with a density of 0.92 g/cm^3 and Tween® 80 with 1.08 g/cm^{3,} which was converted to %m/m for simplicity purposes.

Table A.2: Formula of **S1** used during HPLC sample preparation

Ingredients		%m/m
A: Water phase	Water Surfactant: Span® 60	80.0 2.0
B: Oil phase	Safflower oil Surfactant: Tween® 80 Actives: CLF	9.2 7.8 1.0

Table A.3: Formula of **S2** used during HPLC sample preparation

Ingredients		%m/m
A: Water phase	Water	80.0
	Surfactant: Span® 60	2.0
B: Oil phase	Safflower oil	9.2
	Surfactant: Tween® 80	7.8
	Actives: ART	1.0

Table A.4: Formula of **S3** used during HPLC sample preparation

Ingredients		%m/m
A: Water phase	Water	80.0
	Surfactant: Span® 60	2.0
B: Oil phase	Safflower oil	9.2
	Surfactant: Tween® 80	7.8
	Actives: DQ	1.0

Table A.5: Formula of **S4** used during HPLC sample preparation

Ingredients		%m/m
A: Water phase	Water	80.0
	Surfactant: Span® 60	2.0
B: Oil phase	Safflower oil	9.2
	Surfactant: Tween® 80	7.8
	Actives: CLF	1.0
	ART	1.0
	DQ	1.0

Table A.6: Formula of **O1** used during HPLC sample preparation

Ingredients		%m/m
A: Water phase	Water	80.0
	Surfactant: Span® 60	2.0
B: Oil phase	Olive oil	9.2
	Surfactant: Tween® 80	7.8
	Actives: CLF	1.0

Table A.7: Formula of **O2** used during HPLC sample preparation

Ingredients		%m/m
A: Water phase	Water Surfactant: Span® 60	80.0 2.0
B: Oil phase	Olive oil Surfactant: Tween® 80 Actives: ART	9.2 7.8 1.0

Table A.8: Formula of **O3** used during HPLC sample preparation

Ingredients		%m/m
A: Water phase	Water Surfactant: Span® 60	80.0 2.0
B: Oil phase	Olive oil Surfactant: Tween® 80 Actives: DQ	9.2 7.8 1.0

Table A.9: Formula of **O4** used during HPLC sample preparation

Ingredients		%m/m
A: Water phase	Water Surfactant: Span® 60	80.0 2.0
B: Oil phase	Olive oil Surfactant: Tween® 80 Actives: CLF ART DQ	9.2 7.8 1.0 1.0 1.0

A.3.3 Placebo preparation

The placebo was prepared as mentioned above, only the API was excluded from the formula.

A.3.4 Sample preparation for diffusion studies

Samples were collected from Franz diffusion cells, filtered and transferred into HPLC vials and analysed without any further preparation. See Appendix C.

A.4 Validation parameters

To validate the analytical method the following parameters were used: linearity, limit of detection (LOD) and limit of quantification (LOQ), accuracy, precision (inter- and intra-day), ruggedness and system suitability.

A.4.1 Linearity

The linearity of a certain API can be defined as the ability to elicit experimental procedure results that are directly proportional to the concentration (amount) of analyte in the samples, which are in a given range of a regression curve (Bansal & DeStefano, 2007:113; ICH 1994:5; Johnson & Van Buskirk, 2007:103; USP, 2013:986). During linearity determination, a series of three to five injections is typically used (ICH, 2005). The correlation coefficient (R^2) of 0.998 is required for a valid relation between the regression line and the data (Singh, 2013), which indicates the method has accurate and trustworthy linearity and is reliable and precise for analysis of the samples (Araujo, 2009:2229).

Linear regression analysis determined the linearity of the HPLC response (peak areas) versus API concentration (µg/ml). The data is described by a linear equation, namely:

$$y = mx + c \qquad \textbf{Equation A.1}$$

Where: y = Peak area ratios of the different API

m = Slope

x = Concentration of the different API in µg/ml

c = y-intercept

The linearity results of clofazimine, artemisone and decoquinate are given in Tables A.10, A.11 and A.12, respectively (where SD is the standard deviation), and the linear regression curves can be seen in Figures A.1, A.2 and A.3, respectively.

Table A.10: Linearity results of CLF

Concentration (µg/ml)	Peak area		
	1	2	Mean (± SD)
1.68	242.00	241.10	241.60 (± 0.64)
3.35	483.10	482.30	482.70 (± 0.57)
8.38	1217.80	1200.90	1209.40 (± 11.95)
16.75	2405.10	2399.70	2402.40 (± 3.82)
25.13	3590.00	3591.70	3590.90 (± 0.78)
33.50	4797.60	4772.50	4785.10 (± 17.75)
41.88	5993.10	6009.90	6001.50 (± 11.88)
50.25	7241.50	7216.40	7229.00 (± 17.75)
R^2	0.99998		
Intercept	-1.2419		
Slope	143.4621		

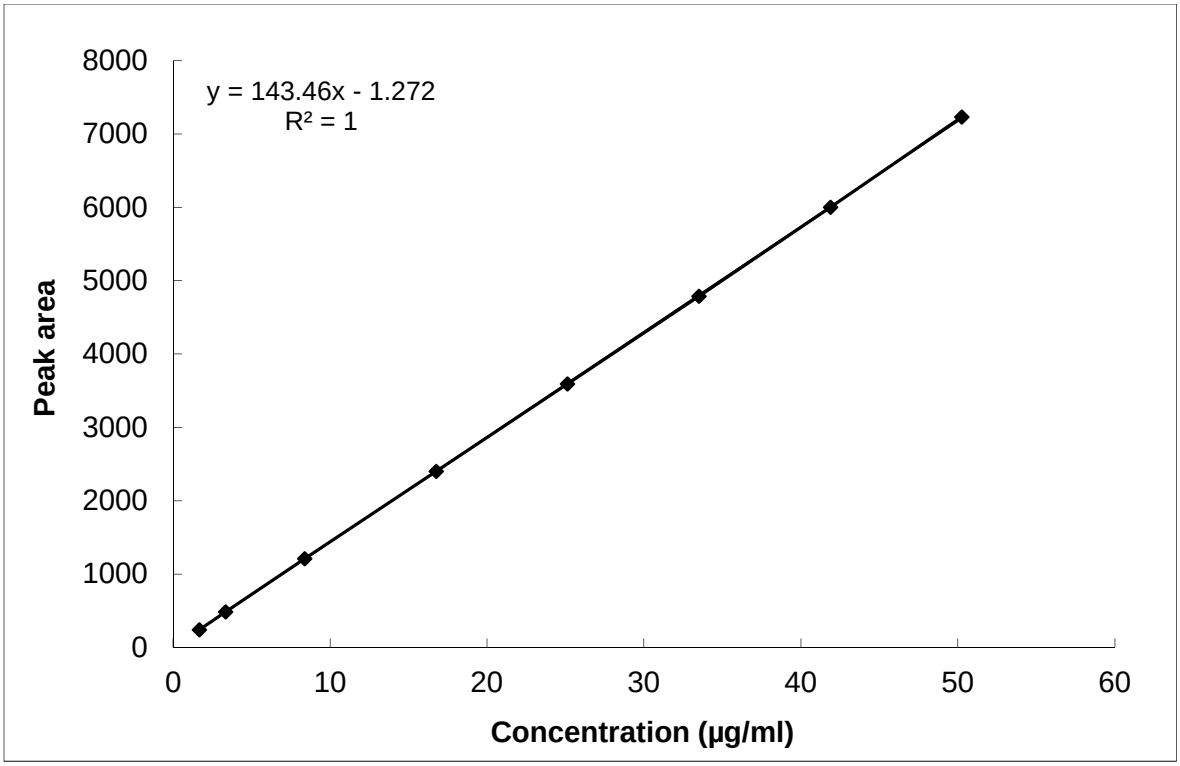

Figure A.1: Linear regression curve of CLF

Table A.11: Linearity results of ART

Concentration (µg/ml)	Peak area		
	1	2	Mean (± SD)
5.00	5.10	5.10	5.10 (± 0.00)
10.00	10.30	10.00	10.20 (± 0.21)
20.01	19.90	19.90	19.90 (± 0.00)
30.01	33.20	33.10	33.20 (± 0.07)
40.01	43.70	43.60	43.70 (± 0.07)
100.03	107.60	107.50	107.60 (± 0.07)
200.05	216.50	216.00	216.30 (± 0.35)
300.08	321.10	320.40	320.80 (± 0.49)
400.10	432.40	433.80	433.10 (± 0.99)
R^2	0.99993		
Intercept	-0.3746		
Slope	1.0793		

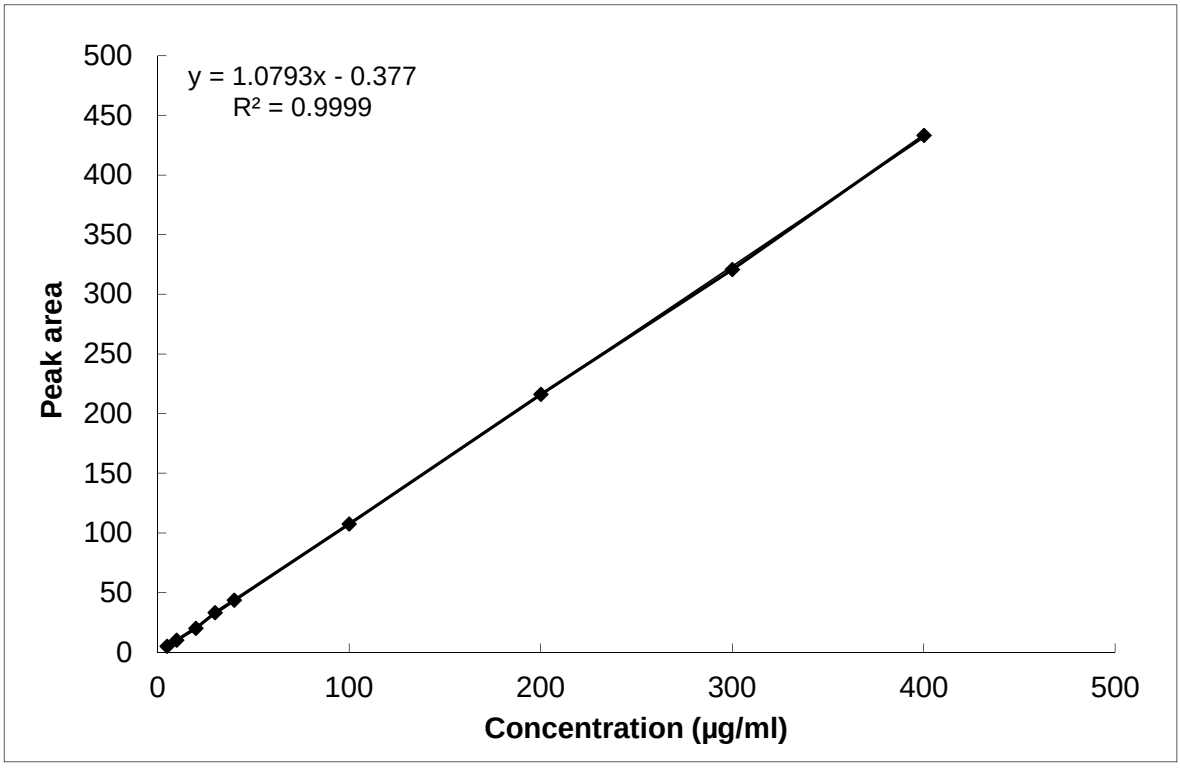

Figure A.2: Linear regression curve of ART

Table A.12: Linearity results of DQ

Concentration (µg/ml)	Peak area		
	1	2	Mean (± SD)
1.50	47.00	49.90	48.50 (± 2.05)
3.00	98.20	98.60	98.40 (± 0.28)
6.01	197.40	197.90	197.70 (± 0.35)
9.01	296.10	296.20	296.20 (± 0.07)
12.01	395.60	395.60	395.60 (± 0.00)
30.03	713.30	718.90	716.10 (± 3.96)
60.05	1432.20	1431.20	1431.70 (± 0.71)
90.08	2140.70	2144.40	2142.60 (± 2.62)
120.10	2856.60	2858.90	2857.80 (± 1.63)
R^2	0.9989		
Intercept	51.8663		
Slope	9.303		

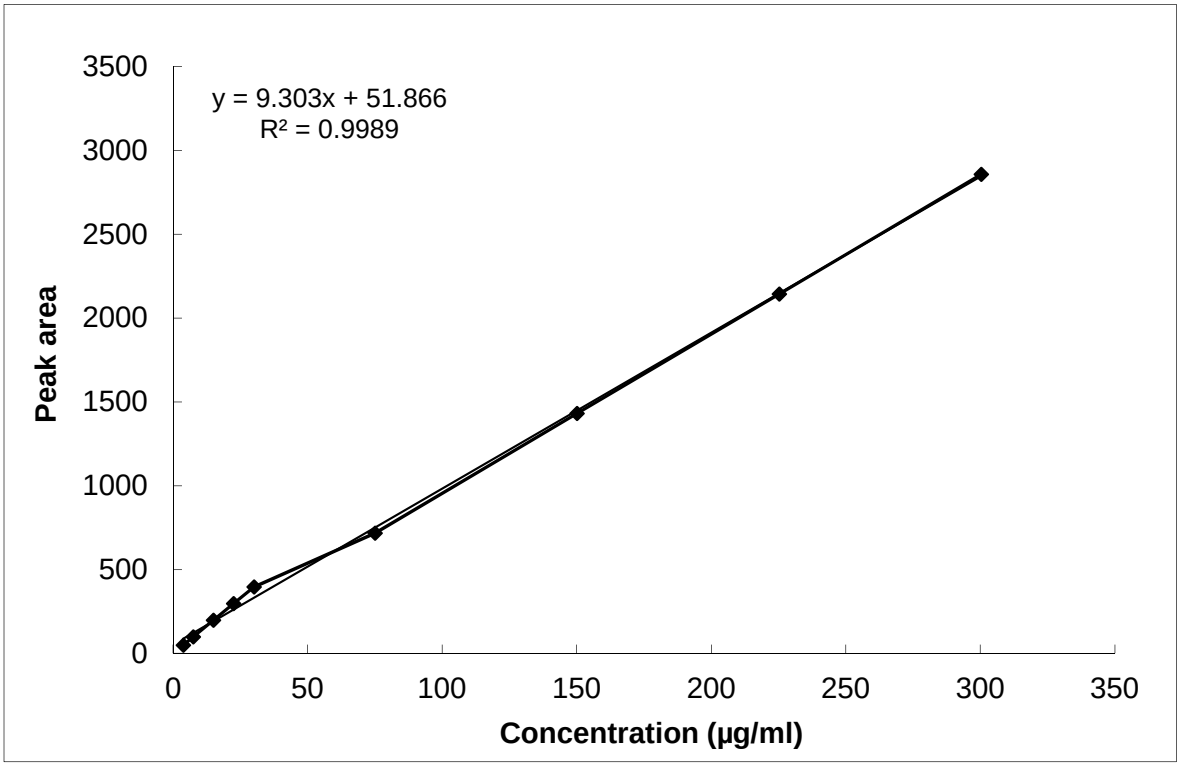

Figure A.3: Linear regression curve of DQ

Linear regression analysis should yield a regression coefficient (R squared) of at least 0.98 but 0.99 is preferred (Johnson & Van Buskirk, 1998:96). The regression value (R^2) obtained, was within the acceptance criteria of 0.99, as seen in Figures A.1 ($R^2 = 1.0000$), A.2 ($R^2 = 0.9999$) and A.3 ($R^2 = 0.9989$), which indicates a high degree of linearity and therefore demonstrating good response of the analytical system.

A.4.1.2 Detection limit (LOD) and quantitation limit (LOQ)

The LOD is the lowest amount of an API in a sample that can be detected, but cannot be quantified as a numerical value by the method. The LOQ can be described as the lowest probable quantity or concentration of an API present in a sample, which can be quantitatively measured with acceptable accuracy and precision of an analytical method (FDA, 2001:10; ICH, 2005:17; VICH, 2015:23). To determine the LOD and LOQ, different standards were prepared of low concentrations and injected into the samples six consecutive times. The %RSD (percentage relative standard deviation) should not exceed 20% for LOD and 15% for LOQ. The LOD-values of CLF, ART and DQ were determined to be 0.04 µg/ml, 4.42 µg/ml and 0.70 µg/ml, with a %RSD of 17.28%, 19.17% and 14.47%, respectively. The LOQ was calculated to be 0.05 µg/ml, 5.50 µg/ml and 4.00 µg/ml for CLF, ART and DQ, respectively. The %RSD of the LOQ was determined to be 7.6%, 12.15% and 8.32% for CLF, ART and DQ, respectively, which confirms less variation between the samples while precision and accuracy were maintained. The %RSD for the APIs are in range, as they did not surpass the %RSD of 20% (Huber, 2010:65).

A.4.2 Accuracy

The accuracy of an analytical method, which is sometimes termed trueness (ICH 1994:4), can be defined as the closeness of experimental results compared to those of the true value (USP, 2013:984), thus the measured value and true value (Johnson & Van Buskirk, 1998:102). Since this process does not include any sample preparation, accuracy and precision can only be completed by preparing a set of standards and comparing them against another set.

A.4.2.1 Accuracy analysis of clofazimine, artemisone and decoquinate

The accuracy of CLF, ART and DQ was determined using the following method:

1. Approximately 7 mg of CLF, 40 mg of ART and 12 mg of DQ were accurately weighed and transferred into a 100 ml volumetric flask and dissolved in ethanol absolute (99.7%).
2. 5 ml of this solution was transferred into a 50 ml volumetric flask and diluted to volume with ethanol absolute (99.7 %).

These yielded solutions containing approximately 1.83, 3.65 and 9.13 µg/ml of CLF, 15.0, 20.0 and 99.8 µg/ml of ART and 2.90, 3.80 and 19.00 µg/ml of DQ. These solutions were then transferred to HPLC vials, after filtering with 0.45 µm PVDF filters. The subsequent solutions were analysed during the accuracy experiment against a standard solution.

Table A.13: Accuracy results of CLF

Concentration spiked (µg/ml)	Peak area			Recovery	
	Area 1	Area 2	Mean	µg/ml	%
1.825	265.30	265.40	265.40	1.80	99.80
1.825	265.90	265.50	265.70	1.80	99.90
1.825	264.50	263.60	264.10	1.80	99.30
3.650	530.90	632.50	531.70	3.70	100.50
3.650	528.70	529.30	529.00	3.60	100.00
3.650	530.90	530.10	530.50	3.70	100.20
9.125	1322.50	1318.70	1320.60	9.10	100.10
9.125	1317.90	1319.30	1318.60	9.10	100.00
9.125	1323.10	1311.40	1317.30	9.10	99.90

Table A.14: Statistical analysis results of CLF

Statistical analysis	
Mean	100.00
SD	0.309
%RSD	0.309

Table A.15: Accuracy results of ART

Concentration spiked (µg/ml)	Peak area			Recovery	
	Area 1	Area 2	Mean	µg/ml	%
15.00	17.90	17.80	17.90	14.70	98.30
15.00	17.80	17.70	17.80	14.60	97.60
15.00	17.90	17.90	17.90	14.80	98.60
20.00	23.60	23.60	23.60	20.20	101.20
20.00	23.40	23.70	23.60	20.10	101.00
20.00	23.70	23.90	23.80	20.40	102.20
99.80	106.90	107.20	107.10	99.80	100.10
99.80	107.10	107.00	107.10	99.80	100.10
99.80	106.90	106.70	106.80	99.60	99.80

Table A.16: Statistical analysis results of ART

Statistical analysis	
Mean	99.90
SD	1.392
%RSD	1.394

Table A.17: Accuracy results of DQ

Concentration spiked (µg/ml)	Peak area			Recovery	
	Area 1	Area 2	Mean	µg/ml	%
2.90	131.40	132.40	131.90	2.50	88.90
2.90	130.10	130.00	130.10	2.50	87.30
2.90	139.00	138.80	138.90	2.70	95.10
3.80	198.00	198.40	198.20	4.20	110.70
3.80	188.00	187.40	187.70	3.90	103.70
3.80	194.90	194.60	194.80	4.10	108.40
19.00	776.10	777.50	776.80	18.80	98.90
19.00	781.50	780.10	780.80	18.90	99.40
19.00	797.00	795.00	796.00	19.30	101.40

Table A.18: Statistical analysis results of DQ

Statistical analysis	
Mean	99.32
SD	7.490
%RSD	7.540

Recovery should yield a percentage of 98 to 102% (Johnson & Van Buskirk, 2007:99) and the mean of the observed concentration should not exceed 15% of all concentrations (within ± 15% of the nominal concentration) (Bansal & DeStefano, 2007:111). The mean %recovery of clofazimine, artemisone and decoquinate was 100.0%, 99.9% and 99.32%, respectively, over the tested range of 1.83 to 9.13 µg/ml (CLF), 15.00 to 99.80 µg/ml (ART) and 2.90 to 19.00 µg/ml (DQ), which are all within the accepted criteria of 98 – 102% (Shabir, 2004:215). The %RSD of CLF (0.309%) and ART (1.394%) are satisfactory and should yield a percentage less than 2% (Shabir, 2004:215). Decoquinate %RSD (7.540%) does not fall within limits and can be explained by the percentage recovery column, where the criteria for individual recoveries range between 85 – 115% and not 98 – 102% since individual recoveries are higher.

A.4.3 Precision

The precision (variability) of an analytical technique is usually expressed as the SD, variance (S2), or coefficient of variation (%RSD) of a sequence of measurements. Precision is an analytical procedure, which depicts the closeness of agreement where a series of measurements are obtained from multiple samples of the standardised (uniform) sample under the prescribed conditions (USP 2013:985). Precision was investigated by terms of repeatability (intra-day), and reproducibility (inter-day).

A.4.3.1 Intra-day precision (repeatability)

Repeatability states the precision (spread of the data, variability) within the laboratory over a short interlude of time using the same equipment and analyst (ICH 1994:5; USP 2013:985). Repeatability (better known as intra-assay precision) was tested as follows:

1. Three samples were prepared, each of low, medium and high concentration (n = 9).
2. A set of standards were prepared as described under sample preparation.
3. The samples were injected into the HPLC in duplicate and analysed.

Table A.19: Repeatability results of CLF

Concentration spiked (µg/ml)	Peak area			Recovery	
	Area 1	Area 2	Mean	µg/ml	%
2.80	398.20	397.90	398.10	2.80	99.80
2.80	397.90	398.90	398.40	2.80	100.00
2.80	396.90	398.30	397.60	2.80	99.80
4.60	667.10	668.30	667.70	4.60	99.90
4.60	669.70	668.50	669.10	4.60	100.10
4.60	670.20	66.80	669.50	4.60	100.20
18.50	2685.10	2683.00	2684.10	18.40	99.70
18.50	2690.30	2688.60	2689.50	18.50	99.90
18.50	2700.40	2708.00	2704.20	18.60	100.40
				Mean	99.99
				SD	0.22
				%RSD	0.22

Table A.20: Repeatability results of ART

Concentration spiked (µg/ml)	Peak area			Recovery	
	Area 1	Area 2	Mean	µg/ml	%
14.70	16.90	16.90	16.90	14.60	99.00
14.70	17.00	16.80	16.90	14.60	99.00
14.70	16.70	16.90	16.80	14.50	98.40
24.60	28.20	27.90	28.10	25.00	101.70
24.60	27.80	27.20	27.50	24.50	99.60
24.60	28.00	27.90	28.00	24.90	101.30
98.30	107.60	106.30	107.00	98.40	100.20
98.30	106.10	106.50	106.30	97.80	99.60
98.30	107.00	106.80	106.90	98.40	100.10
				Mean	99.86
				SD	1.02
				%RSD	1.02

Table A.21: Repeatability results of DQ

Concentration spiked (µg/ml)	Peak area			Recovery	
	Area 1	Area 2	Mean	µg/ml	%
4.70	154.40	153.90	154.20	4.40	93.60
4.70	155.10	155.30	155.20	4.40	94.70
4.70	153.70	155.00	154.40	4.40	93.80
6.20	197.60	197.30	197.50	6.40	103.10
6.20	202.00	201.80	201.90	6.60	106.40
6.20	199.50	199.70	199.60	6.50	104.70
31.00	711.30	714.50	712.90	30.60	98.80
31.00	720.40	720.90	720.70	31.00	100.00
31.00	726.70	728.70	727.70	31.30	101.00
				Mean	99.60
				SD	4.48
				%RSD	4.50

Precision should yield a percentage up to 2%, but should not exceed 15% at all concentrations (Bansal & DeStefano, 2007:111) or coefficient of variation (cGMP, 2001:10). The mean %recovery of CLF, ART and DQ was 99.98%, 99.86% and 99.57%, respectively, which are all within the accepted criteria of 98 – 102% (Shabir, 2004:215). The %RSD was satisfactory with a %RSD of 0.22%, 1.02% and 4.49% for CLF, ART and DQ, respectively; the DQ %RSD does not

fall in the less than 2% category, however for the individual recovery it falls within the criteria, which is less than 5% (Shabir, 2004:215).

A.4.3.2 Inter-day precision (reproducibility)

Reproducibility expresses precision between laboratories, which is usually collaborative studies applied to standardise methodology (ICH 1994:5).

Table A.22: Inter-day results of CLF

Concentration spiked (µg/ml)	Peak area			Recovery	
	Area 1	Area 2	Mean	µg/ml	%
2.63	384.60	384.40	384.50	2.62	99.87
2.63	383.70	384.10	383.90	2.62	99.72
2.63	384.90	386.30	385.60	2.63	100.16
3.50	513.90	513.70	513.80	3.50	100.09
3.50	513.20	512.60	512.90	3.50	99.92
3.50	514.20	514.40	514.30	3.51	100.19
17.50	2569.00	2560.40	2564.70	17.49	99.92
17.50	2566.80	2570.10	2568.45	17.51	100.06
17.50	2565.90	2568.40	2567.15	17.50	100.01
				Mean	99.99
				SD	0.14
				%RSD	0.14

Table A.23: Inter-day results of ART

Concentration spiked (µg/ml)	Peak area			Recovery	
	Area 1	Area 2	Mean	µg/ml	%
15.26	17.70	17.20	17.45	14.96	98.00
15.26	17.30	17.80	17.55	15.05	98.63
15.26	17.70	17.40	17.55	15.05	98.63
20.35	23.60	23.00	23.30	20.57	101.10
20.35	23.50	23.40	23.45	20.72	101.81
20.35	23.30	23.20	23.25	20.53	100.87
101.75	107.90	107.70	107.80	101.72	99.97
101.75	108.20	107.70	107.95	101.86	100.11
101.75	108.00	107.40	107.70	101.62	99.88
				Mean	99.89
				SD	1.20
				%RSD	1.20

Table A.24: Inter-day results of DQ

Concentration spiked (µg/ml)	Peak area			Recovery	
	Area 1	Area 2	Mean	µg/ml	%
4.69	131.40	132.40	131.90	4.17	88.99
4.69	130.10	130.00	130.05	4.09	87.35
4.69	139.00	138.80	138.80	4.46	95.09
6.25	198.00	198.40	198.40	6.93	110.86
6.25	188.00	187.40	187.40	6.47	103.56
6.25	194.90	194.60	194.60	6.77	108.34
31.25	776.10	777.50	777.50	30.94	99.02
31.25	781.50	780.10	780.10	31.05	99.37
31.25	797.00	795.00	795.00	31.67	101.34
				Mean	99.33
				SD	7.49
				%RSD	7.54

Table A.25: Reproducibility results of CLF

	Day 1	Day 2	Day 3	Between days
	99.80	100.10	100.20	
	100.20	100.20	100.20	
	100.20	100.20	100.00	
Mean	100.07	100.17	100.12	100.12
SD	0.19	0.05	0.08	0.13
%RSD	0.19	0.05	0.08	0.13

Table A.26: Reproducibility results of ART

	Day 1	Day 2	Day 3	Between days
	98.40	98.80	98.60	
	101.30	101.00	100.90	
	100.10	98.90	99.90	
Mean	99.93	99.57	99.79	99.76
SD	1.19	1.01	0.92	1.06
%RSD	1.19	1.02	0.92	1.06

Table A.27: Reproducibility results of DQ

	Day 1	Day 2	Day 3	Between days
	98.90	100.80	99.00	
	99.40	99.10	99.40	
	101.00	100.00	101.30	
Mean	99.78	99.96	99.91	99.88
SD	0.92	0.68	1.02	0.89
%RSD	0.92	0.68	1.02	0.89

Inter-day precision must be 5% or less. The intra-day, intermediate precision inter-day %RSD total values of 0.19%, 0.05% and 0.08% were within acceptable limits, as shown in Table A.25, for CLF. The intra-day, intermediate precision inter-day %RSD total values of 1.19%, 1.02% and 0.92% were within acceptable limits for ART, as shown in Table A.26. The intra-day, intermediate precision inter-day %RSD total values of 0.92%, 0.68% and 1.02% were within acceptable limits for DQ, as shown in Table A.27 (Shabir, 2004:215; Singh, 2013:29).

A.4.4 Ruggedness

A.4.4.1 Sample stability

Sample stability refers to the physical or chemical stability of an analyte in a given matrix under very specific conditions over several time intervals (Bansal & DeStefano, 2007:113). The %RSD should be less than 2% (Ermer & Miller, 2005; Huber, 2015). Ruggedness is a critical component in validation as it depicts the interval between sample collection and analysis (Huber, 2015). A sample was left on the auto sampler tray and re-analysed over several time intervals to determine stability during which all the test parameters were kept the same.

Table A.28: Results of sample stability of CLF

Time (h)	Peak area	%Remaining
0	430.90	100.0
1	428.80	99.50
2	432.30	100.30
3	430.60	99.90
4	429.80	99.70
5	429.50	99.70
6	429.40	99.70
7	430.70	100.00
8	430.10	99.80
9	429.90	99.80
10	430.40	99.90
11	429.60	99.70
12	430.00	99.80
13	431.20	100.10
14	431.30	100.10
15	431.20	100.10
16	431.20	100.10
17	430.90	100.00
18	431.40	100.10
19	431.50	100.10
20	432.00	100.30
21	431.70	100.20
22	431.40	100.10
23	431.30	100.10
24	432.00	100.30
Mean	430.80	100.00
SD	0.90	0.21
%RSD	0.21	0.21

Table A.29: Results of sample stability of ART

Time (h)	Peak area	%Remaining
0	23.20	100.00
1	23.50	101.30
2	23.20	100.00
3	23.30	100.40
4	23.30	100.40
5	23.20	100.00
6	23.20	100.00
7	23.40	100.90
8	23.40	100.90
9	23.30	100.40
10	23.30	100.40
11	23.00	99.10
12	22.90	98.70
13	23.00	99.10
14	23.00	99.10
15	23.00	99.10
16	23.10	99.60
17	23.00	99.10
18	23.20	100.00
19	23.30	100.40
20	23.20	100.00
21	23.50	101.30
22	23.20	100.00
23	23.00	99.10
24	23.10	99.60
Mean	23.20	100.00
SD	0.16	0.70
%RSD	0.70	0.70

Table A.30: Results of sample stability of DQ

Time (h)	Peak area	%Remaining
0	179.10	100.0
1	186.80	104.30
2	186.90	104.40
3	186.60	104.20
4	186.70	104.20
5	186.90	104.40
6	187.10	104.50
7	187.50	104.70
8	186.70	104.20
9	186.90	104.40
10	186.60	104.20
11	187.60	104.70
12	187.80	104.90
13	187.80	104.90
14	187.50	104.70
15	187.70	104.80
16	187.80	104.90
17	188.10	105.00
18	187.60	104.70
19	188.00	105.00
20	187.80	104.90
21	188.00	105.00
22	188.40	105.20
23	187.80	104.90
24	187.70	104.80
Mean	187.1	104.5
SD	1.71	0.96
%RSD	0.92	0.92

Sample solutions should not be used for a period longer than it takes to degrade by 2% and in this case, distinctive provisions should be followed to compensate for the degradation. The clofazimine sample solution was stable over a period of 24 h, with only a 0.21% variation in concentration over this period; the artemisone sample solution was stable over a period of 24 h with a 0.70% variation in concentration over this period; the decoquinate sample solution was also stable over a period of 24 h with only a 0.92% variation in concentration over this period.

Instability of decoquinate was observed within the first hour and stabilised thereafter, indicating it was stable during the 24 hr analysis.

A.4.4.2 System repeatability (system suitability)

System repeatability is known as the ability of the method to yield a similar concentration for one sample when measured at different time intervals (Bansal & DeStefano, 2007:113). A sample was injected ten times in order to test the repeatability of the peak area as well as the retention time. The %RSD criteria for system repeatability for both peak areas, as well as the retention times, should be < 1% (Shabir, 2004:217).

Table A.31: Results of system repeatability of CLF

	Peak area	Retention time (min)
	2361.10	6.23
	2361.90	6.22
	2356.30	6.27
	2354.80	6.27
	2358.70	6.27
	2358.40	6.28
	2363.10	6.28
	2361.80	6.28
	2382.20	6.28
	2365.00	6.28
Mean	2362.30	6.26
SD	7.25	0.021
%RSD	0.31	0.342

Table A.32: Results of system repeatability of ART

	Peak area	Retention time (min)
	105.10	7.32
	105.00	7.32
	104.80	7.32
	104.40	7.31
	103.70	7.31
	103.60	7.31
	103.80	7.31
	103.50	7.31
	103.70	7.32
	103.60	7.30
Mean	104.10	7.31
SD	0.60	0.005
%RSD	0.58	0.073

Table A.33: Results of system repeatability of DQ

	Peak area	Retention time (min)
	620.80	9.86
	624.50	9.88
	624.20	9.84
	623.30	9.84
	623.10	9.84
	623.70	9.84
	625.60	9.85
	629.20	9.85
	631.00	9.86
	632.70	9.82
Mean	625.80	9.85
SD	3.65	0.014
%RSD	0.58	0.140

The peak area and retention times should have a %RSD of 2% or less. System performance proved to be well within the acceptable range, with %RSD values of 0.31% for peak area and 0.34% for retention time for CLF, %RSD values of 0.58% for peak area and 0.07% for ART and %RSD values of 0.58% for peak area and 0.14% for DQ, respectively.

A.5 Conclusion

The method performed well and should be appropriate to analyse clofazimine, artemisone and decoquinate during transdermal and topical drug delivery studies. In addition, the analytical method will be suitable for stability testing, quality control and batch release purposes of all three APIs. The method can be considered to be stability-indicating.

References

Araujo, P. 2009. Key aspects of analytical method validation and linearity evaluation. *Journal of Chromatography B*, 877:2229.

Bansal, S. & DeStefano, A. 2007. Key elements of Bioanalytical Method Validation for Small Molecules. *The American Association of Pharmaceutical Scientists*, 9:109-114.

British Pharmacopoeia. 2001. http://www.fda.gov/downloads/Drugs/Guidances/ucm070107.pdf Date of access: 10 Feb 2016.

Current good manufacturing practice (CGMP). 2011. Guidance for Industry. Process validation: General principles and practices. 19p.

Ermer, J. & Miller, J.H., *eds*. 2005. Method validation in pharmaceutical analysis: A guide to best practice. Weinheim: Wiley-VCH Verlag. 403p.

FDA ***see*** FOOD AND DRUG ADMINISTRATION

Food and Drug Administration. 2001. U.S. Department of Health and Human services. Guidance for Industry: Bioanalytical method validation. Rockville. 22p.

Huber, L. 2010. Validation of analytical methods. Agilent Technologies: Germany. 65p.

ICH ***see*** INTERNATIONAL CONFERENCE ON HARMONISATION

International Conference on Harmonisation of Technical Requirements for Registration of Pharmaceuticals for Human Use (ICH). 1994. Validation of analytical procedures: text and methodology, ICH-Q2(R1). 5p. Oct.

International Conference on Harmonisation of Technical Requirements for Registration of Pharmaceuticals for Human Use (ICH). 1995. Guideline for industry: text on validation of analytical procedures, ICH-Q2A. 8p. Mar.

International Conference on Harmonisation of Technical Requirements for Registration of Pharmaceuticals for Human Use (ICH). 1996. Validation of analytical procedures: methodology, ICH-Q2B. 8p. Nov.

International Conference on Harmonisation of Technical Requirements for Registration of Pharmaceuticals for Human Use. 2005. Validation of analytical procedures: text and methodology Q2 (R1). 13p.

International Conference on Harmonisation of Technical Requirements for Registration of Pharmaceuticals for Human Use (ICH). 2005. Validation of analytical procedures: Text and methodology Q2(R1). 17p. Jun.

International Conference on Harmonisation of Technical Requirements for Registration of Pharmaceuticals for Human Use (ICH). 2014. Guideline for industry: text on validation of analytical procedures, ICH-Q2A. 7p.

Johnson, J.D. &. Van Buskirk, G.E. 1998. Analytical method validation. *Journal of Validation Technology,* 2:88-105.

Shabir, G.A. 2004. A practical approach to validation of HPLC methods under current good manufacturing practices. *Journal of Validation Technology,* 10:210-218.

Singh, R. 2013. HPLC method development and validation – an overview. *Journal of Pharmaceutical Education and Research,* 4(1):26-33.

USP. 2013. General Information- Validation of Compendial Procedures, www.ofnisystems.com/wp/12/USP36_1225.pdf Date of access: 10 Feb 2016.

VICH: International cooperation on Harmonisation of Technical Requirements for Registration of Veterinary Medicinal Products. 2015. Guidance for industry. Studies to evaluate the metabolism and residue kinetics of veterinary drugs in food-producing animals: Validation of analytical methods used in residue depletion studies (VICH GL49(R)). 23p.

Appendix B:

Pre-formulation, formulation and characterisation of nano-emulsions containing a natural oil and clofazimine, artemisone and decoquinate

B.1 Introduction

Pre-formulation can be defined as studies that should be done prior to the development of the formulation. The main goal of pre-formulation is to allow coherent development of efficacious, stable and safe drug dosage forms, which are mostly concerned with the characterisation of the API's physicochemical properties. Therefore, in the pre-formulation stage, all the required aspects must be covered by the protocols (Waters & Brain, 2002:321).

Emulsions have been studied extensively, as potential carrier systems, for drug delivery to specific regions in the body (Davies *et al.,* 1985; Donovan & Flanagan, 1996; Fernandez *et al*., 2000; Izquierdo *et al*., 2007:263). Nano-emulsions are promising drug carrier systems used for enhancing transdermal drug delivery (Shakeel *et al*., 2007:104) and are frequently used in the pharmaceutical and cosmetic fields for topical applications. Advantages of nano-emulsions include solubilising both lipophilic and hydrophilic APIs (Förster & Von Rybinski, 1998; Izquierdo *et al*., 2007:263).

Studies show that nano-emulsions commonly increase skin permeation of drug molecules when compared to simple solutions, since there is a relative increase of the API concentration in the dispersed phase (Förster & Von Rybinski, 1998; Izquierdo *et al*., 2007:263). Two natural oils will be examined, safflower and olive oil, and eight nano-emulsions will be formulated, i.e. **S1** to **S4** and **O1** to **O4**.

B.2 Materials

B.2.1 Ingredients used to formulate nano-emulsions

The ingredients used during the pre-formulation of the nano-emulsions, as well as the supplier and batch number are listed in Table B.1.

Table B.1: Ingredients used in the study

Ingredient	Supplier	Batch number
Safflower oil	CJP Chemicals	-
Olive oil	CJP Chemicals	-
CLF	Cipla (India)	-
ART	Cipla (India)	-
DQ	Hohance Chemistry	HH10121001
Span® 60	Merck	5361721034
Tween® 80	Merck	1042689
Milli-Q® Water	Millipore	-

B.2.1.1 Natural oils

The oil phase of an o/w nano-emulsion can consist of a variety of mineral, synthetic or natural oils with either medium or long chain triglycerides (Baibhav *et al*., 2011:68). An important function of the oil phase is that the oil should solubilise the lipophilic API, for maximum drug loading to be achieved, as well as to facilitate the formation of the o/w nano-emulsion (Reddy *et al*., 2013:87; Setya *et al*., 2014:2218). In this study, two natural oils were used, safflower and olive oil, which contain linoleic acid (C_{18}-unsaturated fatty acid) that forms the oil phase of the o/w nano-emulsion (Williams & Barry, 2012:132).

B.2.1.2 Clofazimine

CLF is classified as lipophilic antibiotic riminophenazine (Cholo *et al*., 2011:291), which demonstrates efficacy against TB in animal models even though it was primarily used for leprosy. The compound possesses anti-inflammatory and antimycobacterial activities (Cholo *et al*., 2011:291), but physiochemical properties, such as tissue accumulation (which causes skin discoloration) and an extremely long half-life of the API, limits the use thereof (Lu *et al*., 2011:5813).

B.2.1.3 Artemisone

ART can be described as a 10-alkylaminoartemisinin, which was developed as a potent antimalarial drug. Artemisone is a derivate of artemisinin, which is a thermally stable compound, and has a log D of 2.49 and an aqueous solubility of 89 mg/l. This compound is classified as a non-lipophilic drug even though it is poorly soluble in water. The low lipophilicity reduces cyto- and neurotoxicity in *in vivo* and *in vitro* assays (Haynes *et al*., 2006:2; Nagelschmitz *et al.*, 2008:3087).

B.2.1.4 Decoquinate

DQ is a 4-hydroxy quinolone, which is currently an approved veterinary drug (Biamonte *et al.*, 2013:2838). DQ's mechanism has an anticoccidial activity through disruption of the electron transport in the mitochondrial cytochrome system of coccidia (Mikota & Plumb, 2014; Williams, 1997:102).

B.2.1.5 Emulsifiers

Emulsifiers, also known as surfactants, are incorporated within a nano-emulsion to decrease interfacial tension, existing between the oil and the water phase. Other functions include promoting emulsification during the manufacturing process (Setya *et al*., 2014:2218). For the formulation of an o/w nano-emulsion, a hydrophilic/lipophilic balance (HLB) of 9 to 18 is required and therefore a combination of hydrophilic and lipophilic surfactant was used (Setya *et al*., 2014:2218).

B.2.1.5.1 Emulsifiers classified by hydrophilic/lipophilic balance

Emulsifiers, known as surfactants, are amphiphilic molecules (contains both lipophilic and hydrophilic groups). The HLB number is used as a measure of ratio for both the hydrophilic and lipophilic groups and range from 0 to 20. A number lower than 10 has affinity for lipophilic molecules and higher than 10 has an affinity for hydrophilic molecules. Tween® 80 has a HLB value of 14.9, while Span® 60 has a HLB of 4.7 (HLB Sigma, 2011).

B.2.1.5.2 Sorbitan monostearate (Span® 60)

Span® 60, which is classified as a sorbitol monostearate ester, is a non-ionic surfactant possessing the function of emulsifying, dispersing and suspending (Zhang, 2009b:675). Span® 60 possesses a HLB value of 4.7, indicating it is a lipophilic surfactant and should be incorporated in the oil phase of the nano-emulsion (Zhang, 2009:678).

B.2.1.5.3 Polysorbate 80 (Tween® 80)

Tween® 80 can be classified as a polyoxyethylene 80 sorbitan fatty acid, which acts as a non-ionic hydrophilic surfactant in the nano-emulsion (Zhang; 2009:678). Functions of Tween® 80 include decreasing energy needed to create the nano-emulsion and therefore contributes to stable formulations (Chime *et al*., 2014:91). Tween® 80 possesses a HLB value of 14.7 (HLB Sigma, 2011), indicating it is a hydrophilic surfactant and should consequently be incorporated in the water phase nano-emulsion (Reddy *et al*., 2013:87).

B.2.1.6 Water

The water phase of an o/w nano-emulsion constitutes the greatest part and consists of aqueous material, such as alcohols or water, which is primarily used as the solvent (Williams & Barry, 2012:132). In this study, Milli-Q® water was used as the water phase within the o/w nano-emulsion.

B.3 Compatibility studies

Prior to pre-formulating the nano-emulsions, compatibility studies were done. Drug/excipient compatibility forms an important part of the pre-formulation stage in all dosage forms, as it determines potential chemical and physical interactions between a drug and excipient because it can affect the bioavailability and stability of the API (Corvi *et al.,* 2006) and in turn the therapeutic efficacy and safety (Bharate *et al*., 2010: 1,2). Differential scanning calorimetry (DCS) results should be confirmed with thermal activity results, since DCS results alone can be inconclusive and misleading (Bharate *et al*., 2010: 1, 2).

B.3.1 Differential scanning calorimetry

Physical mixtures of the API were prepared for the compatibility studies by mixing the API and individual excipients in a mortar and pestle (1:1 (w/w) ratio). Using the differential scanning calorimetry (DSC), the mixtures and single compounds were analysed. To determine if there were any incompatibilities, the resulting DSC thermograms of the mixtures were compared. Possible incompatibilities were shown as the presence of a peak shift, appearance of new peaks, or the disappearance of peaks in the DSC thermograms of the mixtures. The DSC-60 Shimadzu instrument (Shimadzu, Japan) was used in this study to record the DSC thermograms. Samples weighing approximately 3 to 5 mg were placed in aluminium-crimped cells then heated to the desired temperature; the heating rate was 10 °C/min and the nitrogen gas flow was 35 ml/min. Table B.2 represents the experimental setup and conditions for the DSC analysis.

Table B.2: Experimental setup and conditions for DSC analysis

Starting temperature	25 °C
Maximum temperature	300 °C
Heating rate	10 °C/min
Nitrogen flow rate	35 ml/min

As observed in Figure B.1, CLF, ART and DQ were melted apart and a physical mixture of 1:1. No interference of compatibility can be detected in Figure B.1 after the APIs were combined.

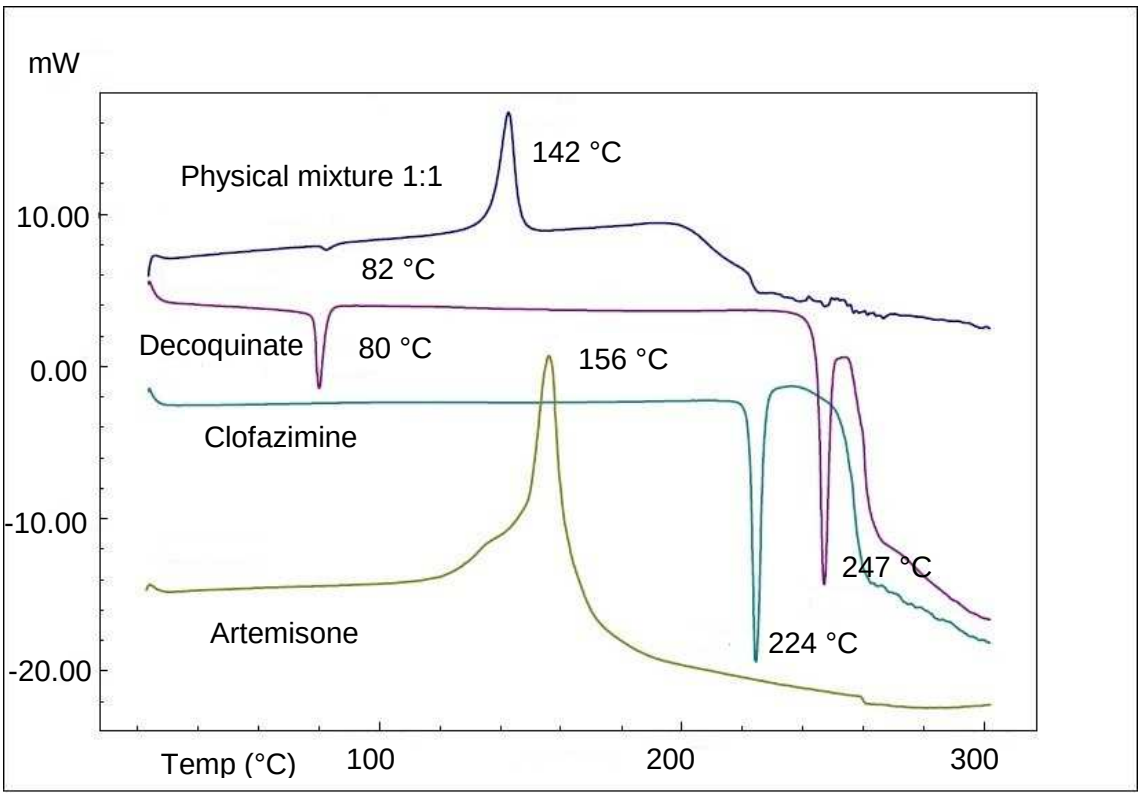

Figure B.1: CLF, ART and DQ combination differential scanning calorimetry

B.3.2 Thermal activity monitor

A 2277 Thermal Activity Monitor (TAMIII) (TA Instruments, USA), equipped with an oil bath, with a stability of ± 100 µK over 24 h was used for compatibility testing. The temperature of the calorimeters was set and maintained at a specific temperature. The temperature was determined through preliminary thermal analyses of all compounds tested. For compatibility studies, the heat flow was measured for the single components, as well as the mixtures. The observed calorimetric outputs for the individual samples are summed to give a theoretical response. This calculated hypothetical response represents a calorimetric output that would be expected if the two materials do not interact with each other. If the materials interact, the measured calorimetric response would differ from the calculated theoretical response. The mixtures were prepared in duplicate, therefore two individual heat flow signals will be compared with the theoretical response. For each sample, approximately 50 mg was weighed. The following matrix was used for compatibility testing:

- olive oil and CLF combination;
- olive oil and ART combination;
- olive oil and DQ combination;
- safflower oil and CLF combination;
- safflower oil and ART combination;

- safflower oil and DQ combination;
- olive oil with combination of CLF, ART and DQ;
- safflower oil with combination of CLF, ART and DQ.

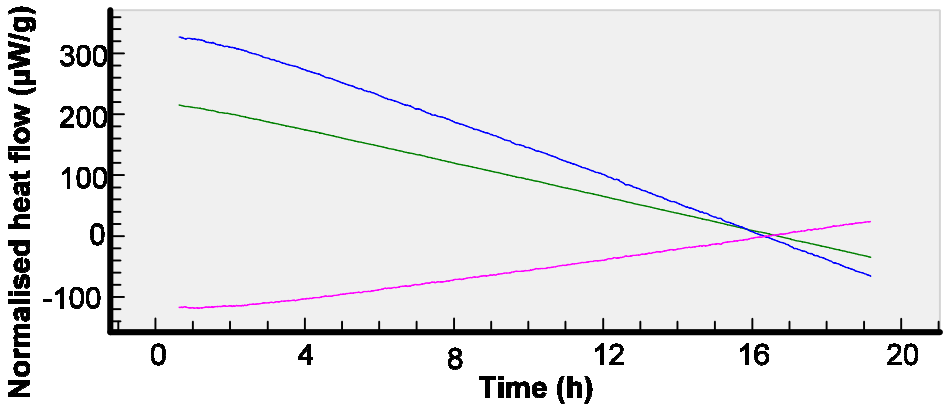

Figure B.2: Heat flow *versus* time graph obtained for a 1:1 combination of CLF and Tween® 80. The green, blue and pink lines represent measured, theoretical and interaction, respectively.

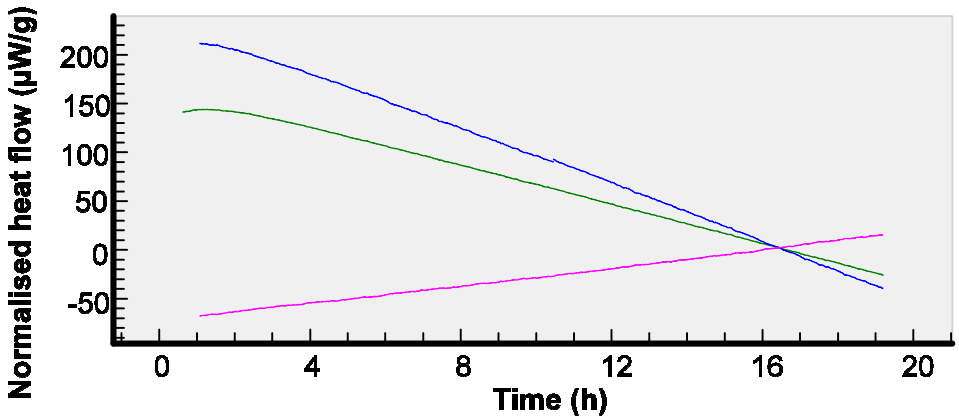

Figure B.3: Heat flow *versus* time graph obtained for a 1:1 weight combination of CLF, Tween® 80 and safflower oil. The green, blue and pink lines represent measured, theoretical and interaction, respectively.

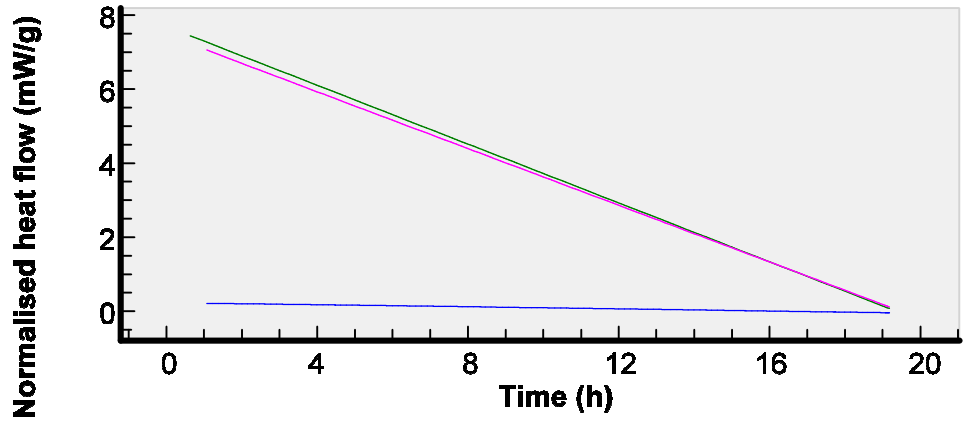

Figure B.4: Heat flow *versus* time graph obtained for a 1:1 weight combination of CLF, Tween® 80 and olive oil. The green, blue and pink lines represent measured, theoretical and interaction, respectively.

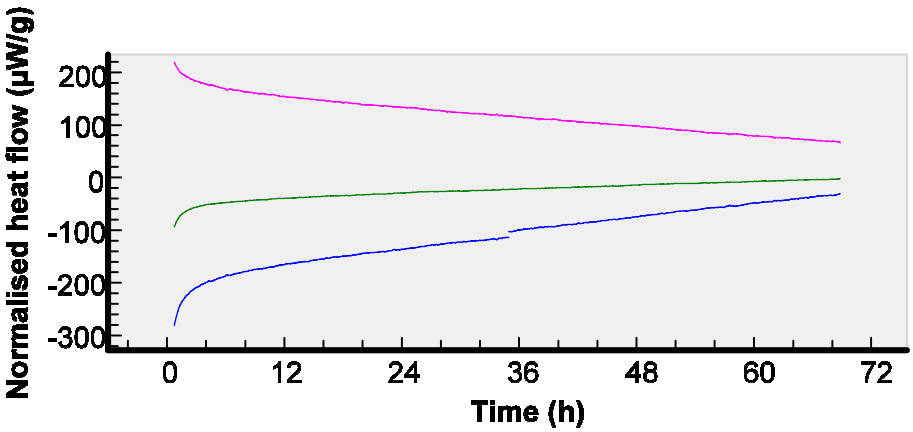

Figure B.5: Heat flow *versus* time graph obtained for a 1:1 weight combination of ART and Tween® 80. The green, blue and pink lines represent measured, theoretical and interaction, respectively.

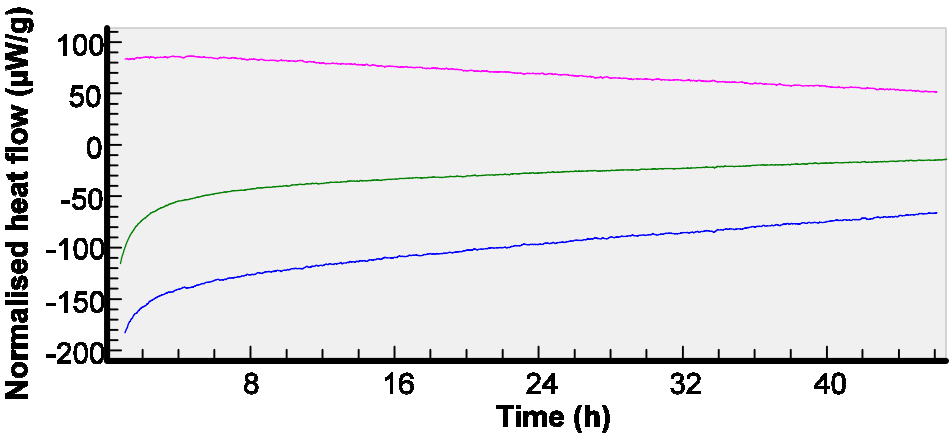

Figure B.6: Heat flow *versus* time graph obtained for a 1:1 weight combination of ART, Tween® 80 and safflower oil. The green, blue and pink lines represent measured, theoretical and interaction, respectively.

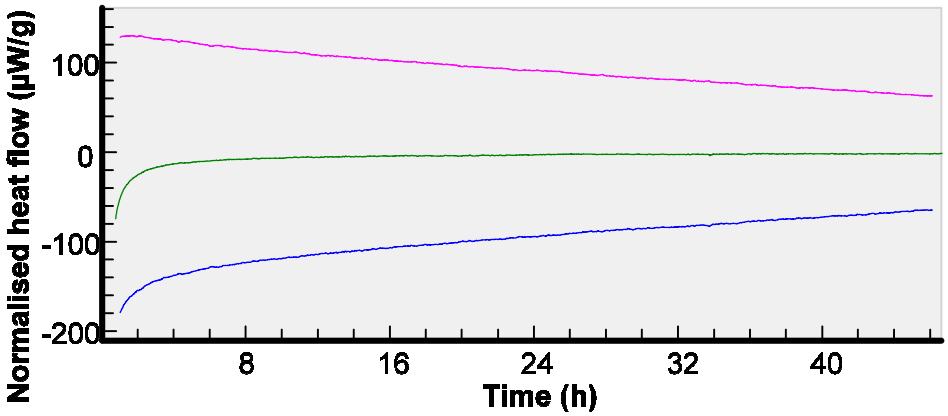

Figure B.7: Heat flow *versus* time graph obtained for a 1:1 weight combination of ART, Tween® 80 and olive oil. The green, blue and pink lines represent measured, theoretical and interaction, respectively.

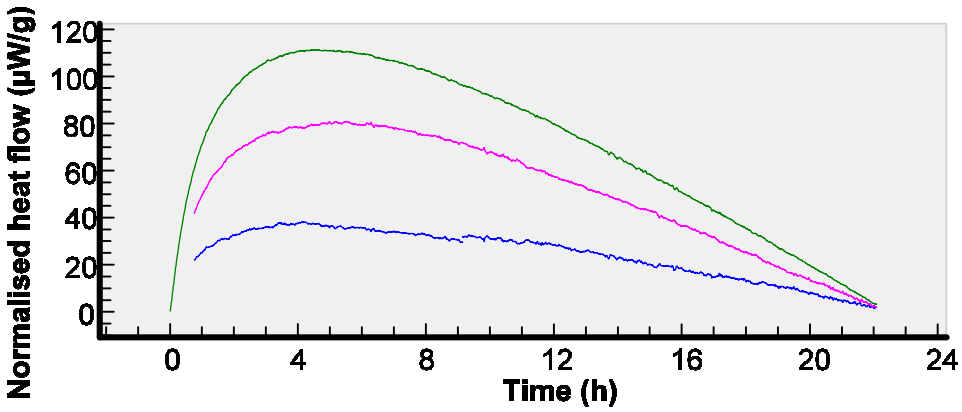

Figure B.8: Heat flow *versus* time graph obtained for a 1:1 weight combination of ART, Span® 60 and safflower oil. The green, blue and pink lines represent measured, theoretical and interaction, respectively.

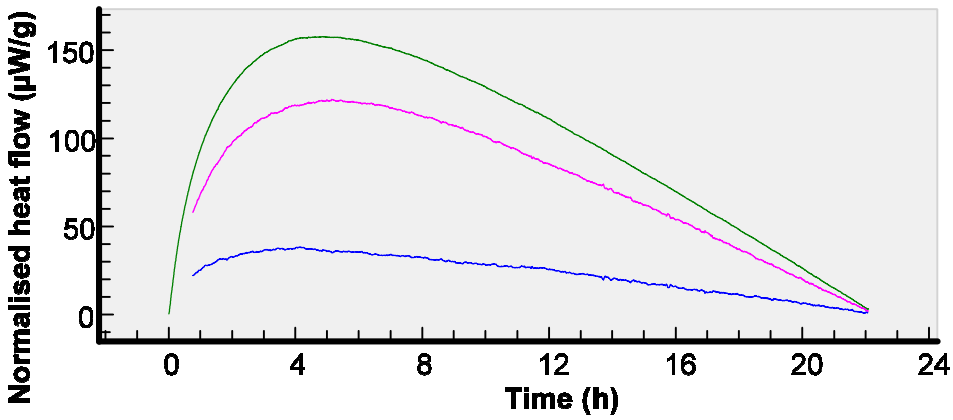

Figure B.9: Heat flow *versus* time graph obtained for a 1:1 weight combination of ART, Span® 60 and olive oil. The green, blue and pink lines represent measured, theoretical and interaction, respectively.

Table B.3 depicts the microcalorimetry results (interaction heat flow) obtained, together with an indication if any incompatibilities were identified. Incompatibilities between the API, oil or surfactant were represented in Figures B.2 to B.9. All samples were tested at a temperature of 32 °C in a combination ratio of 1:1 (w/w).

Table B.3: Interaction heat flow results of TAM

Excipients	Interactive heat flow (µW/g)	Incompatibility identified
CLF and olive oil	2.33 ± 2.81	None
CLF and safflower oil	2.16 ± 2.59	None
CLF and Tween® 80	65.86 ± 0.00	Possible incompatibility
CLF, Tween® 80 and safflower oil	-27.71 ± 36.35	Possible incompatibility
CLF, Tween® 80 and olive oil	3580.00 ± 0.00	Possible incompatibility
CLF and Span® 60	6.82 ± 7.46	None
CLF, Span® 60 and safflower oil	-19.14 ± 25.41	None
CLF, Span® 60 and olive oil	-22.420 ± 29.83	None
ART and olive oil	16.79 ± 16.82	None
ART and safflower oil	20.89 ± 20.91	None
ART and Tween® 80	93.43 ± 0.00	Possible incompatibility
ART, Tween® 80 and safflower oil	69.82 ± 70.61	Possible incompatibility
ART, Tween® 80 and olive oil	93.26 ± 95.16	Possible incompatibility
ART and Span® 60	-6.43 ± 6.68	None
ART, Span® 60 and safflower oil	48.47 ± 53.42	Possible incompatibility
ART, Span® 60 and olive oil	77.32 ± 85.45	Possible incompatibility
DQ and olive oil	4.25 ± 4.39	None
DQ and safflower oil	4.52 ± 4. 67	None
DQ and Tween® 80	2.63 ± 8.37	None
DQ, Tween® 80 and safflower oil	17.84 ± 20.11	None
DQ, Tween® 80 and olive oil	8.50 ± 12.23	None
DQ and Span® 60	13.35 ± 15.39	None
DQ, Span® 60 and safflower oil	0.71 ± 1.15	None
DQ, Span® 60 and olive oil	-7.64 ± 9.11	None
Olive oil combination of CLF, ART and DQ	16.54 ± 16.59	None
Safflower oil combination of CLF, ART and DQ	13.04 ± 13.12	None

Incompatibilities were observed, as clear and distinct deviations were evident from the slopes of the individual curves. The heat flow (which was measured) also differed significantly compared to the calculated heat flow error. It is evident, by looking at Figures B.2 to B.9 that the compatibility decreased after the surface-active agents (Tween® 80 and Span® 60) were added. As seen in Table B.3, when the APIs (CLF, ART and DQ alone and in combination) were mixed with the natural oils (safflower and olive oil), no interaction existed; indicating that the APIs can be combined with natural oils separately and in combination without any incompatibility. Futhermore, no incompatibility was observed when the APIs where separately combined with Span® 60.

However, an incompatibility was observed when CLF was separately combined with Tween® 80 (Figure B.2) and in combination with either safflower- (Figure B.3) or olive oil (Figure B.4). Similar results were noticed when ART was separately combined with Tween® 80 (Figure B.5) and in combination with either safflower- (Figure B.6) or olive oil (Figure B.7). ART also depicted an incompatibility when it was combined with Span® 60 and either safflower- (Figure B.8) or olive oil (Figure B.9). DQ indicated no incompatibility when combined with Tween® 80, Span® 60 or either natural oil separately or in combination.

B.3.3 Hot stage microscope (HSM)

During this study, a small amount of sample was placed on a microscope slide and either covered with silicon oil (Fluka Chemika, Switzerland) and a cover slide (in the case of solvates), or only a cover slide. A Nikon Eclipse E400 thermo-microscope (Tokyo, Japan) with a Leitz 350 heating unit (Wetzlar, Germany) and a Metratherm 1200d thermostat were used for the hot-stage microscopy. A Nikon Simple Polarising Attachment (Tokyo, Japan) was used on the same microscope for the polarising optical microscopy. Photographs were taken using a Nikon Coolpix 5400 digital camera (Tokyo, Japan), which was attached to the microscope. Tables B.4 to B.7 depict the hot stage microscope (HSM) results with corresponding thermal events.

Table B.4: Results of hot stage microscopy for **CLF**

Micrograph	Temperature	Remark
	20.8 °C	CLF raw material Was observed as a red powder
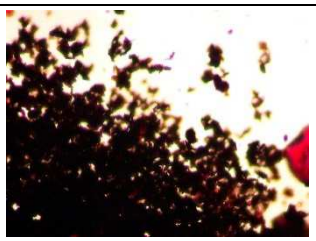	230.0 °C	CLF starts to melt
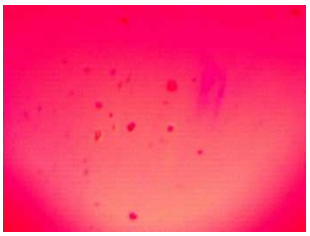	242.2 °C	CLF completely melted

Table B.5: Results of hot stage microscopy for **ART**

Micrograph	Temperature	Remark
	34.9 °C	ART raw material clear, rectangular shaped crystals
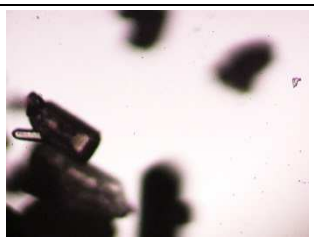	137.0 °C	ART starts to melt (Simultaneous degradation and melting)
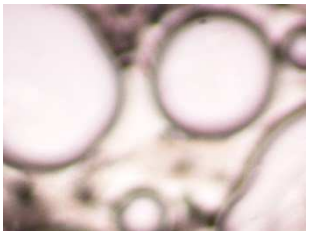	162.0 °C	ART completely melted

Table B.6: Results of hot stage microscopy for **DQ**

Micrograph	Temperature	Remark
	34.5 °C	Raw material identified as a very dense powder
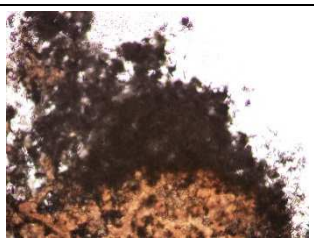	249.5 °C	DQ starts to melt
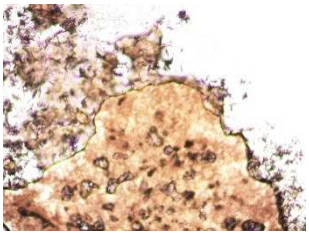	250.7 °C	DQ almost completely melted

Table B.7: Results of hot stage microscopy for the combination of **CLF**, **ART** and **DQ**

Micrograph	Temperature	Remark
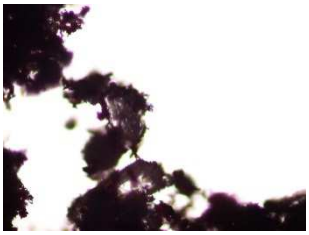	50.1 °C	Combined raw materials
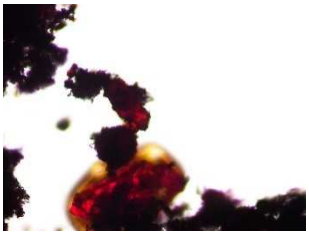	154.3 °C	ART starts to melt
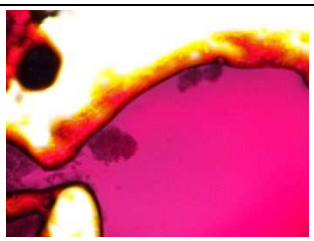	189.7 °C	CLF and DQ dissolves in ART

During HSM studies, the three APIs were melted separately and in combination. When combined, it is evident that ART has the lower melting point starting at 137 °C. It is noticeable that CLF and DQ start to dissolve within ART's liquid, which results in a molten soluble mass. Neither thermal events, phase transitions or crystallisation were observed.

B.4 Pre-formulation of nano-emulsions

B.4.1 Natural oil solubility of CLF, ART and DQ

As can be seen with the compatibility studies, the natural oils were safe to use during the pre-formulation studies. During the solubility study, the solubility of all three APIs was tested separately and in combination for both the safflower and the olive oil. The study was conducted by preheating a water shaker bath to 32 °C. For each natural oil (safflower and olive oil), 5 ml was placed within test tubes and an excess amount of API was added, i.e. CLF in safflower oil, CLF in olive oil, ART in safflower oil, ART in olive oil, etc. The test tube was sealed and placed in the bath for 24 h for saturation to take place. Afterwards, 2 ml of each test tube was removed with a micropipette, placed into a 2 ml microcentrifuge tube and centrifuged. After centrifugation, 2 µl of the supernatant (oil) was removed using a micropipette and placed in a new test tube. Tetrahydrofuran (5 ml) was added to this test tube and mixed by means of vortex. After mixing, it was transferred to a HPLC vial and by means of HPLC, the concentration was determined in the

oil. Table B.8 depicts the amount of API that can be incorporated within the oil-phase for 4.6 ml of natural oil.

Table B.8: Pre-formulation nano-emulsion API concentrations

Oil phase	API	Weight (w/v)
Olive oil	CLF	61.5 mg
Olive oil	ART	179.8 mg
Olive oil	DQ	1.9 mg
Olive oil	CLF ART DQ	70.8 mg 379.2 mg 8.1 mg
Safflower oil	CLF	72.1 mg
Safflower oil	ART	199.3 mg
Safflower oil	DQ	3.4 mg
Safflower oil	CLF ART DQ	136.0 mg 210.4 mg 8.4 mg

B.4.2 Formulation of the nano-emulsion

Nano-emulsions were pre-formulated using a trial and error approach, utilising existing formulas and changed as necessary. Table B.9 depicts the first formulas used in the nano-emulsions with and without API (placebos). In this study eight nano-emulsions containing CLF, ART and DQ, separately and in combination, with natural oils (safflower and olive oil) were formulated using a high energy emulsification method, i.e. ultrasonification, together with their placebos, **S1** to **S5** and **O1** to **O5**.

Table B.9: Pre-formulation nano-emulsion formulas

Formula	Water phase	Weight (v/v)	Oil phase	Weight (w/v)
O1	Water Tween® 80	40.0 ml 3.6 ml	Olive oil Span® 60 CLF	10% (4.6 ml) 1000.0 mg 61.5 mg
O2	Water Tween® 80	40.0 ml 3.6 ml	Olive oil Span® 60 ART	10% (4.6 ml) 1000.0 mg 179.8 mg
O3	Water Tween® 80	40.0 ml 3.6 ml	Olive oil Span® 60 DQ	10% (4.6 ml) 1000.0 mg 1.9 mg
O4	Water Tween® 80	40.0 ml 3.6 ml	Olive oil Span® 60 CLF ART DQ	10% (4.6 ml) 1000.0 mg 70.8 mg 379.2 mg 8.1 mg
O5	Water Tween® 80	40.0 ml 3.6 ml	Olive oil Span® 60	10% (4.6 ml) 1000.0 mg
S1	Water Tween® 80	40.0 ml 3.6 ml	Safflower oil Span® 60 CLF	10% (4.6 ml) 1000.0 mg 72.1 mg
S2	Water Tween® 80	40.0 ml 3.6 ml	Safflower oil Span® 60 ART	10% (4.6 ml) 1000.0 mg 199.3 mg
S3	Water Tween® 80	40.0 ml 3.6 ml	Safflower oil Span® 60 DQ	10% (4.6 ml) 1000.0 mg 3.4 mg
S4	Water Tween® 80	40.0 ml 3.6 ml	Safflower oil Span® 60 CLF ART DQ	10% (4.6 ml) 1000.0 mg 136.0 mg 210.4 mg 8.4 mg
S5	Water Tween® 80	40.0 ml 3.6 ml	Safflower oil Span® 60	10% (4.6 ml) 1000.0 mg

Of importance, since the initial %concentration of API was too low, it was decided to increase each concentration to 1% (w/v) to ensure that enough API was present in the nano-emulsion, thereby making sure that if no API was found in or through the skin, it would not be due to too low an initial concentration. With the initial formulation, a 5% oil phase was used, but it separated after a brief time, hence it was decided to increase the oil phase to 10%, while the other 10% comprised of the surfactants.

B.5 Methods

B.5.1 General formulation method of the nano-emulsion

Various methods exist to formulate nano-emulsions. Nano-emulsions consist of oil and water and can be formulated into an oil in water (o/w) formulation or a water in oil (w/o) formulation and contain surfactants to prohibit phase-separation and when mixed, form a heterogeneous, two phase mixture (Chime *et al*, 1014:77). Energy, i.e. low-energy emulsification method (LEE), high-energy emulsification (HEE) method or a mixture of both, is required to mix the separate phases and form nano-sized droplets, since nano-emulsions are thermokinectically stable, but not thermodynamically stable (Abolmaali *et al*., 2011:140). LEE methods include phase inversion composition (PIC), spontaneous emulsification and phase inversion temperature (PIT), which uses internal chemical energy of the system, only requiring simple stirring to form a nano-emulsion with a small droplet size (Sole *et al*.,2012:133). HEE methods include high-pressure homogenisers, ultrasonicators (Tadros *et al*., 2004:305) and microfluidisers (Bouchemal *et al*., 2006:3187) using mechanical devices, which operate by producing disruptive forces to form nano-emulsions. The mechanical device, together with processing attributes (temperature, operating cycles and formulation composition), will influence the formation of nano-sized droplets (Ganta *et al*., 2014:698)

B.5.2 Formulation method of the eight pre-formulation natural oil nano-emulsions

The nano-emulsions were formulated by firstly mixing Tween® 80 and water (water phase) in a beaker. In another beaker, Span® 60 and olive or safflower oil (oil phase) were mixed. Both mixtures were heated using a magnetic stirrer hotplate (60 °C). After the temperature of 60 °C had been reached and each phase was stable, after 15 min of mixing, the oil phase was added very slowly to the water phase, while continuing to mix at 60 °C. Subsequently, it was placed in a beaker with ice and sonicated for 10 min at a power of 40 Watt (Borhade *et al.,* 2012:150).

B.6 Characterisation of pre-formulation nano-emulsions

The following physical characterisation tests of the pre-formulated nano-emulsions were performed to determine the effectiveness of the formula:

- pH,
- viscosity,
- droplet size,
- zeta-potential,
- drug EE%,
- morphology.

B.6.1 pH

A Mettler Toledo SevenMulti pH meter (InLab® 410 NTC electrode 9823) (Greifensee, Switzerland) was used to determine the pH of the eight prepared nano-emulsions, to establish whether they would irritate the skin after topical application. In order to measure the pH of each nano-emulsion, the probe of the pH meter was submerged into each sample (50 ml) and measurements taken. Despite the fact the skin can withstand products with a pH range of 3 to 9, the acceptable limits for a formulation on the skin is between pH 5 to 9 (Naik *et al.,* 2000:319) and when the pH transfers out of these ranges, it can influence the integrity and permeability of the skin (Barry,2002:512). The test was performed in triplicate and the accuracy of the pH meter was verified by calibrating it each time prior to use.

Table B.10: Results of pH of pre-formulated nano-emulsions

Nano-emulsions	pH
O1	5.01 ± 0.10
S1	5.10 ± 0.05
O2	5.15 ± 0.07
S2	5.08 ± 0.02
O3	5.30 ± 0.08
S3	5.24 ± 0.04
O4	5.19 ± 0.08
S4	5.26 ± 0.07

The pH of a compound determines the ionised or unionised species, indicating whether the compound is a suitable candidate to permeate through the skin. Although the ionised form has a higher aqueous solubility, it also possesses lower permeability than the unionised form. CLF, ART and DQ are dissociated at 99.69%, 0.098% and 99.98%, respectively, at pH 5 where CLF and DQ can permeate through the skin (Admescope, 2012), nevertheless ART does indicate some difficulty. As can be seen in Table B.10, all eight nano-emulsions were close to pH 5, for maximum dissociation, and within the acceptable range (pH 5 to 9) (Naik *et al.,* 2000:319) and therefore, it can be proposed that the eight nano-emulsions would not pose any harm or irritation to the skin.

B.6.2 Viscosity

The viscosity of a formulation specifies the resistance (fluid versus flow) and ultimately, if a high level of resistance were present within a formulation, the flow would indicate a high level of viscosity (Quiñones & Ghaly, 2008:62). The viscosity of the nano-emulsions was measured using a Brookfield® Viscometer (Stoughton, United States of America (US)). A water bath was

connected to the viscosity meter and maintained at 25 °C by means of a Brookfield® temperature controller. Depending on the consistency of the nano-emulsions, the appropriate LV spindles and Helipath attachments were chosen to ensure appropriate torque. The Helipath stand (D20733) lowered and raised the spindle at a rate of 7/8 inch/min. During this time, the T-bar spindle rotated at different rates in the dispersion. Viscosity readings were taken every 10 sec over a period of 5 min, giving 32 readings.

Table B.11: Results of viscosity of pre-formulated nano-emulsions

Nano-emulsions	Viscosity (cP)
O1	2.59 ± 0.50
S1	2.91 ± 0.08
O2	2.60 ± 0.08
S2	2.62 ± 0.05
O3	2.72 ± 0.08
S3	2.73 ± 0.03
O4	2.63 ± 0.07
S4	2.56 ± 0.08

All the viscosity readings of the eight nano-emulsions were very low (2.59 – 2.91 cP), and whilst the larger part of an o/w nano-emulsion is water, the viscosity is therefore very low (Chime *et al*., 2014:97). All eight nano-emulsions were measured at 200 rpm, at a temperature of ± 25°C. Water is known to possess a viscosity of 1 cP, consequently it can be presumed that the viscosity of the nano-emulsions measured close to the viscosity of water (V&P Scientific Inc., 2010); this could be because 95% of the nano-emulsion consists of water and because of the low amount of Tween® 80 and oil used (Djordjevic *et al*., 2004:13).

B.6.3 Droplet size

The droplet size was determined using a Zetasizer Nano ZS (Zen 3600) (Malvern® Instruments LTD, Worcestershire, United Kingdom (UK)) at a temperature of 25 °C (room temperature). For the analysis, a helium - neon (He-Ne) laser (633 nm), at a scattering angle of 175 °, was used at room temperature. During droplet size determination, a polydispersed index (PdI) value is also obtained, which distinguishes whether the nano-emulsions oil droplets were uniform throughout in the water phase (uniformity throughout the dispersion) (Shakeel *et al*., 2007), and is measured on a scale from 0 to 1 (Shaw, 2016). Eight nano-emulsion samples were prepared the day prior to analysis. Eight samples were injected into eight disposable cells (2 ml), respectively. The study was performed in triplicate for each sample and analysed.

Table B.12: Results of droplet sizes of pre-formulated nano-emulsions

Nano-emulsions	Droplet size (nm)	PdI
O1	101.36 ± 2.05	0.230 ± 0.10
S1	126.47 ± 1.75	0.267 ± 0.03
O2	101.47 ± 1.56	0.208 ± 0.08
S2	104.63 ± 1.42	0.219 ± 0.03
O3	91.39 ± 1.30	0.199 ± 0.03
S3	83.61 ± 1.72	0.175 ± 0.03
O4	83.05 ± 0.90	0.210 ± 0.03
S4	88.14 ± 1.52	0.193 ± 0.10

Accumulation of the compound within the skin is preferred for topical delivery (Wiechers, 2008:174). Studies report there is a relationship between the permeability coefficient of a compound and the droplet size of the nano-emulsion, which states that when the size of the droplet changes, there is a change in total area of the dispersed phase (Wiechers, 2008:175). Droplet sizes of the eight nano-emulsions ranged from 83 to 130 nm, which falls within range of emulsions from 10 nm to 10 µm (Wiechers, 2008:173). A PdI value of 1 indicates the dispersion is seen as polydispersed (hence the droplet sizes vary), whilst a PdI closer to 0 is seen as monodispersed (homogenous) (Gaumet *et al*., 2008:5). The PdI value measured for all eight nano-emulsions was < 0.267, therefore it is proposed that the PdI is closer to 0 and thus reasonably monodispersed; nano-emulsions are characteristically seen as heterogeneous dispersions (created through oil and water) (Chime *et al*., 2014:77).

B.6.4 Zeta-potential

Zeta-potential is an indication of how stable a colloidal system is, as it indicates the repulsion degree to institute the formulations' physical stability (Shah *et al*., 2014:66). The zeta-potential was determined for each dispersion by means of the Zetasizer Nano ZS (Zen 3600) (Malvern® Instruments LTD, Worcestershire, United Kingdom (UK)) at a temperature of 25 °C (room temperature). Eight low concentration samples were prepared and injected into eight disposable cells, respectively. This study was performed in triplicate and the average was calculated.

Table B.13: Results of zeta-potential of pre-formulated nano-emulsions

Nano-emulsions	Zeta-potential(mV)
O1	-33.30 ± 1.10
S1	-30.00 ± 0.10
O2	-36.60 ± 0.12
S2	-37.90 ± 0.05
O3	-35.40 ± 0.80
S3	-34.40 ± 1.33
O4	-32.00 ± 1.28
S4	-30.10 ± 0.05

Literature suggests that highly negatively charged zeta-potential is needed to permeate the skin successfully, as the skin is also negatively charged which could lead to an increase of API flux. It is also suggested that zeta-potential values should range from below - 30 mV or above 30 mV, where the nano-emulsions can be viewed as stable (Duangjit *et al*., 2011:6; Eid *et al*., 2014:2; Silva *et al*., 2012:860). As observed in Table B.13, results differ from - 30 mV to - 38 mV, which is in the acceptable range of above 30 mV or below - 30 mV, indicating that the nano-emulsions are stable and would possibly permeate the skin.

B.6.5 Drug entrapment efficacy

The Optima™ L-100 XP ultracentrifuge (Beckman Coulter, Brea, California, USA) was used to determine the drug entrapment efficiency (EE%). The EE% is used to determine the difference between the free drug and the total amount of drug in a sample. The eight nano-emulsion samples (10 ml) were added to Eppendorf® tubes and centrifuged at 25 000 rpm for 30 min at room temperature (23 °C). The supernatant fluid (free drug) was separated from the sediment material (nano-emulsions containing the entrapped API), thereafter the supernatant was diluted (x 10) with the ethanol absolute (99.7%) and transferred to HPLC vials to be analysed. The trapped and free API were determined by means of HPLC. The drug EE% was determined using Equation B.1 (Xuan *et al.,* 2006:583).

$$\text{Drug entrapment (\%)} = \{(\text{drug}_{\text{total}} - \text{drug}_{\text{supernatant}}) \div \text{drug}_{\text{total}}\} \times 100 \qquad \textbf{Equation B.1}$$

The results of the EE% are depicted in Table B.14 for all eight nano-emulsions.

Table B.14: Results of EE% of pre-formulated nano-emulsions

Nano-emulsions	Drug entrapment efficiency (%)
O1	94.12 ± 1.20
S1	91.35 ± 1.38
O2	96.30 ± 1.01
S2	98.95 ± 2.05
O3	93.01 ± 1.45
S3	91.90 ± 0.99
O4: CLF **ART** **DQ**	94.12 ± 2.40 96.30 ± 1.34 93.01 ± 1.57
S4: CLF **ART** **DQ**	94.42 ± 1.20 98.50 ± 1.75 98.02 ± 1.35

As observed in Table B.14, all the nano-emulsions had a drug EE% of > 96%, indicating that the APIs have been entrapped in the oil phase and dispersed through the nano-emulsions. Since the drug entrapment is very high, the nano-emulsions are proposed to be ideal candidates for topical delivery.

B.6.6 Morphology

Light microscopy was performed using a Nikon Eclipse E4000 microscope, fitted with a Nikon DSFi1 camera (Nikon, Japan Linkam THMS600) equipped with a T95 LinkPad temperature controller (Surrey, England) to determine whether formation of droplets took place. A small amount of the nano-emulsions was placed on a 20 mm 16 microscope slide. The sample was covered with a 16 mm cover slip and the microscopic viewing of the nano-emulsions was done using magnifications of 10, 20 or 40 x. The following images have been taken by light microscopy to illustrate the droplet sizes of the natural oil nano-emulsions.

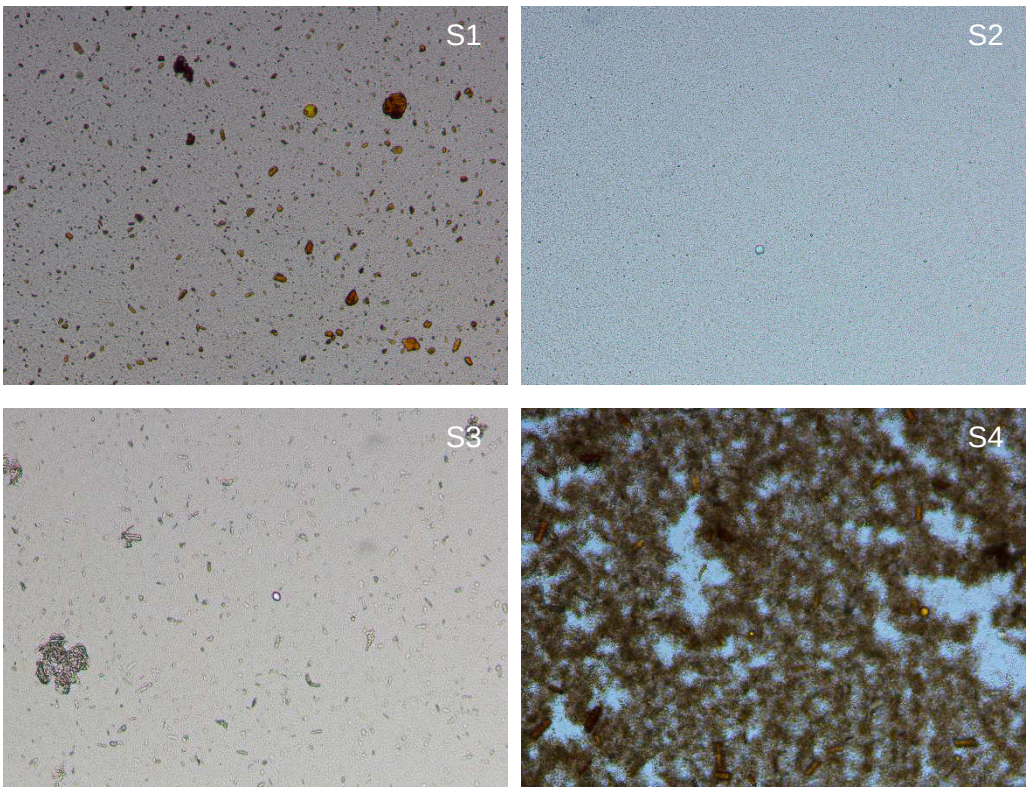

Figure B.10: a) Light microscopy micrographs of the nano-emulsion containing safflower oil (**S1**, **S2**, **S3** and **S4**).

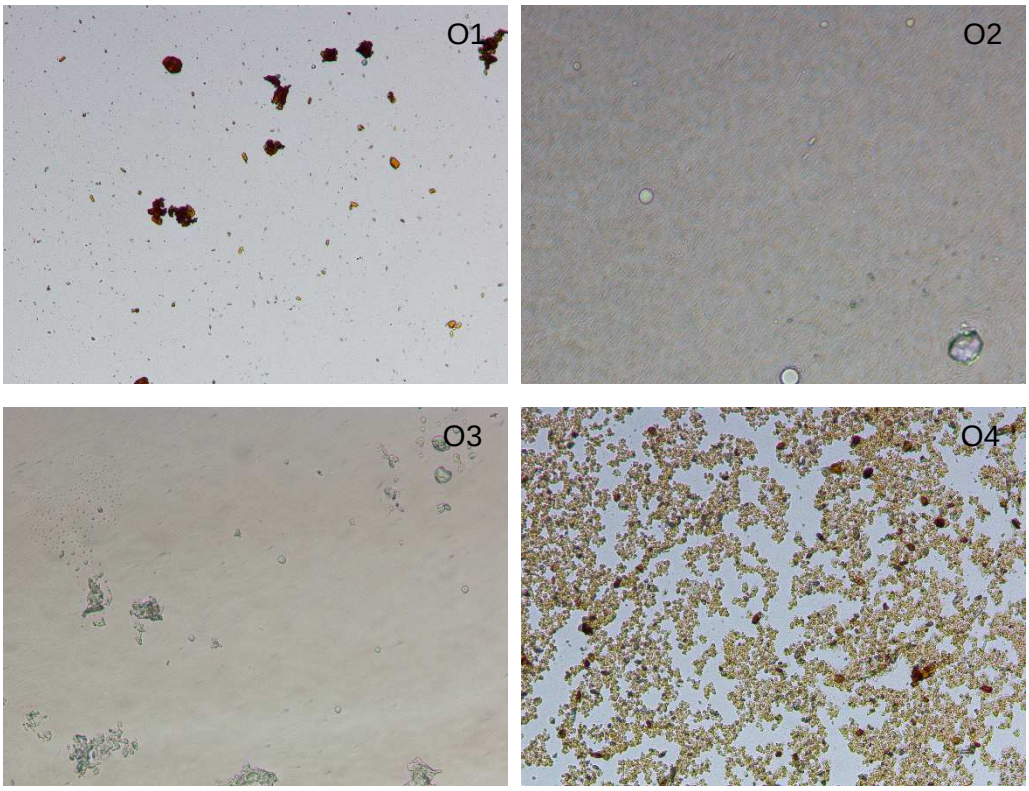

Figure B.11: a) Light microscopy micrographs of the nano-emulsion containing olive oil (**O1**, **O2**, **O3** and **O4**).

B.7 Conclusion

Nano-emulsions containing natural oils were formulated into different combinations, i.e. (**S1**, **S2**, **S3**, **S4**, **S5**, **O1**, **O2**, **O3**, **O4** and **O5**).

In this study, the compatibility was investigated by means of DSC, TAM and HSM. The DSC indicated that all the APIs were compatible, either separately or in combination. Some incompatibility was seen during the TAM studies when surface-active agents, such as Span® 60 or Tween® 80, were added, but no incompatibility was seen between the APIs when tested separately or in combination. HSM studies indicated that while ART melted first, DQ and CLF dissolved within the ART resulting in a molten solubilised mass whereby no phase transitions, thermal events or crystallisation was seen, indicating the APIs were compatible with each other.

Physicochemical properties were also tested, which included pH, zeta-potential, viscosity, droplet size and drug EE%. All eight nano-emulsions indicated a pH of close to 5, which is still within the acceptable range for a skin formulation (pH 5 to 9) (Naik *et al.,* 2000:319). When the viscosity was measured of all eight nano-emulsions, it was evident that due to the small amount of oil and Tween® 80 and the high amount of water used, viscosity readings were very low. , Droplet size values were within the acceptable range of between 10 nm to 10 µm (Wiechers, 2008:173), which was measured at 83 to 130 nm. PdI values of the nano-emulsions were measured at < 0.267, indicating a value closer to 0 (Gaumet *et al*., 2008:5), therefore the nano-emulsions were seen as monodispersed. The eight nano-emulsions were stable with zeta-potential ranging from - 30 mV to - 38 mV, the ideal range being above 30 mV or below - 30 mV, indicating that formulations were stable and skin permeation would be effective (Duangjit *et al*., 2011:6; Eid *et al*., 2014:2; Silva *et al*., 2012:860). The %EE was significantly high, ranging from 91 to 99%, which indicates the APIs were successfully encapsulated within the oil droplets within the nano-emulsions. During the morphology, it was indicated that droplets formed within the nano-emulsions. As stated before, TEM could not be used as the APIs could damage the equipment. The pre-formulation of CLF, ART and DQ in the nano-emulsions containing natural oil provided additional information about the physical and chemical properties when formulated separately and in combination.

References

Admescope. 2012. pKa-Dissociation constant, pH partition. http://www.admescope.com/learnadme/physicochemical-properties/pka-dissociation-constant-ph-partition.html Date of access: 13 Apr 2016.

Baibhav, J., Gurpreet, S., Rana, A.C., Seema, S. & Vikas, S. 2011. Emulgel: a comprehensive review on the recent advances in topical drug delivery. *International Research Journal of Pharmacy*, 2:66-70.

Barry, B. 2002. Transdermal drug delivery. (*In* Aulton, M.E., *ed*. Pharmaceutics: the science of dosage form design. 2nd ed. London: Churchill Livingstone. p. 499-533.)

Bouchemal, K., Briançon, S., Couenne, F., Fessi, H. & Tayakout, M. 2006. Stability studies on colloidal suspensions of polyurethane nanocapsules. *Journal of Nanoscience and Nanotechnology*, 6:3187-3192.

Chime, S.A., Kenechukwu, F.C. & Attama, A.A. 2014. Nanoemulsions – Advances in Formulation, Characterization and Applications in Drug Delivery, Application of Nanotechnology in Drug Delivery, http://www.intechopen.com/books/application-of-nanotechnology-in-drug-delivery/nanoemulsions-advances-in-formulation-characterization-and-applications-in-drug-delivery Date of access: 1 Mar 2015.

Cholo, M.C., Steel, H.C., Fourie, P.B., Germizhuizen, W.A. & Anderson, R. 2011. Clofazimine: current status and future prospects. *Journal of Antimicrobial Chemotherapy,* 67(2):290-298.

Corvi, M.P., Cirri, M. & Mura, P. 2006. Differential scanning calorimetry as a screening technique in compatibility studies of DHEA extended release formulations. *Journal of Pharmaceutical and Biomedical Analysis,* 42:3-10.

Davis, S.S., Hadgraft, J. & Palin, K.J. 1985. Medical and pharmaceutical applications of emulsions. (*In* Becher, P., *ed.* Encyclopedia of Emulsion Technology. Vol. 2. New York: Marcel Dekker. p. 159-238.)

Djordjevic, L., Primorac, M., Stupar, M. & Krajisnik, D. 2004. Characterization of capryocaproyl macrogolycerides based microemulsion drug delivery vehicles for an amphilic drug. *International Journal of Pharmaceutics,* 271:11-19.

Donovan, M.D. & Flanagan, D.R. 1996. Bioavailability of disperse dosage forms. (*In* Lieberman, H.A., Rieger, M.M. & Banker, G.S., *eds.* Pharmaceutical Dosage Forms. Disperse Systems. Vol. 1. New York: Marcel Dekker. p. 315-376.)

Duangjit, S., Opanasopit, P., Rojanarata, T. & Ngawhirunpat, T. 2011. Characterization and *in vitro* skin permeation of meloxicam-loaded liposomes versus transferosomes. *Journal of Drug Delivery*, 83:1-9.

Eid, A.M., El-Enshasy, H.A., Aziz, R. & Elmarzugi, N.A. 2014. Preparation, characterization and anti-inflammatory activity of *Swietenia macrophylla* nanoemulgel. *Journal of Nanomedicine and Nanotechnology*, 5:1-10.

Fernandez, C., Marti-Mestres, G., Ramos, J. & Maillols, H. 2000. LC analysis of benzophenone-3. II. Application to determination of '*in vitro*' and '*in vivo*' skin penetration from solvents, coarse and submicron emulsions. *Journal of Chromatography B: Biomedical Sciences*, 24:155-165.

Foldvari, M., Gesztes, A., and Mezei, M.(1990) Dermal drug delivery by liposome encapsulation: clinical and electron microscopic studies. *Journal of Microencapsulation: Micro and Nano Carriers*, 4:479–489.

Förster, T. & Von Rybinski, W. 1998. Applications of emulsions. (*In* Binks, B.P., *ed.* Modern Aspects of Emulsion Science. London: The Royal Society of Chemistry. p. 395-426.)

Fresta, M. & Puglisi, G. 1996. Application of liposomes as potential cutaneous drug delivery systems: *in vitro* and *in vivo* investigation with radioactively labelled vesicles. *Journal of Drug Targeting*, 4:95-101.

Ganta, S., Talekar, M., Singh, A., Coleman, T.P. & Amiji, M.M. 2014. Nanoemulsions in translational research – opportunities and challenges in targeted cancer therapy. *American Association of Pharmaceutical Scientists*, 15:694-708.

Gaumet, M., Vargas, A., Gurny, R. & Delie, F. 2007. Nanoparticles for drug delivery: the need for precision in reporting particle size parameters. *European Journal of Pharmaceutics and Biopharmaceutics*, 69:1-9.

Haynes, R. K., Fugmann, B., Stetter, J., Rieckmann, K., Heilmann, H.D., Chan, H.W., Cheung, M.K., Lam, W.L., Wong, H.N., Croft, S.L., Vivas, L., Rattray, L., Stewart, L., Peters, W., Robinson, B.L., Edstien, M.D., Kotecka, D.E., Kyle, M., Gerisch, M., Radtke, G., Schmuck, W., Steinke, U., Wollborn, K., Schmeer, K. & Romer. A.S. 2006. Artemisone: a highly active antimalarial drug of the artemisinin class. *Angewandte Chemie*, 45:1-8.

Izquierdo, P., Wiechers, J.W., Escribano. E., García-Celma, M.J., Tadros, T.F., Esquena, J., Dederen, J.C. & Solans, C. 2007. A Study on the Influence of Emulsion Droplet Size on the Skin Penetration of Tetracaine. *Skin Pharmacology and Physiology,* 20:263-270.

Kreilgaard, M., Kemme, M.J.B., Burggraaf, J., Schoemaker, R.C. & Cohen, A.F. 2001. *Journal Pharmaceutical Research*, 18:593-599.

Lee, P.J., Langer, R. & Shastri, V.P. 2003. Novel microemulsion enhancer formulation for simultaneous trans-dermal delivery of hydrophilic and hydrophobic drugs. *Pharmaceutical Research*, 20:264-269.

Lu, Y., Zheng, M., Wang, B., Fu, L., Zhao, W., Li, P., Xu, J., Zhu, H., Jin, H., Yin, D., Huang, H., Upton, A.M. & Ma, Z. 2011. Clofazimine Analogs with Efficacy against Experimental Tuberculosis and Reduced Potential for Accumulation. *Antimicrobial Agents and Chemotherapy,* 55:5183-5193.

Mikota, S.K. & Plumb, D.C. 2014. http://www.elephantcare.org/Drugs/decoquin.htm Date of access: 20 Oct 2017.

Nagelschmitz, J., Voith, B., Wensing, G., Roemer, A., Fugmann, B., Haynes, R.K., Kotecka, B.M., RIieckmann, K.H. & Edstein, M.D. 2008. First assessment in humans of the safety, tolerability, pharmacokinetics, and *ex vivo* pharmacodynamics antimalarial activity of the new artemisinin derivative artemisone. *Antimicrobial Agents and Chemotherapy,* 52(9):3085-3091.

Naik, A., Kalia, Y.N. & Guy, R.H. 2000. Transdermal drug delivery: overcoming the skin's barrier function. *Pharmaceutical Science and Technology Today,* 3(9):318-326.

Paolino, D., Ventura, C.A., Nistico, S., Puglisi, G. & Fresta, M. 2002. Lecithin microemulsions for the topical administration of ketoprofen: percutaneous adsorption through human skin and *in vivo* human skin tolerability. *International Journal of Pharmaceutics*, 244:21-31.

Radd, B. 1994. Efficient formulation of cosmeceutical products. *Cosmetics and Toiletries,* 109(10):50, 51.

Reddy, A.K., Debnath, S. & Babu, M.N. 2013. Nanoemulsion a novel approach for lipophilic drugs – a review. *Asian Journal of Pharmaceutical Research*, 3:84-92.

Setya, S., Talegaonkar, S. & Razdab, B.K. 2014. Nanoemulsions: formulation methods and stability aspects. *World Journal of Pharmacy and Pharmaceutical Sciences*, 3:2214-2228.

Shah, P., Bhalodia, D. & Shelat, P. 2010. Nano-emulsions: a pharmaceutical review. *Systematic Review in Pharmacology*, 1:24-32.

Shakeel, F., Baboota, S., Ahuja, A., Ali, J., Aqil, M. & Shafiq, S. 2007. Nanoemulsions as vehicles for transdermal delivery of aceclofenac. *American Association of Pharmaceutical Scientists*, 8:104.

Shakeel, F., Baboota, S., Ahuja, A., Ali, J. & Shafiq, S. 2009. Celecoxib Nanoemulsion for Transdermal Drug Delivery: Characterization and *In Vitro* Evaluation. *Journal of Dispersion Science and Technology*, 30:834-842.

Shaw, R. 2016. Dynamic lightscattering training: achieving reliable nano particle sizing. http://149.171.168.221/partcat/wp-content/uploads/Malvern-Zetasizer-LS.pdf Date of access: 14 Nov 2017.

Silva, H.D., Cerqueira, M.A. & Vicente, A.A. 2012. Nanoemulsions for food applications: development and characterization. *Food Bioprocess Technology,* 5:854-867.

Sigma-Aldrich. 2011. Surfactants classified by HLB numbers, http://www.sigmaaldrich.com/materials-science/material-science-products.html?TablePage=22686648 Date of access: 21 Oct 2017.

Solè, I., Maestro, A., González, C., Solans, C. & Gutiérrez, J.M. 2006. Optimization of nano-emulsion preparation by low-energy methods in an ionic surfactant system. *Langmuir*, 22:8326-8332.

Tadros, T., Izquierdo, P., Esquena, J. & Solans, C. 2004. Formation and stability of nano-emulsions. *Advances in Colloid and Interface Science*, 108:303-318.

Walters, K.A. & Brain, K.R. 2002. Dermatological formulation and transdermal systems. *(In* Swarbrick, J., *ed.* Dermatological and transdermal formulations. Vol. 119. New York: Marcel Dekker. p. 321, 322.)

Wiechers, J.W., Kelly, C.L., Blease, T.G. & Dederen, J.C. 2008. Formulating for efficacy. *International Journal of Cosmetic Science,* 26:173-175, 177.

Williams, A.C. & Barry, B.W. 2012. Penetration enhancers. *Advanced Drug Delivery Reviews*, 64:128-137.

Xuan, T., Zhang, J.A. & Ahmad, I. 2006. HPLC method for determination of SN-38 content and SN-38 entrapment efficiency in a novel liposome-based formulation, LE-SN38. *Journal of Pharmaceutical and Biomedical Analysis,* 41:582-588.

Zhang, D. 2009. Sorbitan esters. (*In* Rowe, R.C., Sheskey, P.J. & Quinn, M.E., *eds*. Handbook of pharmaceutical excipients. 6th ed. USA: Pharmaceutical Press. p. 675-678.)

Appendix C:

Franz cell diffusion studies of natural oil nano-emulsions containing clofazimine, artemisone and decoquinate

C.1 Introduction

The transdermal route of administration has established extensive applications and gained significant industrial triumph in the rivalry with other dosage forms such as intramuscular, intravenous and oral routes (Tavano *et al*., 2013:281; Thong *et al*., 2007:272). Topical formulation development ought to enhance drug absorption, to alleviate skin diseases by amplifying the skin hydration to surmount the low skin permeability and encourage the prolonged delivery period to the embattled skin sites (Foldvari, 2000:417-425; Lam & Gambardi, 2013:26).

Transdermal drug delivery is a non-invasive approach (Delgado-Charro & Guy, 2014:64) to apply medication to the skin, thus avoiding the first-pass metabolism and shortcomings from oral dosage administration, i.e. enzymatic degradation and rapid clearance in the gastrointestinal tract (Khafagy *et al*., 2007; Lam & Gambardi, 2013:27;; Prausnitz *et al*., 2004; Thomas & Finnin, 2004), regimens which are inconvenient, have high prevalence of adverse effects caused by the first-pass metabolism and low oral bioavailability (Cleary, 1993; Delgado-Charro & Guy, 2001; Prausnitz & Langer, 2008; Wiedersberg & Guy, 2014:150). When drug delivery is targeted to skin sites, it can promote patient compliance and convenience for treatment (Khafagy *et al*., 2007; Lam & Gambardi, 2013:27; Prausnitz *et al*., 2004; Thomas & Finnin, 2004). Other advantages include prolonged period of administration, inexpensive and portable dosage forms (Drakiluc *et al*., 2008:40; William & Barry, 2004), reduced frequency of dosing (since the API's duration of action is extended) and lower variability (Cleary, 1993; Prausnitz & Langer, 2008; Wiedersberg & Guy, 2014:150). Transdermal skin-targeted drug delivery still presents limitations even though the skin is relatively large and a readily accessible surface area for drug adsorption (Lam & Gambardi, 2013:27; Prow *et al*., 2011). For a drug to be a feasible candidate for transdermal drug delivery, there are appropriate conditions, such as pharmacodynamics, pharmacokinetic and physicochemical properties (Delgado-Charro & Guy, 2014:64; Watkinson, 2013), and factors the APIs must adhere to for drug delivery across the skin to take place, namely a) log P should be between 1 and 3, b) molecular weight of <500 Da is required and c) the API should have both

lipophilic (to permeate through the stratum corneum) and aqueous (to permeate through the epidermis to the other layers to the blood circulation) solubility qualities (Cleary, 1993; Wiedersberg & Guy, 2014:150;). Typically, an API's melting point should also be below 200 °C (Finnin & Morgan, 1999; Thomas & Finnin, 2004:699).

Transdermal drug delivery's effectiveness depends solely on the API to permeate through the skin adequately to reach therapeutic levels (Baek *et al*., 2013:358; Dos Anjos & Alonso, 2008). Problems arise when most of the APIs have low permeability to overcome the powerful barrier of the skin, which leads to limited drug uptake, dosage flexibility, slow penetration rates (Lam & Gambardi, 2013:27) and skin tolerability (Wiedersberg & Guy, 2014:151). The APIs used in this study (CLF (10 mg/l), ART (89 mg/l) and DQ (0 mg/l)) have very poor to no aqueous soluble properties, which indicates skin penetration might be challenging.

Penetration enhancers are used to overcome the skin's barrier properties by facilitating drugs across the skin to disrupt the stratum corneum structure and in effect, promote drug diffusion (Foldvari, 2000:419). Nano-emulsions, containing natural oils, were chosen as carriers for this study. The natural oils that will be used during this study are olive and safflower oil, as they contain linoleic acid (C_{18} fatty acid) (Vermaak *et al.*, 2011:920-933), which is also found naturally in the skin (Williams & Barry, 2012:132). Another advantage of linoleic acid is that it is expected to be less harmful, or irritating to the skin, than other penetration enhancers (Dingler, 2002:11). The nano-emulsions to be investigated during this study are proposed to enhance drug penetration. Nano-emulsions have several advantages over other nano-counterparts, such as niosomes, micro-emulsions, liposomes, and nano-particles, including excellent solubilisation capacity of drugs, small droplet sizes with higher entrapment efficiencies offering ease of preparation, optical stability and clarity, all of which contribute to them being attractive candidates for drug vectorisation (Chime *et al.,* 2014). Recently, nano-emulsions have been successfully implemented to improve the transport of hydrophobic compounds (Shakeel *et al*., 2012:953-973). The aim of this study was to investigate whether nano-emulsions containing natural oils, would improve the topical delivery of CLF, DQ and ART, separately and in combination.

C.2 Methods

C.2.1 Preparation of nano-emulsions

During this study, eight nano-emulsions were prepared consisting of safflower or olive oil, and the APIs separate and in combination, i.e. **S1**, **S2**, **S3**, **S4**, **O1**, **O2**, **O3**, and **O4** (see Appendix B).

C.2.2 Preparation of the receptor phase

CLF, ART and DQ are poorly soluble to insoluble in water. The solvent used with validation (absolute ethanol (99.7%)) could not be used during the skin diffusion studies since ethanol has the potential to influence the integrity of the human skin, which could lead to differentiating results (Williams, 2013:685). For the receptor phase during the skin diffusion studies, phosphate buffer solution (PBS: pH 7.4) was used and prepared by dissolving 13.65 g of potassium dihydrogen orthophosphate (KH_2PO_4) in 500 ml of Milli-Q® water and 3.025 g of sodium hydroxide (NaOH) in 800 ml of Milli-Q® water in separate volumetric flasks each containing a magnetic stirrer. Both solutions were placed on a magnetic stirrer and mixed continuously to ensure complete dissolution. Thereafter the NaOH solution was slowly added to the KH_2PO_4 solution. This mixture was stirred continuously with a magnetic stirrer and 700 ml of Milli-Q® water was added to make up to the volume of 2000 ml. The solution pH was adjusted to 7.4 either using orthophosphoric acid or NaOH.

C.2.3 HPLC analysis of clofazimine, artemisone and decoquinate

The analytical HPLC method was developed by Prof Jan du Preez at the ATL of the NWU, Potchefstroom, for the combination analysis of CLF, ART and DQ. The HPLC (Agilent 1200 Series) was equipped with an Agilent 1200 pump and auto sampler injection mechanism, a diode array detector and ChemStation Rev. A.10.01 software for data analysis (Agilent Technologies, Palo, Alto, CA). The UV-detector was set at a wavelength of 210 nm and 238 nm in order for CLF, ART and DQ to be detected. The mobile phase consisted of acetonitrile (650 ml) and 0.05 M sodium octane sulfonate in HPLC water (600 ml), with a 20 µl as injection volume and flow rate of 1.0 ml/min. The runtime was set at 15.0 min and the retention time was approximately 6.3 min for CLF, 7.3 min for ART and 9.8 min for DQ. The solvent used for the HPLC method was absolute ethanol (99.7%). These analytical tests were performed in a laboratory with a controlled environment of 25 °C. Prior to the samples being tested, the mobile phase was filtered through a 0.45 µm PVDF (Agela Technologies, Newark, DE) and degassed.

C.2.4 Standard sample preparation

Prior to skin diffusion studies, a standard sample solution was prepared by dissolving 7 mg of CLF, 44 mg of ART and 12 mg of DQ in absolute ethanol (99.7%) and then injecting it in the HPLC in duplicate at different injection volumes (2.5, 5.0, 7.5, 10.0 and 20.0 µl) to obtain a regression curve.

C.2.5 Solubility and octanol-buffer distribution coefficient determination for clofazimine, artemisone and decoquinate

C.2.5.1 Solubility

All three compounds needed to be dissolved simultaneously, since CLF, ART and DQ were formulated separately and in combination in the different nano-emulsions. Given that CLF and DQ are poorly soluble in water, it was decided to use a variety of solvents during the solubility study. The solvents used were water, acetonitrile, ethanol, isopropanol, tris (hydroxymethyl) aminomethane (TRIS), methanol, PBS, tetrahydrofuran (THF) and acetone. The following method was used to determine the solubility of each API separately.

A water bath was pre-heated to 32 °C (temperature on the skin surface during a diffusion study). The selected API together with a magnetic stirrer bar was added to a test tube; where after 5 ml solvent was transferred into the test tube. An excess of the API was added to the test tube in order for the solution to achieve saturation. Care was taken to check and ensure that saturation is maintained in the solution for the duration of mixing over a period of 24 h. After 24 h the test tube was removed from the water bath and the solution filtered through a 0.45 µm membrane filter and diluted with ethanol (if needed to prevent precipitation) and thereafter transferred to an HPLC vial for subsequent HPLC analysis. This experiment was repeated in triplicate for each API.

C.2.5.2 Octanol-buffer distribution coefficient (log D)

Equal volumes of *n*-octanol and PBS (pH 7.4) (100 ml) were equilibrated with each other for 24 h in order for the two phases to co-saturate. The pre-saturated PBS phase (3 ml) was used as solvent for the API (CLF, ART and DQ, separately). To each of these solutions an equal volume of pre-saturated *n*-octanol (3 ml) was added. Solutions was placed in the shaker water bath for 3 h at 32 °C and left overnight. Thereafter the solutions were centrifuged to ensure complete precipitation. The concentrations of the APIs in the separated phases were determined by means of HPLC. The log D was calculated as the ratio of API concentration in the *n*-octanol phase to the buffer phase (n=4).

C.2.6 Diffusion experiments

C.2.6.1 Membrane release studies

Franz cell release studies are conducted to determine if the APIs are released from the nano-emulsion. The vertical Franz cell consisted of two components, namely the receptor (capacity of approximately 2 ml) and the donor (1 ml) phase, with a magnetic stirring rod placed into the

receptor compartment. Vacuum grease was placed on both the receptor and donor phase to ensure no leaking occurred. PVDF, a synthetic membrane filter (FP Vericel, 0.45 µm, 25 mm, Pall®) was placed on the lower half of the Franz cell. The phases were placed together and secured with a horseshoe clamp. The receptor phase was filled with PBS (pH 7.4) (Fig. C.1) and the donor compartment with the nano-emulsion (**S1**, **S2**, **S3**, **S4**, **S5**, **O1**, **O2**, **O3**, **O4** and **O5**) with a pH of 5 (n = 9). The magnetic stirring rod ensured continuous stirring, whilst diffusion took place. The donor compartment was covered with Parafilm® to avoid any loss of the components. The water bath, in which the diffusion was performed, was maintained at a temperature of 37 °C. Every 6 h the receptor compartment was extracted with a syringe and refilled with PBS (pH 7.4) at 37 °C. By means of HPLC, all the samples were analysed and the concentration of the API that penetrated through the membrane within the receiver fluid and the release rate were determined for all the nano-emulsions.

C.2.6.2 Skin preparation

Caucasian, full-thickness abdominal skin (ethical approval reference number: NWU-00114-11-A5) was collected from plastic surgeons following abdominoplasty surgery. The skin was kept in a freezer at -20 °C for no more than 24 h to ensure easy separation from the fatty layer. Prior to diffusion studies, the skin was defrosted and placed on a paper towel (with the stratum corneum facing upwards), thereafter it was dermatomed using a dermatome™ (Zimmer TDS, United Kingdom) (Fig C.4). By pressing the dermatome (30 - 45°angle) onto the skin with constant pressure, skin samples of approximately 400 µm thickness were cut. Dermatomed skin was cut into circles (± 15 mm in diameter) and placed on Whatman® filter paper to dry, after which they were wrapped in aluminium foil and stored in the freezer at - 20°C. Prior to diffusion studies, the frozen skin samples were thawed, visually examined for defects and mounted onto the diffusion apparatus.

C.2.6.3 *In vitro* skin permeation studies

Franz cell diffusion studies were conducted to determine whether the APIs were delivered transdermally (Wiechers *et al*., 2008:24). Dermatomed skin was positioned on the outer half, i.e. on the receptor compartment of each of the nine Franz diffusion cells (diffusion area of 1.075 cm^2), with the stratum corneum facing upwards to the donor compartment. Seven of the nine Franz cells contained the nano-emulsion with API(s) and two contained the placebo (nano-emulsion without the API). Due to light sensitivity of CLF, amber cells were used to avoid any degradation. The receptor compartment was filled with 2 ml PBS (pH 7.4) and a temperature of 37 °C was maintained. The nano-emulsions, containing the selected APIs, were added to each donor compartment (1 ml). The entire receptor volume was withdrawn after 12 h. Samples were

analysed by means of HPLC to determine the API concentration that permeated through the skin into the receiver fluid (Baert *et al.,* 2011:472, 473).

C.2.6.4 Tape-stripping

The tape-stripping technique was used to determine the API concentration present in the stratum corneum-epidermis (SCE) and epidermis-dermis (ED), after completion of the 12 h diffusion studies. The Franz cells were dismantled and the skin pinned to a solid surface covered with Parafilm®. Any remaining nano-emulsion on the skin was carefully dabbed dry with paper towel (Walter & Brain, 2008:38). 3M Scotch® Crazy™ tape was cut into the same size as the diffusion area. The first tape strip per skin sample was disposed of, due to possible contamination with the nano-emulsion still remaining on the skin. Thereafter, the following 15 tape strips per skin sample were used to remove the SCE until the skin glistened. All tape strips collected from each sample were transferred into a polytop filled with 5 ml of absolute ethanol (chosen based on API solubility) (n = 9). After the tape-stripping procedure, the remaining ED was cut into smaller pieces and placed into another polytop, also containing 5 ml of absolute ethanol. These solutions, containing the tape strips and skin cuttings were stored in a fridge overnight at 4 °C, in order for the API to dissolve in the extraction fluid (Pellet *et al*., 1997:94). The API in the SCE and ED samples were filtered and analysed by means of HPLC.

C.2.7 Data analysis

Each individual Franz cell, together with its mean amount (concentration) of CLF, ART and DQ per area, respectively, which permeated the skin after 12 h was plotted for each nano-emulsion after tape-stripping. A percentage of the applied amount was expressed by using the yield of each cell, where the percentage diffused was also determined after 12 h for diffusion studies.

C.2.8 Statistical analysis

The calculation of the median (middle score in distribution) and mean (with standard deviation (SD)) of the concentration values (diffusion studies) are procedures ascribed to descriptive analysis (Sheskin, 2000:1, 4). The median values and box-plots were used to illustrate data by using first and third quartiles of distribution (Dawson and Trapp, 2004:38). The middle of the data (50%) was represented by the height of the box-plots and the vertical straight lines (whiskers), which extended 1.5 times, ranged above the 25th, and below 75th percentiles were drawn with the bottom as first quartile and top as third quartile. Circles are an illustration of values above or below the whiskers (outliers) (Dawson and Trapp, 2004:39).

By using the analysis of variance (ANOVA), p-values were determined and a p-value of 0.05 or less indicated a statistical significant effect (Steyn *et al.,* 1994:604-606). The tape-stripping and mean concentration were compared by applying a three-way ANOVA, where the different

concentration of the APIs in nano-emulsions were compared within the combination nano-emulsions (safflower combination and olive oil combination). By means of Statistica (Statsoft, 2008) and SAS (SAS Institute Inc., 2005), the above statistical analyses were performed. The median is a more exact method to determine flux or concentration and is used when there is a significant variation between the mean and median values (Dawson and Trapp, 2004:30). The median is used throughout the study to describe the data, although both mean and median values will be depicted.

C.3 Results and discussion

C.3.1 Formulation of natural oil nano-emulsions

Eight natural oil nano-emulsions were prepared containing 1% CLF, ART and DQ as API, respectively, and consisted of four nano-emulsions containing safflower oil with the APIs CLF, ART and DQ, separately and in combination, and four nano-emulsions containing olive oil with the APIs CLF, ART and DQ, separately and in combination.

C.3.2 Physicochemical properties

C.3.2.1 Solubility

Table C.1: Average solubility (mg/ml) results of CLF, ART and DQ in different solvents

Solvent	Clofazimine	Artemisone	Decoquinate
Acetone	2.18 ± 0.02	105.92 ± 6.52	0.02 ± 0.00
Acetonitrile	1.21 ± 0.06	201.96 ± 2.97	0.01 ± 0.00
Ethanol	1.83 ± 0.02	44.60 ± 1.51	0.18 ± 0.00
Isopropanol	1.02 ± 0.04	26.35 ± 0.75	0.16 ± 0.02
Methanol	0.83 ± 0.01	46.54 ± 0.33	0.16 ± 0.00
THF	143.41 ± 0.06	194.19 ± 0.05	0.24 ± 0.03
TRIS (pH 7.4)	0.00 ± 0.00	0.10 ± 0.00	0.00 ± 0.00
PBS (pH 7.4)	0.00 ± 0.00	0.09 ± 0.00	0.00 ± 0.01
Water	0.00 ± 0.00	0.10 ± 0.00	0.00 ± 0.00

The aqueous solubility in water of CLF, ART and DQ was determined as 0.000 mg/ml, 0.100 mg/ml and 0.000 mg/ml, respectively at a temperature of 32 °C. An aqueous solubility of more than 1 mg/ml is required for a molecule to ideally permeate through the skin (Naik *et al.,* 2000:319). Taking the aforementioned into account, CLF and DQ are expected to permeate poorly through the skin or not at all, whereas ART would be expected to penetrate the skin.

In Table C.1, it was evident that DQ was the least soluble in the different solvents and therefore the determining factor for simultaneous dissolution. All the APIs had very poor solubility in water, TRIS (pH 7.4) and PBS (pH 7.4). Consequently, it is proposed that the APIs would not permeate

the skin and therefore both lipophilic (to permeate the stratum corneum) and hydrophilic (epidermal and dermal layer which thereafter leads to blood capillaries) characteristics are important to permeate into and through the skin (Perrie *et al*., 2012:392).

C.3.2.2 Log D

The log D values were obtained from the literature. The log D values of CLF, ART and DQ are 7.60 (US Pharmacopeia online, 2015), 2.49 (Dunay *et al*., 2009:4451) and 7.80 (Chembase, 2014), respectively. The ideal log P value for skin permeation is considered to be between 1 and 3 (Mbah *et al*., 2011:681), therefore only ART depicts a favourable value for possible transdermal drug delivery.

C.3.3 Diffusion experiments

C.3.3.1 Membrane release studies

No results were obtained during the membrane release studies; no API (CLF, ART and DQ) permeated through the membrane into the receptor phase. This could be due to CLF's, ART's and DQ's low aqueous solubility, which means they cannot permeate into the receptor fluid (PBS pH 7.4), or because of CLF's and DQ's high log D value, which indicates it is very lipophilic and cannot permeate across the membrane to the aqueous region (the receptor fluid).

C.3.3.2 Transdermal studies

Prior to diffusion studies, a pilot study was conducted to determine whether extraction should be every 2 h up to 12 h, as per the usual standard operating procedure. After HPLC analysis of the pilot study results, no data was obtained from the receptor phases and it was decided to do a single extraction after 12 h. After the 12 h diffusion studies, samples were analysed by means of HPLC. No API could be detected in the receptor phase for the eight nano-emulsions, which could be explained by non-ideal physicochemical properties of the three APIs, or by the delivery system used. Physicochemical properties, such as aqueous solubility (0.000 mg/l, 0.100 mg/ml and 0.000 mg/l), for CLF, ART and DQ indicated that no aforementioned API would be favourable for transdermal delivery and the log D (7.60, 2.49 and 7.80) indicated only ART might be favourable for transdermal delivery.

C.3.3.3 Tape-stripping results

Mean and median concentrations of CLF, ART and DQ in the SCE and ED are shown in Table C.2. The median concentrations of the SCE and ED are graphically represented in the box-plots in Figures C.5 to C.12 for the eight different nano-emulsions.

Table C.2: Mean and median values of nano-emulsions **S1** – **S4** and **O1** – **O4**

Nano-emulsions	Mean concentration in SCE (µg/ml)	Median concentration in SCE (µg/ml)	Mean concentration in ED (µg/ml)	Median concentration in ED (µg/ml)
S1	2.44 ± 0.10	2.42	3.90 ± 0.13	3.91
S2	19.92 ± 1.58	20.06	0.00 ± 0.00	0.00
S3	15.00 ± 1.06	14.74	9.91 ± 1.49	9.66
S4: CLF	4.04 ± 0.21	4.11	2.79 ± 0.29	2.81
ART	27.46 ± 1.70	27.76	0.00 ± 0.00	0.00
DQ	0.00 ± 0.00	0.00	8.56 ± 0.81	8.36
O1	4.29 ± 0.21	4.30	4.63 ± 0.27	4.55
O2	13.43 ± 1.10	13.36	0.00 ± 0.00	0.00
O3	4.25 ± 0.32	4.22	6.20 ± 0.78	6.24
O4: CLF	9.38 ± 0.36	9.43	1.80 ± 0.35	1.68
ART	19.86 ± 1.24	19.83	0.00 ± 0.00	0.00
DQ	0.00 ± 0.000	0.00	3.99 ± 0.348	3.99

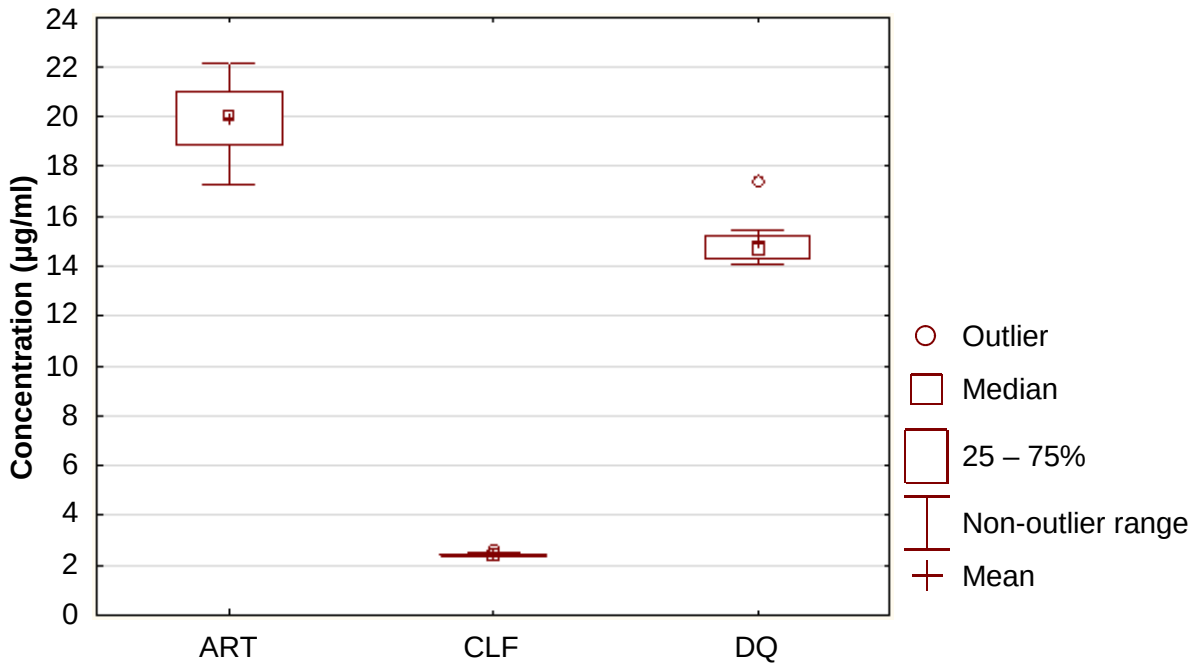

Figure C.5: Box-plot indicating the concentration (µg/ml) of **S1** (CLF), **S2** (ART) and **S3** (DQ) present in the SCE after tape-stripping (n=7). Concentration values are indicated by the lines and squares, respectively.

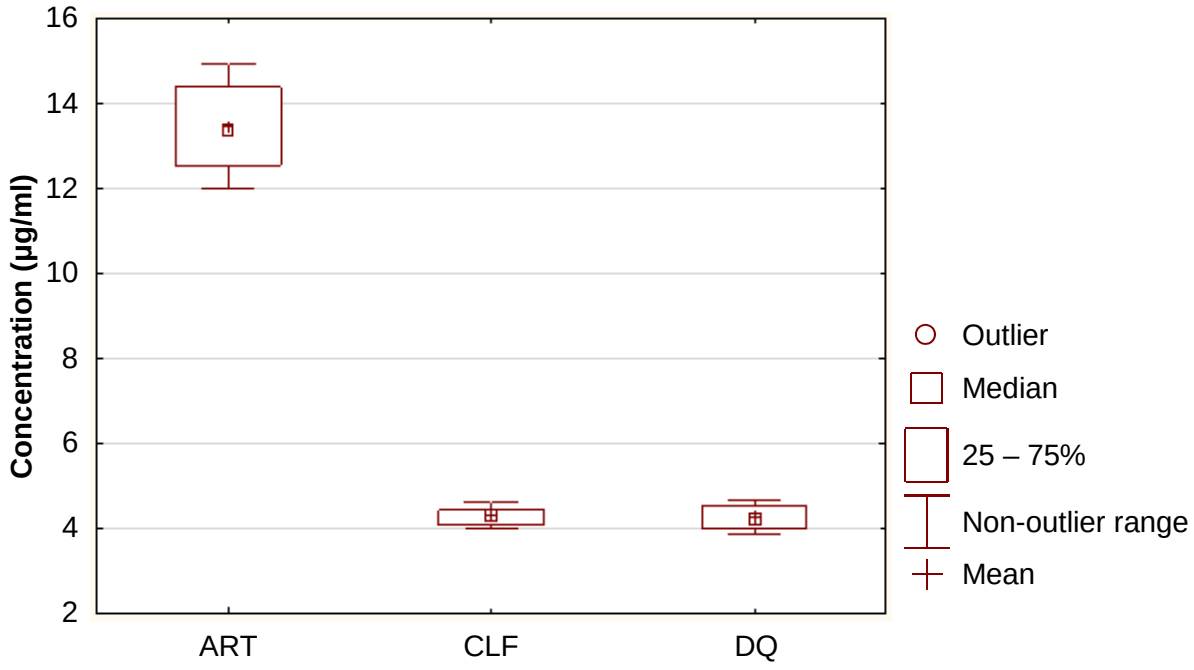

Figure C.6: Box-plot indicating the concentration (µg/ml) **O1** (CLF), **O2** (ART) and **O3** (DQ) present in the SCE after tape-stripping (n=7). Concentration values are indicated by the lines and squares, respectively.

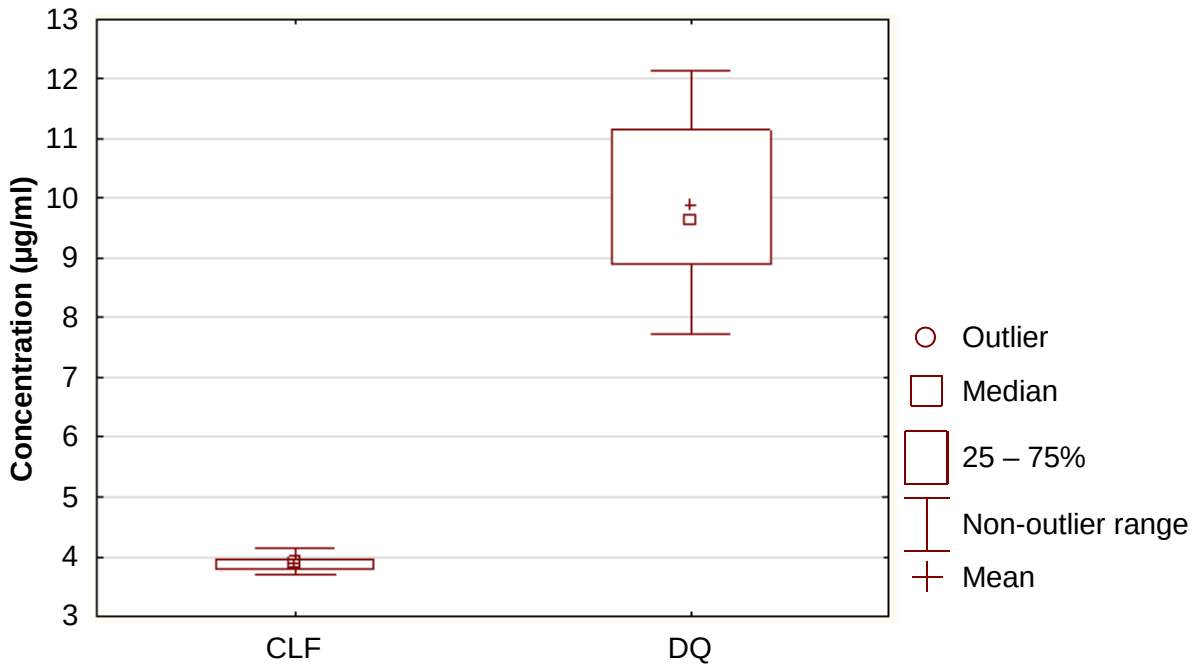

Figure C.7: Box-plot indicating the concentration (µg/ml) **S1** (CLF) and **S3** (DQ) present in the ED after tape-stripping (n=7). Concentration values are indicated by the lines and squares, respectively.

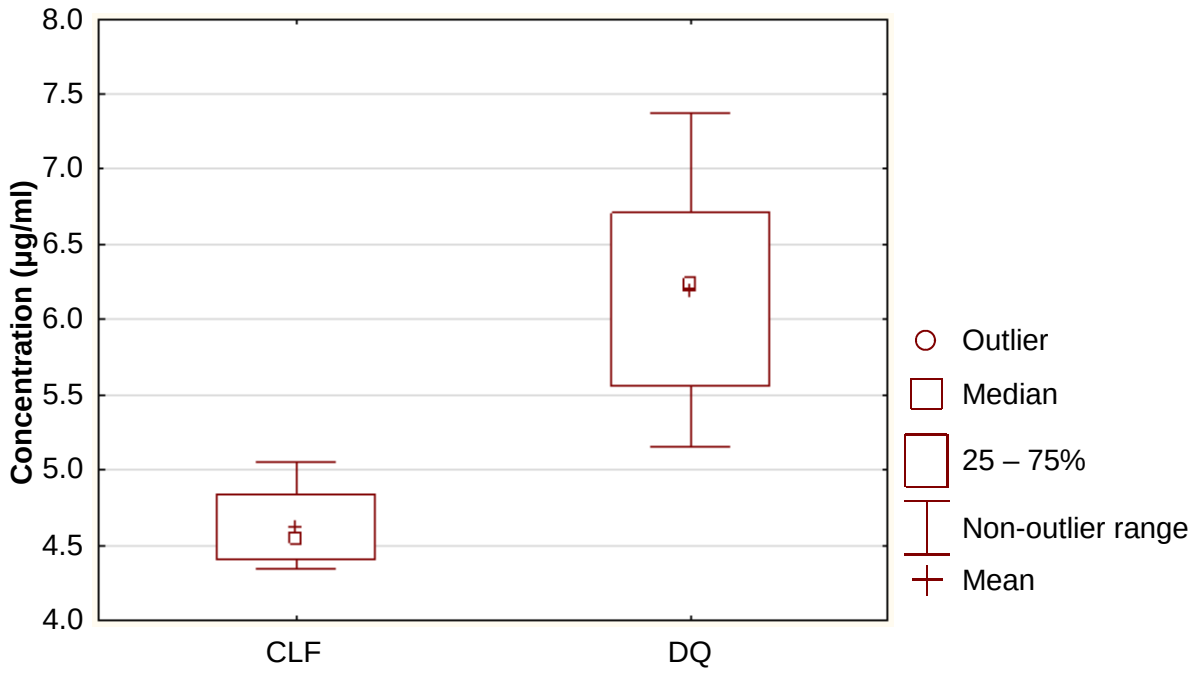

Figure C.8: Box-plot indicating the concentration (µg/ml) **O1** (CLF) and **O3** (DQ) present in the ED after tape-stripping (n=7). Concentration values are indicated by the lines and squares, respectively.

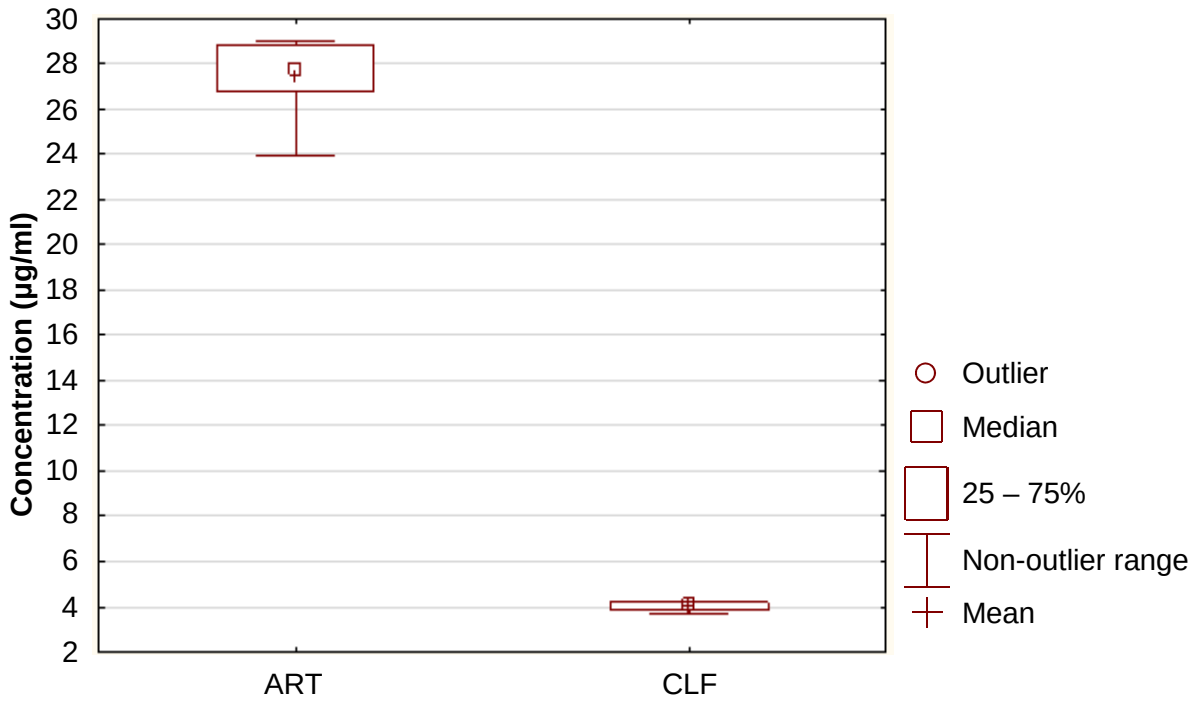

Figure C.9: Box-plot indicating the concentration (µg/ml) CLF, ART and DQ present in **S4** in the SCE after tape-stripping (n=7). Concentration values are indicated by the lines and squares, respectively.

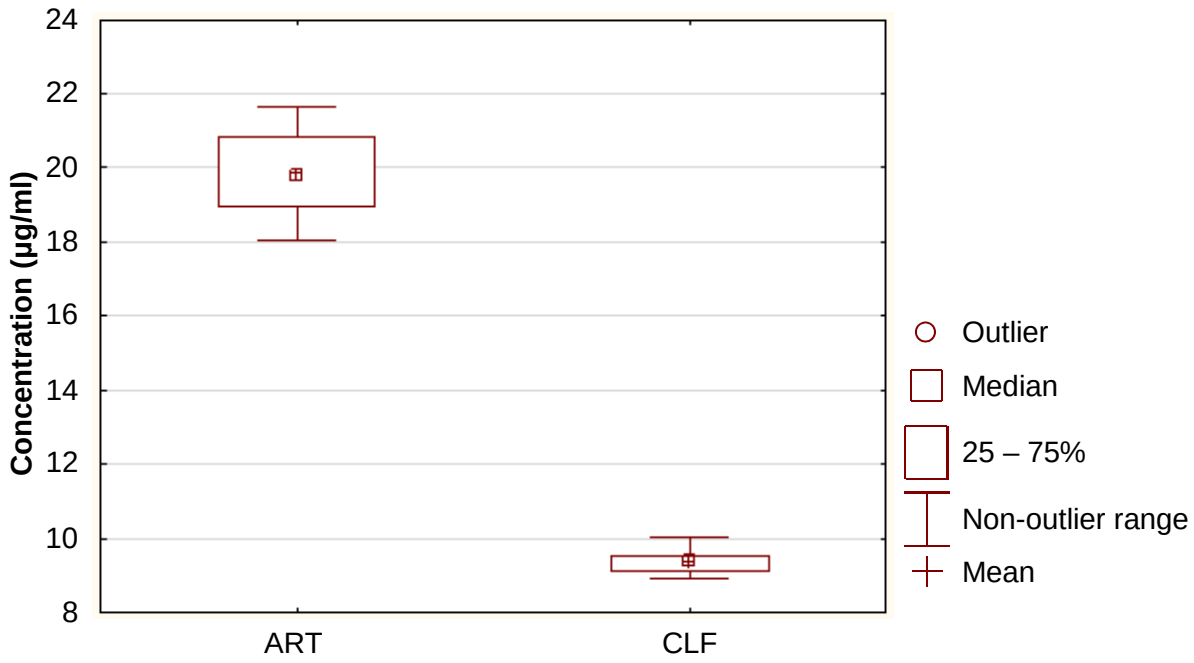

Figure C.10: Box-plot indicating the concentration (µg/ml) CLF, ART and DQ present in **O4** in the SCE after tape-stripping (n=7). Concentration values are indicated by the lines and squares, respectively.

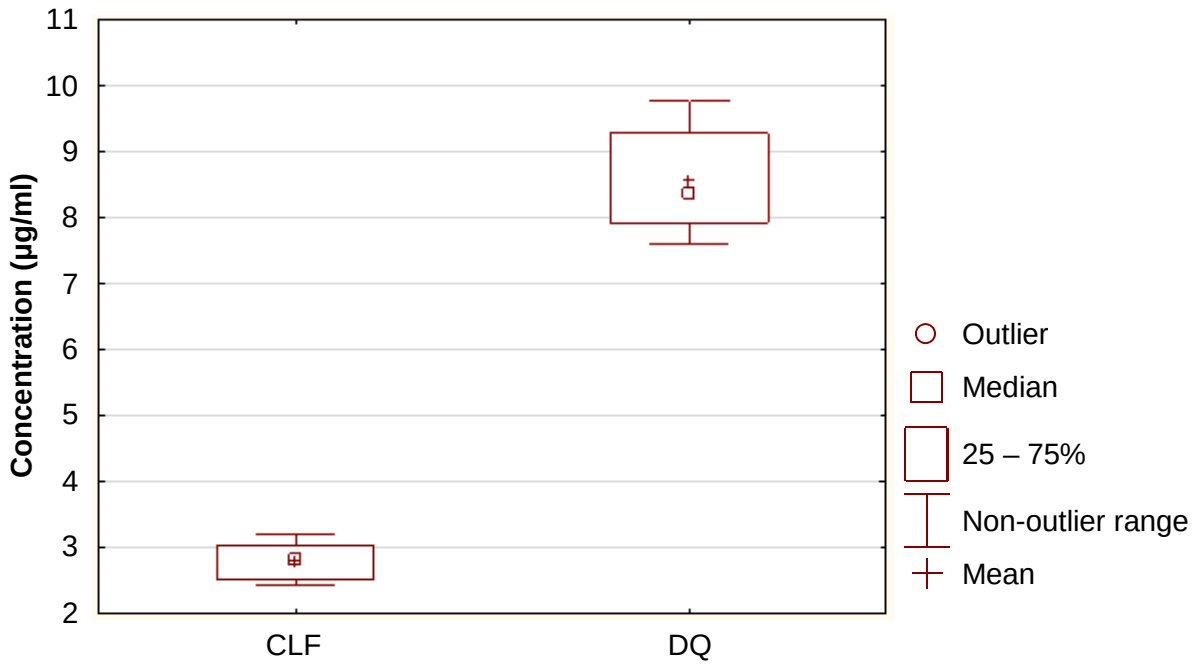

Figure C.11: Box-plot indicating the concentration (µg/ml) CLF, ART and DQ present in **S4** in the ED after tape-stripping (n=7). Concentration values are indicated by the lines and squares, respectively.

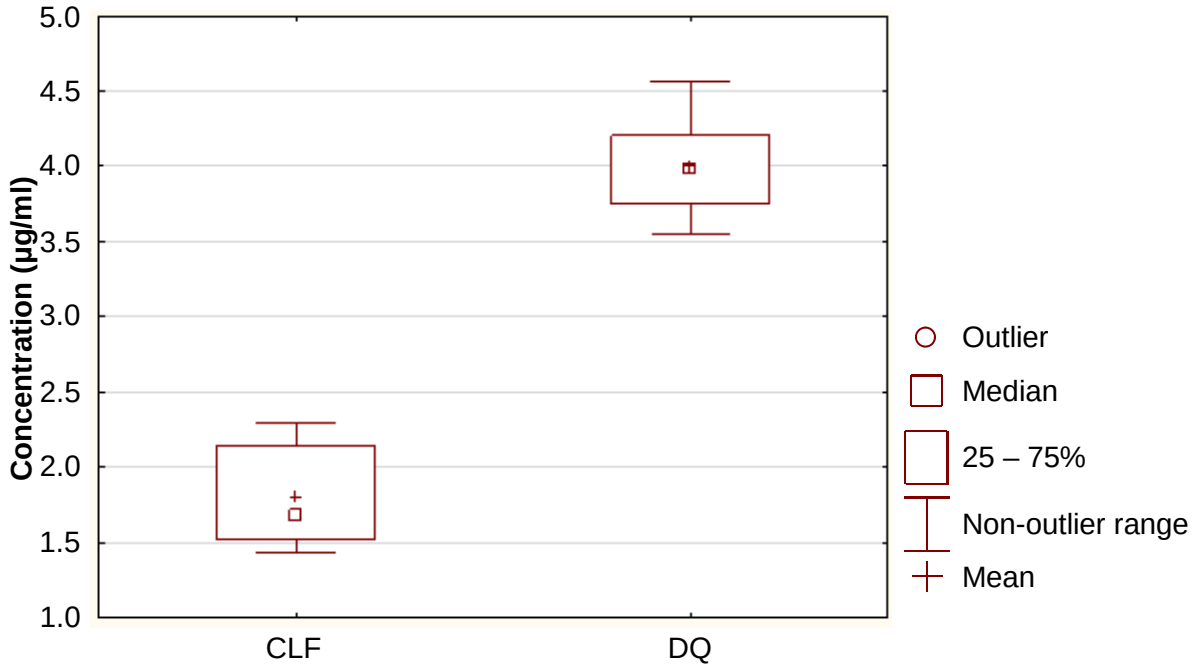

Figure C.12: Box-plot indicating the concentration (µg/ml) CLF, ART and DQ present in **O4** in the ED after tape-stripping (n=7). Concentration values are indicated by the lines and squares, respectively.

C.3.3.3.1 Stratum corneum-epidermis concentration

When the median concentrations of **S1**, **S2** and **S3** are compared, it is observed that **S2** yielded the highest (20.06 µg/ml) median concentration, followed by **S3** (14.74 µg/ml) and lastly, **S1** (2.42 µg/ml). While comparing **O1**, **O2** and **O3**, **O2** (13.36 µg/ml) depicted the highest median concentration, followed by **O1** (4.30 µg/ml) and lastly, **O3** (4.22 µg/ml); it should be mentioned that the median concentration of **O1** and **O3** did not differ greatly. With **S4** it was seen that ART, when compared to CLF and DQ, had the highest median concentration (27.76 µg/ml), followed by CLF (4.11 µg/ml). When **O4** was investigated, it was observed that ART (19.83 µg/ml) had the highest median concentration followed by CLF (9.43 µg/ml). Neither **S4** nor **O4** delivered DQ (0.00 µg/ml) in the SCE.

In Table D.1, it is noticeable that all the nano-emulsions containing the APIs separately (**S1**, **S2**, **S3**, **O1**, **O2** and **O3**) accumulated in the SCE, but the nano-emulsions that contained the safflower oil (**S1**, **S2** and **S3**) improved the permeation of the APIs more than those containing the olive oil (**O1**, **O2** and **O3**), except for CLF (**O1** was higher than **S1**). When comparing the nano-emulsions containing the APIs separately (**S1**, **S2**, **S3**, **O1**, **O2** and **O3**), with regard to the API, it is evident that ART permeated the SCE more than CLF and DQ. When **S4** and **O4** are compared, the same phenomenon as with the nano-emulsions containing the APIs separately (**S1**, **S2**, **S3**, **O1**, **O2** and **O3**) are noticed, where ART permeated the SCE more than CLF and DQ (although DQ did not accumulate in the SCE for both **S4** and **O4**). With **S4** and **O4**, it is not possible to conclude which oil improved delivery, since **S4** delivered ART more than **O4**, while **O4** delivered CLF more than **S4;** the same trend was noticed with the nano-emulsions containing the APIs separately (**S1**, **S2**, **S3**, **O1**, **O2** and **O3**), where the olive oil increased the delivery of CLF more than the safflower oil). In general, when the oils were compared, it was observed that safflower oil increased the delivery of ART and DQ, while olive oil increased the delivery of CLF.

C.3.3.3.2 Epidermis-dermis concentration

When the median concentrations of **S1**, **S2** and **S3** are compared, it is seen that **S3** yielded the highest (9.658 µg/ml) median concentration, followed by **S1** (3.914 µg/ml). On comparing **O1**, **O2** and **O3**, it is observed that **O3** (6.243 µg/ml) depicted the highest median concentration, followed by **O1** (2.812 µg/ml). Neither **S2** nor **O2** delivered ART (0.000 µg/ml) in the ED. When **S4** was examined, it was noticed that DQ, when compared to CLF and ART, had the highest median concentration (8.360 µg/ml), followed by CLF (2.812 µg/ml). While investigating **O4**, it was noticeable that DQ (3.986 µg/ml) had the highest median concentration followed by CLF (1.679 µg/ml). Neither **S4** nor **O4** delivered ART (0.000 µg/ml) in the ED.

In Table C.1, it is evident that the nano-emulsions containing the APIs separately (**S1**, **S3**, **O1**, and **O3**) accumulated in the ED (except for **S2** and **O2**). With the nano-emulsions containing the APIs separately (**S1**, **S3**, **O1**, and **O3**), it is not possible to conclude which oil improved the delivery; since **S3** improved the permeation of the DQ more than **O3**, while **O1** improved the permeation of the CLF more than **S1**. When comparing the nano-emulsions containing the APIs separately (**S1**, **S2**, **S3**, **O1**, **O2** and **O3**), with regard to the API, it was evident that DQ permeated the ED more than CLF and ART. This could possible by ascribed to DQ using other penetration routes other than direct skin permeation, i.e. the annexial route (Williams, 2003:10). The annexial route (sebaceous glands) is located within the hair follicles and secrete sebum, which is a mixture of waxes, triglycerides, fatty acids, cholesterol and cellular debris and consequently, highly lipophilic drugs cross this route due to the lipophilic nature (Montage, 1965:56; Williams, 2003:10). When **S4** and **O4** are compared, the same trend as with the nano-emulsions containing the APIs separately (**S1**, **S2**, **S3**, **O1**, **O2** and **O3**) was noticed, where DQ permeated the ED more than CLF (ART did not accumulate in the ED for any of the nano-emulsions). With **S4** and **O4**, it is observed that safflower oil improved the permeation of the APIs more than the olive oil for both DQ and CLF. The nano-emulsions containing the safflower oil (**S3** and **S4**) permeated better than the nano-emulsions containing the olive oil (**O3** and **O4**). This might be explained by the amount of linoleic acid present in safflower (75.0%) and olive oil (1.5%). Since the stratum corneum also comprises linoleic acid, the increased presence of linoleic acid found in the safflower oil compared to that in olive oil, may cause the safflower oil to increase the delivery of the APIs into the stratum corneum (Applewhite, 1966; Olive oil Source, 2017; Vermaak *et al.*, 2011:920-933). Therefore, since more API is delivered through the first layer of the skin (SCE), more API is available to permeate from the SCE to the ED (Cross & Roberts, 1993:607).

C.3.4 Statistical analysis

Table C.3 consists of the different nano-emulsion combinations used as well as their p-values.

Table C.3: P-values obtained from the three-way ANOVA of all the nano-emulsions

Combinations	p-value
SCE and ED	0.0000
Oils: safflower and olive	0.0531
Interaction: Oils and SCE	0.0035
Interaction: APIs (CLF, ART and DQ) and SCE	0.0000
Interaction: Oils and ED	0.0001
Interaction: APIs (CLF, ART and DQ) and ED	0.0000
Interaction: ART and SCE	0.0000
Interaction: CLF and SCE	0.0000
Interaction: DQ and SCE	0.0000
Interaction: CLF and ED	0.0000
Interaction: DQ and ED	0.0000
Interaction: **O4** and SCE	0.0000
Interaction: Olive oil and SCE	0.0000
Interaction: **S4** and SCE	0.0000
Interaction: Safflower and SCE	0.0000
Interaction: **O4** and ED	0.0000
Interaction: Olive oil and ED	0.0001
Interaction: **S4** and ED	0.0000
Interaction: Safflower oil and ED	0.0000

There is no statistical significance between the two natural oils (safflower and olive oil) ($p = 0.0531$), whereas for all the other combinations everything was statistically significant ($p < 0.05$).

C.4 Conclusion

The aqueous solubility of CLF, ART and DQ (0.000 mg/ml, 0.100 mg/ml and 0.000 mg/ml) indicated that CLF and DQ would either permeate very poorly through the skin or not at all. It is evident from the log D values for CLF (7.60), ART (2.49) and DQ (7.80) that only ART had favourable properties to permeate the skin, whereas CLF and DQ would not be ideal (Naik *et al.,* 2000:319).

After the membrane release studies were conducted, it was evident that no API (CLF, ART or DQ) permeated through the membrane into the receptor phase. Following the membrane studies, diffusion studies were executed. No API was found within the receptor phase during the diffusion studies.

During the pre-formulation studies, it was observed that ART had a higher affinity for both the safflower and olive oil when compared to CLF and DQ, even though ART is classified as polar (Haynes *et al*., 2006:2084). During tape-stripping studies, it was observed that the concentration of ART was higher in the SCE than for CLF and DQ. This could possibly be attributed to the high affinity that ART had for the oil, together with the high affinity the lipophilic oil has with the lipophilic stratum corneum, which may in turn have led to a higher entrapment of ART in the SCE. Consequently, even though ART is more polar in nature, its affinity for the oil phase was higher than its affinity for the hydrophilic ED and therefore ART remained within the SCE rather than permeating to the ED.

When **S4** and **O**4 were investigated, it was noticeable that DQ only appeared in the ED and not in the SCE, which could be attributed to the "saturation effect" in the stratum corneum, as described by Teichmann *et al.* (2005:80). Teichmann *et al.* (2005:80) concluded that the stratum corneum can be saturated and even with prolonged application, no increase in concentration will be observed. Therefore, since three APIs were entrapped within the nano-emulsions, saturation with ART and CLF may have occurred in the SCE before DQ could reach the stratum corneum and therefore DQ may have followed another route of penetration, such as the annexial route (permeating directly to the dermis) (Teichmann *et al*., 2005:80). Since the ART has more ideal physicochemical properties compared to CLF and DQ, it could suggest that ART permeated the SCE first followed by CLF, hence, no DQ was found in the SCE, while ART and CLF followed the intracellular route (permeating into the stratum corneum) (N`Da, 2010:20784). Since the concentration gradient plays a very important role, CLF that was entrapped within the SCE diffused to the ED. Therefore, as CLF permeates from the SCE to the ED, the nano-emulsion still applied on top of the skin supplies the subsequent layers with CLF, hence CLF was found in both SCE and ED.

The following conclusions can be made about the study:

- When the three APIs are compared, with regard to delivery, in the SCE and the ED, ART and DQ had the highest concentration in the SCE and ED, respectively.
- ART might have accumulated within the SCE, since it had a higher affinity for the oil phase than CLF and DQ.
- DQ may have penetrated through other routes to the ED.
- When nano-emulsions containing the APIs separately are examined, it is possible to deliver CLF, ART and DQ into the SCE and CLF and DQ into the ED. ART cannot be delivered in the ED from the nano-emulsions containing the APIs separately.

- When nano-emulsions containing the APIs in combination (all three APIs together in one dispersion) are investigated, it is not possible to deliver all three APIs in the SCE or in the ED. When APIs are combined in a nano-emulsion, DQ cannot be delivered in the SCE, while ART cannot be delivered in the ED.
- Both the **S4** and **O4** performed well regarding the penetration of the SCE (top layer), i.e. ART in **S4** permeated better than ART in **O4**, while CLF in **O4** permeated better than CLF in **S4**.
- When **S4** and **O4** are compared, with regard to the penetration of the ED, both CLF and DQ permeated the ED better from **S4** than from **O4**.
- In general, the nano-emulsions containing the safflower oil increased the delivery of the APIs more than the nano-emulsions containing the olive oil. The improved permeation from the nano-emulsions containing safflower oil, could be ascribed to the increased amount of linoleic acid (75.0%) found in the safflower oil (Applewhite, 1966) compared to the amount of linoleic acid (1.5%) obtained in olive oil (Olive oil Source, 2017), since the skin (stratum corneum) also comprises of linoleic acid (Vermaak *et al.*, 2011:920-933).

References

Anon. The Olive Oil Source. 2017. https://www.oliveoilsource.com/page/chemical-characteristics Date of access: 8 Aug 2017.

Applewhite, T.H. 1966. The composition of Safflower Seed. *Journal of the American Oil Chemists Society*, 43:406.

Baek J.S., Lim, J.H., Kang, J.S., Shin, S.C., Jung, S.H. & Cho, C.W. 2013. Enhanced transdermal drug delivery of zaltoprofen using a novel formulation. *International Journal of Pharmaceutics*, 453(2):358-362.

Baert, B., Vansteelandt, S. & De Spiegeleer, B. 2011. Ion mobility spectrometry as a high-throughput technique for *in vitro* transdermal Franz diffusion cell experiments of ibuprofen. *Journal of Pharmaceutical and Biomedical Analysis*, 55:472, 473.

Chembase. 2014. Decoquinate. http://en.chembase.cn/molecule-157442.html Date of access: 5 Aug 2015.

Chime, S.A., Kenechukwu, F.C. & Attama, A.A. 2014. Nanoemulsions – Advances in Formulation, Characterization and Applications in Drug Delivery, Application of Nanotechnology in Drug Delivery, http://www.intechopen.com/books/application-of-nanotechnology-in-drug-delivery/nanoemulsions-advances-in-formulation-characterization-and-applications-in-drug-delivery Date of access: 1 Mar 2015.

Cleary, G.W. 1993. Transdermal delivery systems; a medical rationale. (*In* Shah, V.P. & Maibach, H.I., *eds.* Topical drug bioavailability, bioequivalence and penetration. Plenum Press. p. 17-68.)

Cross, S.E. & Roberts, M.S. 1993. Subcutaneous absorption kinetics of interferon and other solutes. *Journal of Pharmaceutics and Pharmacolology,* 45:606-609.

Dawson, B. & Trapp, R.G. 2004. Basic & clinical biostatistics. 4th ed. New York: McGraw-Hill. p. 30, 38-39.

Delgado-Charro, M.B. & Guy, R.H. 2014. Effective use of transdermal drug delivery in children. *Advanced Drug Delivery Reviews*, 73:63-82.

Dingler, A. & Gohla, S. 2002. Production of solid lipid nanoparticles (SLN): scaling up feasibilities. *Microencapsulation*, 19:11-16.

Dos Anjos, J.L.V. & Alonso, A. 2008. Terpenes increase the partitioning and molecular dynamics of an amphipathic spin label in stratum corneum membranes. *International Journal of Pharmaceutics*, 350:103-112.

Drakulić, J.B., Juranic, I.O., Eric, S. & Zloh, M. 2008. Role of complexes formation between drugs and penetration enhancers in transdermal delivery. *International Journal of Pharmaceutics*, 363:40-99.

Dunay, I.R., Chi Chan, W., Haynes, R.K. & Sibley, L.D. 2009. Artemisone and artemiside control acute and reactivated toxoplasmosis in a murine model. *Journal of Antimicrobial Agents and Chemotherapy,* 53(10):4450-4456.

Finnin, B.C. & Morgan, T.M. 1999. Transdermal penetration enhancers: Applications, limitations and potential. *Journal of Pharmaceutical Sciences,* 88(10):955.

Foldvari, M. 2000. Non-invasive administration of drugs through the skin: Challenges in delivery system design. *Pharmaceutical Science and Technology Today,* 3:417,418.

Guy, R.H. 2010. Transdermal Drug Delivery. (*In* Schäfer-Korting, M., *eds.* Drug Delivery. Handbook of Experimental Pharmacology. Vol. 197. Berlin, Heidelberg: Springer. p 399-410.)

Haynes, R.K., Fugmann, B., Stetter, J., Rieckmann, K., Heilmann, H.D., Chan, H.W., Cheung, M.K., Lam, W.L., Wong, H.N., Croft, S.L., Vivas, L., Rattray, L., Stewart, L., Peters, W., Robinson, B.L., Edstein, M.D., Kotecka, B., Kyle, D.E., Beckermann, B., Gerisch, M., Radtke, M., Schmuck, G., Steinke, W., Wollborn, U., Schmeer, K. & Romer, A. 2006. Artemisone – a highly active antimalarial drug of the artemisinin class. *Angewandte Chemie,* 45:2082-2088.

Khafagy, E., Morishita, M., Onuki, Y. & Takayama, K. 2007. Current challenges in non-invasive insulin delivery systems: a comparative review. *Advanced Drug Delivery Reviews*, 59(15):1521-1546.

Lam, P.L. & Gambari, R. 2014. Advanced progress of microencapsulation technologies: *In vivo* and *in vitro* models for studying oral and transdermal drug deliveries. *Journal of Controlled Release*, 178:25-45.

Mbah, C.J., Uzor, P.F. & Omeje, E.O. 2011. Perspectives on Transdermal Drug Delivery. *Journal of Chemical and Pharmaceutical Research,* 3(3):680-700.

Montaga, W. 1965. The skin. *Scientific America,* 212:56-66.

Naik, A., Kalia, Y.N. & Guy, R.H. 2000. Transdermal drug delivery: overcoming the skin's barrier function. *Pharmaceutical Science and Technology Today,* 3(9):318-326.

N`Da, D. 2010. Prodrug strategies for enhancing percutaneous absorption of drugs. *Molecules*, 19:20780-20807.

Pellet, M.S., Roberts, M. & Hadgraft, J. 1997. Supersaturated solutions evaluated with an *in vitro* stratum corneum tape-stripping technique. *International Journal of Pharmaceutics*, 151(1):94.

Perrie, Y., Badhan, R.J.K., Kirby, D.J., Lowry, D., Mohammed, A.R. & Ouyang, D. 2012. The impact of ageing on the barriers to drug delivery. *Journal of Controlled Release,* 161:392-393.

Pharmacopeia online. 2014. http://www.uspbpep.com/usp29/v29240/usp29nf245O_m22310.html Date of access: 1 Mar 2015.

Prausnitz, M.R. & Langer, R. 2008. Transdermal drug delivery. *Nature Biotechnology*, 26:1261-1268.

Prow, T.W., Grice, J.E., Lin, L.L., Faye, R., Butler, M., Becker, W., Wurm, E.M., Yoong, C., Robertson, T.A., Soyer, H.P. & Roberts, M.S. 2011. Nanoparticles and microparticles for skin drug delivery. *Advanced Drug Delivery Reviews*; 63(6):470-491.

SAS Institute. 2005. SAS OnlineDoc, version 9.1. http://www.sas.com Date of access: 10 Nov. 2009.

Shakeel, F., Shafiq, S., Haq, N., Alanzi, F.K. & Alsarra, I.A. 2012. Nanoemulsions as potential vehicles for transdermal and dermal delivery of hydrophobic compounds: an overview. *Expert Opinion on Drug Delivery*, 9(8):953-974.

Sheskin, D.J. 2000. Handbook of parametric and nonparametric statistical procedures. 2nd ed. Boca Raton: Chapman & Hall/CRC. p 1, 4, 511, 534.

Statsoft. 2008. Statistica, version 8.0. http://www.statsoft.co.za Date of access: 10 Jul 2017.

Steyn, A.G.W., Smit, C.F., Du Toit, S.H.C. & Strasheim, C. 1994. Modern Statistics in Practice. Pretoria: J.L. van Schaik. 604-606p. Statsoft, 2008. Statistica, version 8.0. http://www.statsoft.co.za Date of access: 10 Sep 2016.

Tavano, L., Gentile, L., RossiI, C.O. & Muzzalupo, R. 2013. Novel gel-niosomes formulations as multicomponent systems for transdermal drug delivery. *Coloids and surfaces B: Biointerfaces,* 110:281-288.

Teichmann, A., Jacobi, U., Weigmann, H.J., Terry, W. & Lademann, J. 2005. Reservoir function of the stratum corneum: Development of an *in vivo* method to quantitively determine the stratum corneum reservoir for topically applied substances. *Skin Pharmacology and Physiology,* 18:75-80.

Thomas, B.J. & Finnin, B.C. 2004. The Transdermal Revolution. *Drug Discovery Today (England)*, 9(16):697-703.

Thong, H.Y., Zhai, H. & Maibach, H.I. 2007. Percutaneous penetration enhancers: an overview. *Skin Pharmacology and Physiology*, 20(6):272-282.

Vermaak, I., Kamatou, G.P.P., Komane-Mofokeng, B., Viljoen, A.M. & Beckett, K. 2011. African seed oils of commercial importance: cosmetic applications. *South African Journal of Botany*, 77:920-933.

Walters, K.A. & Brain, K.R. 2002. Dermatological formulation and transdermal systems. *(In* Swarbrick, J., *ed.* Dermatological and transdermal formulations. Vol. 119. New York: Marcel Dekker. p. 321, 322.)

Watkinson, A.C. 2013. A commentary on transdermal drug delivery systems in clinical trials. *Journal of Pharmaceutical Sciences*, 102:3082-3088.

Wiechers, J.W., Kelly, C.L., Blease, T.G. & Dederen, J.C. 2008. Formulating for efficacy. *International Journal of Cosmetic Science,* 26:173-175, 177.

Wiedersberg, S. & Guy, R.H. 2014. Transdermal drug delivery: 30+ years of war and still fighting! *Journal of Controlled Release*, 190:150-156.

Williams, A.C. 2003. Structure and function of human skin. (*In* Williams, A.C., *ed*. Transdermal and topical drug delivery: from theory to clinical practice. London: Pharmaceutical Press. p. 1-26.)

Williams, A.C. 2013. Topical and transdermal drug delivery. (*In* Aulton, M.E., *ed*. Aulton'spharmaceutics: the design and manufacture of medicines. 4th ed. London: Churchill Livingstone. p. 675-697.)

Williams, A.C. & Barry, B.W. 2012. Penetration enhancers. *Advanced Drug Delivery Reviews,* 64:129-135.

Appendix D:

Cytotoxicity studies of natural oil nano-emulsions containing clofazimine, artemisone and decoquinate

D.1 Introduction

Various approaches have been advanced to study cell proliferation and viability in cell cultures (Cook & Mitchell, 1989). Investigating the cytotoxicity profile, using *in vitro* skin models to determine whether the API entrapped within a formulation indicates any cytotoxic effect to human skin, for instance skin damage or irritation, is an important step in pre-clinical development of pioneering drug delivery systems (Fotakis & Timbrell, 2006:171).

The outer most layer of the skin (which serves as a gatekeeper for the human body and protects the human body from adverse effects of the environment) is comprised of keratinocytes. In order to counter risk and take safety measures, all chemicals which humans may be exposed to need to be tested. Henceforth, measuring the cell viability of cell-based *in vitro* models, after a certain exposure time, will provide concrete evaluation of a substance's toxic potential (accelerate GmbH, 2015) of which the proliferation, growth and viability of the cell is measured (ATCC, 2011:1). Consequently, using *in vitro* human epidermal cells in research investigations could clarify molecular and cellular processes in the keratinocytes affected (Udensi *et al*., 2011:183). It is of utmost importance to understand that cytotoxic studies only reflect what transpires *in vivo* within a system (Fotakis & Timbrell, 2006:171) and no direct correlation can be found between *in vitro* cytotoxicity results and potential *in vivo* results (Yoon *et al*., 2012:634). This could be explained by variances in conditions between *in vitro* and *in vivo*; when the *in vitro* method is used, only cellular level effects are reflected not pharmacodynamics, which is the most important process, such as distribution, excretion metabolism and absorption (Yoon *et al*., 2012:634). Consequently, cytotoxic effects only indicate possible toxic effects of either the API, the nano-emulsion, or API combined with the nano-emulsion on chosen cell lines.

The lactate dehydrogenase (LDH)-assay was employed during this study because it is a quick, reliable and simple test (Decker & Lohmann-Matthes, 1988:62-64; Fotakis & Timbrell, 2006:171). The LDH activity in the extracellular medium is the basis of the LDH-assay, and this can be measured by the cytoplasmic enzyme activity, which is released by cells that are damaged.

Potential candidates for anti-TB drugs have a number of obstacles to overcome. Difficulties such as low levels of stability or retention in cells after uptake, low solubility and degradation before reaching target tissue sites arise when these drugs are used. Due to poor absorption properties or low penetration into cells, there may be some difficulty in achieving optimal concentrations of a drug at the site of infection. A prospective drug may be too harmful, leading to a maximum allowed dose well below what is needed for effective eradication of the infection (Adams *et al*., 1999:1683). Eight nano-emulsions were prepared and investigated during this study as a possible novel topical CTB treatment. Each nano-emulsion contained 1% (w/v) API to determine if any toxic effect was present (Riss *et al*., 2011:103). The common assays used included methylthiazol tetrazolium (MTT; 3-(4, 5-dimethylthiazol-2-yl)-2, 5-diphenyltetrazolium bromide)-assay, LDH-assay and the neutral red. Neutral red is used to detect whether any cytotoxicity is visible after exposure to toxic substances (Fotakis & Timbrell, 2006:171).

In this study, it was determined whether the nano-emulsions, i.e. **S1** – **S5** and **O1** – **O5**, indicated cytotoxicity against:

- HaCaT cells during the LDH study, and
- *M. tuberculosis* H37Rv.

D.2 *In vitro* cell culture toxicity studies

HaCaT and dermal fibroblast cells, cultured in Dulbecco's modified eagle medium (DMEM)/high glucose medium (4 500 mg/l of glucose and 1 mM of sodium pyruvate) were used in this study. This medium was supplemented with 10% foetal bovine serum (FBS), 1% penicillin/streptomycin (Pen/Strep), 4 mM L-glutamine and 1% MEM non-essential amino acids (MEM NEAA). The cells were cultured at 37 °C in a humidified atmosphere (95% air and 5% CO_2) and could be re-distributed to fresh culturing flasks, using trypsinisation. Before any testing could commence, the cells were seeded on appropriate plates (96-well plates) and allowed to grow for 1 – 2 days. This time span allowed the cells to reach the desired confluence of ± 80%, before treatment. Trypsin with Versene® was used to harvest all cells used in this study. The cells were detached from the culturing flasks by removing the growth medium and washing them with phosphate buffered saline to remove any traces of serum and growth medium. To detach the cells from the flask surface, 3 ml of trypsin solution (10%) was added to the 75 cm^2 culturing flask, followed by incubation at 37 °C for 5 min. Cell detachment was confirmed using microscopic visualisation (10 X magnification). Growth medium was added to the flask to inactivate the trypsin enzymatic action, followed by the re-distribution of the required amount of cells to the desired culturing vessel.

D.2.1 Appropriate cell line selection

Different cell types are used depending on the way of contact. A well-accepted model, widely used for various applications including toxicity testing, is the HaCaT cell line. HaCaT is a spontaneous immortalised cell line of human keratinocytes (Ölschläger *et al*., 2009:147; Udensi *et al*., 2011:183), which makes them appropriate *in vitro* models for assessing the toxicity of an API (Lopez-Garcia *et al*., 2010:2846). Generally in skin pathophysiology and homeostasis studies, HaCaT cells have been used (Seo *et al*., 2012:171) for cell cytotoxicity studies, because these cells are diligently comparable to normal skin cells, due to their human skin derivation (Sorrell & Caplan, 2004:667).

D.2.2 Cell line treatment

The HaCaT cells were each treated for 12 h at 37 °C (5% CO_2, 95% humidity) with the placebos (containing no CLF, ART or DQ), i.e. **(S5)** and **(O5)**, the nano-emulsions containing the APIs separately (**S1**, **S2**, **S3**, **O1**, **O2** and **O3**) and in combination (**S4** and **O4**).

D.2.3 Experimental procedures

The cytotoxicity studies were conducted in the Mammalian Cell Culture Laboratory, which is situated in the Laboratory for Applied Molecular Biology (LAMB) of the NWU, Potchefstroom Campus. All experiments were carried out under aseptic conditions. Prior and during the cytotoxic studies, Me A Brümmer conducted all procedures, including cell cultivation, feeding, seeding and the treatment of cell lines.

D.2.3.1 Materials

Table E.1 depicts the materials used in the cytotoxicity. To prevent contamination of the cell cultures and ensure sterility, the materials were handled in the laminar airflow cabinet.

Table D.1: Materials used during the *in vitro* cytotoxicity study

Product	Supplier	Batch number
CytoTox 96® Non-Radioactive Cytotoxicity Assay	Promega™	-
96-Well plate	TPP®	20150301
75 cm^2 Cell culture flask	Corning®	24315044
Trypan Blue solution (0.4%)	Sigma-Aldrich™	RNBC9030
FBS	HyClone®	RZM35923
Phosphate buffered saline (1x)	HyClone®	AAD201744
L-Glutamine	HyClone®	-
DMEM with high glucose, 4.0 mM L-glutamine, sodium pyruvate	HyClone®	AB216032
MEM NEAA (100%)	HyClone®	AAB199680
Pen/Strep	Lonza™	5MB068
Trypsin-Versene® (EDTA)	Lonza™	5MB168

D.3 Cytotoxicity testing

D.3.1 LDH-assay

LDH is a continuous cytoplasmic enzyme present in all cells however, upon damage of the plasma membrane, LDH is rapidly released into the cell culture supernatant (Korzeniewski & Callewaert, 1983). An enzymatic test determines the LDH activity, the first step of which includes the reduction of nicotinamide adenine dinucleotide (NAD) to nicotinamide adenine dinucleotide (NADH). This is done by the LDH catalysed conversion turning lactate into pyruvate. The second step includes the transfer of H/H^+ from $NADH/H^+$ to the tetrazolium salt 2-(4-iodophenyl)-3-(4-nitrophenyl)-5-phenyltetrazolium chloride (INT), by the catalyst diaphorase, which in turn is reduced to a red formazan (Chan *et al*., 2013:66; Decker & Lohmann-Matthes, 1988:62-64; Lappalainen *et al*., 1994; Nachlas *et al.,* 1960; Weyermann *et al*., 2005:369,370).

The LDH-assay is based upon the principle of measuring activity within the extracellular medium. LDH is usually chosen because the evaluation is reliable, quick and very basic (Decker & Lohmann-Matthes, 1988:62-64). The loss of intra-cellular LDH, which is an indicator of irreversible cell death caused by cell membrane damage and the subsequent release of LDH into the culture media (Fotakis & Timbrell, 2006:172; Perche *et al*., 2012:99), is used in the testing of the integrity of the plasma membrane when exposed to nano-emulsion treatment.

Prior to the commencement of the LDH-assay, cultured fibroblast and HaCaT cells were seeded per well in a 96-well plate. The cells were treated with APIs, natural oils and nano-emulsions with and without the APIs. A series of API concentrations were used for the treatment of these cells,

by diluting the appropriate amount of each nano-emulsion containing the API with growth medium and adding these solutions to the cells. The cells were then incubated at 37 °C and 5% CO_2 for a pre-determined period. After the treatment period, the cells were washed with phosphate buffered saline to remove excessive growth medium and serum.

After exposure of the fibroblast and HaCaT cells to the APIs, the cell culture media was aspirated and centrifuged at 3 000 rpm for 5 min to obtain cell free supernatants per test sample. The activity of LDH in the media was determined using an LDH kit (LDL50) (Sigma diagnostics, South Africa). The assay determines the conversion of lactate into pyruvate (in the presence of LDH) and the parallel reduction of NAD^+ (oxidised nicotinamide adenine dinucleotide). The extent to which NADH (reduced) reduces the above reaction is determined by measuring the absorbance at 340 nm. Aliquots of the removed cell culture media are mixed with warm reagent in a 96-well plate and the absorbance recorded using a microplate spectrophotometer system. Results can be analysed using the Soft max pro software and presented as a percentage of control values.

D.3.2 *In vitro* cell culture studies on tuberculous cells

As part of the Flagship Programme, nano-emulsions used for efficacy studies were sent to University of Cape Town (UCT), South Africa, for evaluation. Inoculated bacterial cells were used for the efficacy studies. Currently, no method has been developed for testing on *M. tuberculosis,* but an existing method was adapted for use on surrogate organisms.

D.3.2.1 Determination of the 90% minimum inhibitory concentration (MIC_{90})

To assess the MIC_{90} (minimum concentration of API, which is required to inhibit more than 90% of bacterial population growth) the broth microdilution method (Collins *et al*., 1997) was used. The nano-emulsions were tested in one 96-well microtiter plate. A culture of mutant *M.* tb (M.tb H37RvMA::*gfp*) strain, expressing recombinant green fluorescent protein (GFP) off a plasmid integrated at the phage attachment site (*attB)* locus, was grown to OD_{600} (optical density reading taken at 600 nm) between 0.6 and 0.7 and diluted (1:100) in glycerol–alanine–salts containing iron and Tween® 80 (GAST/Fe) medium. In row 1, 640 µm of the nano-emulsions that were tested were added in duplicate and a total volume of 50 µl of GAST/Fe medium were added to rows 2 – 12 of the plate. Other wells contained GAST/Fe medium, 5% dimethyl sulfoxide (DMSO), kanamycin and rifampicin as control, in addition to the test nano-emulsions in row 1. Two-fold serial dilution was followed by transferring 50 µl of the nano-emulsion containing solution from each preceding row to the following row, ensuring all the wells contained 50 µl (not for control wells). Thereafter plates were incubated for 14 days at 37 °C (humid conditions). Using a Fluostar Optima microplate reader (BMG Labtech), MIC_{90} values were scored using quantitative fluorescence at 7-days and 14-days post inoculation. Digital images were captured and stored.

According to the procedure described by Van der Ven *et al.* (2015), the efficacy of the compounds were determined during growth in different carbon sources.

D.3.2.2 Intracellular efficacy of compounds against *Mycobacterium tuberculosis* H37Rv

The J774 macrophage cell line grown in DMEM was plated on a 96-well plate (100 µl/well) and thereafter incubated overnight in a CO_2 incubator at 37 °C. The plate was transferred to Biosafety Level 3 for infection with the H37RvMA::*gfp* (OD_{600} 0.4 – 0.6) and this culture was grown in 7H9/OADC and DMEM ensuring 10^5 cells per ml. J447 cells were washed with phosphate buffered saline-Tween® 80 then infected with the H37RvMA::*gfp* (100 µl) in DMEM, thereafter H37RvMA::*gfp* in 7H9/OADC was added in appropriate wells and incubated for 4 – 6 h. Ten-fold serial dilutions of plated cells were plated on the agar plates, which contained 7H10/OADC supplemented with hygromycin B resistance gene (Hyg^{50}), and incubated at 37 °C. The medium was replenished with compound containing medium following successful bacterial-uptake by macrophages. Using the Fluostar Optima microplate reader (BMG Labtech), the GFP signal was read and images of representative wells were captured by using the fluorescent cell imager (ZOE Fluorescence Imager, BioRad). The GFP was read daily and the medium was replenished every second day. Following GFP captured fluorescence image analysis, the cells were lysed for enumeration of viable colony-forming units (CFU) and compared with the GFP readouts on day 6. The combination of the APIs were done to determine whether the combination of the APIs in the nano-emulsions would have a synergistic effect on their efficacy or whether the combination would cause cell death.

D.4 Results and discussion

D.4.1 LDH testing results on HaCaT cells

The cell death of HaCaT cells was determined from the eight nano-emulsions (**S1** – **S4** and **O1** – **O4**), together with their placebos (**S5** and **O5**), by means of LDH release assay, whereas the cytoplasmic enzyme, which is present in most cells, was released into the extracellular medium upon cell damage. The results of the cytotoxicity values for the nano-emulsions containing safflower oil and those containing olive oil are depicted in Tables D.2 and D.3, respectively. Cell viability reference values can be described as 1) 40% is measured as non-cytotoxic, 2) a weak cytotoxicity is measured between 40 and 60%, 3) moderate cytotoxicity is measured between 60 and 80% and 4) strong cytotoxicity is measured between 80 and 100% (López-García *et al*., 2014:45). Tables D.2 and D.3 depict the values obtained during the LDH-assay.

Table D.2: LDH results from the nano-emulsions containing safflower oil

	%Cytotoxicity	p-value
Control	0.000	0.000
Lysis	100.000	
S1	11.857	0.010
S2	20.165	0.000
S3	11.699	0.016
S4	53.076	0.000
S5 (Safflower oil placebo)	20.047	0.000

Table D.3: LDH results from the nano-emulsions containing olive oil

	%Cytotoxicity	p-value
Control	0.000	0.000
Lysis	100.000	-
O1	34.072	0.000
O2	28.309	0.000
O3	15.378	0.001
O4	38.580	0.000
O5 (Olive oil placebo)	15.834	0.004

From p-values of all the nano-emulsions, it is there is a statistical significance for all the nano-emulsions ($p < 0.05$). Lysis had a cytotoxic effect of 100% (complete cell death/cytotoxicity), whereas the control had a cytotoxic effect of 0% (no effect on cells). All the nano-emulsions were statistically analysed and compared with the control. Both the nano-emulsions containing safflower oil (**S1** – **S5**) and olive oil (**O1** - **O5**) depicted non-cytotoxic levels regarding the HaCaT cells since all the %cytotoxicity levels were lower than 40%.

D.4.2 *In vitro* cell culture studies on tuberculous cells

Tables D.4 and D.5 tabularise the volumes of nano-emulsions used in 5 ml culture of *M.tb* H37Rv and the %inhibition results of each nano-emulsion (**S1** – **S5** and **O1** – **O5**) used on *M.tb* H37Rv, respectively.

Table D.4: Volumes of nano-emulsions used in 5 ml culture (*M.tb* H37Rv)

Nano-emulsion v/v (µl)				Total in 5 ml bacterial culture (µl)
	CLF	ART	DQ	
S1	2.5			2.5
S2		2.5		2.5
S3			2.5	2.5
S4	2.5			2.5
O1	2.5			2.5
O2		2.5		2.5
O3			2.5	2.5
O4	2.5			2.5
S5	2.5			2.5
O5	2.5			2.5

Table D.5: Percentage inhibition of the nano-emulsions relative to control culture against *M.tb* H37Rv

	CFU/ml	STDEV	%Inhibition (relative to control)
S1	6.67E+07	1.6	60
S2	6.17E+07	1.5	63
S3	8.00E+07	2.9	52
S4	6.67E+07	1.6	60
O1	7.17E+07	1.9	57
O2	7.50E+07	3.7	55
O3	7.67E+07	1.6	54
O4	7.83E+07	0.8	53
S5	1.43E+08	1.6	14
O5	1.30E+08	1.4	22
INH (isoniazid)(1 µg/ml)	3.17E+07	1.7	81
CLF	9.33E+07	2.0	44
ART	1.17E+08	3.4	30
DQ	1.18E+08	2.5	29
Control	1.67E+08	2.4	-

Bacterial cell cultures (*M.tb* H37Rv) were used to test the efficacy of the nano-emulsions to indicate to what extent the nano-emulsions would inhibit the *M.tb* strains. As observed in Table D.4, 2.5 µl of each nano-emulsion was used on these bacterial cells separately. As indicated by Table D.5, the nano-emulsions depicted very good results with regards to %inhibition. Isoniazid (INH), which is known to cause cell death to *Mycobacterium* strains, was

used as a positive control. Compared to the positive control, the eight nano-emulsions (**S1** – **S4** and **O1** – **O4**) showed the %inhibition was exceptionally good, ranging from values 52 – 63% inhibition. Comparing the %inhibition results of the nano-emulsions containing the safflower oil with those of the nano-emulsions containing the olive oil, it is clear the former had higher %inhibition values than the latter. The focus of this part of the study was to determine, whether the nano-emulsions with all the APIs combined in one (**S4** and **O4**) would give better results regarding the %inhibition against *M.tb* H37Rv than those containing the individual APIs (**S1**, **S2**, **S3**, **O1**, **O2** and **O3**). **S4** (60%) yielded a higher %inhibition than **O4** (53%). It is also evident that the placebos (**S5** and **O5**) depicted a little %inhibition, which could possibly be due to the fact natural oils were used during the formulation of the nano-emulsions. These combinations indicate the nano-emulsions with the APIs could possibly be used in the future for the topical treatment of CTB.

D.5 Conclusion

The cytotoxicity assay of the natural oil nano-emulsions containing CLF, ART and DQ were carried out with HaCaT. The LDH-assay used indicated the degree of cytotoxicity from each nano-emulsion. It is evident after investigating the cytotoxicity results, that none of the eight nano-emulsions (**S1** – **S4** and **O1** – **O4**) were cytotoxic. It is also evident the nano-emulsions alone, with no API included (**S5** and **O5**), showed no cytotoxicity.

Low cytotoxicity results could be explained by how the nano-emulsions encapsulated the APIs, suggesting the API is not in direct contact with the skin itself and consequently provides a barrier between the APIs and the interaction with normal healthy cells. These results can be compared to a study by De Godoi *et al*. (2017:6), wherein cytotoxicity was reduced using nano-emulsions, since the API was protected by oil nano-encapsulation. This study shows that CLF, ART and DQ can be successfully entrapped in a nano-emulsion dispersion and possibly be used in the future for the topical treatment of CTB. It is evident that all eight nano-emulsions, together with their placebos, depicted very good results regarding %inhibition with ranges from 52 – 63%; the placebos (**S5** and **O5)** also depicted a small %inhibition, 14% and 22%, respectively. The %inhibition from the nano-emulsions could be ascribed to the natural oils used in the nano-emulsions. No literature was found on cytotoxicity studies conducted on *M.tb* H37Rv treated with a placebo nano-emulsion containing a natural oil, i.e. either safflower or olive oil, and therefore contributes to the absence of information. It is also evident when comparing the %inhibition results of safflower oil with that of olive oil, the safflower oil nano-emulsions had higher %inhibition values than the olive oil nano-emulsion. When the placebo nano-emulsions are compared with the nano-emulsions containing the APIs (CLF, ART and DQ), it is evident the placebo nano-emulsions showed exceptional %inhibition, it can therefore be concluded that the natural oils have

an impact on the %inhibition. These natural oil nano-emulsions combined with the APIs indicate possible future topical treatment of CTB.

References

acCELLerate GmbH. 2015. Use of Assay Ready HaCaT Cells for Cytotoxicity Testing. https://www.accellerate.me/fileadmin/accellerate/Applications/Application_Notes/HaCaT_Assay_Ready_Cells.pdf. Date of access: 15 Aug 2017.

ATCC ***see*** American Type Culture Collection

American Type Culture Collection. 2011. MTT cell proliferation assay. https://www.atcc.org/~/media/DA5285A1F52C414E864C966FD78C9A79.ashx Date of access: 2 Aug 2017.

Chan, F.K., Moriwaki, K. & De Rosa, M.J. 2013. Detection of necrosis by release of lactate dehydrogenase (LDH) activity. *Methods in Molecular Biology*, 979:65-70.

Collins, L. & Franzblau, S.G. 1997. Microplate alamar blue assay versus BACTEC 460 system for high-throughput screening of compounds against *Mycobacterium tuberculosis* and *Mycobacterium avium*. *Antimicrobial Agents and Chemotherapy*, 41:1004-1009.

Cook, J.A. & Mitchell, J.B. 1989. Viability measurements in mammalian cell systems. *Analytical Biochemistry*, 179:1-7.

Decker, T. & Lohmann-Matthes, M.L. 1988. A quick and simple method for the quantitation of lactate dehydrogenase release in measurements of cellular cytotoxicity and tumor necrosis factor (TNF) activity. *Journal of Immunological Methods*, 115(1):61-69.

De Godoi, S.M., Quatrin, P.M., Sagrillo, M.R., Nascimento, K., Wagner, R., Klein, B., Santos, R.C.V. & Ourique, A.F. 2017. Evaluation of Stability and *In Vitro* Security of Nanoemulsions Containing *Eucalyptus globulus* Oil. *BioMed Research International*, 2017:1-10.

Fotakis, G. & Timbrell, J.A. 2006. *In vitro* cytotoxicity assays: comparison of LDH, neutral red, MTT and protein assay in hepatoma cell lines following exposure to cadmium chloride. *Toxicology Letters,* 160:171-177.

Korzeniewski, C. & Callewaert, D.M. 1983. An enzyme-release assay for natural cytotoxicity. *Journal of Immunological Methods*, 64(3):313-20.

Lappalainen, K., Jääskeläinen, I., Syrjänen, K., Urtti, A. & Syrjänen, S. 1994. Comparison of Cell Proliferation and Toxicity Assays Using Two Cationic Liposomes. *Pharmaceutical Research*, 11(8):1127-1131.

Lopez-Garcia, J., Lehocky, M., Humpolicek, P. & Saha, P. 2014. HaCaT keratinocytes response on antimicrobial atelocollagen substrates: extent of cytotoxicity, cell viability and proliferation. *Journal of Functional Biomaterials,* 5:43-57.

Nachlas, M.M., Margulies, S.I. & Seligman, A.M. 1960. A Colorimetric Method for the Estimation of Succinic Dehydrogenase Activity. *The Journal of Biological Chemistry*, 235:499-503.

Ölschläger, V., Schrader, A. & Hockertz, S. 2009. Comparison of primary human fibroblasts and keratinocytes with immortalized cell lines regarding their sensitivity to sodium dodecyl sulfate in a neutral red uptake cytotoxicity assay. *Arzneimittelforschung*, 59(3):146-152.

Perche, F., Patel, N.R. & Torchilin, V.P. 2012. Accumulation and toxicity of antibody-targeted doxorubicin-loaded PEG–PE micelles in ovarian cancer cell spheroid model. *Journal of Controlled Release*, 164:95-102.

Riss, T.L., Moravex, R.A. & Niles, A.L. 2011. Cytotoxicity testing: measuring viable cells, dead cell, and detecting mechanism of cell death. (*In* Stoddart, M.J., *ed.* Mammalian cell 645 viability: methods and protocols. New York: Humana Press. p. 103-114.)

Seo, M., Kang, T.J., Lee, C.H., Lee, A. & Noh, M. 2012. HaCaT keratinocytes and primary epidermal keratinocytes have different transcriptional profiles of cornified envelope-associated genes to T helper cell cytokines. *Biomolecules and Therapeutics*, 20(2):171-176.

Sorrell, J.M. & Caplan, A.I. 2004. Fibroblast heterogeneity: more than skin deep. *Journal of Cell Science*, 117:667-675.

Udensi, U.K., Graham-Evans, B.E., Rogers, C.S. & Isokpehi, R.D. 2011. Cytotoxicity patterns of arsenic trioxide exposure on HaCaT keratinocytes. *Clinical, Cosmetic and Investigative Dermatology*, 4:183-90.

VanderVen, B.C., Fahey, R.J., Lee, W., Liu, Y., Abramovitch, R.B., Memmot, C., Crowe, A.M., Eltis, L.D., Perola, E., Deiniger, D.D., Wang, T., Locher, C.P. & Russel, D.G. 2015. Novel inhibitors of cholesterol degradation in *Mycobacterium tuberculosis* reveal how the bacterium`s metabolism is constrained by the intracellular environment. *Plos Pathogenes,* 11(22):e1004679.

Weyermann, J., Lochmann, D. & Zimmer, A. 2005. A practical note on the use of cytotoxicity assays. *International Journal of Pharmaceutics*, 288(2):369-376.

Yoon, M., Campbell, J.L., Andersen, M.E. & Clewell, H.J. 2012. Quantitative *in vitro* to *in vivo* extrapolation of cell-based toxicity assay results. *Critical Reviews in Toxicology*, 42:633-652.

Appendix E:

Authors guide of 'Drug Development and Industrial Pharmacy'

Drug Development and Industrial Pharmacy is an international, peer reviewed journal, publishing high-quality, original research. Please see the journal's Aims & Scope for information about its focus and peer-review policy.

Please note that this journal only publishes manuscripts in English.

This journal accepts the following article types:

- **Original papers**
- **Critical reviews**: Reviews are written by invitation only, but suggestions of topics are encouraged.
- **Rapid communications**: Highly significant reports that are very original and likely to have considerable impact on the field. These manuscripts contain proof of principle data.
- **Trends articles**: Written by invitation only, but suggestions of topics are encouraged. Trends articles are concise summaries of new and emerging research within the priority topics considered for the journal. Authors will also include their vision of future developments and research directions in the area.

Peer review

Taylor & Francis is committed to peer-review integrity and upholding the highest standards of review. Once your paper has been assessed for suitability by the editor, it will then be single blind peer-reviewed by independent, anonymous expert referees. Find out more about what to expect during peer review and read our guidance on publishing ethics.

Preparing your paper

All authors submitting to medicine, biomedicine, health sciences, allied and public health journals should conform to the Uniform Requirements for Manuscripts Submitted to Biomedical Journals, prepared by the International Committee of Medical Journal Editors (ICMJE).

Structure

Your paper should be compiled in the following order: title page; abstract; keywords; main text, introduction, materials and methods, results, discussion; acknowledgments; declaration of interest statement; references; appendices (as appropriate); table(s) with caption(s) (on individual pages); figures; figure captions (as a list).

Word count

Please include a word count for your paper. A typical paper for this journal should not exceed 8000 words; inclusive of tables, references, figure captions.

A typical rapid communication should not exceed 3,000 words; inclusive of 2 figures/tables.

A typical trends article should not exceed 3500 words; not inclusive of with 4 figures and approximately 30 key references.

Style guidelines

Please refer to these style guidelines when preparing your paper, rather than any published articles or a sample copy.

Please use American spelling consistently throughout your manuscript.

Please use single quotation marks, except where 'a quotation is "within" a quotation'. Please note that long quotations should be indented without quotation marks.

Formatting and templates

Papers may be submitted in any standard format, including Word and LaTeX. Figures should be saved separately from the text. To assist you in preparing your paper, we provide formatting template(s).

Word templates are available for this journal. Please save the template to your hard drive, ready for use.

A LaTeX template is available for this journal. Please save the template to your hard drive, ready for use.

If you are not able to use the templates via the links (or if you have any other template queries) please contact authortemplate@tandf.co.uk

References

Please use this reference guide when preparing your paper. An EndNote output style is also

available to assist you.

Checklist: what to include

1. **Author details**. Please ensure everyone meeting the International Committee of Medical Journal Editors (ICJME) requirements for authorship is included as an author of your paper. Please include all authors' full names, affiliations, postal addresses, telephone numbers and email addresses on the cover page. Where available, please also include ORCiDs and social media handles (Facebook, Twitter or LinkedIn). One author will need to be identified as the corresponding author, with their email address normally displayed in the article PDF (depending on the journal) and the online article. Authors' affiliations are the affiliations where the research was conducted. If any of the named co-authors moves affiliation during the peer-review process, the new affiliation can be given as a footnote. Please note that no changes to affiliation can be made after your paper is accepted. Read more on authorship.
2. A structured abstract should cover (in the following order).
3. A structured **abstract** of no more than 250 words. A structured abstract should cover (with the following headings): Objective, Significance, Methods, Results, Conclusions. Read tips on writing your abstract.
4. You can opt to include a **video abstract** with your article. Find out how these can help your work reach a wider audience, and what to think about when filming.
5. 5-10 **keywords**. Read making your article more discoverable, including information on choosing a title and search engine optimization **keywords**. Read making your article more discoverable, including information on choosing a title and search engine optimization.
6. **Novelty statement**. Please note that a novelty statement is required for submission on the title page. This statement should provide information in one or two sentences as to what is new and novel in the manuscript in relation to prior related work, including the authors' own.
7. **Funding details**. Please supply all details required by your funding and grant-awarding bodies as follows: For single agency grants: This work was supported by the under Grant. For multiple agency grants: This work was supported by the under Grant; under Grant; and under Grant.
8. **Disclosure statement**. This is to acknowledge any financial interest or benefit that has arisen from the direct applications of your research. Further guidance on what is a conflict of interest and how to disclose it.

9. **Biographical note.** Please supply a short biographical note for each author. This could be adapted from your departmental website or academic networking profile and should be relatively brief.
10. **Geolocation information.** Submitting a geolocation information section, as a separate paragraph before your acknowledgements, means we can index your paper's study area accurately in JournalMap's geographic literature database and make your article more discoverable to others. More information.
11. **Supplemental online material.** Supplemental material can be a video, dataset, fileset, sound file or anything which supports (and is pertinent to) your paper. We publish supplemental material online via Figshare. Find out more about supplemental material and how to submit it with your article.
12. **Figures.** Figures should be high quality (1200 dpi for line art, 600 dpi for grayscale and 300 dpi for colour). Figures should be saved as TIFF, PostScript or EPS files.
13. **Tables.** Tables should present new information rather than duplicating what is in the text. Readers should be able to interpret the table without reference to the text. Please supply editable files.
14. **Equations**. If you are submitting your manuscript as a Word document, please ensure that equations are editable. More information about mathematical symbols and equations.
15. **Units.** Please use SI units (non-italicized).

Using third-party material in your paper

You must obtain the necessary permission to reuse third-party material in your article. The use of short extracts of text and some other types of material is usually permitted, on a limited basis, for the purposes of criticism and review without securing formal permission. If you wish to include any material in your paper for which you do not hold copyright, and which is not covered by this informal agreement, you will need to obtain written permission from the copyright owner prior to submission. More information on requesting permission to reproduce work(s) under copyright.

Disclosure statement

Please include a disclosure of interest statement, using the subheading "Disclosure of interest." If you have no interests to declare, please state this (suggested wording: The authors report no conflicts of interest). For all NIH/Wellcome-funded papers, the grant number(s) must be included in the disclosure of interest statement. Read more on declaring conflicts of interest.

Clinical Trials Registry

In order to be published in a Taylor & Francis journal, all clinical trials must have been registered in a public repository at the beginning of the research process (prior to patient enrolment). Trial registration numbers should be included in the abstract, with full details in the methods section. The registry should be publicly accessible (at no charge), open to all prospective registrants, and managed by a not-for-profit organization. For a list of registries that meet these requirements, please visit the WHO International Clinical Trials Registry Platform (ICTRP). The registration of all clinical trials facilitates the sharing of information among clinicians, researchers, and patients, enhances public confidence in research, and is in accordance with the ICMJE guidelines.

Complying with ethics of experimentation

Please ensure that all research reported in submitted papers has been conducted in an ethical and responsible manner, and is in full compliance with all relevant codes of experimentation and legislation. All papers which report *in vivo* experiments or clinical trials on humans or animals must include a written statement in the Methods section. This should explain that all work was conducted with the formal approval of the local human subject or animal care committees (institutional and national), and that clinical trials have been registered as legislation requires. Authors who do not have formal ethics review committees should include a statement that their study follows the principles of the Declaration of Helsinki.

Consent

All authors are required to follow the ICMJE requirements on privacy and informed consent from patients and study participants. Please confirm that any patient, service user, or participant (or that person's parent or legal guardian) in any research, experiment, or clinical trial described in your paper has given written consent to the inclusion of material pertaining to themselves, that they acknowledge that they cannot be identified via the paper; and that you have fully anonymized them. Where someone is deceased, please ensure you have written consent from the family or estate. Authors may use this Patient Consent Form, which should be completed, saved, and sent to the journal if requested.

Health and safety

Please confirm that all mandatory laboratory health and safety procedures have been complied with in the course of conducting any experimental work reported in your paper. Please ensure your paper contains all appropriate warnings on any hazards that may be involved in carrying out the experiments or procedures you have described, or that may be involved in instructions, materials, or formulae.

Please include all relevant safety precautions; and cite any accepted standard or code of practice. Authors working in animal science may find it useful to consult the International Association of

Veterinary Editors' Consensus Author Guidelines on Animal Ethics and Welfare and Guidelines for the Treatment of Animals in Behavioural Research and Teaching. When a product has not yet been approved by an appropriate regulatory body for the use described in your paper, please specify this, or that the product is still investigational.

Submitting your paper

This journal uses ScholarOne to manage the peer-review process. If you haven't submitted a paper to this journal before, you will need to create an account in the submission centre. Please read the guidelines above and then submit your paper in the relevant Author Centre, where you will find user guides and a helpdesk.

If you are submitting in LaTeX, please convert the files to PDF beforehand (you will also need to upload your LaTeX source files with the PDF).

Please note that Drug Development and Industrial Pharmacy uses Crossref™ to screen papers for unoriginal material. By submitting your paper to Drug Development and Industrial Pharmacy you are agreeing to originality checks during the peer-review and production processes.

On acceptance, we recommend that you keep a copy of your Accepted Manuscript. Find out more about sharing your work.

Publication charges

There are no submission fees or page charges for this journal.

Color figures will be reproduced in color in your online article free of charge. If it is necessary for the figures to be reproduced in color in the print version, a charge will apply.

Charges for color figures in print are £250 per figure ($395 US Dollars; $385 Australian Dollars; €315). For more than 4 color figures, figures 5 and above will be charged at £50 per figure ($80 US Dollars; $75 Australian Dollars; €63). Depending on your location, these charges may be subject to local taxes.

Fast Track publication

All publications in this journal are driven entirely by editorial considerations, and independent peer review. As part of the journal's responsive approach to the publication of timely research results, this journal offers an optional, prioritized Fast Track publication.

Articles are published online within 5-7 weeks after submission (subject to 1-2-week author revision following initial peer review, prompt turnaround of proofs, and acceptance of the article).

There is a publication support fee for this service, based on a charge of $850/ €625/ £550 per published page (there are on average 700 words per published page).

Opting for the Fast Track service will in no way influence the quality of the peer review or the editorial decision. Fast Track articles will undergo a peer-review process of the same standard as regular articles submitted to this journal.

If you would like to discuss or select Fast Track publication, please contact the Managing Editor charles.whalley@tandf.co.uk before, or on the day of, submission.

Copyright options

Copyright allows you to protect your original material, and stop others from using your work without your permission. Taylor & Francis offers a number of different license and reuse options, including Creative Commons licenses when publishing open access. Read more on publishing agreements.

Complying with funding agencies

We will deposit all National Institutes of Health or Wellcome Trust-funded papers into PubMedCentral on behalf of authors, meeting the requirements of their respective open access (OA) policies. If this applies to you, please tell our production team when you receive your article proofs, so we can do this for you. Check funders' OA policy mandates here. Find out more about sharing your work.

Open access

This journal gives authors the option to publish open access via our Open Select publishing program, making it free to access online immediately on publication. Many funders mandate publishing your research open access; you can check open access funder policies and mandates here.

Taylor & Francis Open Select gives you, your institution or funder the option of paying an article publishing charge (APC) to make an article open access. Please contact openaccess@tandf.co.uk if you would like to find out more, or go to our Author Services website.

For more information on license options, embargo periods and APCs for this journal please go here.

Accepted Manuscripts Online (AMO)

This journal publishes manuscripts online as rapidly as possible, as a PDF of the final, accepted (but unedited and uncorrected) paper. This is clearly identified as an unedited manuscript and is

referred to as the Accepted Manuscript Online (AMO). No changes will be made to the content of the original paper for the AMO version but, after copy-editing, typesetting, and review of the resulting proof, the final corrected version (the Version of Record [VoR]), will be published, replacing the AMO version.

The VoR is the article version that will appear in an issue of the journal. Both the AMO version and VoR can be cited using the same DOI (digital object identifier). To ensure rapid publication, we ask you to return your signed publishing agreement as quickly as possible, and return corrections within 48 hours of receiving your proofs.

My Authored Works

On publication, you will be able to view, download and check your article's metrics (downloads, citations and Altmetric data) via My Authored Works on Taylor & Francis Online. This is where you can access every article you have published with us, as well as your free eprints link, so you can quickly and easily share your work with friends and colleagues.

We are committed to promoting and increasing the visibility of your article. Here are some tips and ideas on how you can work with us to promote your research.

Article reprints

For enquiries about reprints, please contact the Taylor & Francis Author Services team atreprints@tandf.co.uk. To order a copy of the issue containing your article, please contact our Customer Services team at Adhoc@tandf.co.uk.

Sponsored supplements

This journal occasionally publishes sponsored supplements alongside its schedule of regular issues. Like our articles, all our supplements are expected to meet the same editorial standards as the journal and are subject to approval of the Editor prior to acceptance. They are indexed by the journal and offer targeted, cost-effective and high-impact reach. For more information and to discuss your requirements, please contact charles.whalley@tandf.co.uk.

Appendix F:

International Journal of Pharmaceutics: Guide for Authors

F.1 Scope of the journal

The International Journal of Pharmaceutics publishes innovative papers, reviews, mini-reviews, rapid communications and notes dealing with physical, chemical, biological, microbiological and engineering studies related to the conception, design, production, characterisation and evaluation of drug delivery systems *in vitro* and *in vivo*. "Drug" is defined as any therapeutic or diagnostic entity, including oligonucleotides, gene constructs and radiopharmaceuticals.

Areas of particular interest include: pharmaceutical nanotechnology; physical pharmacy; polymer chemistry and physical chemistry as applied to pharmaceutics; excipient function and characterisation; biopharmaceutics; absorption mechanisms; membrane function and transport; novel routes and modes of delivery; responsive delivery systems, feedback and control mechanisms including biosensors; applications of cell and molecular biology to drug delivery; prodrug design; bioadhesion (carrier-ligand interactions); and biotechnology (protein and peptide formulation and delivery).

Note: In 2004, a new section was started on pharmaceutical nanotechnology. For more details, see Editorials in 279/1-2, 281/1, and 288/1.

F.2 Editorial Policy

The over-riding criteria for publication are originality, high scientific quality and interest to a multidisciplinary audience. Papers not sufficiently substantiated by experimental detail will not be published. Any technical queries will be referred back to the author, although the Editors reserve the right to make alterations in the text without altering the technical content. Manuscripts submitted under multiple authorship, are reviewed on the assumption that all listed authors concur with the submission and that a copy of the final manuscript has been approved by all authors and tacitly or explicitly by the responsible authorities in the laboratories where the work was carried out. If accepted, the manuscript shall not be published elsewhere in the same form, in either the same or another language, without the consent of the Editors and Publisher.

Authors must state in a covering letter when submitting papers for publication the novelty embodied in their work or in the approach taken in their research. Routine bioequivalence studies are unlikely to find favour. No paper will be published which does not disclose fully the nature of the formulation used or details of materials which are key to the performance of a product, drug or excipient. Work which is predictable in outcome, for example the inclusion of another drug in a cyclodextrin to yield enhanced dissolution, will not be published unless it provides new insight into fundamental principles.

F.3 Submission of Manuscripts

Authors are strongly encouraged to submit their manuscript electronically by using the Elsevier submission site at (http://www.elsevier.com/iournals).

After registration, authors will be asked to upload their manuscript and associated artwork. Full instructions on how to use the online submission tool are available at the web address listed above.

If an author cannot submit their manuscript electronically, then for the initial submission of manuscripts for consideration, hardcopies are sufficient. The original plus two copies, complete with two sets of figures (including originals or duplicates of sufficient quality for clarity of reproduction) and tables, must be submitted in English. All data that would help referees to evaluate the paper should also be supplied. Manuscripts should be typewritten with double spacing and adequate margins on one side of the sheet only (not more than 26 lines per page). All pages should be numbered sequentially. Manuscripts should be sent to one of the following Editors-in-Chief according to the geographical origin of the author. Please include full contact information - corresponding author name, e-mail address, telephone and fax numbers, and full postal address.

After final acceptance for publication, your revised manuscript on disk together with two printed hard copies should be submitted to the accepting editor. It is important that the file on disk and the printout are identical. Both will then be forwarded by the editor to Elsevier. In-depth guidelines for submitting artwork/illustrations can be found at: http://www.elsevier.com/ artworkinstructions.

When the paper is to be published as a Rapid Communication, this should be clearly indicated to the Editor-in-Chief.

F.3.1 Europe, Africa, Near East

Prof AT. Florence, The School of Pharmacy, University of London, 29-39 Brunswick Square, London WCIN 1AX, U.K., Fax: +44 20 7837 5092; E-mail: jip(5)pharmacv.ac.uk

F.3.2 The Americas, Australia and New Zealand

Prof J.H. Rytting, Pharmaceutical Chemistry Dept, University of Kansas, 2095 Constant Avenue, Lawrence, KS 66047, U.S.A., Fax: +1 785 864 5736; E-mail: iip@ku.edu

F.3.3 Japan and far East

Prof. T. Sonobe, Department of Pharmaceutical Engineering, School of Pharmaceutical Sciences, University of Shizuoka, 52-1 Yada, Shizuoka-shi 422-8526, Japan. Fax: +81-54-264-5614; E-mail: sonobe@gakushikai.jp

F.4 Manuscript Types

F.4.1 Full length manuscripts

The arrangement of full length papers should accord with the following:

F.4.1.1 Title

The full title should not exceed 85 characters including spaces between words.

F.4.1.2 List of authors

Initial(s) (one given name may be used) followed by the surname of author(s) together with their affiliations. When the work has been carried out at more than one address, the affiliation of each author should be clearly indicated using superscript, lower-case letters. The author to whom correspondence should be directed must be indicated with an asterisk.

F.4.1.3 Affiliation(s) Name(s) and address (es) of the establishment(s) where the work was done designated by superscript, lower-case letters where appropriate.

F.4.1.4 Abstract

An Abstract not exceeding 200 words (a single paragraph) should be provided typed on a separate sheet.

F.4.1.5 Keywords

A maximum of 6 keywords or short phrases suitable for indexing should be supplied. If possible keywords should be selected from Index Medicus or Excerpta Medica Index. Authors may also wish to refer to the Subject Index published in International Journal of Pharmaceutics, for example, Vol. 287/1-2, pp. 205-219.

F.4.1.6 Corresponding author

The author to whom correspondence should be directed should be designated with an asterisk (do not include the address unless different from that indicated by the author's affiliation). Telephone, fax and e-mail address of the corresponding author must be provided.

F.4.1.7 Text

The text should be divided into main sections, such as the following: 1. Introduction; 2. Materials and methods; 3. Results; 4. Discussion; Acknowledgements; References; Figure legends; Tables and Figures. These sections must be numbered consecutively as indicated. Subdivisions of a section should also be numbered within that section, for example, 2.1. Materials, 2.2. Relative humidity measurement, 2.3. Sample preparation, etc.

F.4.1.8 Nomeclature

Standard nomenclature should be used throughout; unfamiliar or new terms and arbitrary abbreviations should be defined when first used. Unnecessary or ambiguous abbreviations and symbols are to be avoided. Data should be expressed in SI units.

F.4.1.9 Figure legends, table legends, footnotes

Figure legends, tables and footnotes should be typed on separate sheets, lines double spaced. Footnotes, to be numbered consecutively in superscript throughout the text, should be used as little as possible.

F.4.1.10 References

See below for full details.

F.4.2 Rapid communications

- These articles should not exceed 1500 words or equivalent space.
- Figures should not be included otherwise delay in publication will be incurred.
- Do not subdivide the text into sections. An Abstract should be included as well as a full reference list.
- No proofs will be sent to the author(s).

F.4.3 Notes

Should be prepared as described for full length manuscripts, except for the following:

- The maximum length should be 1500 words, including figures and tables.
- Do not subdivide the text into sections. An Abstract and reference list should be included.

F.4.4 Reviews and mini reviews

Suggestions for review articles will be considered by the Editors-in-Chief. "Mini-reviews" of a topic are especially welcome.

F.5 References

F.5.1 Text citation

The Harvard system of citation must be used. References should be cited in the text within parentheses: where several citations are given within a single set of parentheses, they should be arranged in ascending order of year of publication; where more than one reference with the same year of publication is cited, they should be arranged in alphabetical order of the first authors' names. When referring to a work of more than two authors, the name of the first author should be given, followed by et al.

Examples of text citations:

(Gesztes et al., 1988; Chestnut et al., 1989; Legros et al., 1990; Mhando and Li Wan Po, 1990; Korsten et al., 1991; Langerman et al., 1991, 1992a,b; Masters et al., 1991; Bonhomme et al., 1992; Kollietal., 1992).

(Shaw et al., 1978; Nakano and Arita 1990b; Nakano et al., 1990a,b; Bone et al., 1992)

F.5.2 Reference list

All references cited in the text should be listed at the end of the paper (typed with double spacing) and assembled alphabetically. More than one paper from the same author(s) in the same year must be identified by the letters a b c, etc. placed after the year of publication.

References must consist of names and initials of all authors, year, title of paper, abbreviated title of periodical, and volume and first and last page numbers. 'Personal communication' and 'unpublished data' should be cited in the text only. Papers referred to as 'submitted for publication' must include the name of the journal to which submission has been made. Journal titles should be abbreviated according to the 'List of Serial Title Word Abbreviations' (available from International Serials Data System, 20, rue Bachaumont, 75002 Paris, France. ISBN 2-904939-02-8).

Example of arrangement in the reference list:

Crowe, J.H., Crowe, L.M., Chapman, D., 1984a. Infrared spectroscopic studies on interactions of water and carbohydrates with a biological membrane. Arch Biochem. Biophys., 232, 400-407.

Crowe, J.H., Crowe, L.M., Hoekstra, F.A., 1989. Phase transitions and permeability changes in dry membranes during rehydration. J. Bioenerg. Biomembr., 21, 77-92.

Crowe, J.H., Crowe, L.M., Carpenter, J.F., Aurell Wistrom, C, 1987. Stabilization of dry phospholipid bilayers and proteins by sugars. Biochem. J., 242, 1-10.

Crowe, J.H., Crowe, L.M., Carpenter, J.F., Rudolph, A.S., Wistrom, C.A., Spargo, B.J., Anchordoguy, T.J., 1988. Interactions of sugars with membranes. Biochim. Biophys. Acta, 947, 367-384.

Crowe, L.M., Crowe, J.H., Womersley, C, Reid, D., Appel, L, Rudolph, A., 1986. Prevention of fusion and leakage in freeze-dried liposomes by carbohydrates. Biochim. Biophys. Acta, 861, 131-140.

Crowe, L.M., Mouradian, R., Crowe, J.H., Jackson, S.A., Womersley, C, 1984b. Effects of carbohydrates on membrane stability at low water activities. Biochim. Biophys. Acta, 769, 141-150.

Examples of presentation for various types of publication

Langerman, L., Chaimsky, G., Golomb, E., Tverskoy, M., Kook, A.I., Benita, S., 1990. A rabbit model for evaluation of spinal anaesthesia: chronic cannulation of the subarachnoid space. Anesth. Analg., 71, 529-535.

Timsina, M.P., Martin, G.P., Marriott, C, Ganderton, D., Yianneskis, M., 1994. Drug delivery to the respiratory tract using dry powder inhalers. Int. J. Pharm., 101, 1-13.

Gibaldi, M. and Perrier, D., 1982. Pharmacokinetics, 2nd Ed., Dekker, New York. 171

Deppeler, H.P., 1981. Hydrochlorothiazide. In: Florey, K. (Ed.), Analytical Profiles of Drug Substances, Vol. 10, Academic Press, New York, pp. 405-441.

US Pharmacopeia XXII, 1990. US Pharmacopeial Convention, Rockville, MD, pp. 1434-1435.

Mueller, L.G., 1988. Novel anti-inflammatory esters, pharmaceutical compositions and methods for reducing inflammation. UK Patent GB 2 204 869 A, 23 Nov.

Du Plessis, J., 1992. Topical liposomal delivery of biologically active peptides. Ph.D Thesis, Potchefstroom University for CHE, South Africa.

F.5.3 Use of digital object identifier (DOI)

The digital object identifier (DOI) may be used to cite and link to electronic documents. The DOI consists of a unique alpha-numeric character string which is assigned to a document by the publisher upon the initial electronic publication. The assigned DOI never changes. Therefore, it is an ideal medium for citing a document particularly "Articles in press" because they have not yet received their full bibliographic information.

The correct format for citing a DOI is shown as follows: doi:10.1016/j.ijpharm.2005.01.041

F.6 Articles in special issues

Please ensure that the words 'this issue' are added (in the list and text) to any references to other articles in this Special Issue.

F.7 Figures and Tables

F.7.1 Figures

Line drawings (including graphs) should be drawn in black ink on white paper or on tracing paper with blue or faint grey rulings; graduation will not be reproduced. Lettering should be large enough to permit photographic reduction. If figures are not to be reduced, their format should not exceed 16 x 20 cm. Photographs (or half-tone illustrations) must be of good quality, submitted as black and white prints on glossy paper, and have as much contrast as possible. The magnification of micrographs should be indicated by a scale bar in the figure. Figures should be clearly marked on the reverse side with the number, orientation (top) and author's name; a soft pencil or a felt-tipped pen should be used for marking photographs. The illustrations should be numbered with Arabic numerals. The legends should be typed separately with double spacing.

Colour illustrations should be submitted as original photographs, high-quality computer prints or transparencies, close to the size expected in publication, or as 35 mm slides. Polaroid colour prints are not suitable. If, together with your accepted article, you submit usable colour figures then Elsevier will ensure, at no additional charge that these figures will appear in colour on the web (e.g., ScienceDirect and other sites) regardless of whether or not these illustrations are reproduced in colour in the printed version. For colour reproduction in print, you will receive information regarding the total cost from Elsevier after receipt of your accepted article. The 2008 price for colour figures is EUR 285 for the first page and EUR 191 for subsequent pages. For further information on the preparation of electronic artwork, please see http://www.elsevier.com/artworkinstructions.

Please note: Because of technical complications which can arise by converting colour figures to 'grey scale' (for the printed version should you not opt for colour in print) please submit in addition usable black and white prints corresponding to all the colour illustrations.

F.7.2 Tables

All tables must be numbered consecutively (with Arabic numerals) and be cited in the text. Titles should be short but descriptive. Tables should be compiled on separate sheets, together with a legend and/or footnotes identified by superscripts a.b.c, etc. Do not use vertical lines and keep horizontal rules to a minimum.

F.7.3 Dna and genbank accession numbers

Many Elsevier journals cite "gene accession numbers" in their running text and footnotes. Gene accession numbers refer to genes or DNA sequences about which further information can be found in the databases at the National Centre for Biotechnical Information (NCBI) at the National Library of Medicine.

Authors are encouraged to check accession numbers used very carefully. An error in a letter or number can result in a dead link. Note that in the final version of the electronic copy, the access/on number text will be linked to the appropriate source in the NCBI databases enabling readers to go directly to that source from the article.

F.8 Copyright guidelines for authors

Upon acceptance of an article, authors will be asked to sign a 'Journal Publishing Agreement' (for more information on this and copyright see http://www.elsevier.com/copyright). Acceptance of the agreement will ensure the widest possible dissemination of information. An e-mail (or letter) will be sent to the corresponding author confirming receipt of the manuscript together with a 'Journal Publishing Agreement' form or a link to the online version of this agreement.

Subscribers may reproduce tables of contents or prepare lists of articles including abstracts for internal circulation within their institutions. Permission of the Publisher is required for resale or distribution outside the institution and for all other derivative works, including compilations and translations (please consult http://www.elsevier.com/permissions).

If excerpts from other copyrighted works are included, the author(s) must obtain written permission from the copyright owners and credit the source(s) in the article. Elsevier has pre-printed forms for use by authors in these cases: please consult http://www.elsevier.com/permissions.

F.9 Authors' rights

As an author you (or your employer or institutions) retain certain rights; for details you are referred to http://www.elsevier.com/authorsrights.

F.10 Proofs, Offprints and Page Charges

One set of page proofs in PDF format will be sent by e-mail to the corresponding author (if we do not have an e-mail address then paper proofs will be sent by post). Elsevier now sends PDF proofs which can be annotated; for this you will need to download Adobe Reader version 7 or higher available free from http://www.adobe.com/products/acrobat/readstep2.html. Instructions on how to annotate PDF files will accompany the proofs. The exact system requirements are given at the Adobe site http://www.adobe.eom/products/acrobat/acrrsvstemreqs.html#70win.

If you do not wish to use the PDF annotations function, you may list the corrections (including replies to the Query Form) and return to Elsevier in an e-mail. Please list your corrections quoting line number. If, for any reason, this is not possible, then mark the corrections and any other comments (including replies to the Query Form) on a printout of your proof and return by fax, or scan the pages and e-mail, or by post.

Please use this proof only for checking the typesetting, editing, completeness and correctness of the text, tables and figures. Significant changes to the article as accepted for publication will only be considered at this stage with permission from the Editor. We will do everything possible to get your article published quickly and accurately. Therefore, it is important to ensure that all of your corrections are send back to us in one communication: please check carefully before replying, as inclusion of any subsequent corrections cannot be guaranteed. Proofreading is solely your responsibility. Note that Elsevier may proceed with the publication of your article if no response is received.

The corresponding author, at no cost, will be provided with a PDF file of the article via e-mail or, alternatively, 25 free paper offprints. The PDF file is a watermarked version of the published article and includes a cover sheet with the journal cover image and a disclaimer outlining the terms and conditions of use. Additional paper offprints can be ordered by the authors. An order form with prices will be sent to the corresponding author.

There are no page charges.

F.11 Language Services

Authors, who require information about language editing and copyediting services pre- and post-submission, please visit http://www.elsevier.com/locate/languagepolishing or contact authorsupport@elsevier.com for more information. Please note Elsevier neither endorses nor takes responsibility for any products, goods or services offered by outside vendors through our services or in any advertising. For more information please refer to our Terms & Conditions http://www.elsevier.com/termsandconditions.

F.12 Funding body agreements and policies

Elsevier has established agreements and developed policies to allow authors who publish in Elsevier journals to comply with potential manuscript archiving requirements as specified as conditions of their grant awards. To learn more about existing agreements and policies please visit http://www.elsevier.com/fundingbodies.

F.13 Author enquiries

For enquiries relating to the submission of articles (including electronic submission where available) please visit this journal's homepage at http://www.elsevier.com/locate/iipharm. You can track accepted articles at http://www.elsevier.com/trackarticle and set up e-mail alerts to inform, you of when an article`s status has changed. Also accessible from here is information on copyright, frequently asked questions and more.

Contact details for questioning arising after acceptance of an article, especially those relating to proofs, are provided after registration of an article for publication. No responsibility is assumed by the Publisher for any use or operation of any methods, products, instructions or ideas contained in the material herein. Because of the rapid advances made in the medical sciences, independent verification of diagnoses and drug dosages should be made.

Gill Smithies

Proofreading & Language Editing Services

59, Lewis Drive, Amanzimtoti, 4126, Kwazulu Natal

Cell: 071 352 5410 E-mail: moramist@vodamail.co.za

Work Certificate

To	Cornel Burger
Address	Centre of Excellence for Pharmaceutical Studies, Division of Pharmaceutics, Potchefstroom Campus, North West University
Date	16/11/2017
Subject	Natural oil nano-emulsion dispersions for the topical delivery of clofazimine, artemisone and decoquinate.
Ref	GS/CB/02

I, Gill Smithies, certify that I have proofed the following thesis,
Natural oil nano-emulsion dispersions for the topical delivery of clofazimine, artemisone and decoquinate,
to the standard as required by NWU, Potchefstroom Campus.

Gill Smithies

Work Certificate